LARGE-SCALE HYDROLOGICAL MODELLING: PHYSICAL PARAMETERISATION FOR GROUNDWATER RECHARGE

by
Luciene Pimentel da Silva

Thesis submitted in fulfilment of the requirements for the degree of Doctor of Philosophy in Civil Engineering

Department of Civil Engineering
University of Newcastle upon Tyne
Newcastle upon Tyne, UK

January 1997

ACKNOWLEDGEMENTS

I wish to thank my supervisor John Ewen for his guidance and advice during all stages of this study. I also wish to thank him for the careful review of the thesis text and his kind support during hard times.

I would like to thank James Bathurst and Enda O'Connell for the kind reception they gave me when I first visit the University and for their friendly support during this study.

I wish to thank CNPq and COPPE/UFRJ for funding this research.

Thanks to Enda O'Connell and John Ewen for giving me the opportunity of interacting with the research group in WRSRU (University of Newcastle) involved in the TIGER programme. This has been an excellent experience for me.

On early stages of this work Sue White, Pascal Lardet and Anton Purnama contributed greatly with many suggestions and criticism.

Steve Birkinshaw contributed greatly reviewing and upgrading the FULCRUM computational code.

Rozi Abdullah gave invaluable support in the use of University machines and UNIX. This has been very important in the FULCRUM simulations in Chapter 4.

I would like to thank Stephen Anderton, Greg O'Donnell and Geoff Parkin for their support and advice on the preparation of the DSATE data set.

I wish to thank Chris Kilsby, who apart from sharing Brazilian's passion for football, gave me lots of good advises, friendly support and invaluable help on the preparation of the data sets in Chapters 4 and 6.

Sarah Dunn also contributed supplying some data sets.

Thanks to Bill Sloan for his friendly support and for the advice in Chapter 5 in the comparison of Richards' equation and the convection-diffusion equation.

Thanks to all my colleagues at the University for their companion and friendship. Julia Sherwood, Judith Stunell, Agnes Chung, Rozi Abdullah, Adhi Suyanto, Faridah Othman and Ali Almasi with whom I shared the office in different times certainly contributed for me to have a great time in Newcastle.

Thanks to Judith Stunell and Ben Lukey for their friendship and invaluable help with the English Language.

I also would like to thank Beto for his friendship, companion and support during all stages of this study.

ABSTRACT

There is currently worldwide interest in the effect of human activity on the global environment, especially the effect of greenhouse gases and land-use change on the global climate, and models are being developed to study both global change and the local effects of global change. The research reported here (funded by CNPq-Brazil) involves the development of GRASP: Groundwater Recharge modelling Approach with a Scaling-up Procedure. GRASP has been integrated into the UP (Upscaled Physically-based) macromodel, developed under the UK NERC TIGER programme, which is designed for studying the effects of climate and land-use change on the availability and quality of water resources. The UP macromodel will be coupled to the UK Meteorological Office's Unified (weather and climate) model to create a state-of-the-art coupled atmospheric/hydrological model.

Several important requirements for the design of new large-scale hydrological models are identified in a wide ranging review on GCMs (General Circulation Models) and physically-based hydrological modelling, and these requirements have been applied in the development of GRASP (and UP). The main requirements are a physical basis, proper treatment of spatial variability, and simplicity.

Using the concept of partial analysis, two point-scale models, SM (Soil Moisture content approach) and TF (Transfer Function approach), are developed for recharge, both based on the one-dimensional Richards' equation. SM is a simple two-parameter model relating recharge to water storage in the unsaturated zone, and several unsuccessful attempts are made to link its parameters to physical properties. TF is a transfer function model, and is parameterised using the matric potential and unsaturated hydraulic conductivity functions using a new approach developed especially for GRASP. Both SM and TF are verified against numerical solutions of Richards' equation.

SM has been adopted for use in the UP macromodel, because of its simplicity and computational efficiency. The basic grid scale for UP is around 10km and SM is parameterised at this scale by calibration against aggregated responses, determined by applying TF to several representative points in the grid. There is scope to improve on this approach by calibrating SM directly against an aggregated transfer function, found by superposing the at-a-point transfer function from TF. GRASP is tested, in a limited fashion, for the Little Washita catchment of the Red River basin, USA.

LARGE-SCALE HYDROLOGICAL MODELLING: PHYSICAL PARAMETERISATION FOR GROUNDWATER RECHARGE

List of Contents

List of Figures

List of Tables

Chapter 1

Introduction

1.1 - Research Overview

The research described in this thesis was funded by CNPq-Brazil and carried out in association with the NERC / TIGER (Terrestrial Initiative in Global Environmental Research) project at the University of Newcastle. The GRASP (Groundwater Recharge modelling Approach with a Scaling-up Procedure) was developed during this research. This is a hybrid approach that comprises two modelling schemes: SM (Soil Moisture content approach) and TF (Transfer Function approach), SM works on the grid- or catchment-element scale (~100 km^2) and groundwater recharge rates are given as a linear function of total soil moisture content. The SM model parameters are fitted to larger scale groundwater recharge rates, aggregated (upscaled) from the point scale. Groundwater recharge at the point scale is given by TF, which is based on the 1-D Richards' equation and the use of transfer functions. TF includes a new approach in which the parameters of the transfer function are obtained directly from soil physical properties. TF is completely free of calibration as it uses only widely available soil property data.

GRASP is intended to be a component of the UP (Upscaled Physically-based) model. UP is a macromodel developed by the Water Resource Systems Research Unit, University of Newcastle, as their contribution to the TIGER programme, and the wider review on large scale modelling presented in this thesis contributed to the design of the modelling framework. The UP model is designed to simulate hydrological and transport process at a range of spatial scales from 10^2 to 10^6 km^2 and over time scales from 1 to 1000 years. UP simulates land surface processes, including the effects of changes in land use and climate. UP can run with meteorological data as input, or in conjunction with atmospheric models. It is intended that UP will be coupled to the UK Meteorological Office Unified (atmospheric) model, to be run at the meso-scale, as a state-of-the-art coupled atmospheric/hydrologic model.

1.2 - Outline of the TIGER Programme

The Terrestrial Initiative in Global Environmental Research (TIGER) is a UK contribution to the world-wide research efforts, currently underway, on environmental and global climate change; e.g. the World Climate Research Programme (WCRP, World Climate Research Programme, 1991), the Global Energy and Water Cycle Experiment (GEWEX, International GEWEX Project Office, 1991), the Hydrological Atmospheric Pilot Experiment (HAPEX, André et al., 1990 and Goutorbe et al., 1994), the Amazonian Region Micrometeorological Experiment (ARME, Shuttleworth, 1988a). The main concern of TIGER is the understanding of the role of the principal greenhouse gases in climate prediction and evaluating the effect of the interaction of these gases on the biosphere (WRSRU/NERC, 1992).

TIGER is divided into four parts (TIGER 1, 2, 3 and 4). TIGER 3 is concerned with understanding the water and energy balance at the surface, and part of TIGER 3 is focused on the development of large scale hydrological models, including the UP model. The University of Newcastle is collaborating with three UK Research groups: the Institute of Hydrology focusing on the channel routing component of UP model; University College London (UCL) whose contribution includes the collection and generation of global land surface data sets including topography, hydrological networks, land cover, soil type and geology; and Imperial College whose contribution is concerned with the disaggregation of climatological data, as input to the hydrological models. An application of the UP model to the Red River basin, USA, is underway.

1.3 - Climate Change and the Hydrological cycle

In recent years man has become increasingly concerned about the effects that land use change associated with land management and, urban and industrial development has on the natural environment. Large scale clearance of tropical rain forests has focused attention on the possible effects of deforestation on climate. Shukla et al. (1990) carried out a study using a General Circulation Model (GCM) to simulate the complete clearance of the Amazon forest, and predicted an increase in surface temperature of up to 2.5°C. At the same time, the build up of the so-called greenhouse gases during the post-industrial period has given rise to speculation about a possible rise in surface temperature (global

warming) due to the increase of the concentrations of carbon dioxide (CO_2), methane (CH_4), ozone (O_3), nitrous oxide (N_2O), chlorofluorocarbons (CFCs) and other gases in the atmosphere (Table 1.1).

Table 1.1 - Concentrations and residence times* of important greenhouse gases, adapted from Loaiciga et al. (1996)

	H_2O ppmv	CO_2 ppmv	CH_2 ppmv	CFC-11 pptv	CFC-12 pptv	N_2O ppbv	O_3[a] ppbv
1750-1800	3000	280	0.8	0	0	285	1-15[b]
1990	3000	353	1.72	280	484	310	10-100
residence time	10-15 days	50-100 years	10 years	65 years	130 years	150 years	na[c]

Symbols: CFC-11: $CFCl_3$, CFC-12: CF_2Cl_2; ppmv, parts per million volume; ppbv, parts per billion volume; pptv, parts per trillion volume.

[a] below 12 km.

[b] estimated value.

[c] ozone is continuously produced by photolisis in the stratosphere.

na, not applicable.

* time that the greenhouse gas remains in the atmosphere.

The theory of global warming is strongly tied to the greenhouse effect, which is based on the assumption that the surface temperature is regulated by the atmosphere, for which the main source of energy is the sun. Most of the solar radiation that passes through the atmosphere is absorbed by the Earth's surface. Some radiation is not absorbed, and is reflected back to the atmosphere. The Earth's surface emits radiant energy approximately like a blackbody, in the infrared range of the electromagnetic spectrum. The atmosphere is generally cooler than the surface: it has an equivalent effective radiative temperature of approximately -18°C, while the Earth's surface global mean is approximately 15°C (Rasmusson et al., 1992). As a consequence of these emissions and absorptions in the surface-atmosphere system, part of the infrared radiation emitted by the surface is trapped by the gases in the atmosphere, increasing the

Earth's surface temperature which gives rise to the greenhouse effect. All the gases in Table 1.1 absorb infrared radiation emitted by the Earth's surface, and therefore contribute to the greenhouse effect.

The effects of global warming on the climate have been predicted using GCM simulations. As CO_2 is an important byproduct of human activities, predictions hypothesising a doubling of CO_2 concentrations have become standard, although the effect of the other gases can not be disregarded (Loaiciga, 1996). Exactly what is going to happen to the global climate due to global warming is a question that has not yet been fully answered. There are differences in the way climate change is simulated, with predictions using either a steady increase in CO_2 until its initial concentration is doubled or an abrupt increase in CO_2 after a period of normal levels. There seems to be general agreement, however, that the global mean surface temperature will rise, and some simulations predict a rise of up to 5°C (Mitchell, 1989). There is even more uncertainty about how this rise in temperature will affect the hydrological cycle and water resources.

With a rise in global mean surface temperature, an increase in global mean evapotranspiration would be expected, leading to an increase in mean precipitation. If the surface and air temperatures increase by the same amount and relative humidities remain fixed, global evaporation will simply increase, and the hydrological cycle will speed up with global warming. From GCM simulations, the Intergovernmental Panel on Climate Change (Intergovernmental Panel on Climate Change (IPCC), 1990) suggest:

(1) In the tropics, surface temperature will increase and seasonal variation will narrow;
(2) At high latitudes (above 50°) will be warmer winters and springs;
(3) In northern midlatitudes summers will be dryer.

It is expected that these changes will have a direct impact on the availability and/or distribution of water resources. Water is vital for life and any change that affects current resources must be taken very seriously. Hence there has been a worldwide effort involving both observational and modelling studies to improve predictions and fully understand all the consequences of land use change and the build up of the concentration of greenhouse gases in the atmosphere (Shuttleworth, 1991 and Liesbscher, 1993).

The observational studies aim to improve the understanding of the energy and water fluxes in the soil-vegetation-atmosphere system at different spatial and temporal scales. These studies use experiments at scales varying from the plot or local-scale (e.g. Anglo-Brazilian Amazonian Climate Observation Study (ABRACOS), Shuttleworth et al., 1991) to larger scales (e.g. Hydrologic Atmospheric Pilot Experiment (HAPEX), André et al., 1990 and Goutorbe et al., 1994). The experiments are generally demanding and involve considerable resources, therefore, field characterisation studies cannot be carried out everywhere. Although remotely sensed data has been traditionally used for mapping, recently its use has been expanded to more physically based characterisation of the data, allowing local observations to be enhanced and extended (Wessman, 1992). It is widely hoped that remotely sensed measurements made with satellite-mounted systems will be of great value in observational studies.

As has been discussed previously, GCMs have been used in the modelling studies associated with land use change and the increase of the concentration of the greenhouse gases in the atmosphere. Although these models have been successful in demonstrating that the climate is sensitive to these changes, there is some concern over the accuracy of these GCM predictions. This is not only related to the level of understanding of physical processes and actual data availability for these simulations, but also to the accuracy of the current modelling schemes.

1.4 - Introduction to General Circulation Models (GCMs)

GCMs represent major features of atmospheric circulation and, for some interactive models, ocean circulation process is also modelled. Their variables are basic indicators of atmospheric conditions, e.g. temperature, humidity, surface pressure, wind velocity and precipitation, with each value representative of an entire grid square which may be tens of thousands of square kilometres in area. They solve the three-dimensional, time-dependent differential equations for the rates of change of air pressure, wind vector, temperature and moisture content; taking account of sources and sinks of heat, moisture, and momentum. To determine unique solutions, the models require input of upper and lower boundary conditions, e.g. solar radiation at the top of the atmosphere, orograph and land-sea distribution, albedo of bare soil, surface roughness and vegetation characteristics.

There are a variety of GCMs available, mostly associated with major laboratories: the Canadian Climate Center model (CCC), the Geophysical Fluids Dynamics Laboratory (GFDL), the Goddard Institute for Space Studies (GISS), the Laboratoire de Meteorologique Dynamique (LMD), United Kingdom Meteorological Office (UKMO) and the National Center for Atmospheric Research (NCAR). The models mainly differ in the number of vertical layers, spatial resolution and horizontal representation (spectral or grid point finite difference models).

There are, however, some unresolved issues related to the way physical processes are represented in these models. The representation of ocean conditions, for example, is poor and models frequently do not include coupled atmospheric-oceanic general circulation. Apart from this, the representation of the land-surface is generally very simple. Hydrological processes such as runoff are either very poorly represented or simply ignored. The need to improve land surface representation in GCMs is now widely agreed (Shuttleworth, 1988b; Wood, 1991a; Avissar, 1992).

1.5 - Land-Surface Parameterisation in GCMs and Large Scale Hydrology

Although the representation of land surface processes in GCMs is currently under review, Budyko's approach (described in Manabe, 1969) is still used in many GCMs. The land-surface component is represented by a large-scale lumped soil-reservoir with one single layer that can be filled to some maximum theoretical "field capacity" and from which the soil water evaporates at a rate proportional to the remaining water content. This parameterisation highly simplifies the hydrological processes of infiltration and evaporation; the model does not explicitly consider vegetation and assumes that parameter values, such as soil moisture capacity, are constant over the entire grid square. Soil moisture content is an important component in GCMs, as energy fluxes and temperature have been shown to be sensitive to soil moisture variations (e.g. Avissar, 1992). In addition, the processes of heat and mass exchange between the surface and the atmosphere that ultimately control evapotranspiration fluxes are modelled as boundary conditions (Loaiciga, 1996). This is inadequate because it does not account for feedback from land surface hydrological processes to the atmosphere. This also affects runoff estimates as they are calculated from water mass balance using evapotranspiration and rainfall.

Another important simplification assumed in many GCMs is that lateral transfer of water within grids can be neglected. Runoff is calculated using water mass balance for each grid box, and then accumulated for each river basin, finally being deposited in the ocean. Therefore, some of the important dynamics of the hydrological cycle are not modelled.

Recently, new parameterisations have appeared in the literature. These have attempted to overcome the problems associated with the use of simplistic soil moisture availability functions based on field capacity and water budget accounting, and modelling evaporation without explicitly accounting for the physiological resistance of vegetation.

To improve the land-surface representation of GCMs Soil-Vegetation-Atmosphere Transfer Schemes (SVATS, e.g. Sellers et al., 1986) have been proposed. These modelling schemes account in a more detailed way for vegetation and its interaction with both the atmosphere and land surface, using the physical and physiological properties of the vegetation and soil. SVATS have in general a very detailed vertical physical representation; however, they usually neglect spatial heterogeneity. The parameters for the soil and vegetation properties are assumed constant within a GCM grid. Because of their detailed vertical resolution in the canopy, but lack of horizontal detail, these models have been referred to as 'big-leaf' models (Wood, 1991a). Entekhabi and Eagleson (1989) proposed a scheme using probability distribution functions to include the effects of spatial variability into GCM's land surface parameterisation. These functions, if introduced for all the physical processes involved in the atmosphere-land surface representation would lead the model to be computationally very time consuming.

The land surface and atmosphere are coupled through the exchange of energy and water and therefore should be treated as interacting components of the climate system. The land surface affects the atmosphere through fluxes of radiation, momentum, heat and moisture. The land surface (hydrological) processes, in conjunction with the the soil and vegetation characteristics, determine the surface moisture availability which controls the partitioning between sensible and latent heat fluxes. Developing more realistic parameterisations which fully account for this coupling is extremely complicated.

It is evident that for more accurate evaluation of the effects of global warming on both climate and water resources, there is a need to enhance the representation of land surface processes in GCMs, as well as the representation of their interaction with the atmosphere. This involves mainly the representation of intergrid lateral transfers and a more realistic modelling approach to represent runoff, which implies implicitly accounting for spatial variability. The study of spatial variability involves searching for patterns. These are associated with the scale at which physical processes occur. The scale issue is complex, and, in addition, the atmosphere-land surface processes comprise a variety of processes that naturally are associated with a variety of different spatial scales.

Becker and Nemec (1987) presented a general overview of scales in the atmospheric, hydrological and geographical sciences (Figure 1.1). In combination with this wide range of spatial scales, the residence time of the land-atmosphere interactions cover a wide range of temporal scales. For the atmosphere, turbulent dynamics in the surface boundary layer occur on scales of seconds to hours contrasting with the annual cycle of the atmosphere's general circulation that is characterised over months, years or decades. For land surface processes, infiltration excess, for example, can be observed on a temporal scale of less than an hour, whereas groundwater-controlled flows have time-scales of months to decades.

GCMs work at the coarsest scale of atmospheric modelling. In hydrology, some models operate at the continental scale (e.g. Solomon, 1968 and Vorösmarty, 1989). These are intended for the evaluation of the water balance at the regional scale and the effects of land use change. However, there is a general belief that the land parameterisation in these models needs to be reviewed (Wood, 1991a). Models constructed to work on the catchment scale (micro- and lower meso-scales) have been successfully used in engineering design, and in estimating some of the effects of land-use change at the catchment scale. In some aspects, the hydrology of large river basins differs from that of small basins. The variety of landscape forms found in large basins, and the diversity of vegetation, land uses, soil types etc. necessitate a different approach. Mathematical relationships that describe a physical phenomenon are mostly scale dependent, so different formulations arise at different spatial-time scales. Thus, there is a need both to improve actual modelling and to overcome the scale gap. This motivated a new discipline in hydrology: Large Scale Hydrology or Macrohydrology, as described in Shuttleworth (1988b).

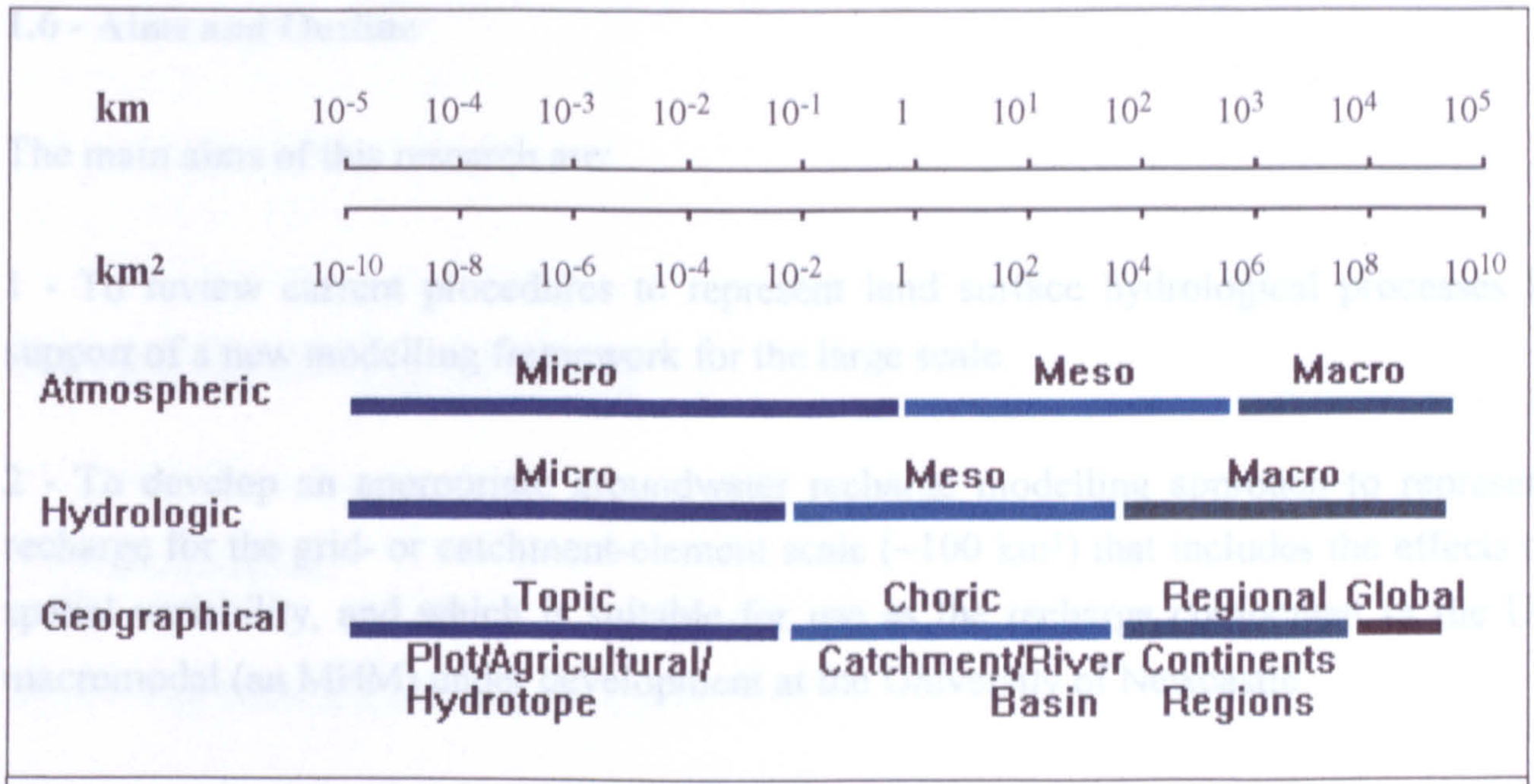

Figure 1.1- Classification of scales in the atmospheric, hydrological and geographical sciences, adapted from Becker and Nemec (1987)

The central consideration in developing Macroscale Hydrologic Models (MHM) is how to build upon the current existing modelling schemes to address water cycling issues at larger scales while simultaneously linking land and atmospheric systems. This research addresses the issue of large scale hydrological modelling. It is believed that progress in this area will enhance the understanding of the effects that land-use change and an increase in greenhouse gas concentration in the atmosphere would have on climate, as well as their consequences for the availability and distribution of water resources.

1.6 - Aims and Outline

The main aims of this research are:

1 - To review current procedures to represent land surface hydrological processes in support of a new modelling framework for the large scale.

2 - To develop an appropriate groundwater recharge modelling approach to represent recharge for the grid- or catchment-element scale (~100 km^2) that includes the effects of spatial variability, and which is suitable for use as the recharge component in the UP macromodel (an MHM) under development at the University of Newcastle.

The thesis is divided into seven chapters. In chapter 2, large scale hydrological modelling is reviewed and the need for a new approach discussed. This review contributed to the design of the UP macromodel. In chapter 3, the UP model is described and the groundwater recharge modelling approach (GRASP) introduced. In chapter 4, the transient one-dimensional Richards equation simulations, which are the basis for GRASP development, are described. GRASP itself is described in chapter 5 and a case study to demonstrate the use of GRASP is presented in chapter 6. Finally, chapter 7 contains overall conclusions and suggestions for future research.

Chapter 2

Large Scale Hydrology

2.1 - Introduction

2.1.1 - The Global Hydrological Cycle

The main source of energy for the planet is the sun. Of the total solar incoming energy (short-wave radiation), 30% is reflected from the atmosphere and the earth's surface, returning to space as short-wave radiation. The remaining 70% is absorbed, 19% by the atmosphere and 51% by the earth's surface. Because the earth is in approximate thermal equilibrium (i.e. no long-term net heating), this 70% is eventually re-radiated back to space as long-wave radiation. However before it returns to space, this energy passes through a complex recycling between the earth's surface and the atmosphere (Rasmusson et al., 1992).

Due to the spherical shape of the planet, the energy emitted by the sun reaches the atmosphere and the earth's surface with different angles of incidence. This leads to a variation in the energy budget according to latitude. There is net radiative heating at low latitudes (near the equator) and net cooling at high latitudes (near the poles). This imbalance leads to a pole-ward transport of energy, and a fundamental coupling exists between the radiation budget and the general circulation of the atmosphere and oceans. It is this circulation, accomplished by ocean currents, that forces and drives the land-surface processes forming the global hydrological cycle. Figure 2.1 shows a one-dimensional (vertical) scheme of the various sinks and fluxes of water, as well as the coupling systems (ocean-land, ocean-atmosphere and atmosphere-land) in the global hydrological cycle.

The vital link between the hydrological cycle and the global energy balance is the atmospheric transport of latent heat (water vapour) which is a major contributor to the heat balance of the earth. In the atmosphere, heat is transported in the form of sensible heat, which is associated with both the temperature of the air parcel and the latent heat of the water vapour the air parcel contains. This latent heat or 'energy parcel' is carried by the evaporated water vapour until it is released to the atmosphere upon vapour condensation in regions of upward atmospheric motion, cloud formation, and precipitation.

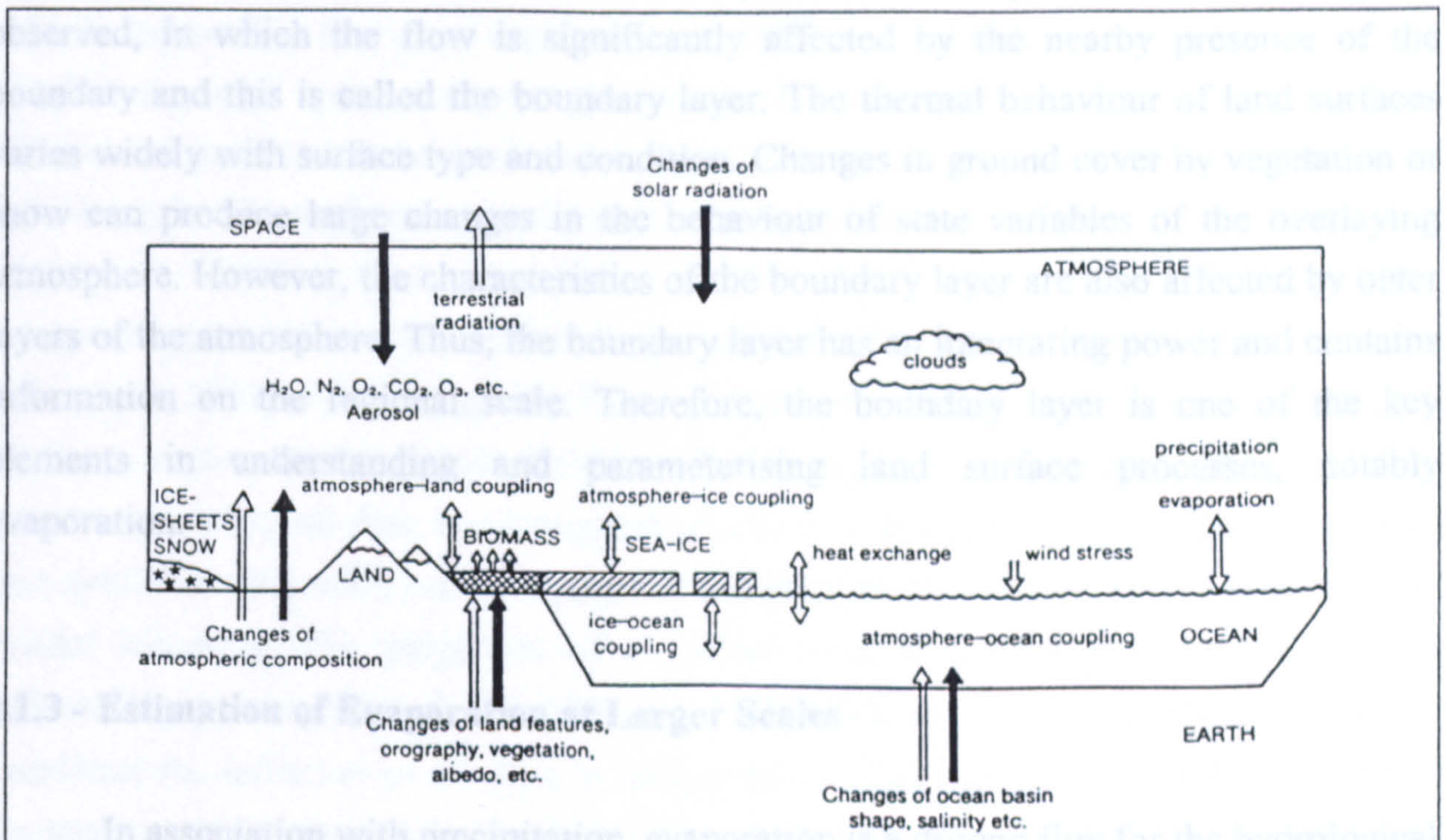

Figure 2.1 - One-dimensional abstraction of the global hydrological cycle, after IPCC (1990)

2.1.2 - The Atmospheric Boundary Layer

The atmosphere forms a distinctive layer about 100 km thick around the earth which is characterised by different sub-layers divided according to the temperature profile. The troposphere is the most important layer for land-surface studies as it contains 75% of the weight of the atmosphere and virtually all its moisture. Although the thickness of these layers vary, the troposphere extends to about 11 km above the earth's surface. The atmospheric circulation in the troposphere is affected by its outer spheres, stratosphere and mesosphere, and by surface features.

As in other fluid flows, in the atmosphere a zone adjacent to the boundary is observed, in which the flow is significantly affected by the nearby presence of the boundary and this is called the boundary layer. The thermal behaviour of land surfaces varies widely with surface type and condition. Changes in ground cover by vegetation or snow can produce large changes in the behaviour of state variables of the overlaying atmosphere. However, the characteristics of the boundary layer are also affected by outer layers of the atmosphere. Thus, the boundary layer has an integrating power and contains information on the regional scale. Therefore, the boundary layer is one of the key elements in understanding and parameterising land surface processes, notably evaporation.

2.1.3 - Estimation of Evaporation at Larger Scales

In association with precipitation, evaporation is a driving flux for the hydrological cycle and is the main mechanism for depletion of the available water. It is also important to represent the catchment "runoff-readiness" in hydrologic modelling. This depends primarily on the initial soil-moisture content of the catchment, and thus on the antecedent evaporative conditions. The initial state of the catchment is the direct result of evaporation and soil drainage between storms.

Transport of momentum, sensible heat, water vapour and other admixtures of air near the earth's surface generally involve turbulence. As the outer region of the Atmospheric Boundary Layer (ABL) is affected by large-scale atmospheric dynamics and weather patterns, and rarely results from equilibrium conditions, most information gained

about the ABL has been in the form of bulk transfer expressions which describe surface fluxes for water vapour and sensible heat. However, mainly due to scarcity of suitable data sets, these equations have been seldom tested. Other studies assume that the ABL behaves as a perfectly mixed "slab" in which the evolution of latent and sensible heat storage are represented by budget equations for the mean specific humidity and potential temperature. The slab approach has been useful in describing the development of elements of the ABL, for example thickness evolution. This approach has also been useful in attempts to simulate evaporation and to gain more insight into existing parameterisations. The closure of the budget equation is not, however, without difficulties and generally neglects advective terms. Another possible method of enhancing the understanding of the ABL is a study of the fluxes using a profile approach which focuses on the inner region of the ABL, and aims to establish mean vertical profiles for wind speed, temperature and specific humidity. For a portion of the inner layer these profiles can be considered quasi-uniform, but it has not been determined yet how irregular the surface can be for such an assumption to be valid.

Progress in studies of the fluxes of the ABL has, however, been very slow (Brutsaert, 1991) and these studies have not yet been able to establish a methodology to estimate regional evaporation. Point-based evaporation can be reliably evaluated from micrometeorological data, but it requires special and expensive instrumentation, which is not available with wide enough spatial distribution to allow good areal estimates to be made. Moreover, the properties of air which control surface evaporation rates are affected by passing through the ABL and the layers above, and feedback may occur to moderate the influence of changes in surface cover. This modification of the atmosphere happens at all horizontal scales from the very small scale of a leaf to the continental scale, and these atmospheric feedback mechanisms may intervene at larger scales to attenuate the effect of surface controls in evaporation. Based on this, Bouchet (1963) and Morton (1965, 1983) proposed eqn. (2.1) to estimate, E, the regional evaporation:

$$E = 2E_{po} - E_o \qquad \text{eqn. (2.1)}$$

where E_{po} is a hypothetical potential evaporation rate that would have occurred if water was freely available and E_o is the potential evaporation calculated using near-surface weather variables. Brutsaert and Stricker (1979) had some success using the Penman

equation to estimate E_{po} and the Priestly and Taylor expression for E_o. Kite et al. (1994) used eqn. (2.1) to estimate areal evaporation in a large scale hydrological model.

In most atmospheric models, evaporation is given by an average rate which is calculated as a function of local potential rates. The assumption in these models is that over uniform surfaces or those where surface variations occur randomly, the mixing of air means that to the atmosphere they appear uniform and regional scale atmospheric feedback can be adequately represented by one-dimensional models. Typically (e.g. Canadian Climate Centre GCM; Mcfarlane et al., 1992), evaporation is given as a function of a reduction factor, β, and the potential rate, E_p.

$$E = \beta E_p \qquad \text{eqn. (2.2)}$$

When it is calculated as a function of soil moisture content, β may indirectly incorporate both vegetation and soil characteristics. E_p can be estimated by the Penman equation and assumes a wet surface. In many GCMs this scheme is related to the land-surface representation by a simple bucket (Manabe, 1969) with a maximum water capacity equivalent to an average field capacity and from which evaporation is taken.

Another current method for estimating E is based on the concept of a resistance factor, r, which may be seen as analogous to a electrical resistance. The expression used is the Penman-Monteith equation (Monteith, 1973). Although there is a correspondence between the Penman-Monteith formula and the approach given by eqn. (2.2) using E_p from the Penman equation (Brutsaert, 1986), the Penman-Monteith expression accounts more explicitly and comprehensively for the soil-plant system.

2.2 - Soil Vegetation Atmospheric Transfer Schemes

2.2.1 - Overview

Biosphere-Atmosphere Transfer Schemes (BATS, Dickinson, 1991), and Soil-Vegetation- Atmosphere Transfer Schemes (SVATS, e.g. Sellers et al., 1986) have emerged in an attempt to enhance the simple land-surface parameterisation (simple bucket model) still in place in many GCMs. BATS and SVATS include the processes of diffusion of water in soils and canopy resistance which are not addressed in the simple bucket model.

There exists a wide range of models that can be called SVATS and these models differ from each other in many features, most particularly in scale which can range from local to regional, and from fractions of hours to days and months. Some SVATS and BATS have been incorporated into GCMs. Geyer and Jarvis (1991) present a detailed review of a large number of SVATS. These models are essentially vertical views of hydrological processes and consider the transport of water and energy below and across the surface, and then within and through the vegetation canopy. Some SVATS also consider CO_2 and other trace gases in addition to heat, water and momentum transfer.

SVATS models include layered parameterisations of the vegetation structure (ground and canopy store) and of the soil. Radiative transfers are processed considering vegetation and soil conditions for given inputs of incoming solar radiation. In addition, soil heat transfer, sensible heat transfer, evapotranspiration and precipitation interception in the canopy are modelled. Precipitation reaching the canopy fills up a store which is subsequently emptied by evaporation and drainage. A fixed proportion of precipitation and drainage form the throughfall which reaches the soil moisture store. From there, it may either evaporate or penetrate further down into the soil profile. Evapotranspiration estimations take into account the effect of light, temperature, vapour pressure deficit, leaf water potential and the canopy's stomatal resistance. As an example Figure 2.2 shows a representation of the Simple Biosphere model (SiB, Sellers et al., 1986).

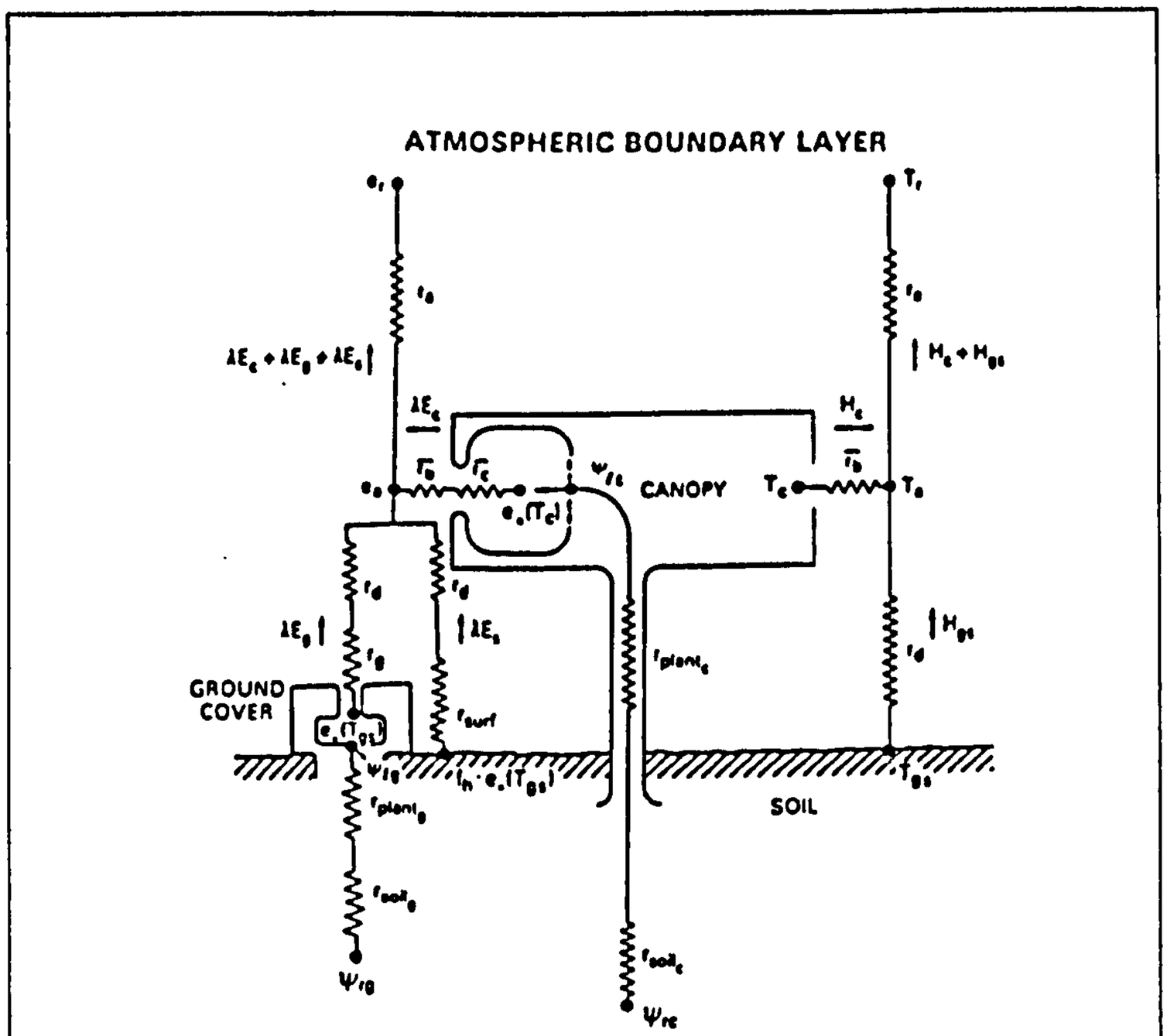

Figure 2.2 - Framework of the Simple Biosphere (SiB) model, after Sellers et al. (1986)

This figure shows how the vertical transfer of mass, momentum and heat is conceptualised as a series of flow paths. The interchange between stores works by analogy with Ohm's law and considers resistance to water and energy movement. These resistance parameters are obtained from basic canopy, leaf and soil structure and, for given precipitation and other meteorological inputs (e.g. temperature and solar radiation), the model calculates evapotranspiration, soil moisture content and runoff.

BATS and SVATS are physically-based representations of land surface-atmosphere interactions, and are more realistic than the simple representations that appear in many atmospheric models. Recent studies (e.g. Chen et al., 1996) using field data have demonstrated that models which adopt this detailed soil-vegetation representation result in more realistic predictions of evaporation rates than those which adopt eqn. (2.2). In contrast with this simple approach, SVATS and BATS demand the

definition of a large number of parameters which may be sometimes difficult to determine. One way to overcome this is by calibration analysis using detailed micrometeorological data. Efforts have been made in observational land-atmosphere studies to provide the data required for the tuning of BATS and SVATS and, at the same time, understand how these models might in due course be calibrated for heterogeneous land surfaces (International Geosphere-Biosphere Programme, IGBP,1990). Most studies presented in the literature use data from these detailed studies (HAPEX, ARME and ABRACOS, discussed in section 1.2). These studies, however, are demanding and not practical to repeat everywhere. It is hoped that remotely sensed measurements made with satellite-mounted systems will ease the problem, allowing general calibration of BATS and SVATS.

2.2.2 - Limitations in BATS and SVATS modelling Schemes

BATS and SVATS have an essentially one-dimensional nature, representing area-average fluxes as vertical interchanges between stores (Shuttleworth, 1991). They do not contain any representation of spatial variability and generally allow for only one type of vegetation and soil. In moving to a larger scale, the size of the stores and the equations describing the exchange between them are likely to lose the local physical and physiological relevance they have at the plot or patch scale. For example, representation of the area-average amount of water stored on the leaves of the plants must recognise that convective rain does not fall uniformly over a large area. Thus, the need to "tune" the value of parameters to area-average values to allow for the representation of land-surface heterogeneity is implicit in the application of SVATS and BATS to larger areas.

Arain et al. (1996) carried out BATS simulations using the FIFE (First International Satellite Land Surface Climatology Project Field Experiment; Sellers et al., 1992) data set. They tested rules for defining the aggregate value of the parameters required to specify surface interactions by application to heterogeneous mixtures of vegetation types. Thus, BATS aggregated responses of individual soil patches within the grid (for sensible and latent heat, and soil heat profiles) were compared to the response using average parameters for the grid and, in most cases, results showed good agreement.

It was pointed out that extra work is needed to estimate spatial contrast thresholds. Aggregation rules for surface resistance remained untested.

The main assumption implicit in the direct application of BATS and SVATS at larger scales is that the understanding of the micro scale elements and processes of the hydrological cycle can, with minor modifications, be extrapolated to larger scales. Although these models have a good physical representation at the plot scale, and it is sensible to examine the micro scale hydrological processes in order to justify the predictions which will eventually be made for larger scales, the micro scale does not require the expression of feedback, spatial variability and other spatial integrational features that need to be included when moving towards larger scales (Dooge, 1986 and Becker and Nemec, 1987).

SVATS and BATS contain a limited procedure to represent runoff, and unsatisfactory runoff simulations have been reported in the literature (e.g. Thomas, 1990). Small and meso-scale variations in land characteristics can play an important role in runoff generation. Avissar (1992) performed numerical experiments showing that water availability for evapotranspiration plays a major role in land-atmosphere interactions. Taking, for example, a hillslope; the foot of the slope would be expected to be wetter than its top. Avissar also reported that differences in surface temperatures can be observed on hillslopes according to their aspect (i.e. spatial orientation, facing North or South). Such heterogeneity can generate strong circulations, which have an impact on the overlying atmospheric layers. It is also reported (Chen et al., 1996) that, in the FIFE experiment, areas with soil moisture contents equivalent to that at wilting point and others much wetter could both be observed within areas equivalent to the grid squares of atmospheric models.

Compared with evapotranspiration, runoff generation develops over different time scales. The absence of a realistic procedure which takes into account the dynamics of the process in many regions can lead to large errors in calculating evapotranspiration (Kuchment, 1992). Moreover, BATS and SVATS do not contain a full procedure to account for lateral flow. Modelling lateral groundwater and surface flow is relevant to land-surface/atmosphere interaction because inter-grid transfers can alter the availability of water for evapotranspiration.

At large spatial scales groundwater generally becomes an increasingly important component of hydrological fluxes, as more permeable soil material and regions of recharge and discharge from subsurface systems are more likely to occur. Although groundwater flows have low velocities they contain large volumes of water. In the Amazon Basin, for example, baseflow accounts for 75%-95% of total discharge. Determining inputs to the groundwater system requires knowledge of spatial and temporal variations of surface fluxes and the behaviour of water in the unsaturated zone beneath, which will both influence recharge rates. The soil unsaturated zone is represented in BATS and SVATS, and improvements in recharge estimates are thus interlinked with improving the model itself.

BATS and SVATS models have added new capabilities to large scale hydrological modelling. They have improved the realism of calculated surface energy/water fluxes and hence the representation of surface climate (as required in studies of future climate change). BATS and SVATS, however, overlook spatial heterogeneity and do not represent lateral transfers. Therefore the grid-average evaporation rate may be over- or under-estimated. This may also lead to misrepresentation of soil moisture content, which directly influences runoff modelling. Considering feedback effects, this would ultimately lead to unrealistic energy partitioning and incorrect evaporation rates. These factors, combined with the number of parameters required by SVATS and BATS, are problems that need to be addressed in order to improve modelling of land-surface processes at larger scales (see e.g. Moore et al., 1991).

The representation of heterogeneity may be enhanced by increasing the overall model resolution and the use of three-dimensional physical differential equations. However, apart from the numerical problems of solving such a complex system, the computer power required would currently be unrealistically expensive. A possible way of simplifying the problem would be to look for patterns and similarities in the spatial organisation within the domain in which the relevant phenomena take place. The concept of pattern is interrelated with scale, as the description of pattern involves the description of variation and the quantification of variation involves the determination of scales (Levin, 1992). Once patterns are detected and described, the determinants of the pattern, and the mechanisms that generate and maintain those patterns can be found.

2.3 - The Scale Issue

2.3.1 - Overview

Land-surface modelling comprises a range of processes that occur over a broad scale spectrum of several orders of magnitude for both space and time. How to represent and couple these processes is central to the development of realistic Macroscale Hydrological Models (MHMs). Mathematical relationships that describe a physical phenomenon are mostly scale dependent, in fact different relationships arise at different spatial-time scales (Dooge, 1986).

The land-atmosphere processes residence times cover a wide range of different temporal scales that can vary from less than one hour to months, years and decades.

Scales are either intrinsic to the system or imposed by our way of looking at it. Length scales are imposed by physical characteristics of components of the interface, e.g. leaf dimensions, vegetation height, topographic features; by the length of external forcing variables, e.g. precipitation cells; by the observation process; by dynamic processes that create boundary layers and other features of various dimensions and even by computational factors.

Ideally, processes should be observed at the same scale as they occur and, based on these observations, one could develop a theory pertinent to that scale. However, this is not always possible and most observations are point-based. One major reason for this is that observational devices cannot be constructed to operate at any arbitrary scale of interest. Apart from this, hydrological processes are generally simultaneously operative at a range of scales. The understanding of scale interactions would allow the application of information known for one scale in the analysis of processes at another scale.

2.3.2 - Current Approaches to the Scale Problem

Scale issues have been discussed in current research considering intermediate sub-scales to cover the gap from the plot- to the large-scale. Kuhnel et al. (1991) used elements of partial analysis in the issue of scales associated with soil water modelling. They described five sub-scales which are associated with the principle variables and parameters represented in the formulation of such models (Table 2.1). The particle scale comprises the region in which the physical laws based on viscosity and surface tension can be applied. At the pendon scale, a one-dimensional form of Darcy's Law is assumed to operate without accounting for spatial variability; differing from the field scale at which there is variability of local parameters. At the basin scale the model formulation depends both on the morphology of the basin and the interaction between the different modules (for example slopes, channels and aquifers). At the biome scale the equilibrium depends on the representation of the vegetation and the physical processes associated with it.

Table 2.1 - Scales in soil moisture accounting, after Kuhnel et al. (1991)

Scale	Variables	Parameters
Particle (10^{-3} - 10^{-6} m)	θ, ψ, K	a, σ, μ shape, packing, size
Pendon (10^{-2} m)	t_p, $f(t)$, t_d, $e(t)$	K(θ), D(θ), void ratio
Field (10^{2} m)	$f(t)$, $e(t)$	S, f_{ult}
Basin (10^{4} m)	$f_p(a)$, $e_p(a)$	S(a), $f_{ult}(a)$
Biome (10^{6} m)	E(t)	climate, soil, vegetation

Key for Table 2.1: θ, *moisture content*; ψ, *matric potential*; K, *hydraulic conductivity*; a, *surface area of the particle*; σ, *the surface tension of water*; μ, *viscosity*; t_p, *time to surface ponding*; t_d, *time for surface desaturation*; *e*, *evaporation rate*; D, *hydraulic diffusivity*; *f*, *infiltration rate*; S, *effective sorptivity*; f_{ult}, *ultimate mean infiltration rate*.

The problem of scale is often approached in mathematical models by a simplistic approach that tends to generalise relationships that were established for a small plot to larger areas, like in the case of SVATS and BATS. However, understanding the interactions among scales poses one of the most challenging problems in hydrology (e.g. Blöschl and Sivapalan, 1995; Milly, 1991).

Natural catchments generally exhibit a high degree of spatial variability both in space and time. The problem lies in determining to what extent spatial variability affects the intrinsic phenomena and how it should be represented at each scale, particularly when computing power will be limiting for a fully three-dimensional approach. The atmospheric response to the variability of land-surface characteristics may be small as long as the land surface features have high spatial frequencies. However, this is seldom verified.

Hydrological processes occur at a range of different length and time scales. Runoff generation by infiltration excess is characterised by a very fast response and is a 'point phenomena', whereas subsurface stormflow is generally much slower and, as with saturation excess, is an integrating process requiring a certain catchment area to operate. Characteristic rainfall-runoff relationships are therefore generated at the catchment, hillslope and point -scale, and this needs to be incorporated in MHMs (Macroscale Hydrologic Models). In contrast, atmospheric processes operate on a larger scale and represent the forcing mechanisms driving the hydrological cycle. Therefore, to build up and operate a realistic MHM, it is necessary to consider transferring and linking information across scales. Conceptually, the problem could be described as:

$$r(s,\omega,i) \underset{down}{\overset{up}{\leftrightarrow}} R(S,\Omega,I), \text{ which may imply scaling}$$

$$s \underset{down}{\overset{up}{\leftrightarrow}} S, \qquad \omega \underset{down}{\overset{up}{\leftrightarrow}} \Omega \quad \text{or / and} \quad i \underset{down}{\overset{up}{\leftrightarrow}} I$$

where,

r (s, ω, i)	- small-scale hydrological response of some hypothetical process;
s	- state variable associated to the formulation of r;
ω	- model's set of parameters;
i	- set of input variables; and,
R (S, Ω, I)	- large scale description

Scaling is associated with linking and transferring information across scales, and can be performed using either a stochastic or a deterministic modelling scheme. The stochastic approach allows the distribution function to be derived more readily but deterministic methods have greater potential to capture physical elements of the catchment. Figure 2.3 illustrates a procedure of linking responses across scales described in Blöschl and Sivapalan (1995). In practice, linking procedures may not be meaningful for all variables, as some may lose their meaning from one scale to another, e.g. hydraulic conductivity.

Linking conceptualisations across scales can follow either a downward or an upward route. The downward approach involves finding a theory or concept directly at the level of interest and then searching for the steps that could have led to it from a lower level. In the case of parameters, for example, it implies that if a determined parameter set is able to represent certain catchment behaviour, it is in some way related to the local physical characteristics (Beven, 1995). Downscaling involves disaggregating and singling out. Conversely the upward approach involves combining, by mathematical synthesis, information or theories that operate at a lower scale level into theories for predicting the associated process at an upper scale. Upscaling comprises two phases. The first step involves distributing 'point-based' measured information, and the second, consists of aggregating the spatial distribution response into one single value. The scale extent through which a concept can be inferred is more limited in the downscaling procedure.

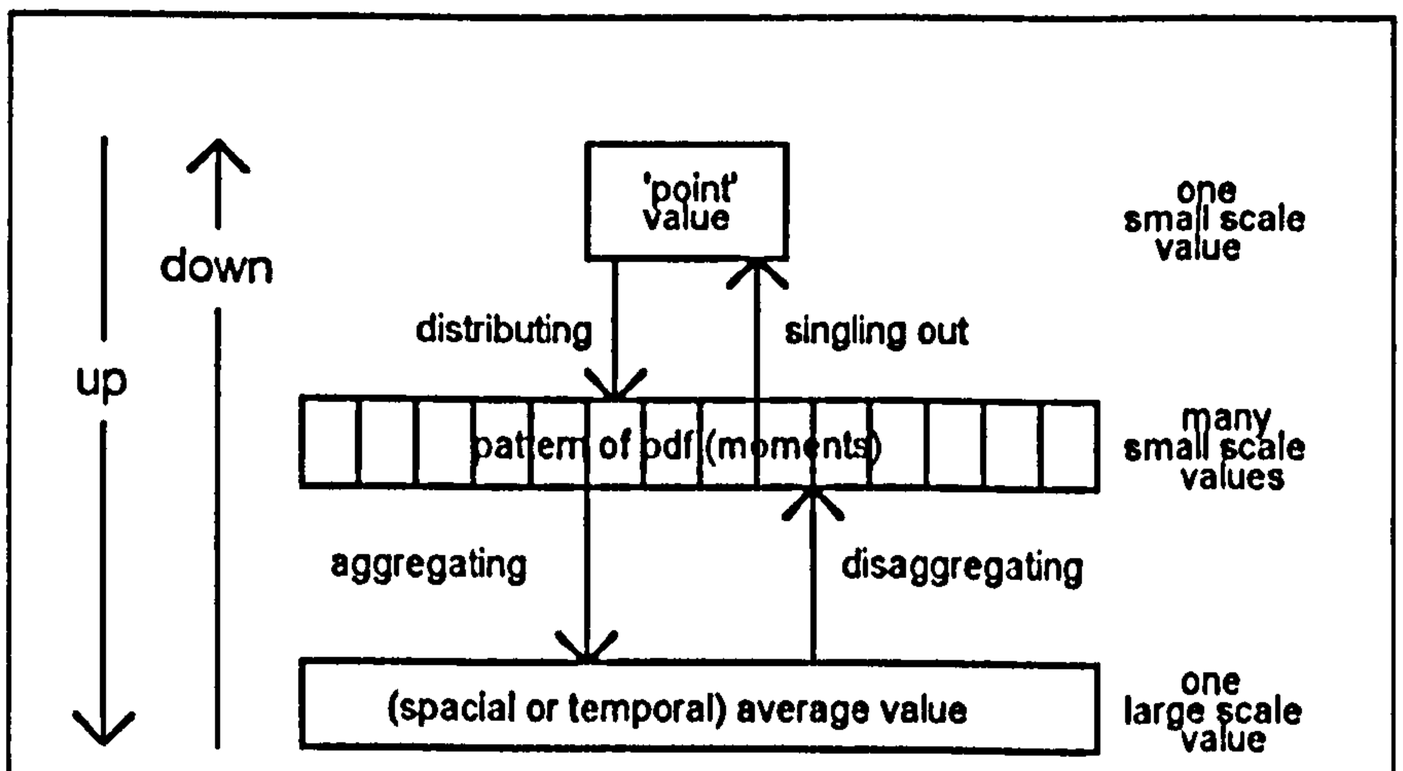

Figure 2.3 - Linkages across scales, after Blöschl and Sivapalan (1995)

2.3.3 - Aggregation Procedures

Different methods exist for aggregating systems. King (1991) analysed four different approaches for scaling up in ecosystems, which may be useful in hydrological problems. These are lumping, direct extrapolation, extrapolation by the expected value and explicit integration.

Lumping is one of the simplest methods for scaling up and the requirements for this approach are easily met. One only needs to estimate model arguments averaged across the landscape. This approach, however, relies on assumptions that should be carefully considered. Lumping assumes that the system properties reflected in the model structure (mathematical formulation) do not change with scale. This is equivalent to assuming that on average the system behaves the same on both the large and small scale. This assumption only holds if the underlying system is linear. Many hydrological processes are non-linear and the accompanying aggregation error can be considerable. However, when the assumption of linearity or the associated errors are acceptable, lumping can be a useful approximation tool. Many conceptual hydrological models employ a lumped approach.

Direct extrapolation assumes that the landscape can be sub-divided into homogeneous sub-elements that are supposed to behave in the same way. The local small-scale model is applied to each element for which the model is appropriate and the scaled-up variables are given by the combination of these individual simulations, which for the case of non-interacting elements, is the simple summation. This method is probably the most commonly applied in estimating the larger scale response of a heterogeneous region (e.g. SHE model, Abbott et al., 1986a,b; Bathurst, 1986a,b). Direct extrapolation may be of limited use when the local model is a large system of differential equations with time consuming numerical solutions and the landscape involves a large number of elements. Another restriction associated with this method is that it does not consider interactions between elements. For example, in the case of evaporation modelling, excess sensible heat emanating from a dry patch of land increases the potential for evaporation from a wetter patch of grass downwind (Milly, 1991).

Extrapolation by the expected value is, to some extent, analogous with direct extrapolation. However, it allows for a probability distribution function to be applied to the modelled process. Therefore, the larger-scale expression of the local, finer-scale behaviour is the product of the region's area and the expected value of the model output simulating the local process. Arguments in the local model that vary spatially across the landscape are treated as random variables, and their joint probability distribution function defines the spatial heterogeneity of the landscape. If the probability density function is known, the expected value can be directly evaluated. If this is not the case, Monte Carlo simulations may be used to calculate the expected value of the local model and the probability density functions can be sampled. In some limited cases, this model can also be applied when interdependence between elements is verified. A limitation of this approach, especially for continental modelling, is that the number of interacting processes to be represented may lead to excessive modelling complexity. Desbarats (1995) applied a probability distribution function in a study to upscale soil capillary pressure-saturation curves.

Explicit integration assumes that landscape heterogeneity can be described by explicit functions of space. The extrapolation from smaller to the larger spatial scale is achieved by explicitly evaluating the integral of the smaller-scale model in exact or in a close form, with space as the integration variable. In contrast with the previous approaches, this method involves a change in model structure. The indefinite integration used in this approach represents a transformation or rescaling of the original small-scale model. The new model describes the larger-scale landscape behaviour as a function of the spatial limits of the landscape rather than as a function of the local spatially distributed variables. One of the difficulties in applying this method is determining the model indefinite integral. Complex functions describing spatial variability or a complex local model may make it difficult or impossible to find an explicit solution by indefinite integration. A further limitation is the validation of this approach, as generally observation of land-surface processes are point-based. However, if these difficulties can be overcome, explicit integration can provide an accurate and efficient estimate of the aggregate behaviour. There is no numerical approximation error in evaluating the definite integral once the indefinite integral is determined, and only one simulation with the rescaled model is needed to estimate the larger-scale landscape behaviour. Chen et al. (1994a,b) applied this aggregation approach to the Richards equation, but the resulting equation was even more complex than the Richards equation itself. Although this method

may be prohibitive for upscaling a full land-surface model, equations derived from this application can be used in verifying models of individual processes originating from simpler approaches.

One limitation of the upward approach is the incomplete knowledge of the larger-scale aggregate and the constraints of mathematical tractability (Dooge, 1986). However, it has a great appeal because it is theoretically straightforward and bears a clear conceptual meaning. As observational data are generally 'point-based' it seems sensible to use the point or local scale as the starting point. It is necessary, however, to develop mechanisms to validate these new larger-scale theories. Nevertheless, in the case of large scale modelling it is likely that both approaches (upwards and downwards) will need to be applied.

2.4 - Hydrological Modelling

2.4.1 - Large Scale Hydrological Modelling

The early attempts at hydrological continental modelling sought mainly to estimate the water mass balance; to calculate the proportions of total precipitation that would evaporate and run off. Solomon (1968) proposed a system that works based on a mesh of grid squares, a large part of which is a data base which stores and retrieves input information (e.g. physiographic characteristics). Precipitation, temperature (evapotranspiration is estimated as a function of temperature using Turc's formula) and runoff for each grid square are estimated by multiple regression, in which surface features, i.e. elevation and type of vegetation, are considered as independent variables. The model was successfully applied in the Amazon basin in Brazil, UNDP/WMO (1983), Canada and Sweden. Later versions of this system focused on improving soil modelling by including an infiltration module and enhancing the overland flow calculation by implementing a routing scheme.

Since then, continental modelling has started to address environmental issues, (in particular the effects of land use change and, more recently, climate change) and the requirements of the modelling approaches have had to be reviewed. There are, however, features from the earlier systems that can be incorporated into the new approaches.

Vorösmarty et al. (1989) proposed a system for which the main goal was the study of biochemical cycles at the global scale. The model includes a global hydrological component which consists of a coupled water balance and transport model. The hydrological component is linked to the terrestrial ecosystem model and trace gas model through soil moisture and evapotranspiration. The water balance model (WBM) is based on a structure of grid cells and for inputs of precipitation, temperature, potential evaporation, vegetation, soil and elevation the model predicts evapotranspiration, soil moisture, and runoff, on a monthly basis.

The soil moisture module shares similarities with the simple bucket (also referred as Budyko's scheme; Manabe, 1969), discussed in section 2.1.3, in which the soil reservoir is regulated as a function of an average field capacity. In the case of the WBM, field capacity is determined from the soil retention function and root depth. The soil retention function is determined as in Saxton et al. (1986) from soil texture analysis with the particle size classification and root depth assigned according to pedological classifications. Therefore, field capacity is dependent both on vegetation and soil characteristics. Runoff is calculated as the excess of soil moisture content (depleted by evapotranspiration) above field capacity.

WBM combined good ideas and represented a move towards more physically realistic continental hydrologic models. However, it is now recognised that to increase the confidence in future climate predictions more detailed modelling has to be introduced. For example, explicit infiltration modelling, and hence a more realistic runoff representation (Wood, 1991a).

Ott et al. (1991) proposed a model for application in the Mosel basin (with an area of approximately 28000 km^2) to evaluate the hydrological and climatological effects of land-use change. The model works on a 30 x 30 m grid basis. Landsat image data, and a digital elevation model were used to provide estimations for the model parameters. The small elements are aggregated into the so-called 'hydrologically similar units' and, for each typical grid cell surface flow is calculated as infiltration excess. Interflow and base flow are represented by a single reservoir with two outlets.

Kouwen et al. (1993) also proposed classification by similar units as a strategy for distributed hydrologic modelling. The Grouped Response Unit (GRU) consists of a sub-catchment which may have a range of land cover characteristics. The size of the sub-catchments (elements) are limited either to an area that is subject to uniform meteorological conditions or to a size where catchment travel times are small compared with either the overall basin travel time or the duration of meteorological events of interest. In each element, runoff is modelled by adding the contributions from each land cover unit which are estimated using a rainfall-runoff model. Model parameters are the same for equivalent land cover units. Runoff from each element is routed to the basin outlet and takes into account topographic features, channel slope, drainage density and pattern.

Both Ott's and Kouwen's approaches have in common the use of hydrologically similar units. Although the GRU classification approach is simplified because it considers only vegetation cover to classify homogeneous elements, it is likely that any large scale hydrological model would benefit from a classification system to optimise computing resources. In both cases (Ott's and Kouwen's classification systems) current catchment-scale hydrological models are applied to each homogeneous element. But are the current hydrological models ready for the task of predicting the effects of future climate change? In the following section some of the current catchment modelling approaches are reviewed.

2.4.2 - Catchment Physically-Based Modelling

Physically-based models have been proposed as a solution to the need to predict catchment changes, spatial representation of input and output variables, the movement of pollutants and sediment through a catchment, and forecasting the hydrological response of ungauged catchments. Although on a different scale and perspective, they share common needs with continental scale modelling.

The development of physically-based approaches has been fragmented (Beven and O'Connell, 1982). There has been a variety of developments on modelling individual hydrological processes, using both analytical and numerical methods to solve the associated physical equations. However, there have been few attempts at building

distributed physically-based hydrological models of whole catchments: the Système Hydrologique Européen (SHE, Abbott et al., 1986a,b and Bathurst, 1986a,b) and the Institute of Hydrology Distributed Model (IHDM, Beven et al.,1987 and Calver, 1988) are some examples.

In both SHE and IHDM the catchment is subdivided into homogeneous small units, and for each of these units, the associated physical equation of each named phase of the hydrological cycle is represented, e.g. interception, evapotranspiration, flow in the saturated and unsaturated zone. Water flow between units is also represented. However, neither SHE nor IHDM are fully three-dimensional representations of the hydrological cycle. It is possible to write general partial differential equations in a three-dimensional domain to represent the processes of mass and energy transfer within the catchment; and develop numerical solutions given physically realistic boundary and initial conditions. However, data provision could limit model results. Apart from this, computer power would limit the run time and spatial resolution of such models, and, therefore, the size of the catchment simulated.

Some success has been achieved using both SHE and IHDM for simulations in small catchments. Although setting up the model demands a great expenditure of time, these models represent a very useful instrument for understanding catchment behaviour. However, there has been a debate about a number of aspects of distributed physically-based catchment modelling, such as the method of discretization of the catchment, scale effects, numerical problems, data provision, validation or philosophical reflections about the quality of the results achieved (see Beven, 1989; Bathurst and O'Connell, 1992; Binley and Beven, 1992, Jensen and Mantoglou, 1992), and further problems may be encountered if it is attempted to extend their application to larger scales.

2.4.3 - Catchment Conceptual Modelling

Conceptual models have been widely and successfully applied in the planning and management of water resources. Conceptual modelling arose first from a systemic view of rainfall-runoff modelling, and one of the main developments is the unit hydrograph concept, which presupposes a time invariant linear system. The impulse response of a linear invariant system was associated with an instantaneous unit hydrograph which in

turn has been interpreted in terms of assemblages of linear reservoirs and linear channels (e.g. the 'Nash cascade' of *n* linear reservoirs). In these models, the instantaneous unit hydrograph is represented as a function of a set of parameters which are, in theory, connected to physical characteristics of the catchment, but in practice the models are calibrated against rainfall and runoff data.

Another generation of rainfall-runoff models, described in O'Connell (1991) as Explicit Soil Moisture Accounting models (ESMA), originated from this background. These, however, accomplished a more descriptive view of hydrological processes and attempt to represent the total catchment response, contrasting with the unit hydrograph theory which considers only stormflow. Their structure is fairly simple, generally comprising two distinct components (Franchini and Pacciani, 1991): the soil water balance (WBC) and the transfer to the basin outlet (TC). The WBC is the most important and characterises the model. The WBC is generally divided into sub-zones which are near surface, sub-surface and deep zone. It expresses the balance between the soil water content, incoming net rainfall and outgoing, evapotranspiration and runoff. The second component, TC, sometimes contains three different sub-elements: these are transfer along hillslopes (TH), transfer to the sub-basin outlet (TN) and the transfer to the succeeding outlets sections (TO) of any basin located downstream (Figure 2.4).

The need to solve different problems has led to the development of a variety of conceptual models (e.g. Stanford Watershed Model, Boughton Model, Sacramento Model, Tank Model). They differ mainly in the level of detail included in the modelling of each process. A review of a wide range of these models is presented in Fleming (1975) and more recently a structural analysis was conducted by Franchini and Pacciani (1991), which includes a discussion of a number of current approaches for rainfall-runoff modelling.

ESMA models generally consist of a network of stores, each representing sub-phases of the hydrologic cycle, with links representing the pathways by which water is transferred between stores and then to either the catchment outlet as simulated streamflow or back to the atmosphere through evapotranspiration. These transfers between stores are regulated by mathematical expressions which are associated with physical descriptions of the processes involved.

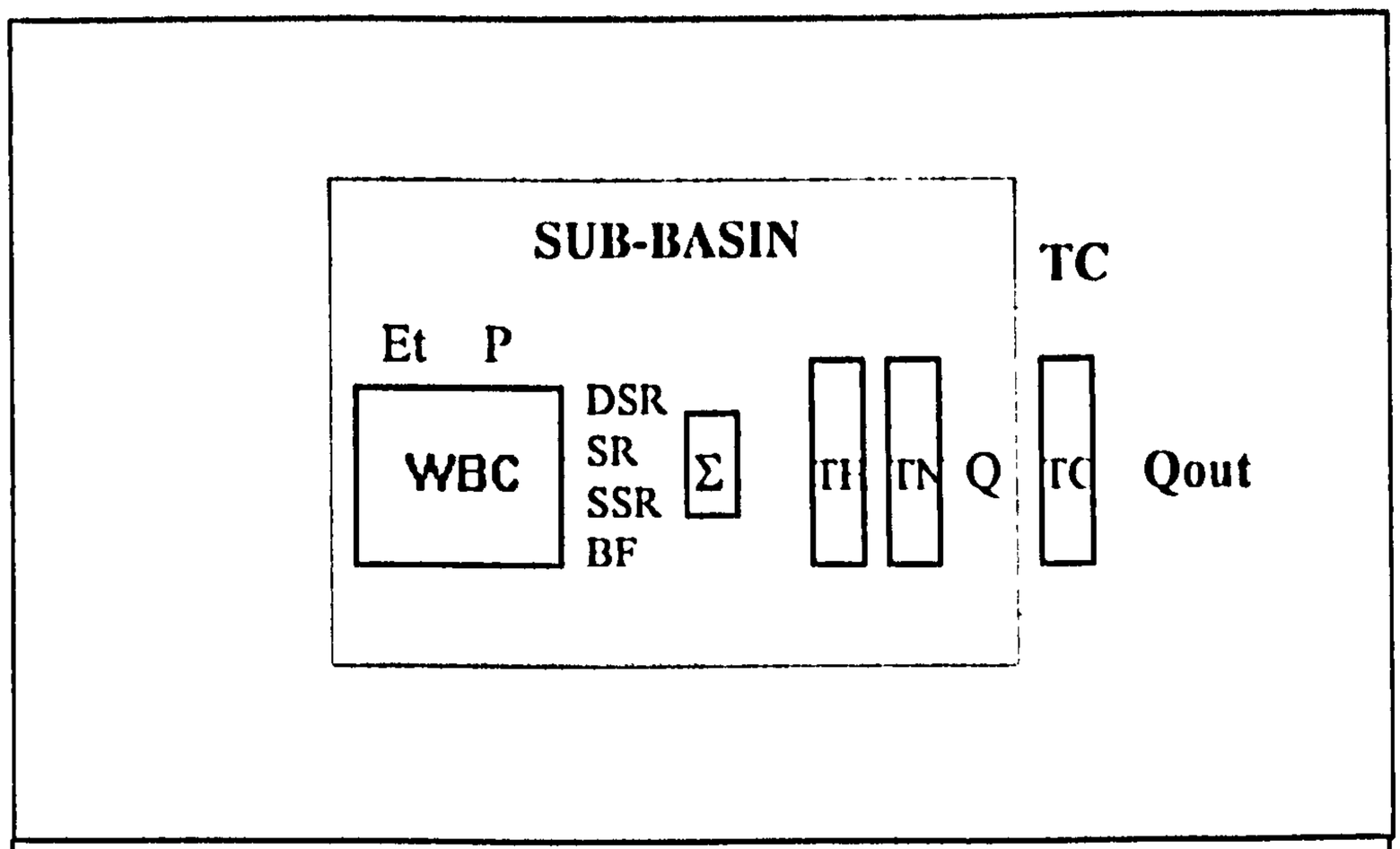

Figure 2.4 - Structure of conceptual models (adapted from Franchini and Pacciani, 1991)

Key for Figure 2.4: *WBC - water balance component at soil level, TC - transfer component, TH - transfer along hillslopes, TN - transfer to the closure section of the watershed (transfer along the drainage network), TO - transfer along the channel to a downstream section, P - precipitation, Et - evapotranspiration, Q - flow rate in the closure section of the sub-basin, Qout - part of the flow rate in the closure section of a sub-basin located further downstream, obtained by transfer of the flow rate Q.*

The mathematical equations that regulate the model's stores generally consist of a state variable (x_t) that corresponds to the level in the reservoir and variable parameters generally associated with the physical characteristics of different catchments. Figure 2.5 shows a typical store in one of these models. The relationship between the model parameters and the physical catchment characteristics is usually unknown and not explicit. The determination of parameter values involves calibration which can be done manually by trial and error or automatically, in which case mathematical search methods are used to find the best set of parameters to match an observed control variable, usually the discharge at the catchment outlet. In either case the process is not straightforward.

In the automatic calibration, an objective function, which measures the deviation between observed and simulated values of the control variable, is established. The problem is then to optimise the objective function by finding the set of parameters that

minimise the errors between the observed and simulated values. There are a number of mathematical functions that can be applied and the choice is associated with the application purpose. The minimum squared function is largely adopted. However, as a result of peculiarities in the formulation of conceptual models, the problem of parameter calibration can be complex.

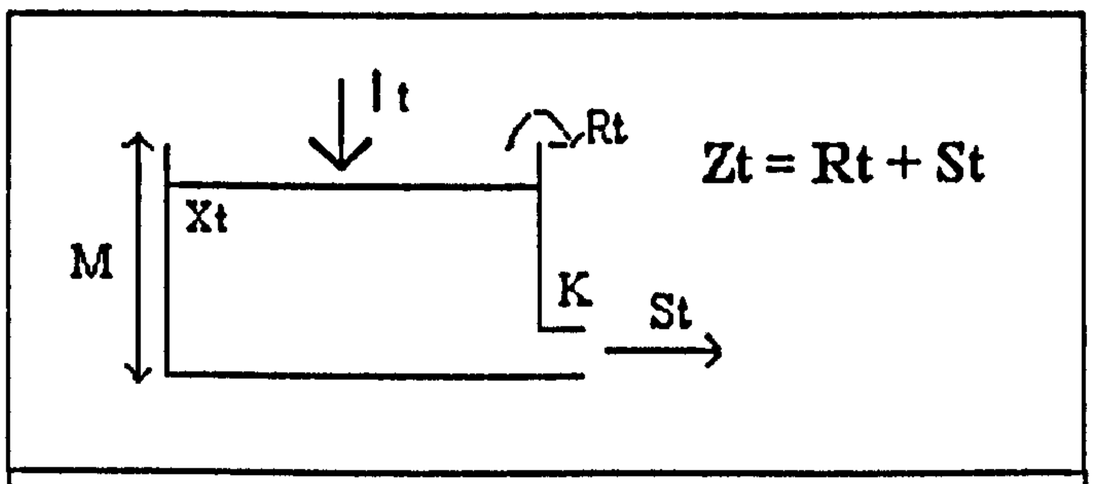

Figure 2.5-Typical storage in ESMA models

Key for Figure 2.5: *I_t - input from precipitation or other model storages; x_t - water level in the reservoir each time step; M - reservoir's maximum capacity, generally a parameter; R_t - outflow component, equals zero for $x_t < M$; S_t - outflow component; K - coefficient of recession for the reservoir, generally a parameter.*

Function z_t from Figure 2.5 can be written as,

$$Z_t = S_t + R_t;$$

where,

$$S_t = K(x_t - R_t)$$

$$R_t = \begin{cases} 0, \text{ if } x_t \le M \\ (x_t - M), \text{ if } x_t > M \end{cases}$$

$$x_t = x_{t-1} + I_t$$

The response surfaces resulting from the objective functions are very complex, characterised by high non-linearity, extensive valleys (due to interdependence between parameters than can be related to parameter redundancy), flat regions (which are regions of indifference) and multiple local minima (Ibbitt and O'Donnell, 1971; Johnston and Pilgrim, 1976). These features are tied to characteristics of model formulation and represent pitfalls for mathematical optimisation algorithms, sometimes leading to a non-representative set of parameters or simply numerical failure. Less robust searching methods are even more susceptible to failure. Some of these problems can also affect trial and error (manual) calibration.

Apart from this, threshold structures common in the formulation of ESMA models can lead to discontinuity that are points in the parameter space at which the objective function, although remaining continuous, is non differentiable. These threshold structures, apart from leading to confusion in the search method, limit the choice of mathematical optimisation routines to less robust methods that do not use derivatives (Sorooshian and Gupta, 1985 and Hendrickson et al., 1988).

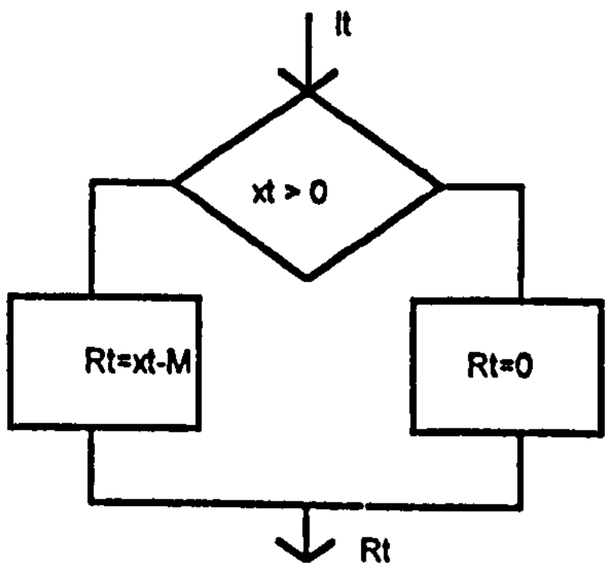

(a) ESMA threshold structure

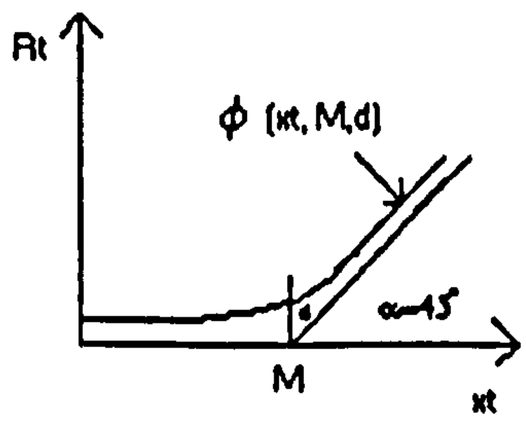

(b) Smoothing Function

Figure 2.6 - Typical threshold structures in ESMA models

Pimentel da Silva (1990) developed a methodology to smooth these threshold structures. A function, with hyperbolic shape (eqn. 2.3; Xavier, 1982) is applied, replacing the original 'if" structures (Figure 2.6).

$$\phi = \frac{\tan\left(\frac{\pi-\alpha}{2}\right)}{\tan^2\left(\frac{\pi-\alpha}{2}\right)-1}\left(x_t - M + \sqrt{(x_t - M)^2 + d^2 \frac{\left(\tan^2\left(\frac{\pi-\alpha}{2}\right)-1\right)^2}{\tan^2\left(\frac{\pi-\alpha}{2}\right)}} \right) \qquad \text{eqn. (2.3)}$$

The function ϕ is continuous and continuously derivable for x_t, including the point x_t=M for d>0, allowing the use of optimisation algorithms that use derivatives. Moreover, ϕ pursues properties that make it particularly useful for the task:

$$\lim_{d\to 0} \phi(x_t, M, d) = \begin{cases} 0, \text{ if } x_t \le M \\ (x_t - M), \text{ if } x_t > M \end{cases}$$

which implies that the deviation between ϕ and the model function can be made as small as required by making the parameter 'd' very small allowing the physical integrity of the model to be maintained. Additionally, ϕ is asymptotically tangent to the linear functions R_1 (x_t, M)=0, and R_2 (x_t, M)=(x_t-M), for d>0; which makes ϕ suitable for smoothing the threshold structures. Apart from this, ϕ is convex and decreasing for d > 0, and convex and non-decreasing for d=0; although this property is not necessarily transferred to the objective function, it is a useful property.

This function was successfully applied to smooth the threshold structures of the model SMAP (Soil Moisture Accounting Procedure; Lopes et al., 1981). The SMAP model is a fairly simple rainfall-runoff model, and its structure is similar to others cited in the literature, e.g. Boughton model, Dawdy and O'Donnell's model. As in Dawdy and O'Donnell (1965), synthetic series for discharge were generated by using the model to simulate discharge with a given set of physically realistic parameters values, rainfall and potential evaporation. This discharge data set was then used for parameter calibration of the smoothed version of the model attached to a second-derivative optimisation algorithm. The version of the SMAP model used has nine parameters. A number of trials

were run assuming different parameter set starting points in the process of optimisation. Deviations up to 75% of the solution were imposed on the initial parameter set. In all cases the model performed well and the values of the objective function always tended towards zero.

Apart from making possible the use of more robust optimisation methods and improving some of the negative aspects related to the shape of the objective function response surface, this approach also allows the objective function to be written analytically and as an explicit function of the parameters. In addition, this has the advantage of allowing the systematic investigation of all the possible optimum areas situated within the region where parameters assume realistic values by analysing the zeros of the derivatives.

Moore and Clarke (1981), reviewed the difficulties associated with parameter estimation in ESMA models and adopted a new approach. The catchment is considered to consist of a statistical population of narrow tubes, representing soil moisture stores. Runoff is estimated by a soil moisture accounting procedure. The resulting number of model parameters is small and the derivatives of the minimum squares objective function are continuous, allowing application of more efficient second order methods for optimisation. Different possibilities for enhancing the calibration of ESMA models are also described in Sorooshian et al. (1993) and Wang (1991).

The motivation behind descriptive modelling is to enhance the understanding of the behaviour of hydrological systems. Observational approaches accompanied by physical laws to explain the observations have an important role in hydrological modelling. Recent advances achieved by detailed field studies on catchment runoff generation are an example of this, and although they have not yet been transformed into physical laws, they have contributed to enhance the physical realism within hydrological modelling.

2.5 - Runoff Generation Processes

Figure 2.7 illustrates the mechanisms of runoff generation. In reality, all these processes occur dynamically over the basin and in practice, their separation is very difficult. These mechanisms are primarily driven by the intensity, duration and spatial distribution of precipitation. The dynamics of runoff generation are controlled by the initial soil moisture content (related to soil texture and structure), vegetation characteristics and topographic features (including the number and size of surface depressions, slope steepness and length of slope). As a result, runoff can be highly variable in space and time.

Early studies of the mechanisms of runoff generation have been centred mainly on Hortonian flow, where runoff is defined as the part of rainfall that cannot be absorbed into the soil by infiltration. However, in recent years, a considerable number of field observations have been carried out and these have identified processes other than infiltration excess that play an important role in runoff generation.

Infiltration excess overland flow is applicable to both impervious surfaces in urban areas and natural surfaces with low infiltration capacity as in semiarid and arid lands. In most humid regions infiltration capacities are higher because vegetation protects the soil from rain packing and dispersal, and because the supply of humus and the activity of microfauna create an open soil structure. Under such conditions, rainfall intensities generally do not exceed infiltration capacities and Hortonian overland flow does not occur over large areas and is restricted to portions of the catchment. Hortonian flow is, therefore, only one of the processes responsible for runoff and other physical mechanisms are necessary to explain the occurrence of runoff. Field evidence has shown that subsurface flows also play an important role in runoff generation (e.g. Dunne, 1978 and Sklash and Farvolden, 1979)

Incoming precipitation is first absorbed by the soil, and may either be stored there or move towards stream channels via several routes. If the soil or rock is deep and permeable, the water moves vertically down to the zone of saturation and then follows a curving path to the nearest stream channel. Heterogeneity of geological structure may disrupt this simple flow pattern in the groundwater zone. Some of the groundwater discharge contributes to stormflow and the antecedent baseflow to which stormflow is

added from other sources is an important factor in determining the size of flood peaks. In very permeable rock formations, the rate of subterranean water movement may be so rapid that considerable amounts of stormflow originate from the groundwater. But generally, water taking the long subsurface pathways contributes more the baseflow of a stream rather than its stormflow.

Sometimes, however, the water percolating through the soil reaches an impeding zone which is generally characterised by soil layers of lower conductivity (e.g. clayey soils), and a portion of water will be diverted horizontally and will reach the stream by a much shorter, quicker route, arriving fast enough to contribute to stormflow. Water in the unsaturated zone may flow through macropores. In some regions pipe flow can be significant, and contribute to stormflow. These pipes are open passageways in the soil and may be of any size ranging from a couple of centimetres up to a number of metres in diameter. They are commonly circular in cross section and smaller ones are often originated from animal burrows (Beven and Germann, 1982).

Subsurface discharge can also be generated by an upward movement of groundwater. This takes place when the soil becomes saturated throughout its depth, leading to water flowing through the shallow subsurface emerging from the soil surface reaching the stream channel as overland flow. This contribution is sometimes referred to as return flow.

Rainfall on saturated or near saturated areas also contributes to runoff as a fast component. The water falling onto such surfaces does not infiltrate but runs over the surface, reaching the channels very quickly. This component is generally difficult to distinguish from return flow and these two mechanisms together are referred to as saturation excess flow.

2.6 - The Contributing Area Concept

2.6.1 - Definition

The realisation of the number of different mechanisms and dynamics involved in catchment runoff generation gave rise to the contributing area concept. This is based on the division of the catchment into areas that produce runoff during a storm event and those that do not (van de Griend and Engman, 1985), which can shrink or expand depending both on the rainfall amount and on the antecedent wetness of the soil. This concept is also referred by Hewlett and Hibbert (1967) and Dunne (1978) as the 'variable source area concept'. The terms 'dynamic watershed concept' and 'partial area concept' (first applied by Betson (1964) for Hortonian runoff conditions) have also been used to refer to the same idea. This spatial delineation concept, and recognition of the variability of contributing areas, has provided the framework for using spatially distributed modelling in the prediction of the water movement and associated transport of chemical contaminants and sediment.

Although the contributing area is generally accepted as a basic concept in hydrology which has been validated in a number of field experiments and regarded as a basic approach in catchment modelling, contributing areas are difficult to identify and quantify. There are two basic problems associated with the identification and quantification of the contributing area: firstly, contributing areas are strongly dependent on hydrogeological, geomorphological, topographical and pedological conditions; secondly the characterisation of this potential runoff generation region is made even more difficult by the dynamic nature of those areas which is seasonal and varies even during storms (van de Griend and Engman, 1985).

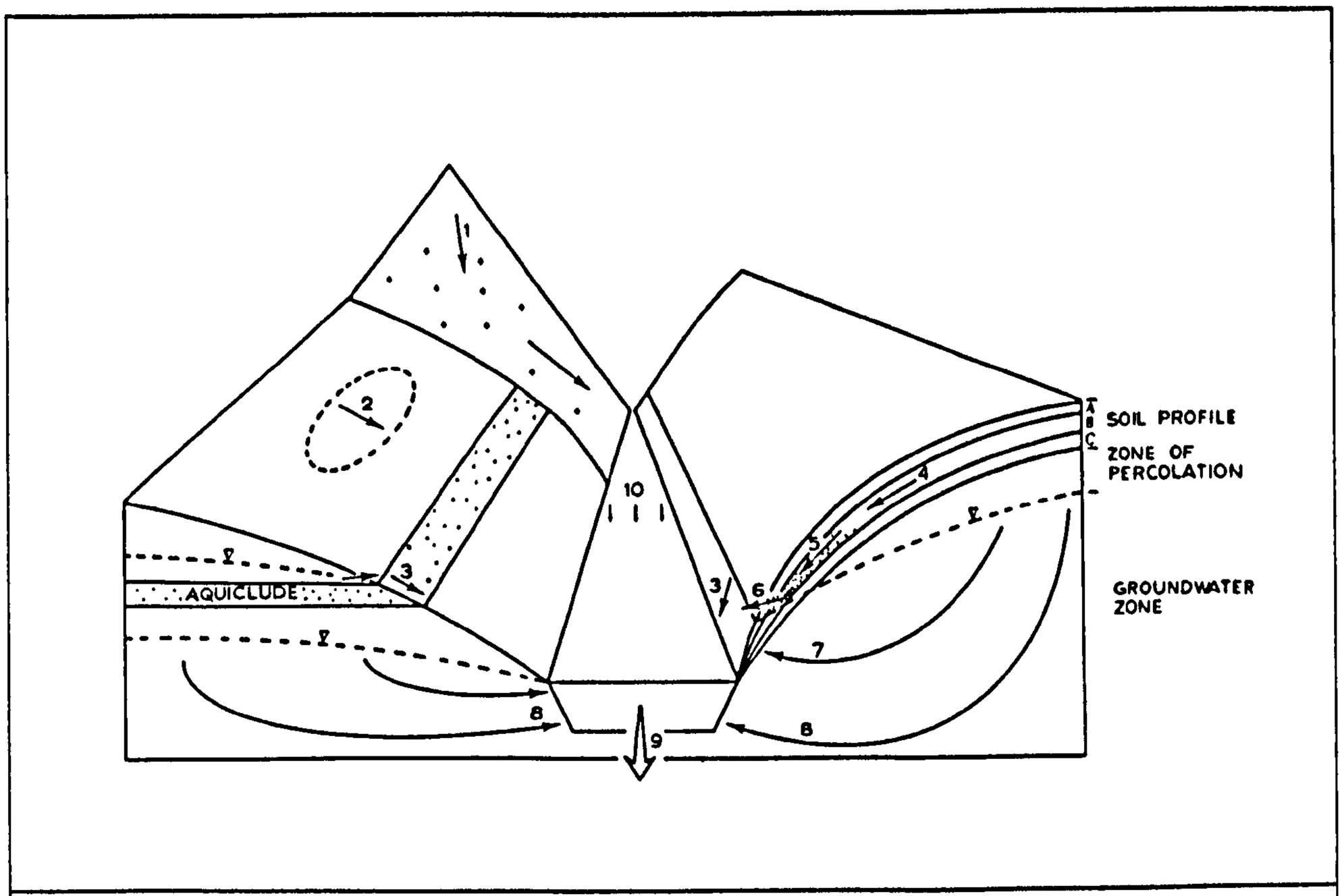

Figure 2.7 - Flow mechanisms that contribute to runoff, after van de Griend and Engman (1985)

Key for Figure 2.7 - *(1)(2) hortonian overland flow; (3) saturation overland flow; (4) unsaturated soil moisture movement; (5) saturated soil moisture movement; (6) return flow; (7) groundwater seepage flow; (8) groundwater flow; (9) turbulent channel flow; (10) direct channel precipitation.*

2.6.2 - The Contributing Area Concept and Catchment Hydrological Modelling

A very early attempt to include spatial variability into runoff modelling was made by Crawford and Linsley (1966), who represented runoff from infiltration excess in the Stanford Watershed Model using a linear distribution to describe the soil infiltration capacity and evaporation. The use of probability distribution functions (pdfs) considers the frequency of occurrence of hydrological variables (model inputs, parameters or elements) across the catchment without regard to the location of a particular occurrence within the catchment. This means that random assemblages of different parts are

considered more important than the relationship between parts. Further developments of the work by Moore and Clarke (1981), described in section 2.4.2, led to a range of new possibilities using pdf's in hydrological modelling. For example, the derivation of a spatial-temporal description of the infiltration process based on a log-normal distribution for infiltration capacity is demonstrated in Moore (1983). Later, Moore also derived expressions that consider interaction among storage elements (Moore, 1985).

Zhao et al. (1980) proposed an approach which was applied in the Xinanjiang model and uses a power distribution function for soil storage capacity,

$$F(w) = 1 - \left(1 - w/w_{\max}\right)^{bb}, \quad 0 \le w \le w_{\max} \qquad \text{eqn. (2.4)}$$

where, w is the soil storage capacity; w_{max} is the maximum storage capacity; bb is a coefficient that controls the degree of spatial variability of soil storage capacity (bb=0 implies a constant capacity over the catchment, Zhao et al. suggested that 'bb' could be interpreted as being related to the catchment topography); F(.) is the distribution function, and defines the saturated area over the catchment.

This function, presented by Zhao et al., has been implemented in the ARNO model (Todini, 1996). Soil moisture accounting in ARNO is given by the expression:

$$w(t+dt) = w(t) + P(t) - R(t) - E(t) - D(t) - I(t) \qquad \text{eqn. (2.5)}$$

where,

P(t) - rainfall

R(t) - surface runoff, generated according to the Zhao et al. expression for saturation excess overland flow

E(t) - loss through evapotranspiration

D(t) - outflow as subsurface flow (drainage)

I(t) - loss through percolation to the groundwater

w(t) was described in eqn. (2.4).

The drainage component is given by:

$$D(t) = D_{\min} \frac{w}{w_{\max}}, \; w < w_{\lim}$$

$$D(t) = D_{\min} + D_{\max}\left(\frac{w - w_{\lim}}{w_{\max} - w_{\lim}}\right)^{d\exp}, \; w \geq w_{\lim} \qquad \text{eqn. (2.6)}$$

where, D_{max} (maximum allowed drainage), D_{min} (minimum allowed drainage) and dexp are variable parameters which are determined by calibration.

The percolation abstraction only takes place for $w > w_{lim}$, and is estimated by:

$$I(t) = \frac{pp_{\max}(w - w_{\lim})}{w_{\max} - w_{\lim}} \qquad \text{eqn. (2.7)}$$

where, pp_{max} is a parameter determined by calibration.

The ARNO model also includes a detailed routing component that consider transfers both within sub-catchments and from sub-catchments towards the outlet of the catchment modelled.

Beven and Kirkby (1979) proposed the use of a topographic index, $h(x)$, to delimitate the extent of the contributing area,

$$h(x) = \ln(a / \tan b) \qquad \text{eqn. (2.8)}$$

where, a is the area drained by per unit contour length, and b is the slope of ground surface at the location. This concept has been incorporated into TOPMODEL (Beven and Kirkby, 1979 and Beven et al., 1984). The model also represents Hortonian runoff.

O'Loughlin (1981,1986) derived a criterion for delimiting saturated areas on draining hillslopes, which was also expressed in terms of a topographic index similar to the one used in TOPMODEL,

$$h'(x) = A / BM \qquad \text{eqn. (2.9)}$$

where A is the area above a reference location at the hillslope (generally associated with the slope's foot), B is the contour length, and M is the slope. The areas considered as contributing areas are those associated with the emergence of ground water at the foot of a slope or with channel expansion areas which are often due to development of perched water tables at shallow depth. This scheme was adopted by Fett et al. (1990) and also used with minor modifications by Moore and Grayson (1991) and Grayson et al. (1992).

Later versions of TOPMODEL also account for soil spatial variability, in which case the transmissivity of the subsurface zone is included in modelling. The contributing area is then predicted by a topographic-soil index, $h''(x) = \ln(a / T\tan b)$ (where T is the transmissivity of the subsurface zone). Quinn et al. (1991) demonstrated the topographic index calculation using Digital Elevation Maps (DEMs). A high index value usually indicates a wet part of the catchment which can arise from either a large drainage area (valley bottoms, convergent hollows) or very flat slopes. Areas with low index value are usually drier resulting from either steep slopes or a small drainage area.

Sivapalan et al. (1987) applied a variant of TOPMODEL which uses equations expressed in a dimensionless form. This led to the identification of five dimensionless catchment similarity parameters and three dimensionless auxiliary conditions which govern scaled storm response. The similarity parameters are: two scaled hydraulic conductivity parameters, two scaled soil moisture characteristic parameters and a scaled soil-topographic distribution parameter. Catchments are assumed to be hydrologically similar if their similarity parameters are identical or are within a pre-established range for each parameter, regardless of scale. It is suggested that a continuum representation of runoff production may be possible beyond a certain threshold spatial scale (called a representative elementary area, REA; Wood et al., 1988). This means that at scales of the order of the REA, the actual catchment with all soil and physiographic heterogeneity can be replaced with a spatially integrated representation.

2.7 - Topographic Index and Large Scale Hydrological Modelling

Famiglietti and Wood (1994a,b) proposed the macromodel TOPLATS (TOPMODEL-Based Land Atmosphere Transfer Scheme), in which the concept of the topographic-soil index is incorporated to a SVATS model, and fluxes are aggregated to larger scales in two steps, namely grid to catchment-scale and catchment to macroscale. Sivapalan et al. (1987) derived an expression for the local water table depth, z^i, in terms of the local topographic-soil index, $\ln\{(a\,T_e)/(T^i\,\tan b)\}$:

$$z^i = \bar{z} - \frac{1}{f}\left\{\ln\left(\frac{a\,T_e}{T^i\,\tan b}\right) - \lambda\right\} \qquad \text{eqn. (2.10)}$$

where,

$\bar{z}$ - catchment average water table depth,

i - local grid element index,

f - parameter that describes the exponential decay of saturated hydraulic conductivity with depth, in which, $K_s(z) = K_0\,\exp(-fz)$,

T_e - catchment average value of the saturated transmissivity coefficient (saturated hydraulic conductivity divided by f),

T^i - local value of the transmissivity coefficient, and

λ - is the catchment average value of the topographic variable $h(x)$ defined in section 2.6.2.

TOPLATS involves coupling TOPMODEL's saturation excess runoff modelling scheme with a SVATS, via a common variable, depth to the water table (determined by eqn. 2.10). The resulting model is then applied to catchment sub-grids. Both saturation and infiltration excess (modelled by the SVATS model) are represented in the runoff modelling. The aggregation scheme 'grid to catchment scale' considers that root-zone soil moisture content spatial variability (sub-grid) is dominant among other variables that control grid-scale water and energy balance. To model this soil moisture dynamics, it is assumed that the redistribution of soil water is dominated by the variations in topographic-soil index spatial distribution which can be represented either by a

probability density function or by its sample histogram. To perform the water and energy balance, the distribution of the topographic-soil index is sub-divided into a number of intervals and the SVATS applied to each of these intervals. This procedure involves the concept of similarity in the REA approach, described in section 2.6.2. The macroscale hydrological fluxes are the result of the weight average of these patch area fluxes.

Very recent work has, however, been analysing the extent of the physical realism in TOPMODEL assumptions and parameterisation. Moore and Thompson (1996) suggested, based on some observations made on a shallow forest soil, that it might be that the contributing area modelling in TOPMODEL is not applicable for the whole catchment and for any landscape, but should be limited to specific parts of the hillslope, and/or landscapes. They suggested an extension to TOPMODEL conceptualisation of runoff generation by constructing a two-zone catchment model; one for upslope flows and the other for lower slope zones.

Franchini et al. (1996) performed a sensitivity analysis of TOPMODEL's parameterisation applying it to a number of catchments in Italy and one in France. Parameters were calibrated by trial and error, and generally quite good agreement with observed discharge was obtained. However, results showed limited sensitivity to the actual catchment index curve (contributing area versus topographic index). Different DEM grid sizes, ranging from 60x60m to 480x480m, were considered. It was verified that the index curve and the values of parameter K_0 (saturated hydraulic conductivity) were both affected greatly by the size of the DEM grid. Furthermore, K_0 may sometimes assume unrealistically high values, looking unrealistic. As a result of this, runoff originating from infiltration excess is underestimated. This affects both the interflow regime and, together with parameter f ($T_0 = K_0/f$), the flow exchange between the unsaturated and saturated zones, thus leading to high values of percolation which always cause the soil surface to dry out.

2.8 - Probability Distribution Function and Large Scale Hydrological Modelling

Spatial distribution functions have been used in catchment scale hydrological models (as described in section 2.4). This is a common approach in the literature, to represent spatial distribution in modelling. Johnson et al. (1993) introduced land-surface hydrology parameterisation with sub-grid spatial variability (as derived by Entekhabi and Eagleson, 1989) in the NASA Goddard Institute for Space Studies GCM. Precipitation intensity over a fraction κ of the grid is considered to be exponentially distributed and near-surface soil saturation is taken to be distributed according to a gamma probability function. Surface runoff is represented by two different generating processes: infiltration and saturation excess. Infiltration is simulated using the Darcy equation for steady vertical flow in porous media. Evaporation is accounted by;

$$E = \beta E_p$$

(see eqn. (2.2) section 2.1.3) and a probability distribution function was derived to represent β. There are uncertainties in the determination of some parameters introduced into the new modelling scheme, e.g. κ. However, results from the model showed that introducing spatial variability improved the predictions at the cost of an increase of 10% in the CPU (Computing central Processing Unit) usage.

Eltahir and Bras (1993) proposed an interception modelling scheme which combines the Rutter model and a statistical description of the spatial variability in rainfall and canopy storage. It is assumed that rainfall and canopy storage capacity follow an exponential probability density function. It was also assumed that the distribution of canopy storage is independent from the distribution of rainfall. It was found that this new scheme enhanced the representation of interception compared with the original Rutter model, a simple BATS model scheme and the interception scheme described in Shuttleworth, 1988b (in which rainfall is assumed to be exponentially distributed but the canopy storage is assumed constant in space).

In early stages of this work the possibility of using ARNO modelling scheme as the land-surface component of an MHM was considered. Dümenil and Todini (1992) incorporated ARNO modelling scheme into the Hamburg OGCM (Coupled Ocean and GCM model) using a functional relationship between soil storage capacity and

topographic slope to obtain regionalisation of parameters at the GCM scale. Although rainfall was not considered spatially distributed and there was no attempt to differentiate other model parameters between grid squares, the version of the model incorporating ARNO as the land-surface scheme appeared to generate sensible results. Wood et al. (1991) compared different large scale land surface parameterisations, including a scheme using the Xinanjiang runoff expression, and concluded that the introduction of spatial variability led to more dynamic and realistic short-term variations in soil moisture. Moreover, they also highlighted the importance of the introduction of an explicit baseflow component, which was found to generate more realistic simulations for between-storm runoff.

ARNO includes a drainage component, eqn. (2.7). Nevertheless, it involves the calibration of four arbitrary parameters and is formulated using a threshold structure (which as has been discussed in section 2.4 may cause problems for parameter calibration). A study was carried out, therefore, to investigate this scheme. The study involved elements of recession analysis and aimed at establishing a new equation for the drainage component. Tallaksen (1995) presented a review on recession analysis. Drainage is taken here in a wide context, intending to represent the contribution of both the unsaturated and saturated zones to streamflow.

The recession analysis was based on hourly observed discharge rates for Featherstone and Alston, both sub-catchments of the Tyne river basin, in Northeast England. The hydrographs for this analysis were selected from extended dry periods, with little or no precipitation. The water available for drainage, i.e. catchment storage, was determined by integrating the recession curve, assuming storage was equal to zero for the last time step of the interval analysed. Evaporation rates were given from SHE simulations and were forced into the model.

A new drainage equation analogous to ϕ (eqn. 2.3) was obtained by regression using the integrated storages and corresponding discharges. In the regression analysis, all recession segments were arbitrarily shifted together, to form a characteristic recession. The new drainage function is then a hyperbolic-form function which fitted very well to the data. More detail on this study is given in Appendix A.

This new modelling scheme has simplified the parameter choice compared with the original drainage scheme in ARNO. The new function has the advantage of being continuous and overcomes the problems caused by threshold structures in conceptual models (discussed in section 2.4). The new drainage approach was then put together with the Xinanjiang runoff function and some simulations were carried out using evaporation given by the SHE model. Although this approach was not tested extensively, some parameter sensitivity problems were identified in the Zhao function. A priori, this would make difficult the association of the parameters to catchment physiographic characteristics, which is important if the model is to be used to predict future climate. This study, however, needs to be further extended using other catchments and other data sets before these results can be generalised.

2.9 - Data Requirements and Availability

2.9.1 - Introduction

The data required for MHMs (Macroscale Hydrological Models) do not differ significantly from the data needed in other hydrological applications. However it is likely that, due to the scale on which such models are designed to operate, large data bases need to be developed. A number of experiments particularly focused on hydrology (e.g. HAPEX and FIFE) are currently underway, providing valuable data for MHMs. Data are required for MHMs for three different purposes: model development, model initialisation and model validation. Table 2.2 shows the types of data required for each of these modelling phases (Arnell, 1993).

Table 2.2 - Data requirements for MIIMs, adapted from Arnell (1993)

Data type	Modelling purpose		
	Development	Initialisation & operation	Validation
Physiographic data	x	x	
Dynamic properties	x	x	
Climatological data	x	x	x
Hydrological data	x	x	x

2.9.2 - Data Types Required

Physiographic data

These data are constant in time and include topographic information and soil properties. They are fundamental for developing and operating an MHM. The basic source of topographic data for MHMs are Digital Elevation Models (DEMs) which consist of a digitised database of elevations. DEMs can be constructed from topographic maps, digitised contours, stereo aerial photographs, satellite images or from satellite altimetric or interferometric data. High resolution DEMs with a grid spacing of 50m or less are available for some countries. It is, however, unlikely that these data would be readily available for less developed countries. High resolution DEMs can be applied to automatically define hill and channel slopes, catchment boundaries and stream flow directions. Information about river networks can be added to DEMs to improve the representation of these features. This information can be useful for runoff estimation and routing.

Soil properties needed in MHMs include porosity, saturated hydraulic conductivity, and soil hydraulic conductivity and retention functions, which are obtained from field measurements. It is also important to consider the possibility of estimating these properties from soil texture data using pedofunctions (e.g. Saxton et al., 1986 or Rawls and Brakensiek, 1989). At the global scale, the FAO/UNESCO Soil Map of the World (FAO/UNESCO, 1974) shows the distribution of a number of soil types each of which can be associated to a number of soil properties including typical values for field capacity and saturation capacity plus characteristics that can be associated to soil texture (Vorösmarty et al., 1989). The scale of these maps is, however, very coarse. An IGBP project is currently under development to derive a new global soil data base which would be more useful for high-resolution modelling (Arnell, 1993). In the case of an MHM to be applied linked with an atmospheric model, there is also a need for estimates of properties such as albedo, heat capacity and thermal conductivity, which are necessary for modelling energy exchange and its effect on evaporation.

Dynamic properties

Dynamic properties are necessary for development, initialisation and operation of MHMs. Some soil properties, such as infiltration capacity, may change with time due to cracking and crust formation as a result of variation in soil moisture content. Ideally MHMs should be able to simulate fully the dynamics of the soil properties.

Vegetation cover may also vary with time. MHMs require information both on vegetation interception capacity, and the plant characteristics that regulate the release of water through leaves and soil uptake. Some of these characteristics can be determined in the laboratory, or from detailed field experiments, or estimated from physically-based evapotranspiration models that are calibrated against field data. There are global vegetation maps at coarse resolution but MHMs need detailed data sets. Spatial distribution can also be acquired through remote sensing, resulting in higher resolution maps.

Climatological data

Climatological data are the driving forces for MHMs. They include precipitation and the meteorological observations needed to estimate evaporation (such as net radiation, temperature, wind speed, humidity). The key issue with climatological data is in matching the correct spatial and temporal scale for MHMs. When MHMs are operated on their own it will be necessary to develop tools to spatially interpolate the observed data, to replace information which would otherwise come from another model. The simplest way to achieve this is to consider only the distances between observation points (as in the Thiessen polygons method). However, more sophisticated correlation methods can be applied. Another possibility is to use data provided by weather radar which allows rainfall to be estimated with high spatial and temporal resolution. Remote satellite-based systems can also be used to estimate climatological data. Holwill and Stewart (1992), for example, used thermal infrared data to estimate the brightness temperature which can then be correlated with ground measurements to estimate the surface temperature.

MHMs should also be able to be run in conjunction with atmospheric models, in which case, generation of climatological inputs is likely to require a special approach. Atmospheric models running as climate models work on a much larger scale than MHMs and some method to improve the resolution of the variables that are to be forced into MHMs is therefore necessary. One way that more spatial detail can be added is to distribute the climatic variables according to an appropriate probability distribution function (e.g. Entekhabi and Eagleson, 1989 and Johnson et al., 1993). Other possibilities involve either developing spatial patterns using land-surface features which interface with geographically-distributed hydrological models or, stochastic modelling techniques (e.g. Neyman-Scott model; Cowpertwait et al., 1996).

Hydrological data

River discharge, groundwater levels, and soil moisture contents are needed in all three phases. River discharge is generally used for validation and is usually readily available. Hydrological models are frequently tested by their performance in estimating the river flow at a fixed controlling point, generally located at the basin's outlet. Groundwater levels and soil moisture content are needed both for model initialisation and validation. Groundwater levels are obtained from observational wells spatially distributed across catchments. These wells are not widespread, and are not found in all basins. From groundwater levels, subsurface fluxes and gradients can be estimated. Moreover, groundwater levels delimit the depth of the soil unsaturated zone. It is important to initialise the model with physically meaningful variables as this shortens the model initialisation period. Soil moisture contents are even less widely available than other soil and groundwater data.

2.9.3 - Estimation of Soil Moisture Content using Remotely Sensed Data

Spatial fields of soil moisture content can be determined based on remotely sensed measurements which depend on reflected and emitted radiation. Current procedures only allow determination of soil moisture content for the soil top layer. Estimation of soil moisture content is focused on three regions of the radiation spectrum: **γ-rays** (gamma radiation); **thermal infrared** (8 - 14 μm, consisting of the measurement

of diurnal surface temperature or crop canopy temperature); and **microwave** (1 - 50 cm) which may be either **active** (consisting of measurement of the radar back scatter coefficient) or **passive** (consisting of the measurement of the microwave emission or brightness temperature).

The gamma radiation technique is based on detecting the difference between the natural terrestrial gamma radiation flux for wet and dry soils. The presence of water in the upper soil layers increases the attenuation of the gamma radiation from below; thus the flux is less for wet soils then for dry soils. Quantitative estimates of soil moisture require calibration flight lines to determine a background soil moisture value and a background gamma count rate. Because the atmosphere also attenuates the gamma radiation flux from the soil this approach is limited to aircraft flying at 100-200 m. The spatial resolution for a 150m flight altitude is 250m.

Surface temperature (thermal infrared technique) is primarily dependent upon the thermal inertia of the soil which is dependent upon both the thermal conductivity and the heat capacity, and increases with soil moisture (Price, 1982). The thermal inertia represents the ability to absorb and transmit heat, which is a function of both soil matrix properties and soil moisture content. By measuring the amplitude of the diurnal temperature change, a relationship can be found between the temperature change and the soil moisture content.

Much research has been done in this area, especially following the Heat Capacity Mapping Mission in 1978. One of the principal investigations in the mission was made by European scientists through the 'Tellus' project, sponsored by the Joint Research Centre of the European Economic Community whose specific objective was to map diurnal soil temperature variations so that, by correlation with ground samples, thermal inertia models could be developed for the prediction of variations in soil moisture content. The principle adopted was that soils of high water content would show lower diurnal variations in surface temperature than drier soils. This technique is strongly affected by cloud cover and vegetation.

In the case of microwave techniques the sensors are not affected by cloud cover. The theoretical basis for measuring soil moisture by microwave techniques is based on the large contrast between the dielectric properties of liquid water and dry soil. For the

passive microwave sensing, a radiometer measures the intensity of emission from the soil surface. This emission is proportional to the product of the surface temperature and the surface emissivity which is commonly referred to as the microwave brightness temperature (TB). The measurement of brightness temperature and consequently the emissivity, is dependent on soil texture, surface roughness and any vegetation present, so actual soil moisture is usually empirically related to TB using ground data.

In the case of active microwave sensing, a pulse at a specific frequency is emitted by a radar and the back scatter energy is detected. This is given by a scattering coefficient, σo, which is highly correlated with the moisture content of the top 5cm of the soil. This coefficient is made up of backscatter from vegetation, soil and the attenuation caused by the vegetation canopy. A relationship can be established with the soil moisture content and surface roughness and although the coefficients of this relationship are known to vary with the wave length, polarisation and incidence angle, there is no satisfactory theoretical model to estimate each term independently. So an empirical relationship with ground data is generally required, as in the case of the passive microwave.

Both techniques, passive and active, are very similar and usually need calibration against ground data. The passive approach appears to be less affected by surface roughness and overlying vegetation, but as distance from the target increases a serious degradation in spatial resolution is observed. This contrasts with active systems using the synthetic aperture concept which have a spatial resolution independent of sensor altitude. Methods for improving the resolution and attenuating the effects of vegetation have been studied by several researchers.

An additional approach to the use of microwaves is through change detection. This can be used for both passive and active microwave data. The change detection method reflects the change of target variables such as soil texture, roughness and vegetation because these tend to change slowly, if it all, over time. It is simply assumed that the only target variable changing is soil moisture content and for most hydrological applications the changes in soil moisture content are more important than the actual absolute value of soil moisture content (Engman and Gurney, 1991).

Theis et al. (1984) demonstrated the use of visible and infrared data to calculate a perpendicular vegetation index (PVI), which in turn was used to correct the emissivity determined with a passive microwave radiometer. This suggests the possibility of a total satellite remote sensing approach for determining soil moisture without any ground sampling.

Remote sensing of soil moisture content has been shown successful mainly in regard to the soil top-layer. Recently, however, Ragab (1995) has shown new possibilities of using top soil moisture content to predict soil moisture content in deeper soil layers.

2.9.4 - Monitoring the Runoff Contributing Area using Remotely Sensed Data

Soil moisture states are closely related to runoff production and the ability of a model to correctly represent the spatial pattern of soil moisture content translates into its performance for estimating runoff. Runoff cannot be directly measured using remote sensing techniques, but, as the surface overland flow is highly dependent on the actual moisture content of the soil, establishing a threshold and monitoring the moisture content of the soil may allow the contributing area to be mapped. Runoff is an areal phenomenon and remote sensing measurements of surface soil moisture content could define the dynamic nature or range of the size of contributing areas. The dynamic aspect of the source areas can be defined by making measurements before, during and immediately after runoff-producing rains and by collecting data at various times through the year.

The main problem in the use of remote sensing to identify contributing areas is associated with the temporal and spatial resolution that can be achieved. For thermal infrared sensing, the temporal discretization will be poor for LANDSAT data, as there will be 16 days of lag between successive measurements. Additionally, the spatial resolution is 120x120m (using data from LANDSAT 5 thermal infrared band 6 - 10.40 to 12.50 μm), which is too large for the detection of contributing areas (van de Griend and Engman, 1985). The same is true for gamma radiation sensing in which the resolution is only 250m for a flight at an altitude of 150m.

Engman et al. (1983) reported results from a passive L-band radiometer mounted on an aeroplane as part of an experiment conducted to define saturated soil moisture

conditions for a small (7.8 km^2) basin in Minnesota, USA. As expected, the sensitivity to surface conditions increased for the low altitude data collection. The ground surface resolution for this altitude was 60m and thus it was not suitable for detecting the changes in soil moisture content adjacent to streams. Topography effectively changes the incidence angle and thus the microwave measurement. van de Griend and Engman (1985) suggested that as many of the basins where contributing area research has been conducted have rather abrupt changes in slope and elevation and as partial-area hydrology seemed to be related to topography some procedure for normalising data to a plane surface should be developed and used in these cases. This may be a complex procedure involving the use of topographic data and, spatial resolution or other characteristics of the sensor.

Active microwave or radar may be more sensitive to topographic changes than passive systems and can be used in such a way as to minimise the effects of vegetation and surface roughness. Brun et al. (1990) reported results of a physical simulation of the European Earth Resources Satellite (ERS 1) for contributing area hydrology approach. The configurations of the radar were reproduced and a flight 350m high was undertaken in order to reproduce the spatial resolution given by the satellite (30x30 m). A C-band scatterometer was used to avoid effects of absorption or diffusion from the canopy (Jackson and Schmugge, 1981). The experimental area was a small site (2.3 km^2) in a catchment of 10 km^2 in western France which was characterised by gentle, concave slopes of less than 5%, a variety of vegetation canopies, bare soil, annual crops and grass lands. The soils are deep silty loam. Measurements were taken during three days and samples were taken from the top 2 cm of the soil. Gravimetric water content of the samples was determined and used in both the calibration of the radar and to generate a map of soil surface moisture content. Additionally, the interface between the saturated zone around the river and the surrounding unsaturated zone was determined by field mapping of the interface.

Although for the time of the year (autumn and winter) saturation conditions were expected, results were quite reasonable considering the small number of flights, plot positions and days sampled. Another advantage of this approach is that ERS 1 has a 3 day repeat cycle, guaranteeing good temporal resolution. This can be useful as a tool to monitor the contributing area and validate actual hydrological models that consider this concept for runoff modelling.

Apart from this type of application, remotely sensed data can also be used to indirectly determine potential runoff areas by sensing other phenomena or features of the landscape (e.g. topography, geomorphology, vegetation) that are indicative of runoff.

2.10 - Discussion and Conclusions: The Need for a New Approach

GCMs (General Circulation Models) have been used to predict the effects on the climate of the build up in concentration of the greenhouse gases in the atmosphere. GCMs generally operate on large grid squares of the order of hundreds of kilometres and land-surface processes are generally represented using a lumped approach. Land-surface processes play an important role in the energy balance. The way energy loss from the land surface is partitioned between latent and sensible heat is highly dependent on the amount of water stored in the soil layer. However, most modelling schemes overlook spatial variability and do not account for lateral transfers of water between grids. Runoff is calculated from a water budget and transferred directly to the nearest ocean grid point.

SVATS and BATS have proved to be more realistic than the simple lumped soil reservoir still in place in many GCMs. However, SVATS and BATS are essentially vertical approaches. There is in reality a gap between the vertical (profile) detail included in the model and its spatial representation. Another problem with these models is the number of parameters to be calibrated, and also their representation of runoff. Most, if not all, SVATS and BATS account only for runoff generated by infiltration excess which is partly related to their profile point-based (plot) representation. As reviewed in section 2.5, Hortonian overland flow is more frequently observed in arid and semi-arid regions or is restricted to small portions of the catchment, where, for example, forests have been cut. Subsurface flow also plays an important role in generating runoff and this is not accounted for in SVATS and BATS. The subsurface contribution to runoff is more spatially-associated (it is an areal phenomenon). In addition, although it is also a 'fast' component, it operates on different time scales from infiltration excess runoff.

Although actual GCM predictions are useful to show the possible consequences of global warming and how the climate system is sensitive to land-surface representation, in absolute terms, these predictions might not be fully accurate. One way of improving the spatial representation in GCMs is by increasing the model's resolution. However, land

surface processes cover a range of spatial-temporal scales. Spatially these may go down to the size of a hillslope and actual computer power is a practical constraint when bringing the resolution of GCMs down to the small catchment or hillslope scale.

Recent work has introduced the use of statistical distribution functions to represent spatial variability in GCMs. Although results have been encouraging, there are some underlying simplifying assumptions that may jeopardise the use of these models for future climate forecasts. Generally, these approaches are designed assuming that variables are independent and also land-surface feedbacks are not taken into consideration (Moore et al., 1991). Moreover, as the number of variables or processes for which distribution functions are incorporated increases, models also increase in complexity. A fully spatially distributed system may become very complex. Johnson et al. (1993) reported increases of up to 10% CPU (Computing Central Processing Unit) time when a distributed function is introduced into runoff modelling.

One way of bridging the gap between scales is designing land surface schemes to operate at an intermediate scale. In the case of hydrology, this would mean going up to scales larger than the small catchments which are normally applied in hydrological studies. In the case of GCMs this means increasing resolution to the scale usually applied in weather forecast models (meso-scale, 10 km grid approximately).

Vorösmarty et al. (1993) suggested a structural approach for MHMs, in which the model could be viewed as hierarchical structures with finer scale, site-specific submodules interacting with simulations over broader domains. The GCM outputs within a particular simulation time step when using this approach serve as boundary or initial conditions or both for the higher resolution model nested within it. Table 2.3 shows the scales and resolution for this multiple scale structure. The coarsest scale level serves as an integrator of the numerous sub-scales effects, and the link between the GCM and the macroscale hydrologic model is interactive, as the simulation in the GCM progresses inputs to the macroscale hydrological model are updated. This configuration seeks to extract and identify the impacts of global climate change down to the regional and local levels, while simultaneously propagating physically valid dynamics towards larger scales. Figure 2.8 illustrates the approach.

This approach has the advantage of allowing land-surface feedbacks to be accounted for in the atmospheric model simulation and vice-versa. The macroscale hydrological model would have to incorporate in some way the dynamics of the land-surface processes that take place within the small catchment. One way of approaching this problem, which involves both a range of different scales and the tied issue of spatial variability, is looking for patterns.

Table 2.3 - Scales and resolutions for multiple scale analysis, after Vorösmarty et al. (1993)

Scale	Model	Boundary	Resolution	
			Atmosphere	Hydrology
Continental	Linked GCM-MHM	Interactive in GCM	≥ 100 km (sub hourly)	10-50 km (weekly to monthly)
Meso-scale (regional)	Linked Meso-MHM	Prescribed or interactive in nested GCM	10-50 km (minutes)	1-10 km (daily)
Local	Hillslope - small catchment	Topographically determined	Prescribed point forcings (sub daily)	≤ km (sub daily)

Different classification schemes have been applied in hydrological modelling to search for similarities in the catchment hydrological behaviour. Kouwen et al. (1993) proposed the GRU (Group Response Unit, section 2.4) which prioritises vegetation in the definition of the similar hydrologic units. Vorösmarty et al. (1989) proposed a scheme that is based on the relationship between vegetation types and the underlying soil texture characteristics. Sivapalan et al. (1987) proposed the use of the REA (Representative Elementary Area, section 2.6) based on the soil-topographic index concept. However, all these approaches contain some simplifications about the relevance of each surface feature in the catchment general hydrological behaviour. However it seems that ideally, if there is no physical evidence that one feature is more relevant than another, a system of land-surface classification should take into account as much of the available information as possible.

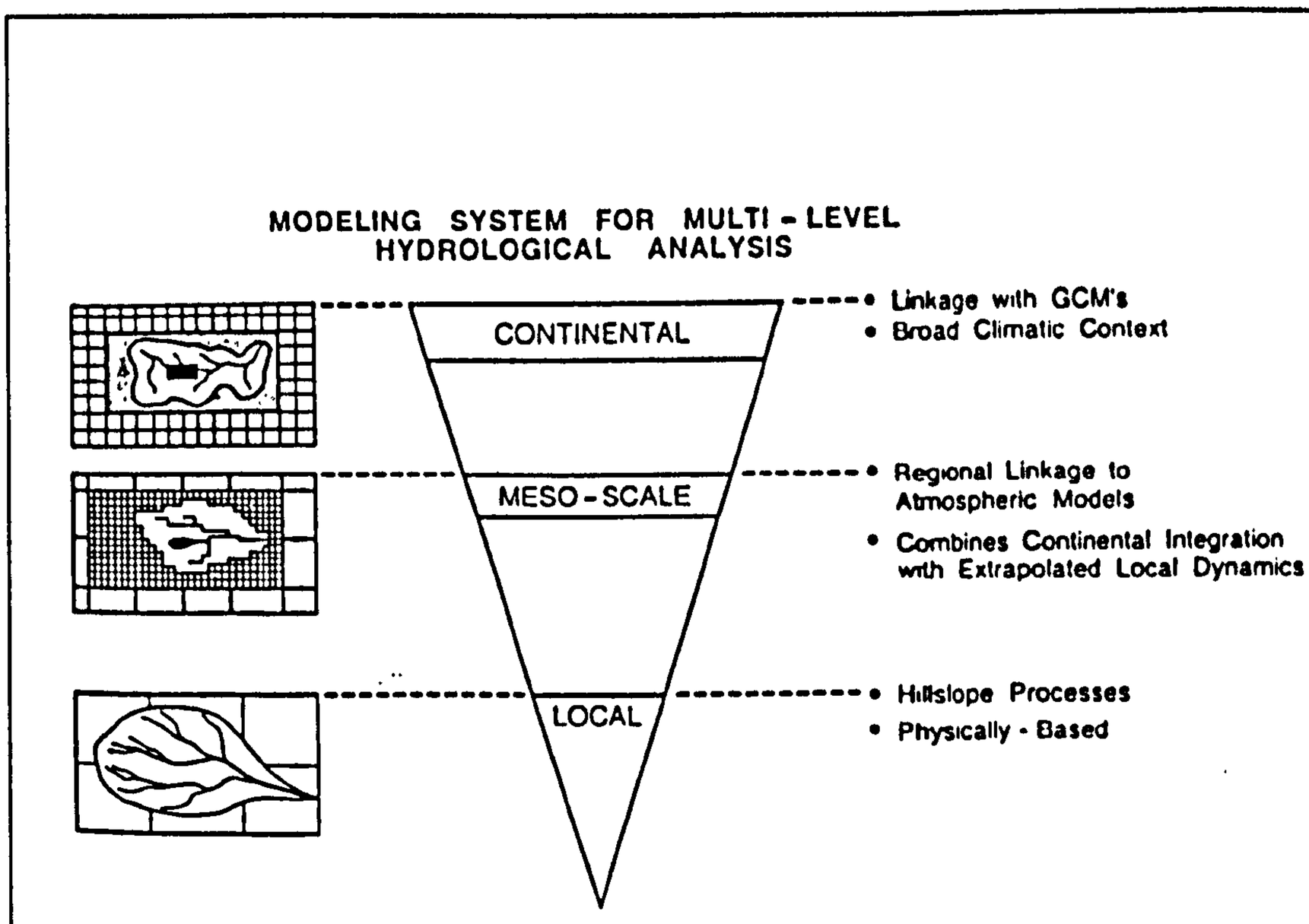

Figure 2.8 - Strategy to develop linked atmosphere-macrohydrology models, after Vorösmarty et al. (1993)

As these similar units or small catchments are defined, there is then a need to establish a hydrological modelling approach suitable for the small unit or catchment scale. It is desirable that this approach associates variables and parameters measured or observed at the local (point- or plot-based) scale to those values at the small unit or catchment scale, thus closing the gap at the lower bound of the scales range.

A number of hydrological approaches have been reviewed, some of these have already been incorporated into large scale hydrologic models. Conceptual models have the advantage of a simple structure. However, the determination of parameters is not straightforward, and in most models the parameters are not directly connected to physiographic catchment features. This last characteristic makes these approaches unsuitable for land use and climate change studies. In contrast, physically-based approaches have been built partly to support land use change studies at the catchment scale, but are demanding to set up. They require large data sets which are not always

available world-wide and are computationally very expensive. Kite (1994) applied a hydrologically distributed model to GRUs (similar units according to vegetation) of a proposed continental model. However, the parameters of the hydrological model need calibration, and are not explicitly associated to land-surface features, which is a problem when predicting effects of land use and climate change. Becker (1992) suggested that, ideally, hydrological models for the large scale should combine the simplicity of conceptual approaches and the physical meaning and realism of physically-based modelling.

Initially, the new generation of conceptual models that embody land-surface spatial variability representation would seem suitable for the task. The TOPMODEL soil-topographic index represents spatial variability and allows for a link between model parameters and soil-topographic features. This concept has been incorporated in the macromodel TOPLATS (Famiglietti and Wood, 1994 a,b). However, very recent research (Franchini et al., 1996), has reported problems of identifiability on the topographic-index curve and associated model parameters. These results may introduce uncertainty to approaches such as TOPLATS, as the model relies on water table levels predicted by TOPMODEL whose parameterisation have been identified by Franchini et al. (1996) to assume sometimes unphysical parameter values. Apart from this, some field experimental evidence has led to the conclusion that some of the assumptions in TOPMODEL are limited to certain types of hillslope (Moore and Thompson, 1996).

Probability distribution function approaches also brought spatial distribution into hydrological modelling. Models such as ARNO have been applied successfully in a range of areas. ARNO incorporates a power distribution function into the runoff generation scheme proposed by Zhao et al. (1980) and embodies a very detailed routing modelling scheme. In early stages of this research, a new drainage modelling approach was designed to enhance the original ARNO scheme. Some trials were carried out using data from the Tyne basin, Northeast England. Although the approach was not tested extensively, identifiability problems related to some of the parameters in the Zhao runoff function were found. In addition to this, there is also the problem of relating ARNO parameters to catchment physical attributes. Zhao et al. (1980) suggested that 'bb', the runoff function's power exponent could be related to the catchment topography (section 2.6). However, at first, this link seems to be somewhat unclear. This issue brings in the question of *scaling up* or *scaling down* in large scale hydrology ?

Vorösmarty et al. (1993) indicate that the interaction between GCMs and MHMs does not have to be necessarily of the 'top-down' type. They suggest the possibility of propagating the physical local dynamics up to the larger scales, thus creating a coupled 'top-down' and 'bottom-up' linkage between the various models.

The 'top-down' approach, if applied to the scale range of small-catchment to point, involves connecting variables and parameters encountered for the catchment as a whole to local characteristics (e.g. expression relating the average water table depth to local values, Sivapalan et al., 1987). Nevertheless, the observation of physical processes are more associated to the local or point-based scale. In addition, parameters need to be sensitive to changes that are observed at the scale where phenomena are observed in order to be able to incorporate the effects of change. Following this it seems more natural to use the local scale as a starting point; which means instead of a scaling down procedure looking for a scaling up scheme. Although those in favour of scaling down (e.g. Beven, 1995) would advocate that the link between these parameters and local characteristics is implicit (as the chosen parameters set are able to represent the average catchment behaviour), the task of looking for an effective procedure to go downwards and identify the surface features which are responsible for a certain average value does not seem trivial. Apart from this, well established physical laws, such as the Darcy flow equation for porous media, have been established from laboratory and column-based field observations and therefore it seems more appropriate to start from here and build up to larger scales.

The central problem in going up across scales is how to aggregate the acquired local information on the larger scale. From the systematic analysis discussed in King (1991) it seems that the fully analytical integration approach would be the most adequate when searching for physical-meaning to be incorporated into modelling. However, the numerical problem of deriving all expressions, if possible, seems to be too complex. Nevertheless, the most simple approaches rely on linearity of the underlying smaller scale modelling scheme and this is seldom verified in land-surface processes.

One way of approaching the problem is by searching for simplified modelling schemes that may not be valid for the overall system but that approach transient stages bounded by realistic initial and boundary conditions of the underlying system keeping physical realism. Kuhnel et al. (1991) discussed the concept of partial analysis, in which

a determined process can be represented by different stages of the whole system, and for each of these stages a more simple relationship than the full representation of the overall system may be found. In the case of evaporation different stages can be defined by analysing the phase in which evaporation is soil-controlled, atmosphere controlled and so on. More recently, Wang and Dooge (1994) pointed out that in the case of the Richards' equation, for example, there are a variety of simplified solutions that, while limited, bound the solutions for real soils.

Thus, based on the discussion above a set of basic requirements for a new approach in large scale hydrologic modelling have been established:

- Ideally, a large scale hydrological model should incorporate as much physical realism as possible. As reviewed, heterogeneity representation, and runoff and lateral transfers modelling are weak points in actual large scale land-atmosphere schemes that need to be enhanced. On accounting for land-surface/atmosphere interactions, the model should be able to represent feedback. The nested approached discussed by Vorösmarty seems to be appropriate for this.

- The nested approach requires large amounts of data and information at a variety of scales, for which large data bases are required. When developing these data bases, it is important to have good spatial-temporal resolution, and the system should allow growth; the data base may need to be frequently updated with new information. Moreover, systems to interpret, classify and seek patterns across the landscape are required. As this approach covers a variety of scales, systems to aggregate and disaggregate data sets are necessary.

- A new hydrological modelling approach is required for the similar units with size equivalent to small catchments. It should, while bearing physical meaning, avoid complex approaches, excessive computing-time and be simple to set up. Hydrological conceptual models have simple structure and are relatively easy to operate. Their descriptive view of the hydrological cycle, which represents named phases of the process, such as infiltration, groundwater recharge, saturated flow, etc. could well be incorporated on these sub-elements of the large scale hydrological model. However, there are problems associated with model parameters in conceptual models that mean

they may not to be immediately suitable for the task of predicting climate and land-use change. Model parameters should be associated with physical characteristics and, if possible, be directly measurable in the field or able to be evaluated from maps or remote observation systems; thus avoiding extensive parameter calibration. Moreover, the model should be sensitive to these parameters in order to be able to simulate the effects of change.

- Although fully physically-based models bear enough physical detail, they are very demanding to run. To design these new modelling schemes partial and transient analysis can be useful to produce schemes which, although simple, have a physically sound basis.

- In designing this new approach the amount of information and data that are reasonably widely available for developing, validating and applying the model should be taken into consideration.

- A land-surface and channel routing system and a large scale groundwater model should be developed to represent the lateral transfers between the sub-elements of the large scale hydrological modelling system. In addition, the understanding of flow pathways and residence times can help explain hydrochemical fluxes.

CHAPTER 3

The UP Macromodel

3.1 - Introduction

The UP (Upscaled Physically-based) macromodel developed by the Water Resource Systems Research Unit (WRSRU), University of Newcastle, was designed to simulate hydrological and transport process at a range of spatial scales from 10^2 to 10^6 km^2 and over time scales from 1 to 1000 years. It is intended for simulations of land surface processes including the effects of land use and climate change. It was designed to run on its own, with meteorological data as input, or in conjunction with atmospheric models. It is intended that UP will be coupled to the UK Meteorological Office Unified (atmospheric) model, and run at the meso-scale, as a state-of-the-art coupled atmospheric/hydrological model (as conceptualised by Vorösmarty et al. (1993) and described in section 2.10).

The model has been designed bearing in mind the basic requirements discussed in section 2.10. These can be summarised as:

- all aspects of the model should have a physical interpretation;
- the model should mainly represent explicit named physical processes (e.g. exfiltration, groundwater recharge);
- parameters should be measurable or derived based on physical features (e.g. topography, mapped river networks, land cover, soil type, etc.), minimising the need for calibration, and also be sensitive to environmental change;
- the required data should be, as far as possible, globally available;
- the model should be computationally efficient, fast and simple to run.

The data required to run UP are relatively simple, comprising hydrometeorological time series, land cover maps, digital elevation maps (given by Digital Elevation Models, DEMs), subsurface hydraulic characteristics often derived from geological maps, and mapped river networks.

For running UP, the catchment or region to be modelled is divided into sub-areas. Each of these sub-areas is represented by a single UP element (Figure 3.1). The sub-areas can be defined hydrologically, as sub-catchments or, arbitrarily as grid squares. Horizontal transfers across the landscape are represented by the overland flow (surface water subgrid routing) and channel routing (main channel intergrid routing, which includes groundwater transfers) modules.

In this chapter some of the features in the UP modelling scheme are briefly introduced to give the reader the necessary background for understanding the groundwater recharge modelling approach for UP which is developed later in this thesis.

3.2 - Overland Flow and Channel Routing Representation

Overland flow is described using sub-grid transfer functions, which are established based on results from a simple two-dimensional overland flow model. This overland flow routing representation enables the spatial variability in surface flow velocities to be accounted for explicitly. Surface water is assumed to accumulate in rills and ditches and travel to the river with a velocity that is locally dependent both on land cover and slope. It is intended that the two-dimensional flow fields used in creating the transfer functions will be used in the UP model contaminant transport component.

Surface water is assumed to travel towards a neighbouring river channel and, consists of rainfall falling over saturated areas plus exfiltrated water from the subsurface. When developing the transfer function for incident rainfall, the saturated area is split into pixels using a fine grid and a unit of water is routed from each pixel to the river channel using a velocity field. Then, the travel times are collated to construct a transfer function for a uniformly distributed unit pulse of rain incident on the saturated contributing area.

For exfiltration areas, the transfer function for routing a unit pulse to the river is derived by routing numerical fractions (water volumes) which are proportional to the exfiltration rate from each pixel. At any time the current groundwater and interflow water storage volumes (discussed in the next section) control the extent of the saturated area and the spatial variability in exfiltration rates. This transfer function is used to route water discharged from the interflow and groundwater compartments of the UP element to the main channel network.

Surface water reaching the channel is routed by the channel module which is based on the network-width-function linear diffusion-wave approximation model (Naden, 1993) under development at the Institute of Hydrology, Wallingford, UK.

3.3 - The UP Element and its Compartments

Typical element sizes for the model when used with a weather forecasting or climate model are 10x10 km or 50x50 km. The modelling scheme for an element was conceptualised to represent all the processes involved in runoff formation, according to their temporal scale. Therefore, a model element comprises sub-elements (compartments), each representing one of these phases. Runoff is a multidimensional and dynamic phenomenon influenced by surface and subsurface characteristics, and atmospheric processes. In a simplified way, the sub-elements seek to represent each phase of these dynamic process. In the current version an element comprises four compartments: (i) canopy/snowpack and (ii) soil water (fast surface processes), (iii) interflow (slower), and (iv) groundwater (the slowest). Figure (3.1) shows a typical UP element with its compartments.

The moisture status of each UP element compartment is described by one or more simulation variables. Most of these are simply the volumes of water in the compartments. The UP approach is still under development, and new types of variables are regularly being considered. The water transfers between compartments (Figure 3.1) are calculated at each time step using algebraic equations or look-up tables. These are generated using aggregated results from detailed physically-based simulations run prior to setting up the UP simulation model, and take account of the small scale spatial variability of the physical properties of the area being modelled. Therefore, the application of the model

uses a two-stage approach. The second stage is the use of the UP elements to give a fast running, simple simulation model, and the first stage is the use of a suite of physically-based process models to give the look-up tables and equations which parameterise the UP elements.

Mass continuity is maintained for each compartment using hourly mass balance calculations, so the simulation variables represent the dynamic moisture status of the land surface and subsurface and its variation hour by hour.

3.3.1 - Canopy/Snowpack Compartment

In this compartment the processes of rainfall interception, evapotranspiration and snow modelling (not described here) are represented. A detailed parameterisation model is not run for the canopy, and at present only one canopy layer is represented. The formulation of the interception model is similar to that used in the UM (UK Meteorological Office's Unified Model; Gregory and Smith, 1993). No account is taken of the spatial distribution of rainfall amounts at the sub-grid scale, but the model is easily extended to include this effect. The throughfall rate is assumed to be related to the depth of storage in the canopy, and the evaporation rate from storage is calculated using the Penman-Monteith equation.

Transpiration removes water from the soil water compartment (unsaturated zone). The Penman-Monteith equation is used and the calculated transpiration rate is appropriately reduced if the canopy is partially wet. The effect of physiological controls on transpiration are represented via the canopy resistance. The specification of this resistance is simple at present, but empirical functions relating the resistance to meteorological variables are available and will be included in the future.

The spatial heterogeneity of vegetation is allowed for by weighting all canopy calculations according to the fractional cover of each vegetation type. A separate canopy water store is used for each vegetation type present in the grid.

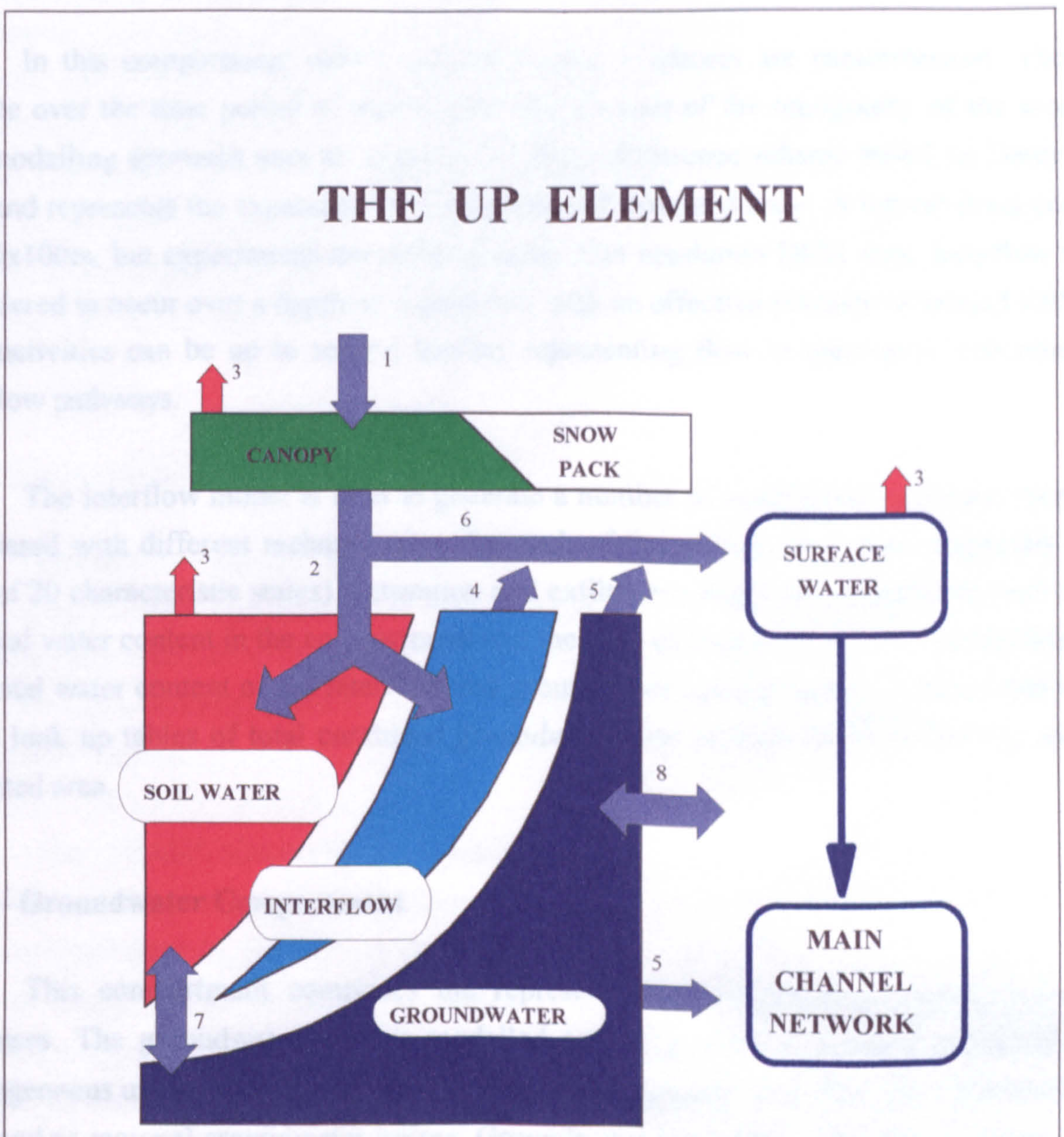

Figure 3.1 - UP element

3.3.2 - Interflow Compartment

In this compartment runoff and exfiltration responses are parameterised. They operate over the time period of storms and take account of the topography of the area. The modelling approach uses an implicit 2-D finite difference scheme based on Darcy's Law and represents the expansion and contraction of saturated areas. A typical pixel size is 100x100m, but experiments are planned using 30m resolution DEM data. Interflow is considered to occur over a depth of around 1m, with an effective porosity of around 0.05. Conductivities can be up to several km/day representing flow in macropore and other interflow pathways.

The interflow model is used to generate a number of equilibrium interflow states associated with different recharge rates, for each of the groundwater states (typically a total of 20 characteristic states). Saturation and exfiltration maps are produced as well as the total water content in the compartment and the total exfiltration rate from the surface. The total water content of the interflow and groundwater compartments are then used to index look up tables of total combined groundwater and interflow exfiltration rate and saturated area.

3.3.3 - Groundwater Compartment

This compartment comprises the representation of exfiltration and baseflow responses. The groundwater zone is modelled assuming there is a single anisotropic, heterogeneous unconfined aquifer. Water may enter the aquifer both from the unsaturated zone and as regional groundwater inflow. Groundwater is currently modelled as being in steady state, using a two-dimensional Boussinesq approximation (e.g. Bear, 1972).

$$\varnothing \frac{\partial h}{\partial t} = \frac{\partial}{\partial x}\left[K_x h \frac{\partial h}{\partial x}\right] + \frac{\partial}{\partial y}\left[K_y h \frac{\partial h}{\partial x}\right] + r_t \qquad \text{eqn. (3.1)}$$

$\varnothing$ - specific yield;

h - elevation of water table;

(x, y) and t - directions on an horizontal plane and time respectively;

$K_{x,y}$ - hydraulic conductivity components for the aquifer;

r_t - recharge rate.

The groundwater model is used to generate a number of groundwater states, each associated with a given recharge rate, the values for which are derived from rainfall and evaporation data or estimates. Exfiltration rates to the surface, the rate of direct groundwater discharge into the main channel, and the area fraction of saturation excess are all calculated, as well as values for the total water content. These are used as an index in the lookup tables produced in conjunction with the interflow module. The soil water compartment supplies recharge to the groundwater compartment at a rate depending on the current status of both compartments.

3.3.4 - Soil Water Compartment

Infiltration, surface flow and groundwater recharge are represented in the soil water compartment. The description of the ground surface is currently under review in a separate programme of work (John Ewen, personal communication). The emphasis there is to develop a consistent description of coupled heat and moisture transfer, infiltration and related runoff.

The GRASP (Groundwater Recharge modelling Approach with a Scaling-up Procedure) is the main topic of this thesis, and was developed for use in the unsaturated zone compartment of the UP element. GRASP is a simple and efficient modelling scheme using a physical parameterisation. The strategy adopted in its development includes a type of partial analysis, as discussed by Kuhnel et al. (1991). GRASP is consistent with the one-dimensional Richards equation (Richards, 1931) for flow in unsaturated porous media, and allows for the effect of spatial variability in soil properties via a scaling-up procedure.

3.4 - Discussion and Overview of the UP Macromodel

For an UP simulation the modelled area is divided into sub-catchments or grid squares, and each small sub-catchment or grid square is modelled using a single UP element. To parameterise the UP elements, a suite of physically-based parameterisation models is used. These make full use of the physical property data that are available. With this approach, parameterisation is a data-intensive and time-consuming task. However, it

only has to be done once for a given area and only for certain representative catchments or grid squares, since the parameterisations are extended to other, data-poor, sub-catchments or grid squares using a simple scaling and classification approach.

Data are stored and manipulated on a pixel basis in a GIS (Geographical Information System) for use by the parameterisation suite of models. A wide variety of data types and sources can be used, but the basic data sets are:

- DEMs;
- land cover maps;
- subsurface hydraulic property maps;
- hydrometeorological data;
- river network maps.

The basic elements of the current parameterisation suite are:

- two-dimensional surface water (overland flow) model;
- lumped channel flow routing model;
- one-dimensional soil and vegetation column model;
- lumped snow-pack model (not described);
- two-dimensional interflow module;
- two-dimensional groundwater flow module.

Each UP element has only a few compartments (soil water, groundwater, etc.) and the moisture status of each of these is described using only one or two variables (e.g. stored volume). The physical transfers of water (e.g. recharge and exfiltration) are calculated using simple equations or look-up tables, parameterised in terms of the simulation variables.

The description of the UP model given here was brief and aimed mainly to provide the reader with some background for placing the proposed groundwater recharge modelling approach within the framework of the UP macromodel as a whole. Chapters 4, 5 and 6 discuss the GRASP approach for groundwater recharge modelling proposed in this research.

Chapter 4

Groundwater Recharge Simulation using One-dimensional Richards' Equation

4.1 - Introduction

The basis for the GRASP (Groundwater Recharge modelling Approach with a Scaling-up Procedure) approach developed in Chapter 5 is the one-dimensional RE (Richards Equation) to model groundwater recharge at-a-point, which is discussed here.

Recharge is generally used as the term describing the entry of water into the saturated zone. Here for convenience the term is used more broadly, to describe the transfer of water between the soil's unsaturated and saturated zones. Thus it involves both percolation from the unsaturated to the saturated zone, and capillary rise where transfers occur in the opposite direction (negative recharge).

Natural groundwater recharge is a very dynamic process and affected by a number of factors. Although soil properties such as porosity and hydraulic conductivity have a strong influence on natural groundwater recharge, rainfall, the slope of the water-bearing layer, and the soil moisture content of the unsaturated zone also affect recharge rates. Because of this, the recharge process is quite variable spatially and there is no widely accepted method available to represent recharge in a direct and explicit way. Field techniques to evaluate recharge usually involve the use of geochemical methods (tracers), lysimeters, or indirect inference using other hydrological variables and estimating recharge by the soil water budget method (Sharma, 1986). In addition, recharge can also be estimated indirectly by measuring change in the hydraulic head (Δh) in observation wells:

$$rchrge_t = \Delta h_t . \varnothing$$

where $\varnothing$, specific yield, can be determined by pumping tests.

Modelling recharge is not simple, partly as a result of the inherent difficulties of modelling the (highly non-linear) unsaturated zone. This is affected at its top surface by rainfall and other quickly changing processes, and at its base by the complex behaviour of the capillary fringe. A number of techniques have been used to model the recharge process. The methods include simulation using only the unsaturated zone or saturated zone, or both. Assuming equilibrium between recharge and discharge from the groundwater, recharge rates can be evaluated roughly by hydrograph separation from the part of the streamflow which could have contributed to recharge (Sharma, 1986). Conceptual rainfall-runoff models may be applied allowing recharge to be estimated by water balance in the subsurface buckets (e.g. Johansson, 1988).

Morel-Seytoux and Miracapillo (1989) proposed a model in which the multidimensional character of the recharge process is approximated by a technique that links vertical (unsaturated zone) and horizontal (saturated zone) fluxes. The process consists of modelling fluxes into and out of the water table mound (transition zone between the soil unsaturated and saturated zones). The evolution of water table fluctuations is modelled by a linear form of the Boussinesq equation. Recharge rates flowing into the mound are estimated by integrating hydraulic conductivity over the vadose zone in which the relationship between hydraulic conductivity and moisture content is given by a power function.

In the so called inverse problem, recharge rates are determined using the Boussinesq equation (e.g. Bear, 1971) based on spatially observed hydraulic heads. Parameters are generally identified by means of calibration. In the more realistic situation in which there is substantial spatial variation in the parameters and only scarce point measurements are known, the mathematical problem becomes 'ill-posed' (i.e. it does not allow unique solution). Yeh (1986) presented an extensive review of the inverse problem.

Recently, Su (1994) presented an analytical solution for the Boussinesq equation. The solution is given in a simple form but requires the knowledge of a range of parameters not always available. The solution can be useful to verify numerical models or even to estimate recharge rates with the aid of some in-situ measurements of soil properties.

In this research the development of the groundwater recharge modelling scheme was based on unsaturated zone elements. The problem was approached by searching for a simple model that would be able to simulate recharge rates for the macromodel element, with physical interpretation. Spatial variability within the macromodel element is represented using a scaling up (bottom-up approach) procedure. This is strongly based on the fact that most information available for soil modelling design, operation and validation is point-based. It seems therefore more reasonable to use this scale as a starting point. The possibility of establishing a simpler model, preferably linear, eases the problem of scaling the recharge rates up to the macromodel element (as discussed in section 2.10). In addition, for the case of large scale modelling this framework is very advantageous in terms of enhancing computing efficiency.

Since the recharge process is complex and very dynamic, the strategy adopted here involves the analysis of a series of temporal recharge rates on an at-a-point-basis, associated with transient stages of flow in the unsaturated zone. These consider different stages of soil moisture content and associated phreatic surface depths. The recharge rates used in the analysis were obtained from a number of physically reasonable soil scenarios simulated using FULCRUM which incorporates a numerical algorithm for predicting water flow in the soil unsaturated zone by solving Richards' equation. These simulations provided realistic time series of soil water infiltration rates, soil unsaturated zone moisture content and, recharge rates which are simulated using the water flux at the lower boundary of the unsaturated zone. Very recently, Wu et al. (1996), also used RE simulations as an aid to estimating recharge rates.

The aim of this chapter is to describe the soil water unsaturated zone point-based simulations that comprise a range of different transient scenarios which provided a solid basis for developing the groundwater recharge modelling approach for the UP macromodel element which was decribed in Chapter 3.

4.2 - Modelling Soil Water in the Unsaturated Zone

Soil water movement in the unsaturated zone is described by the Richards Equation (RE), which is obtained by applying the mass conservation law,

$$\frac{\partial \theta}{\partial t} = -\nabla q \qquad \text{eqn. (4.1)}$$

and the Darcy flow law generalised for unsaturated media:

$$q = -K.\nabla H \qquad \text{eqn. (4.2)}$$

where,

q (z,t) - soil water flux (Darcian flow) taken as positive vertically downward (L T^{-1});

K - soil hydraulic conductivity function (L T^{-1});

θ (z,t) - local volumetric soil water content (L^3 L^{-3});

z - depth below soil surface (L);

t - time (T).

∇H is the hydraulic head gradient, which for unsaturated soils includes both suction (ψ) and gravitational (z) components (H=ψ+z). RE can be derived for all three dimensions. However, only the vertical unidimensional RE is presented here. The equation of continuity (eqn. 4.1) for vertical flow in a soil column is therefore,

$$\frac{\partial \theta}{\partial t} + \frac{\partial q}{\partial z} = 0 \qquad \text{eqn. (4.3)}$$

The Darcian flow equation for unsaturated media (equation of motion) for vertical movement of soil water is,

$$q = -K(\psi)\left(\frac{\partial \psi}{\partial z} - 1\right) \qquad \text{eqn. (4.4)}$$

where ψ (negative in the unsaturated zone) is the matric potential (L).

Equations (4.3) and (4.4) combined give;

$$\frac{\partial\theta}{\partial t}=\frac{\partial}{\partial z}\left(K(\psi).\frac{\partial\psi}{\partial z}-K(\psi)\right) \qquad \text{eqn. (4.5)}$$

This result is the RE (Richards, 1931). If the matric potential (ψ) and the hydraulic conductivity (K) are both taken as single-valued functions of soil water content (θ), RE can be written in different forms,

$$\frac{\partial\theta}{\partial t}=\frac{\partial}{\partial z}\left(K(\theta).\frac{\partial\theta}{\partial z}-K(\theta)\right) \quad (\theta\text{- form}) \qquad \text{eqn. (4.6)}$$

or even in terms of soil water diffusivity $D(\theta)=K(\theta)\frac{d\psi}{d\theta}$,

$$\frac{\partial\theta}{\partial t}=\frac{\partial}{\partial z}(D(\theta).\frac{\partial\theta}{\partial z})-\frac{dK(\theta)}{d\theta}\frac{\partial\theta}{\partial z} \qquad \text{eqn. (4.7)}$$

Equation (4.7) is sometimes referred to as the non-linear Fokker-Planck diffusion-convection equation.

Alternatively, if specific water capacity, C(ψ), is defined as $C(\psi)=\frac{d\theta}{d\psi}$, RE becomes;

$$C(\psi).\frac{\partial\psi}{\partial t}=\frac{\partial}{\partial z}\left(K(\psi).\frac{\partial\psi}{\partial z}-K(\psi)\right) \quad (\psi\text{- form}) \qquad \text{eqn. (4.8)}$$

4.3 - Soil Hydraulic Property Functions

Soil hydraulic property functions play a central role in predicting flow. Matric potential function $\psi(\theta)$ (sometimes called the retention or moisture release or tension curve) and the hydraulic conductivity function, $K(\theta)$ or $K(\psi)$, are all highly non-linear for natural soils. Numerous mathematical functions have been proposed in the literature to represent soil hydraulic properties (e.g. Brooks and Corey, 1964; van Genuchten, 1980;

Rawls et al., 1983; and Saxton, 1986). Generally, these functions are not fully physically-based and were derived by fitting field and laboratory measurements.

The approach of van Genuchten (1980) and Mualem (1976) (VG-Mualem model) is widely used in estimating soil hydraulic properties (e.g. Carsel and Parish, 1988). Like the Brooks-Corey approach (BC model; Brooks and Corey, 1964), this is usually classified as a pore-size distribution model. Such models interpret the matric potential function of a porous medium as a measure of its pore-size distribution (Ragab and Cooper, 1990; Durner, 1994). The van Genuchten function is;

$$\theta = \theta_r + \frac{\theta_s - \theta_r}{[1+|\alpha\psi|^n]^m} \text{ , for } \theta_r \le \theta \le \theta_s \qquad \text{eqn. (4.9)}$$

and the hydraulic conductivity function of Mualem (1976) is;

$$K = K_s \frac{\{[1+|\alpha\psi|^n]^m - |\alpha\psi|^{n-1}\}^2}{[1+|\alpha\psi|^n]^{m(x+2)}}, \; x = 0.5 \qquad \text{eqn. (4.10)}$$

The subscripts "r" and "s" indicate residual and saturation values, respectively. Eqn. (4.9) is an "S-shape" curve. The steepness towards more negative values of matric potential is reflected by parameter n and the point where it bends down towards saturation is reflected by α. The parameter m has been proposed by van Genuchten (1980) as equal to [1-(1/n)]. θ_S is usually considered to be equal to the porosity and is not difficult to obtain. θ_r can be more complicated to obtain. It can be determined in the laboratory, but values of this parameter are not often quoted in the literature. In addition, θ_r may be determined, like n and α, by fitting the VG-Mualem model to field observations. However, low moisture contents are not often observed in the field, so extrapolation is likely to be necessary. Moreover, some interactions between parameters have been reported, for example a decrease of the value θ_r causes a shift of parameter n toward a smaller value. A similar effect is caused by an increase of θ_S (Durner, 1994). Rawls et al. (1983) proposed empirical functions that relate VG-Mualem model parameters to particle size distribution and alternatively to BC model parameters.

Khaleel et al. (1995) tested the VG-Mualem relationship's ability to predict hydraulic conductivities (K) at relatively low moisture contents in coarse textured soils. Using a laboratory-measured saturated K as a fixed parameter they found that the standard VG-Mualem functions are a poor representation of unsaturated K at low moisture content for dry regions. They concluded that predictions improve if, instead of using saturated hydraulic conductivity as the matching point, a measured K value for low moisture is used.

Compared with the BC model, the VG-Mualem model has the favourable property of having a continuous derivative $d\theta/dpF$ ($pF=\log_{10}\psi$) and of being asymptotically zero towards large and fine pores (Durner, 1994). Rossi and Nimmo (1994) proposed a model that combines the power law of the BC model with a logarithmic function for higher suction values (lower values of moisture content) and takes θ_r as zero. van Genuchten and Nielsen (1985) compared various water retention models and concluded that eqn. (4.9) fits the water retention data of most soils very well, and better than the BC model. However, the complicated form of the VG-Mualem model may limit its use in analyses that require analytical evaluation of the integral of the function (Russo, 1988).

Mishra and Parker (1989) examined the errors in predictions of unsaturated flow which result from parameter uncertainty when parameters are derived either from the particle size distribution, or by fitting directly to transient flow measurements. Error intervals on model predictions, evaluated by a first-order error analysis procedure, were found to bracket reasonably the behaviour of the system in both cases.

Recently, Durner (1994) proposed a bi-modal function based on the VG-Mualem model. The new function was found to improve the representation of hydraulic properties of field soils. However, it involves the use of more parameters.

4.4 - Analytical Solutions for Richards' Equation

RE (Richards Equation) is a second-order, parabolic partial differential equation and can also be derived from the Navier-Stokes equation. Its high non-linearity is caused by the soil hydraulic properties ($K(\theta)$ and $\psi(\theta)$) which are required for its solution. The

functions $K(\theta)$ and $\psi(\theta)$ are usually highly non-linear and hysteretic, therefore an exact analytical solution for Richards' equation is difficult to obtain. Existing analytical solutions rely on simplifying assumptions which can lead to solution. Moreover, solutions are generally obtained for specific initial and boundary conditions, covering different real scenarios.

One of the best known solutions for RE is the so called Boltzmann solution in which RE is reduced to an ordinary differential equation by neglecting gravitational flow and assuming no hysteretic effects. This solution has been adopted by different authors. The solution given in terms of soil water infiltration rates is known as the Philip model (Philip, 1957).

Some analytical solutions are obtained by converting RE to the linear Convection-Diffusion equation (CDE). There are different ways of writing RE in terms of the CDE. These solutions are usually referred to as quasilinear solutions.

Taking RE as the non-linear Fokker-Planck diffusion-convection equation (eqn. 4.7) and introducing the variable Θ (L^2/T) where,

$$\Theta = \int_{\psi_1}^{\psi} K d\psi \equiv \int_{\theta_1}^{\theta} D(\theta) d\theta$$

where θ_1 and ψ_1 are reference values and $\psi_1=\psi(\theta_1)$, eqn. (4.7) then becomes,

$$\frac{1}{D(\theta)}\frac{\partial \Theta}{\partial t} = \frac{\partial^2 \Theta}{\partial z^2} - \frac{1}{D(\theta)}\frac{\partial K}{\partial \theta}\frac{\partial \Theta}{\partial z} \qquad \text{eqn. (4.11)}$$

or by expanding (chain rule) the last term on the right hand side,

$$\frac{1}{D(\theta)}\frac{\partial \Theta}{\partial t} = \frac{\partial^2 \Theta}{\partial z^2} - \frac{1}{K(\theta)}\frac{dK}{d\psi}\frac{\partial \Theta}{\partial z} \qquad \text{eqn. (4.12)}$$

This transformation is often referred to as Kirchhoff's transformation and Θ is Kirchhoff's potential (Kirchhoff, 1894). By applying particular forms for functions K(0) and ψ(θ), the term $(1/K(\theta))(dK/d\psi)$ becomes constant, and the right hand side of the above equation is linearised, allowing solution. This condition implies that,

$$K \propto e^{\alpha\psi}$$

Generally, soils that obey this functional form are called Gardner soils, because Gardner was probably the first to introduce such models.

With $(1/K(\theta))(dK/d\psi) = \alpha$ (a constant) the steady state version of eqn. (4.12) becomes,

$$\frac{\partial^2\Theta}{\partial z^2} = \alpha\frac{\partial\Theta}{\partial z}$$

Srivastava and Jim-Yeh (1991), presented an analytic solution for RE based on the following functional forms,

$$K = K_s\, e^{\alpha\psi} \qquad \text{eqn. (4.13)}$$

$$\theta = \theta_r + (\theta_s - \theta_r).e^{\alpha\psi} \qquad \text{eqn. (4.14)}$$

By adopting these equations RE was re-written as,

$$\frac{\partial^2 K}{\partial z^2} + \alpha\frac{\partial K}{\partial z} = \frac{\alpha(\theta_s - \theta_r)}{K_s}\frac{\partial K}{\partial} \qquad \text{eqn. (4.15)}$$

which is equivalent to the linear Convection-Diffusion Equation (CDE) that possesses known solutions. Srivastava and Jim-Yeh presented a solution for this in the form of RE by Laplace transformation.

A detailed review on quasilinear approaches for unsaturated flow problems was presented by Pullan (1990).

Other solutions for RE are based on relating RE to Burgers equation (Burgers, 1948),

$$\frac{\partial \theta}{\partial t} = D\frac{\partial^2 \theta}{\partial z^2} - (A\theta + B)\frac{\partial \theta}{\partial z} \qquad \text{eqn. (4.16)}$$

with A, B and D constants. This constitutes a weak-nonlinear form of the Fokker-Planck equation [$(dK(\theta)/d\theta) = (A\theta + B)$-eqn.(4.7)]. Particular forms of functions K(θ) and ψ(θ) can be derived to allow solution.

Philip (1974) presented a solution for eqn. 4.16 (originally given by J.H.Knight) subject to constant flux or constant moisture content boundary conditions, preserving nonlinearity in the coefficient of $\partial\theta/\partial z$.

More recently (e.g. Broadbridge and White, 1988; Sanders et al., 1988; Hills and Warrick, 1993 and Warrick and Parkin, 1995), a series of solutions have been presented using Fujita functions (Fujita, 1952),

$$D = \frac{a}{(b-\theta)^2} \qquad \text{eqn. (4.17)}$$

$$K = \beta + \gamma(b-\theta) + \frac{\lambda}{2(b-\theta)} \qquad \text{eqn. (4.18)}$$

with a, b, β, γ and λ as constants.

Broadbridge and White (1988), re-parameterised the Fujita functions (eqns. 4.17 and 4.18) using commonly used soil physical parameters. The constants β, γ and λ in eqn.(4.18) were expressed as a function of a new introduced constant *c* given by:

$$c = \frac{(b-\theta_n)}{(\theta_s-\theta_n)} \qquad \text{eqn. (4.19)}$$

Then,

$$\lambda = 2c^2(c-1)\,\Delta\theta\Delta K$$
$$\beta = K_s - [1 + 2c(c-1)\Delta K]$$
$$\gamma = (c-1)\Delta K/\Delta\theta$$

where,

c - is a dimensionless parameter;

θ_n - value of moisture content for which $dK(\theta = \theta_n)/d\theta = 0$ (dry case);

$\Delta\theta$ - $= (\theta_s - \theta_n)$;

K_n - hydraulic conductivity at ($\theta = \theta_n$);

ΔK - $= (K_s - K_n)$.

By introducing the variable Θ' [1] (reduced moisture content) given by:

$$\Theta' = \frac{(\theta - \theta_n)}{(\theta_s - \theta_n)} \qquad \text{eqn. (4.20)}$$

the soil hydraulic properties functions become,

$$\frac{K(\Theta')}{K_s} = \frac{(c-1)\Theta'^2}{(c-\Theta')} \qquad \text{eqn. (4.21)}$$

$$D(\Theta') = \frac{\lambda K_s c(c-1)}{\Delta\theta(c-\Theta')^2} \qquad \text{eqn. (4.22)}$$

Eqns. (4.21) and (4.22) were used to solve eqn. 4.16 (with the dependent variable (which was θ) changed to the reduced moisture content, Θ') for initial uniform moisture content and constant rate rainfall infiltration. Warrick et al. (1991), extended Broadbridge and White's solution for time-varying infiltration, expressed as a series of constant rates with arbitrary time intervals. Hills and Warrick (1993) extended the Broadbridge and White solution for a finite depth in the vadose zone. Warrick and Parkin (1995) derived the solution in terms of drainage.

---

[1] Originally, Broadbridge and White (1988) used the symbol Θ. However, Θ has already been used here to denote the Kirchhoff potential. Therefore, Θ' was used here to denote the Θ of Broadbridge and White.

Burgers equation preserves a "profile at infinity" unlike the fully linearised RE (with A=0). In other words, as time and water penetration depth become large, steady infiltration into initially drier soils leads to a fully developed wetting front profile. Additionally, Fujita (1952) functions seems to better represent observed soil data than the exponential forms.

Sander et al. (1988) derived a solution using Fujita functions based on the solution presented by Rogers et al. (1983) for two phase oil and water flow, but with a non-linear general functional-form for hydraulic conductivity,

$$K(\Theta') = \frac{K_1 + K_2\Theta' + K_3\Theta'^2}{1 - \upsilon\Theta'} \qquad \text{eqn. (4.23)}$$

with K_1, K_2, K_3 and n as constants, which can be reduced down to three by assuming K(0)=0, implying K_1=0.

Barry et al. (1993) derived a solution using the following form for the soil hydraulic function,

$$\Theta'(\psi) = \begin{cases} \dfrac{\alpha\psi_a}{K_s}\displaystyle\int_{-\infty}^{\psi} \frac{1}{\psi + B}\frac{dK(\psi)}{d\psi} & \psi < \psi_a \\ 1 & \psi \geq \psi_a \end{cases} \qquad \text{eqn. (4.24)}$$

where α is taken as an arbitrary constant and ψ_a is the air-entry moisture tension (also in the BC model). Although the authors claim that this form is a general one for soil hydraulic functions, they admit that Burdine models (i.e. the BC and Mualem models) are more useful for water modelling in field soils.

Although these solutions are based on simplified forms for soil hydraulic property functions (to a certain extent unrealistic), they are useful in giving insight into soil physics modelling, providing answers that bound the solutions for real soils and enhance confidence in numerical solution schemes (Srivastava and Jim-Yeh, 1991; Wang and Dooge, 1994).

4.5 - Numerical Solutions for Richards' Equation

Richards' Equation (RE) can be solved numerically using either finite difference or finite element methods. In general, the problems arising are the common problems found in numerical approaches (e.g. convergence, precision and stability). There exists a variety of solutions using different forms of RE (eqns. 4.5 to 4.8). Solutions are frequently given in terms of soil water infiltration or drainage rates for specific boundary and initial conditions.

Some problems on global mass balance errors have been reported on solving the ψ-form of RE (Celia et al., 1990). Rathfelder and Abriola (1994) demonstrate that efficient mass conservative solutions can be obtained by adopting an approximation for the capacity coefficient.

The accuracy of numerical solutions for the one-dimensional RE is frequently discussed (e.g. Haverkamp et al., 1977; Ross, 1990). Simple mass balance checks are widely applied to validate numerical solutions, Thomas and Rees (1991) validated a solution which used the finite element method against measurements from a field experiment. Gottardi and Venutelli (1993) presented a range of codes for solving the one-dimensional RE. Solutions were given in terms of soil infiltration rate for different forms of Richards' equation (θ, mixed and ψ forms) and validated by inter-comparison. In addition, numerical solutions can be validated using analytical solutions.

In this study the one-dimensional RE was applied to simulate water fluxes in the soil unsaturated zone. The model FULCRUM which adopts a numerical solution for RE was used.

4.6 - The FULCRUM Soil Column Model

FULCRUM is a computational FORTRAN module in which water flow and contaminant migration are modelled in a soil column. It includes the ground surface, the unsaturated zone and the top part of the saturated zone. The movement of water in the unsaturated zone is modelled using the one-dimensional Richards equation which is

solved numerically using an implicit finite-difference scheme. For this study only the water flow component of FULCRUM was applied.

The model allows vertical variations in soil physical properties but assumes that the soil is areally homogeneous and the soil properties are non-hysteretic. The soil water is assumed to be incompressible and the effects of temperature are not considered. Macropore flow is not considered and flow in the unsaturated zone is assumed to occur only in the vertical direction. The model considers lateral groundwater inflow and outflow below the phreatic surface and, there is a vertical input from regional groundwater. Figure (4.1) shows schematically the fluxes represented in FULCRUM.

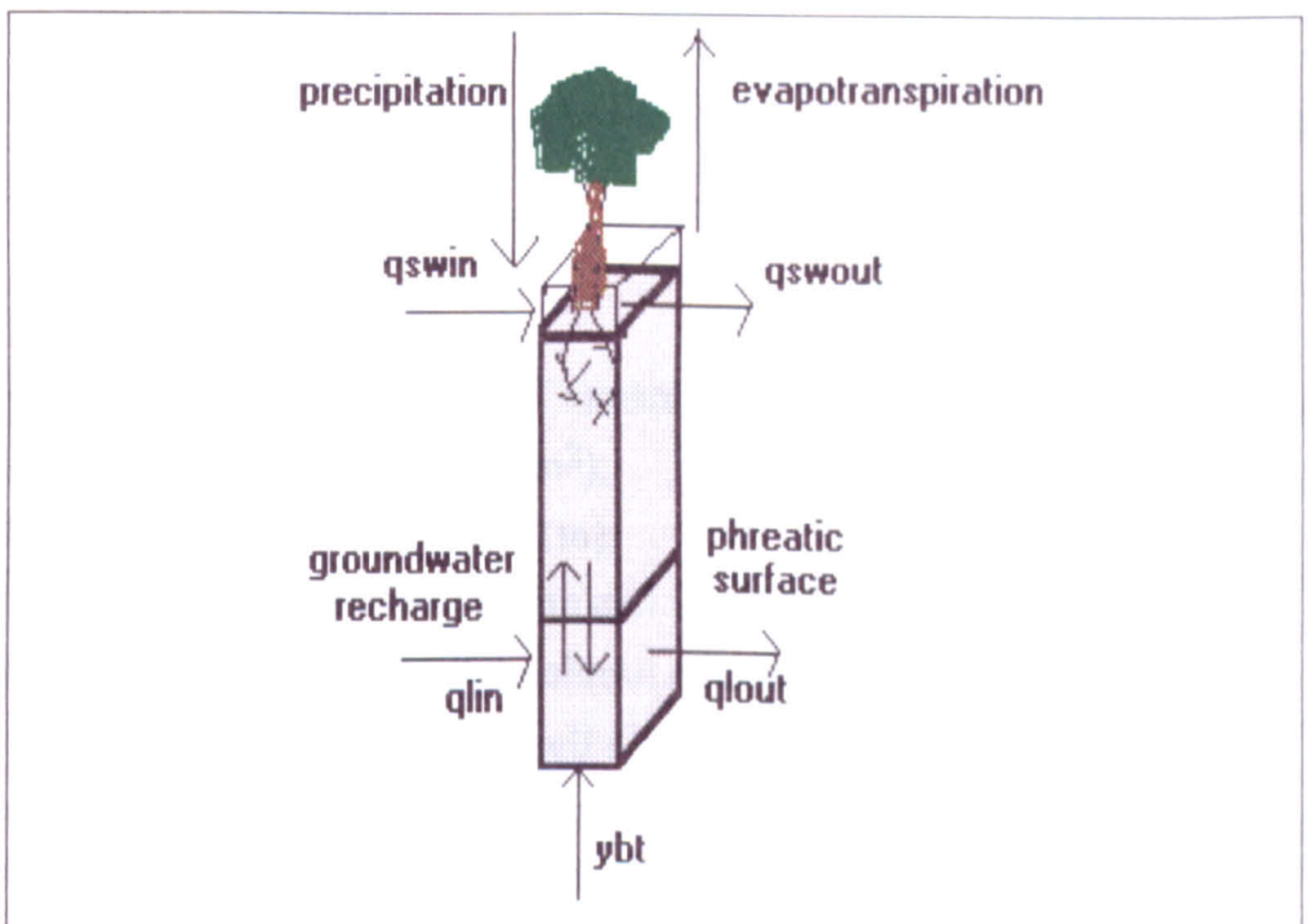

Figure 4.1 - The FULCRUM soil column components

The model was developed by Dr. John Ewen - Civil Engineering Department - University of Newcastle upon Tyne. Partial descriptions of the model are given in Whittaker(1992) and Birkinshaw (1993). Recently, the interception, evapotranspiration and snowmelt components of the FULCRUM have been updated to be consistent with the UM model (UK Meteorological Office's Unified Model, described in Gregory and Smith, 1993).

4.6.1 - Water Flow in the Soil Column Model

The soil column is divided into cells for finite difference solution of the physical equations. The general mass balance equation for each cell i, is given by:

$$\Delta\theta_i \,.\, A \,.\, \kappa_i \;=\; \{\, q_{i\,in} - q_{i\,out} + Y_i + A \,.\, u_i - S_i \,\} \,.\, \Delta t \qquad \text{eqn. (4.25)}$$

where,

$\Delta\theta_i$ - variation of the volumetric soil moisture content of soil column cell i (m^3m^{-3});
A - area of column cross section (m^2);
κ_i - thickness of soil column cell i (m);
$q_{i\,in}$ - lateral inflow rate to soil column cell i ($m^3\ s^{-1}$);
$q_{i\,out}$ - lateral outflow rate from soil column cell i ($m^3\ s^{-1}$);
Y_i - source terms for soil column cell i ($m^3\ s^{-1}$);
u_i - resultant vertical flow velocity for soil column cell i ($m\ s^{-1}$);
S_i - sink terms for cell i ($m^3\ s^{-1}$), in this case evapotranspiration;
Δt - time step (s).

4.6.2 - Lateral Flow Components

Below the phreatic surface in the soil column, lateral inflow and outflow and vertical flows are represented. The rate of lateral inflow is given by:

$$q_{l_{in}} = \frac{b_i . \kappa . A . K_{sI}}{K_{sI}} \frac{1}{t_{gw_{in}}} (a_1 + (1 - a_1) . w / \overline{w}) \qquad \text{eqn. (4.26)}$$

where,

$q_{l_{in}}$ - lateral inflow rate for the i^{th} soil column cell ($m^3 s^{-1}$);

b_i - proportion of the cell that is below the phreatic surface;

κ_i - thickness of the i^{th} soil column cell (m);

K_{si} - saturated hydraulic conductivity for the i^{th} soil column cell ($m s^{-1}$);

K_{sI} - saturated hydraulic conductivity integrated over the full depth of the saturated zone ($m s^{-1}$);

t_{gwin} - groundwater inflow time (s);

a_1 - a factor associated with the long term persistence of groundwater inflow/outflow;

w - average volume of rainfall over the previous week ($m^3 s^{-1}$);

$\overline{w}$ - long term average of w.

The lateral outflow is given by:

$$q_{l_{out}} = \frac{b_i . \kappa_i . A . K_I}{K_I} \frac{1}{t_{gw_{out}}} \frac{(z_1 - z_m)}{(z_2 - z_m)} \qquad \text{eqn. (4.27)}$$

where,

$q_{l_{out}}$ - lateral outflow rate for the i^{th} cell soil column ($m^3.s^{-1}$);

$t_{gw_{out}}$ - groundwater outflow time (s);

z_1 - groundwater thickness (m);

z_2 - total soil column depth (m);

z_m - given minimum height of the phreatic surface (m).

4.6.3 - Top Cell Source Term

For the top cell the source Y_i is equivalent to the net precipitation and surface fluxes into and out of the cell. The net precipitation is due to the net rainfall and snow melt. For the top cell, Y is given by:

$$Y_{top} = P_{net} + q_{in_{sw}} - q_{out_{sw}} \qquad \text{eqn. (4.28)}$$

where,

Y_{top} - top cell inflow rate ($m^3 s^{-1}$);
P_{net} - net precipitation volume inflow rate ($m^3 s^{-1}$);
q_{insw} - steady rate of surface water inflow rate ($m^3 s^{-1}$);
q_{outsw} - surface water outflow rate ($m^3 s^{-1}$).

Surface water outflow is generated only when the top cell is saturated. For convenience, surface water is lumped with the soil moisture in the top cell;

$$\theta_{top} = \theta'_{top} + dsw / k_{top} \cdot z_2 \qquad \text{eqn. (4.29)}$$

where,

θ_{top} - effective volumetric moisture content in the top cell after accounting for ponding water;
θ'_{top} - actual volumetric moisture content in the top cell;
d_{sw} - depth of the surface ponding (m);
κ_{top} - thickness of the top cell (m);
z_2 - length of the soil column (m).

The rate of lateral surface outflow is assumed simply to be:

$$q_{out_{sw}} = \xi \frac{\Lambda d_{sw}}{t_{sw}} \qquad \text{eqn. (4.30)}$$

where,

ξ - a coefficient equal to 0.693;
t_{sw} - half-life for surface water storage (s).

Net Rainfall and Interception

The canopy interception modelling scheme of FULCRUM is in line with the UK Meteorological Office approaches. Up to three land-surface covers (v) for the soil column are allowed, being two different types of vegetation and a bare soil. For the two allowed vegetation types the canopy is represented by a single layer with maximum water capacity C_v^{max}. The throughfall T_v is given by:

$$T_v = \begin{cases} P-(C_v^{max}-C_v)/dt, \text{ if } P > (C_v^{max}-C_v)/dt \\ PC_v/C_v^{max}, \qquad \text{if } P \le (C_v^{max}-C_v)/dt \end{cases} \qquad \text{eqn. (4.31)}$$

where C_v is the current water storage depth. Drainage from the canopy is not modelled, so the effective rainfall (that reaches the ground) is given by :

$$T_v+(1-\beta_v)P \qquad \text{eqn. (4.32)}$$

where β_v is the ground cover fraction and P is the rainfall rate. The canopy water content is depleted by throughfall (T_v) and evaporation.

Snow Modelling

The FULCRUM snowmelt component is based on the existing SHETRAN snow component (Bathurst and Cooley, 1996) and is briefly described below.

If the air temperature falls below 0°C, all precipitation is assumed to occur as snow. Otherwise, precipitation is assumed to fall as rainfall and the calculation of effective rainfall proceeds as described above. Snow passing through the canopy, snow interception and accumulation are not described.

It is assumed that rain falling on the snowpack is added to melted snow, so, rain and snowmelt may not freeze in the snowpack even if the temperature falls below 0°C. If the air temperature is at or below 0°C, all evapotranspirative fluxes are considered zero and the canopy storage freezes. Sublimation from the snow pack is not represented.

Snowmelt is calculated using the degree day method,

$$M = k(T_a - T_o)dt \qquad \text{eqn. (4.33)}$$

where,

M - melted snow (mm of water);
k - degree-day factor ($mm.s^{-1}.°C^{-1}$);
T_a - air temperature (°C);
T_o - air temperature above which snow start to melt (°C);
dt - time step (s).

The snowpack thickness increases by precipitation as snow ($T_a \leq 0°C$) and, decreases by melting at the snowpack surface (eqn. 4.33). The time, t_m, taken for a melt 'slug' to reach the ground is governed by the snowpack thickness:

$$t_m = 0.745(Z_s/1000)^2 + 1.429(Z_s/1000) \qquad \text{eqn. (4.34)}$$

where,

t_m - travel time from the top to the bottom of the snowpack (s);
Z_s - snowpack thickness at the beginning of the passage of the melt water (mm of water).

At each time step it is checked if the the 'slug' has reached the ground surface, and if it has, it is treated as effective rainfall. Ponded water or overland flow generated at the ground surface while a snowpack is present is not affected by the presence of the snowpack.

4.6.4 - Source Term for the Bottom Cell

For the bottom cell the input from the regional groundwater is considered to be equal to:

$$y_{bt} = \frac{z_2 . A}{t_{gwr}} (a_1 + (1 - a_1) . w / \overline{w} \qquad \text{eqn. (4.35)}$$

where,

y_{bt} - input from the regional groundwater ($m^3 s^{-1}$);
z_2 - length of the soil column (m);
t_{gwr} - deep groundwater inflow time (s);
a_1 - factor relating long term persistence of groundwater inflow or outflow.

Apart from the top and bottom cells, the source term is zero for all cells.

4.6.5 - Flow Velocity

The flow velocity in the soil matrix is given by Darcy's law;

$$u = -K(\frac{\partial \psi}{\partial z} - 1) \qquad \text{eqn. (4.36)}$$

where,

u - vertical velocity at an upper or lower horizontal face of the cell i ($m s^{-1}$);
K - hydraulic conductivity ($m s^{-1}$);
ψ - matric potential (m).

Both K and ψ are given as functions of soil moisture content and are input to the model as look up tables.

4.6.6 - Evapotranspiration Modelling for the Soil Column

The total evapotranspiration has three components: loss from intercepted water, evaporation from bare soil and transpiration by plants. Evapotranspiration from each of the three types of land cover is calculated independently using the Penman-Monteith equation. The column average value is calculated by areal weighting.

The rate of canopy interception is calculated independently for each vegetation type, and the canopy storage for each type is updated each time step. However, the effective rainfall derived for each cover type is aggregated and applied uniformly over the soil column surface.

Transpiration water is considered to be taken from soil water storage at a rate related to the density of roots for each soil layer. For bare soil, evaporation water is taken only from the top cell at a rate controlled by the cell's water content and by tuning parameters r_c (the surface resistance) and r_a (the aerodynamic resistance of the Penman-Monteith equation).

The Penman-Monteith equation (Monteith, 1973) may be written as:

$$\lambda E = \frac{\Delta R_N + \rho C_p (e_s - e)/r_a}{\Delta + \gamma(1 + r_c/r_a)} \quad (\mathrm{Wm^{-2}}) \qquad \text{eqn. (4.37)}$$

where,

λ - latent heat of vaporisation (=2.465 x 10^6 Jkg^{-1})

E - rate of evapotranspiration ($kgm^{-2}s^{-1}$)

Δ - rate of change of e_s with temperature (mbK^{-1})

R_N - net radiation (longwave and shortwave) (Wm^{-2})

ρ - air density (=1.2 kg m^{-3})

C_p - specific heat of air (=1005 J kg^{-1})

e - ambient vapour pressure (mb)

e_s - saturation vapour pressure at the air temperature (mb)

(e_s-e) - saturation vapour pressure deficit (mb)

γ - psychrometric constant (=0.66mb K^{-1})

r_a - aerodynamic resistance (s m^{-1})

r_c - canopy resistance (s m^{-1})

e, R_N, r_a, r_c are all given as input variables. c_s and Δ are calculated as functions of temperature.

The rates of interception loss, evaporation from bare soil and transpiration are partly controlled by the parameters r_a and r_c and limited by the soil water content and the amount of water present in the canopy.

Canopy evaporation is controlled mainly by the aerodynamic term (r_a). When the canopy is completely wet all evaporation is considered to be taken from the canopy storage, so there is no transpiration, the value of r_c is equal to zero and the evaporation rate is calculated by the Penman-Monteith equation. If the canopy is not entirely wet than the evaporation rate from the canopy is reduced by a factor C_v/C_v^{max}, and transpiration is allowed.

The effect of soil moisture availability is accounted for by multiplying the maximum possible transpiration from a soil column cell ($ETRA_i^{max}$) by a factor f, varying linearly from 0 at a lower limit for a specified moisture content to an upper limit. The effect of vertical root distribution and the extraction of water from different soil layers is accounted for by using a vegetation specific normalised root distribution function (RDF_i), giving the fraction of root present in each layer (constant input data). Water is then taken from each layer as a transpiration rate which is given by:

$$ETRA_{iv} = RDF_{iv} f(\theta_v) ETRA_i^{max} \qquad \text{eqn. (4.38)}$$

FULCRUM was adapted for this study, so that the phreatic surface level could be kept constant through time. To achieve this, the matric potential at the phreatic surface is treated as a boundary condition and set equal to zero.

4.7 - Verification of FULCRUM Numerical Solution

In this study the numerical scheme implemented in FULCRUM was verified against the analytical solution presented by Srivastava and Jim-Yeh (1991). As described in section 4.4, Srivastava and Jim-Yeh (1991) developed an analytic solution based on rewriting RE in the form of the CDE using K (hydraulic conductivity) as an independent variable and adopting exponential functions for both the soil hydraulic conductivity and retention functions. Solutions are derived both for homogeneous and layered soils. Only the case for the homogeneous soil column was considered in the FULCRUM verification. Two different scenarios (as in Srivastava and Jim-Yeh) wetting and draining profiles, have been considered in this study. The initial pressure profile is set to correspond to steady state infiltration at a rate of 0.1 cmh^{-1}. Then at an arbitrary time step the infiltration rate is increased to a steady rate of 0.9 cmh^{-1}. For the drainage scenario the infiltration rate is suddenly reduced from 0.9 back to 0.1 cmh^{-1}. Equivalent soil properties were adopted and the same trial was reproduced using FULCRUM. The results showed that soil moisture and pressure profiles for both wetting and draining scenarios simulated using FULCRUM were in good agreement with the profiles presented in Srivastava and Jim-Yeh (1991).

The FULCRUM code also includes an automatic water mass-balance checking procedure that is executed each time step, and this showed that the mass balance errors were negligible in the verification simulations.

4.8 - Input Data for FULCRUM Simulations

The data used in the simulations are based on the DSATE catchment data set. DSATE is a hypothetical catchment that includes a realistic drainage system, a flood plain and a range of surface soil types (Anderton et al., 1994). This basin has been established for use in research studies undertaken at the WRSRU (Water Resource Systems Research Unit), University of Newcastle upon Tyne.

4.8.1 - Meteorological Data

The DSATE catchment meteorological data set was obtained via the WRSRU from the Finland National Board of Waters and the Environment for the Kotioja catchment, Finland. The data set is considered to be of high quality and comprises hourly precipitation (1984-1989), daily pan evaporation, minimum, mean and maximum temperatures (1980-1989). Simulations were conducted for a single year (1989) and utilised the hourly precipitation data, hourly temperature (derived from daily observed values by Anderton et al., 1994), hourly net radiation and vapour pressure deficit which were both obtained using the observed values of daily pan evaporation in line with recommendations of the UK Meteorological Office (Thompson et al., 1981).

Figure 4.2 shows hourly rainfall, temperature, net radiation and vapour pressure deficit time series data for 1989 which were used in the FULCRUM simulations.

4.8.2 - Snowmelt Parameters

In FULCRUM all precipitation is assumed to fall as snow whenever the air temperature falls below 0°C and melting is assumed to occur only when air temperatures are above 3°C in order to inhibit excessive melting early in spring. Table 4.1 shows the parameters adopted for snowmelt modelling.

Table 4.1 - Summary of snowmelt parameters

Initial depth of snow (mm)	0
Initial snow pack depth (mm of water)	0
Specific gravity of snow	0.4
Degree day factor (mm s^{-1} $°C^{-1}$)	5.0×10^{-5}
Temperature above which melt starts (°C)	3

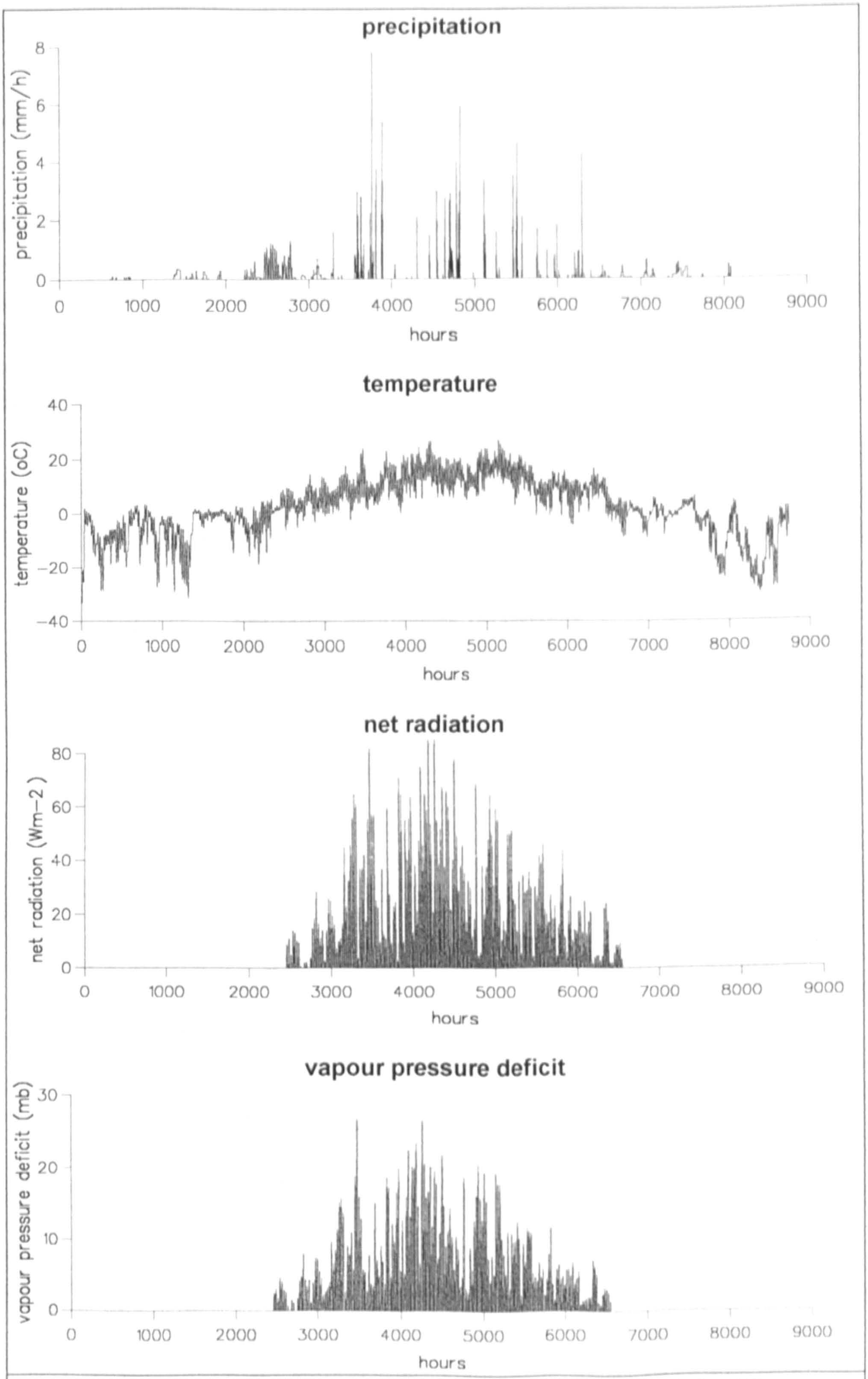

Figure 4.2 - Hydrometeorological input data for FULCRUM

4.8.3 - Evapotranspiration Parameters

Only one type of vegetation (grassland) was considered in this study. The vegetation height was chosen as 0.1m and assumed to cover 90% of the column surface, leaving the remaining 10% as bare soil. Root depth was taken as 0.6m with root density decreasing exponentially with depth. The canopy resistance (r_c) was taken to be 69sm^{-1} (Shuttleworth, 1992) and the aerodynamic resistance (r_a) was 50sm^{-1}. The values of r_c and r_a for bare soil were set to 100sm^{-1} and 10sm^{-1}, respectively (Thompson et al., 1981). The full data set for evapotranspiration parameters is given in Table 4.2.

Table 4.2 - Summary of evapotranspiration parameters

Vegetation parameters (grassland)	
Land cover fraction	0.90
Canopy cover fraction	1.0
Height of vegetation (m)	0.10
Initial canopy storage (mm)	0.25
Maximum canopy storage (mm)	0.50
Canopy resistance (sm^{-1})	69.
Aerodynamic resistance (sm^{-1})	50.
Bare soil parameters	
Fraction of soil covered	0.10
Canopy resistance (sm^{-1})	100.
Aerodynamic resistance (sm^{-1})	10.
Penman-Monteith constants	
Air density (kg m^{-3})	1.2
Psychrometric constant (mb K^{-1})	0.66
Specific heat capacity of air (J kg^{-1})	1005.
Latent heat of vaporisation (J kg^{-1})	2.465 x 10^6
Soil matric potential control constants	
Upper matric potential (m)	-1.
Lower matric potential (m)	-150.

4.8.4 - Soil Parameters

The soils in the DSATE catchment are representative of soils which are present in the Pennines, UK (Anderton et al., 1994). Field data for these soils were obtained from the Soil Survey and Land-use Research Centre (SSLRC). The soil hydraulic properties functions ($K(\theta)$ and $\psi(\theta)$) were obtained by fitting the van Genuchten-Mualem model (eqn. 4.9 and 4.10) to these field data. Five soils were chosen for this study and a summary of their hydraulic properties is given in Table 4.3. Figure 4.3 shows $K(\theta)$ and $\psi(\theta)$.

Table 4.3 - Summary of soil hydraulic properties

soil no.	soil type	θ_s	θ_r	θ_{fc}	K_{sat} (m/day)	n	α (cm^{-1})
1	upper sand	0.430	0.090	0.247	0.660	1.588	0.0103
2	silt clay	0.530	0.220	0.397	0.001	1.552	7.15e-03
3	lower sand	0.360	0.060	0.294	1.900	1.700	2.68e-03
5	Anglezarke A	0.602	0.135	0.275	2.120	1.400	0.060
8	Blackwood A	0.595	0.093	0.230	3.030	1.408	0.072

Moisture content at field capacity (θ_{fc}) are the values corresponding to a matric potential of -333 cm.

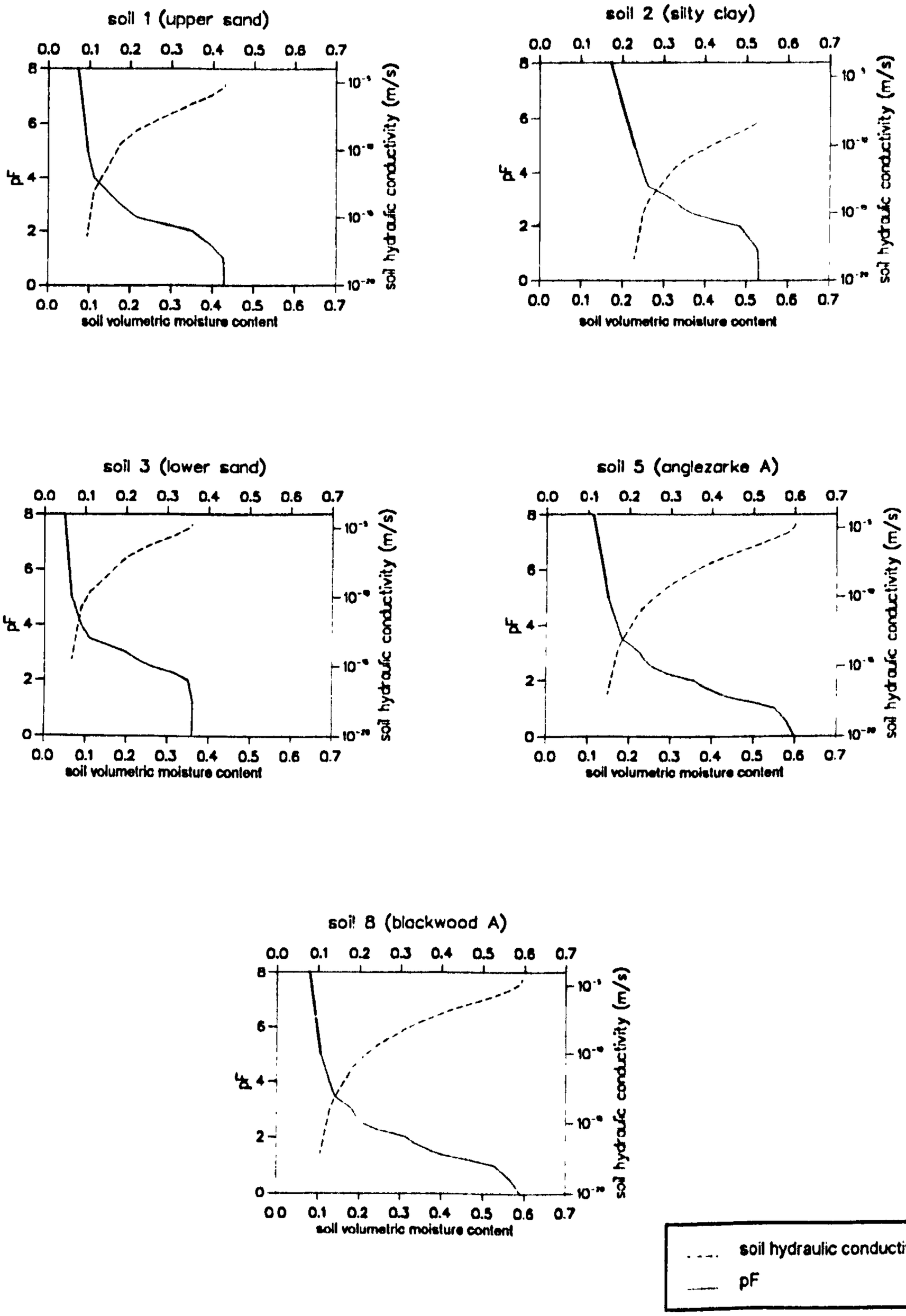

Figure 4.3 - Soil hydraulic properties

4.9 - FULCRUM Simulations

The series of FULCRUM simulations comprised 18 trials with 5 uniform soil columns and 1 non-uniform soil column (containing 2 different soil types). The same land cover and hydrometeorological data described in section 4.7 were used in every trial. For each soil column a number of different phreatic surface depths (LL) were used in the simulations. Table 4.4 summarises the trials.

Table 4.4 - Summary of FULCRUM simulations

Simulation	Column soil type	LL (m)
1	upper sand (soil 1)	-1.0; -1.5; -2.0; -3.0
2	silt clay (soil 2)	-1.0
3	lower sand (soil 3)	-1.0; -1.5; -2.0; -3.0
4	anglezarke A (soil 5)	-1.0; -1.5; -2.0
5	blackwood A (soil 8)	-1.0; -1.5; -2.0
6	half upper sand and half lower sand (soil 1-3)	-1.0; -2.0; -3.0

The soil columns are sub-divided into small cells for numerical solution. For these simulations the columns were typically divided into around 70 cells. The initial conditions were set so as to ensure equilibrium during the initial time steps (both infiltration and groundwater recharge rates are equal to zero at the beginning of each simulation). The simulations use time steps of one hour and run for 52 weeks from January to December. Figures 4.4 to 4.13 show FULCRUM simulation results for hourly infiltration rates, total soil-column moisture content and groundwater recharge rates (negative when capillary rise occurs). Except for the case of the silt clay soil, in which overland flow is generated, infiltration is very similar for all soils. Infiltration for the upper sand soil (LL = -2.0 m) is shown (Figure 4.4) as an example.

During execution FULCRUM presented some occasional numerical problems, but these could all be overcome by reducing the simulation time step. The resulting time series all look very consistent. Groundwater recharge hydrographs (Figures 4.5, 4.8, 4.10, 4.11 and 4.12) become smoother as the depth to the phreatic surface increases for each soil type. It can also be observed that the peaks and recessions are consistent both with the infiltration and total soil moisture content hydrographs (Figures 4.4, 4.6, 4.7, 4.9,

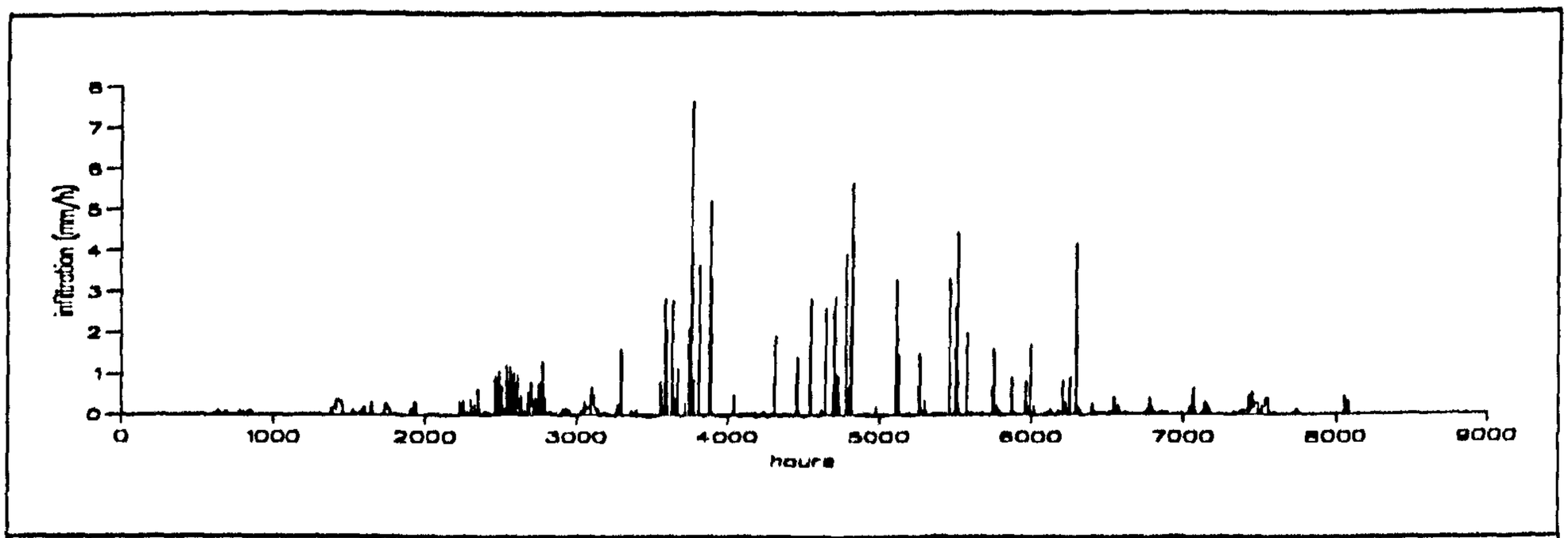

Figure 4.4 - Infiltration for soil 1 (LL=-2.0 m)

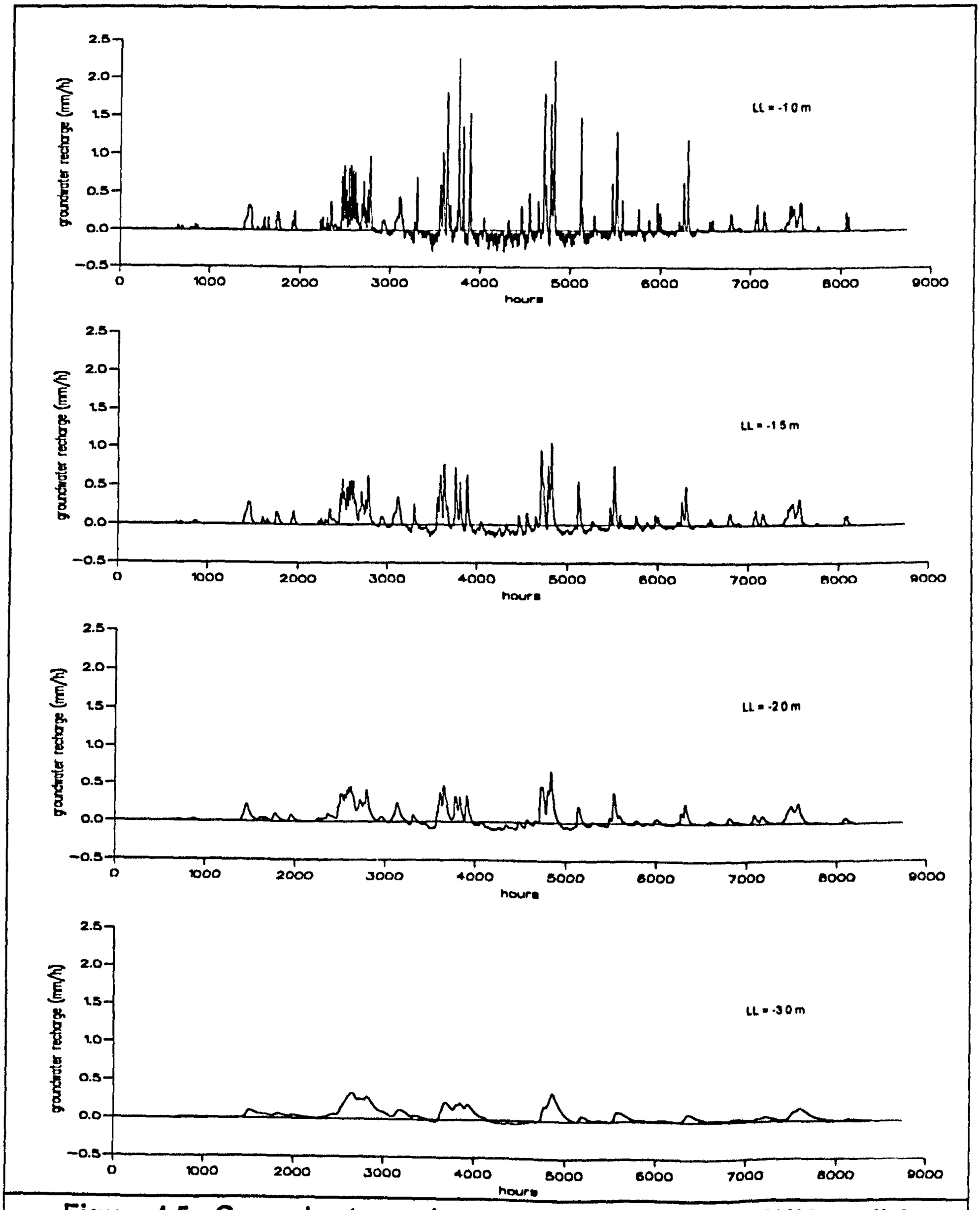

Figure 4.5 - Groundwater recharge simulated by FULCRUM - soil 1

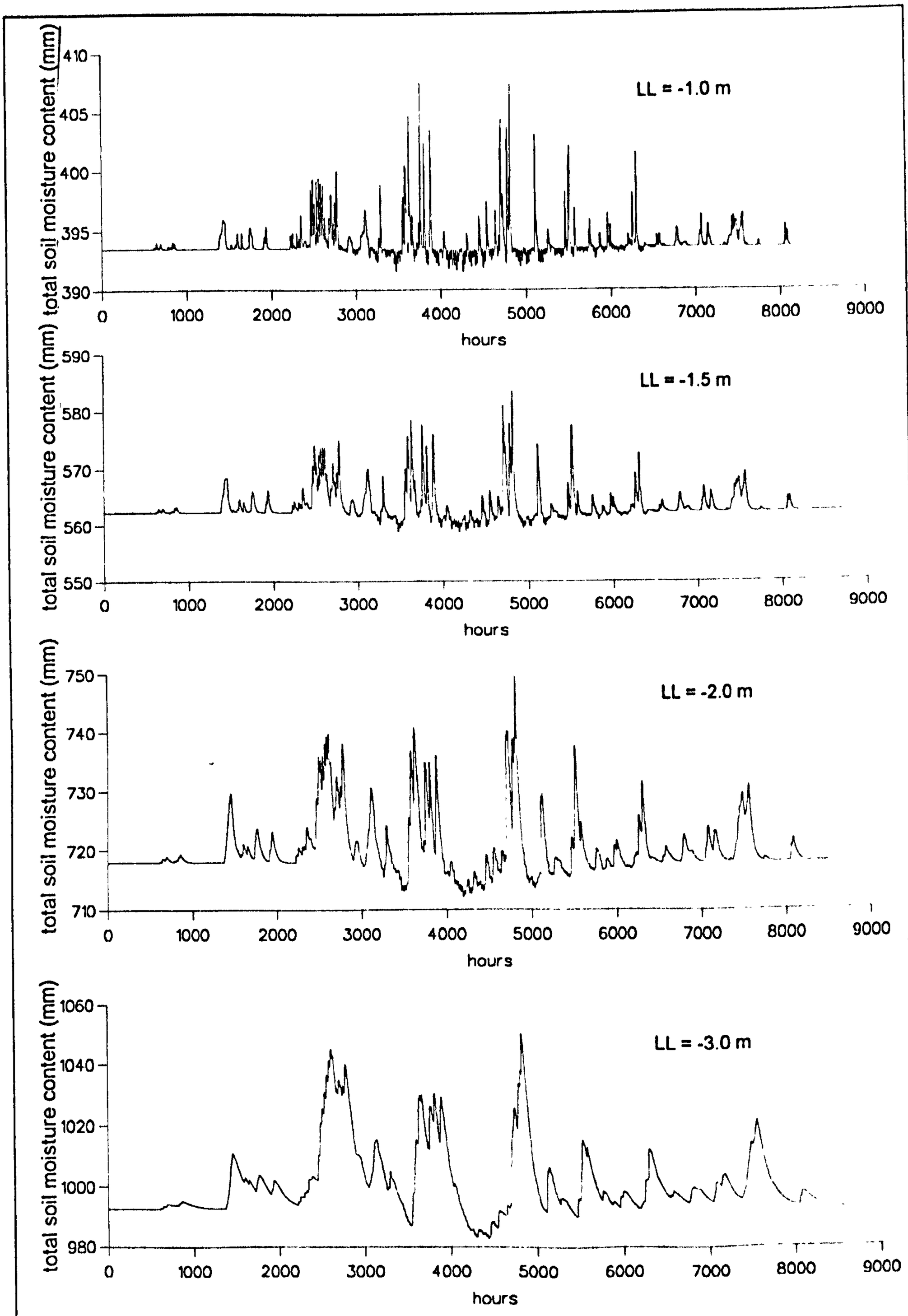

Figure 4.6 - Total soil moisture content simulated using FULCRUM - soil 1

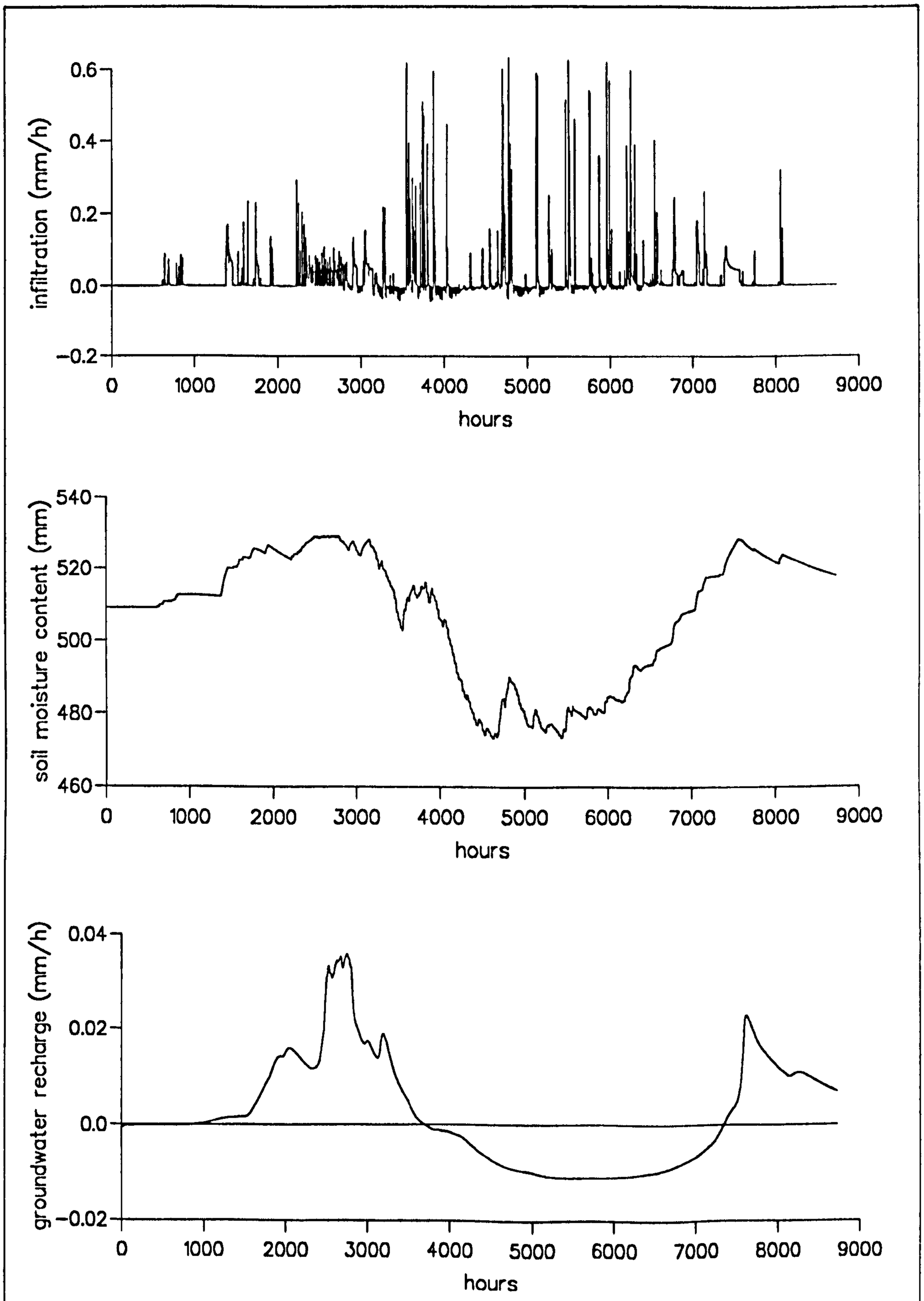

Figure 4.7 - Infiltration, total soil moisture content and groundwater recharge simulated using FULCRUM - soil 2 (LL = -1.0 m)

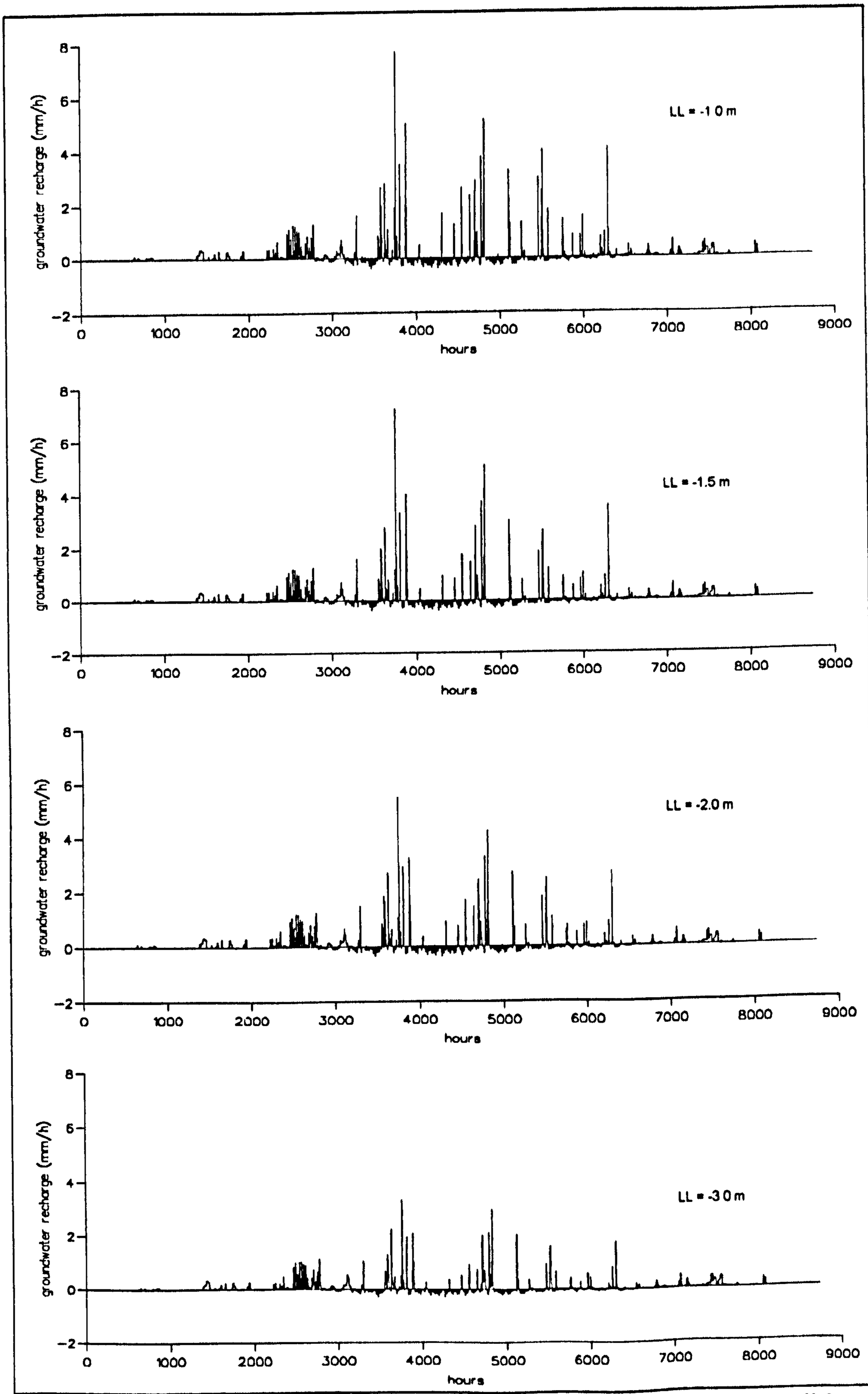

Figure 4.8 - Groundwater recharge simulated using FULCRUM - soil 3

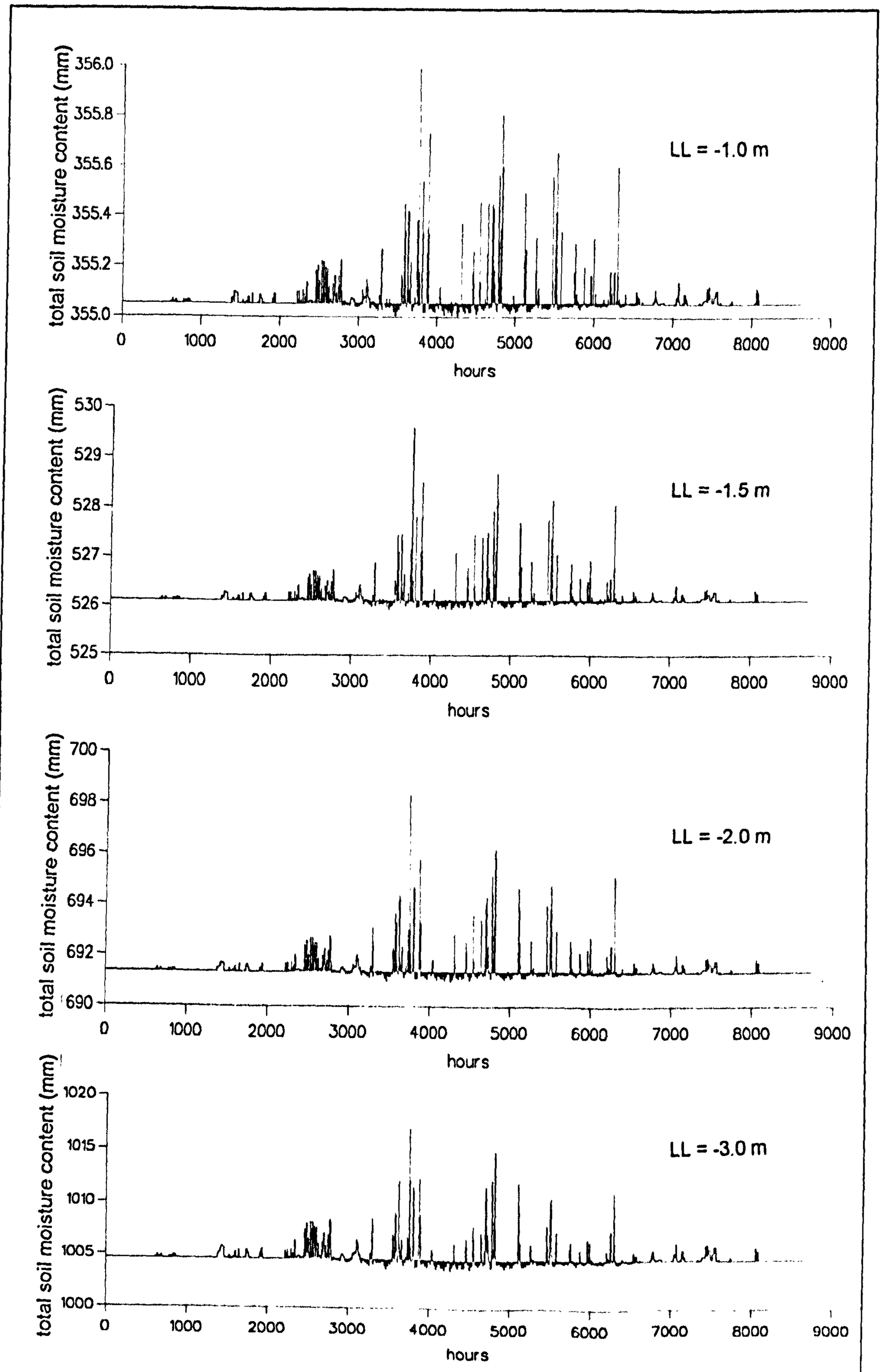

Figure 4.9 - Total soil moisture content simulated using FULCRUM - soil 3

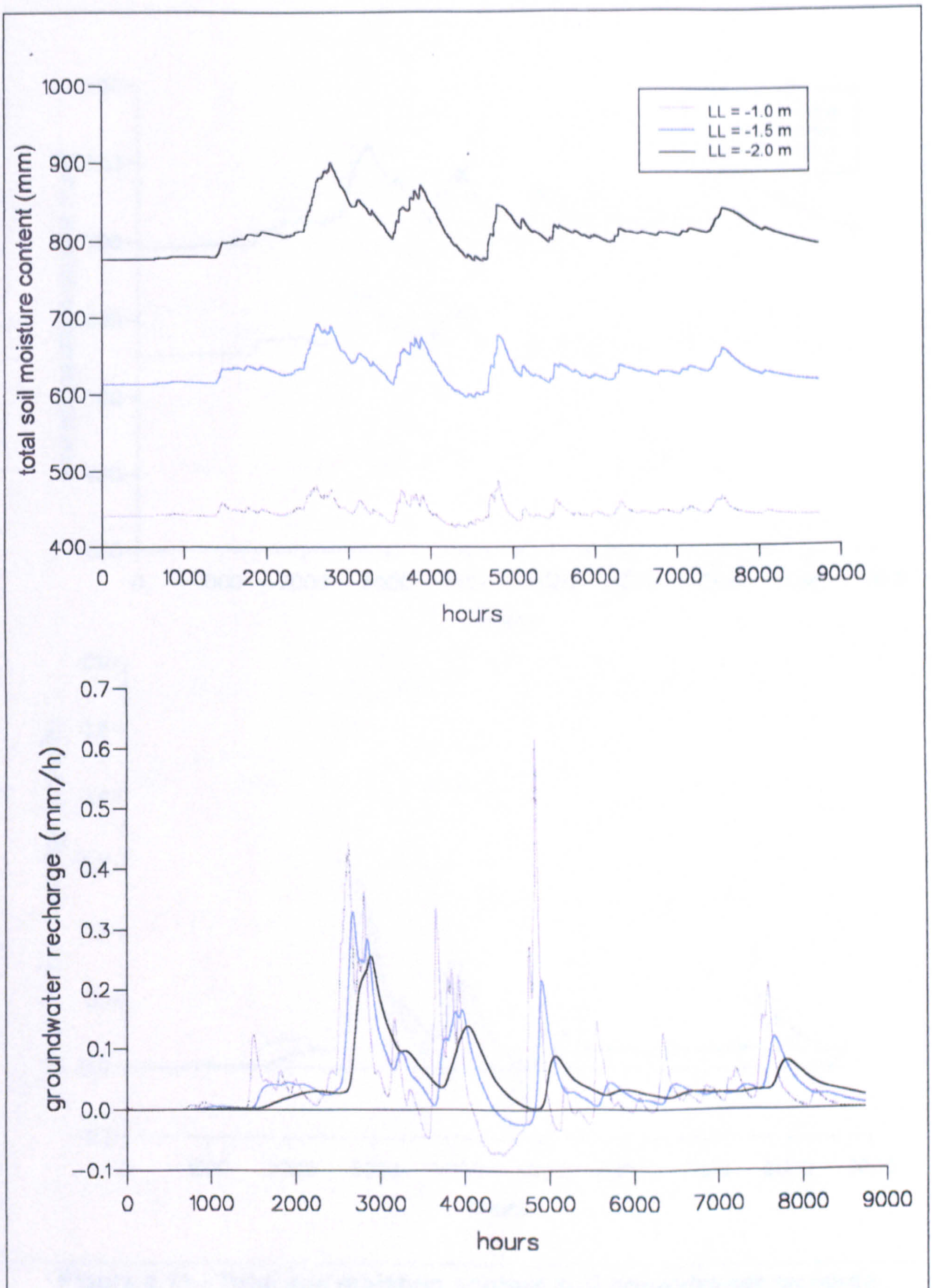

Figure 4.10 - Total soil moisture content and groundwater recharge simulated using FULCRUM - soil 5

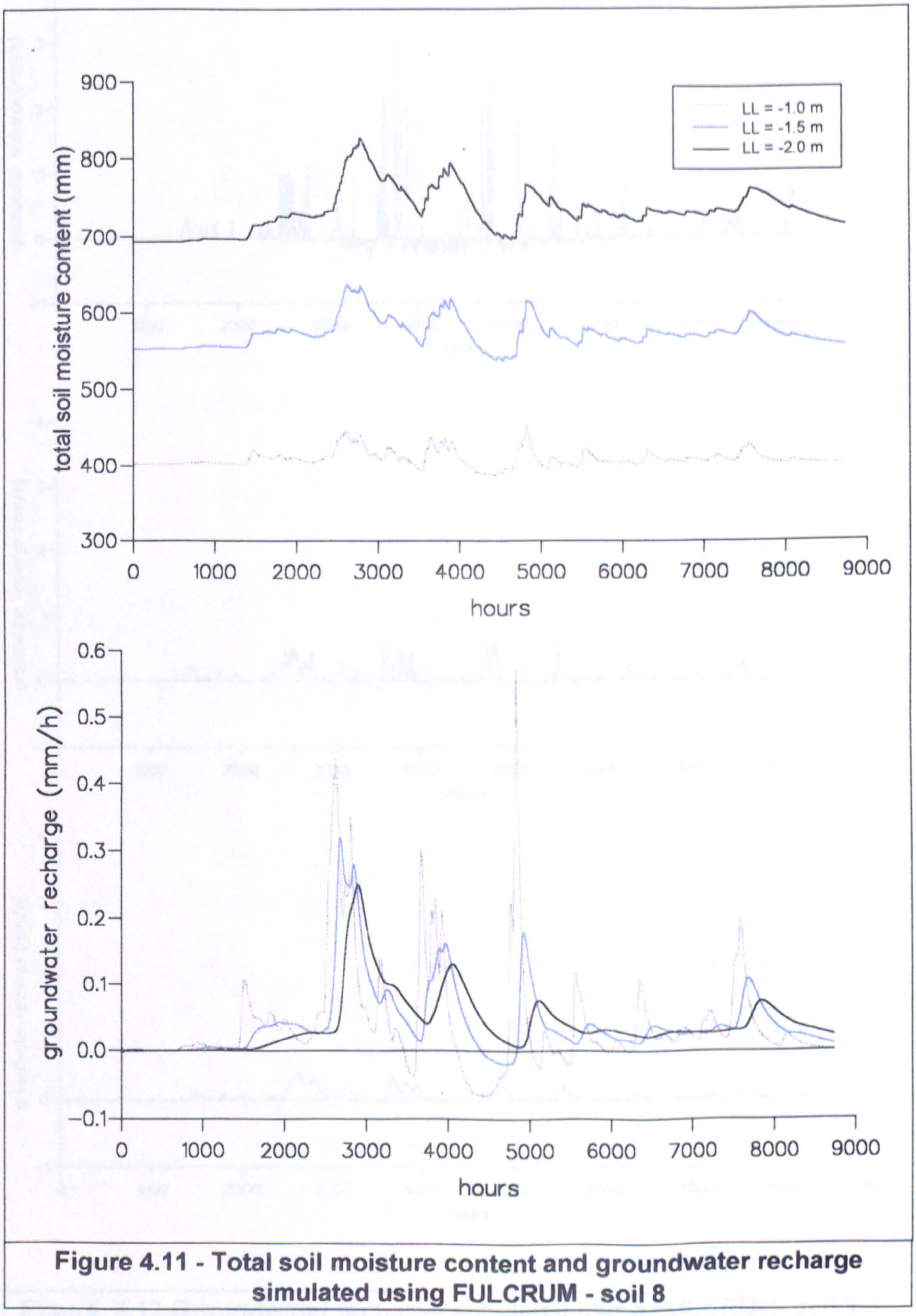

Figure 4.11 - Total soil moisture content and groundwater recharge simulated using FULCRUM - soil 8

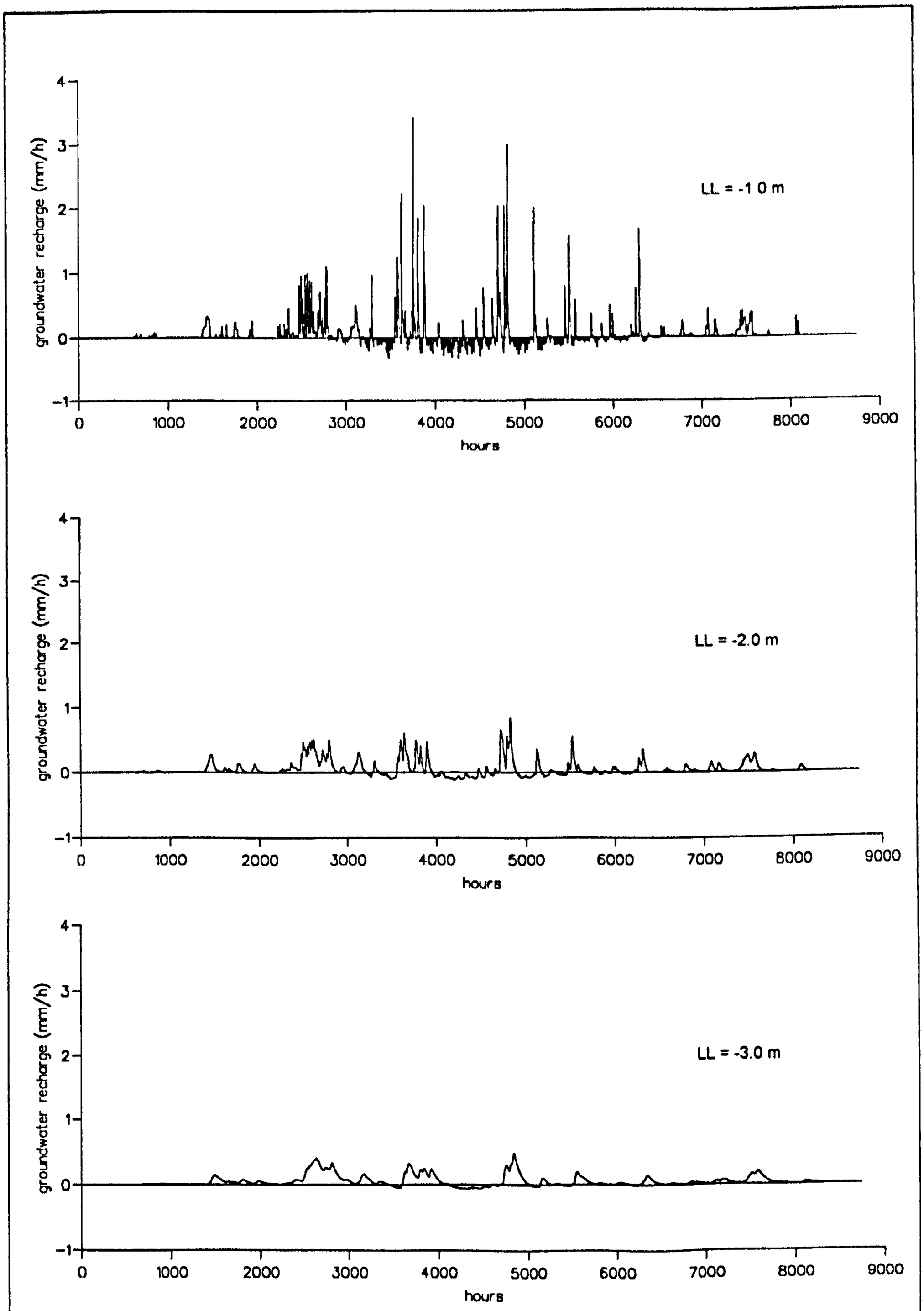

Figure 4.12-Groundwater recharge simulated using FULCRUM- soil 1-3

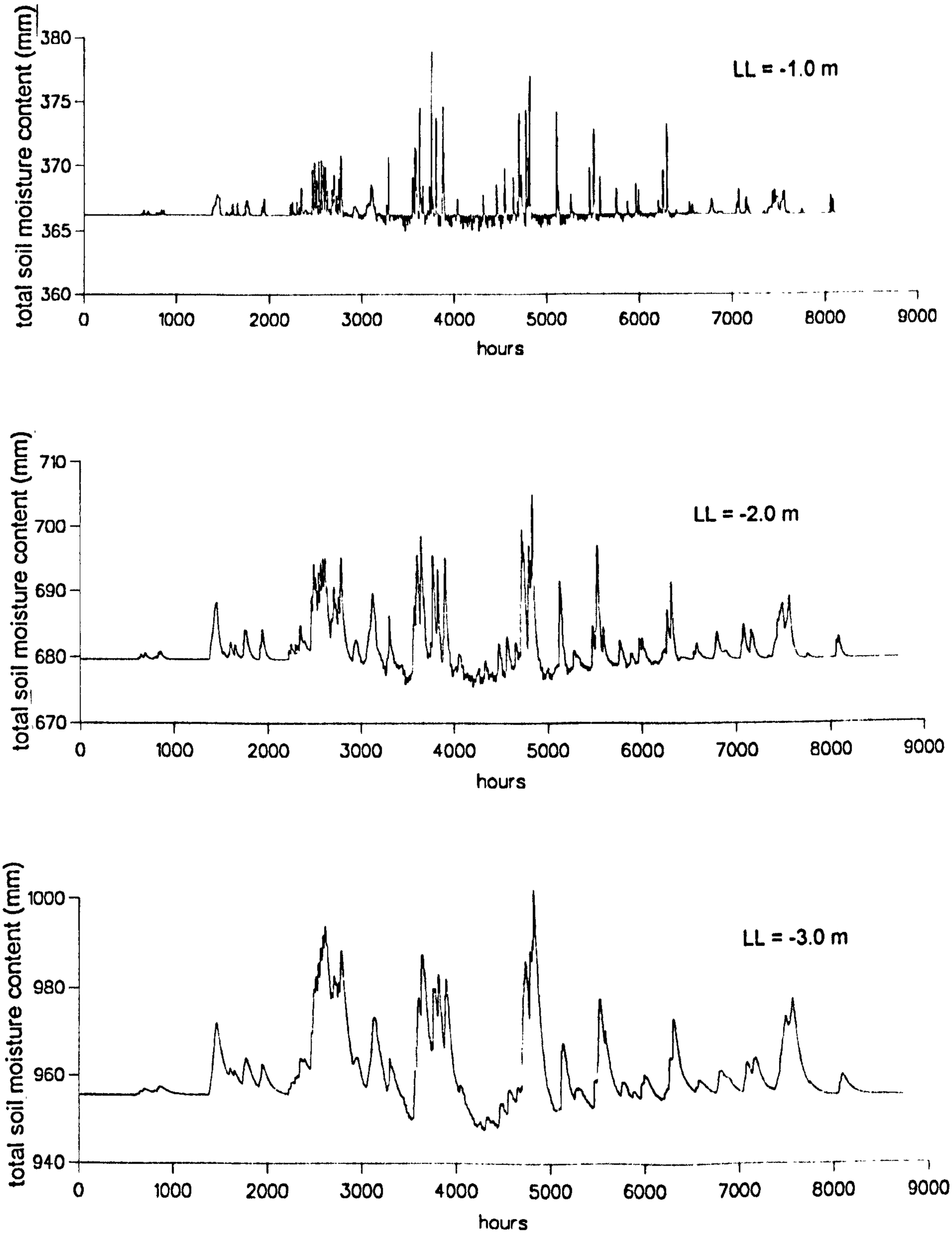

Figure 4.13-Total soil moisture content simulated using FULCRUM- soil 1-3

4.10, 4.11 and 4.13). In the case of soil 2 (Figure 4.7), between 4500 and 5000 hours the groundwater recharge hydrograph is decreasing while the soil moisture content is increasing. This is due to evaporation. As expected, soil 2 (silt clay) present a much smoother groundwater recharge hydrograph compared with the same phreatic surface depth (LL) for soils 1 and 3 (sand soils).

Mass balance errors were checked in two ways: for each time step during the execution of the code, and for the entire time series created using FULCRUM simulations. This showed that moisture is very well conserved in the simulations. The performance of FULCRUM was also tested in simulations using several different data sets which showed it to be very consistent.

4.10 - Summary

In this Chapter the simulation of at-a-point groundwater recharge rates using soil unsaturated zone elements was described. The model FULCRUM which represents water fluxes in the soil unsaturated zone by solving the one-dimensional Richards Equation (RE) was used in the simulations. FULCRUM includes the representation of interception and evaporation, and incorporates a numerical procedure to solve RE. The numerical solution implemented in FULCRUM was verified against the analytical solution presented by Srivastava and Jim-Yeh (1991).

A number of simulations were carried out for a period of one year and soil water infiltration rates, total soil moisture content and groundwater recharge rates were determined. These involved several different realistic scenarios, for a number of different soil types and groundwater phreatic surface depths. Mass balance verifications showed that moisture is very well conserved in the simulations. The time series form the basis for the design of the GRASP groundwater recharge component for the UP model element, developed in the next Chapter.

Chapter 5

Recharge Modelling for the UP Element

5.1 - Introduction

As a result of the study presented in this Chapter, the model GRASP (Groundwater Recharge modelling Approach with a Scaling up Procedure) is proposed to represent groundwater recharge for the UP (Upscaled Physically-based) macromodel element which was described in Chapter 3. GRASP consists of a hybrid approach comprising two different modelling schemes which are SM (Soil Moisture approach) and TF (Transfer Function approach). SM works on the macromodel element-scale (~100km^2) and groundwater recharge rates are given as a linear function of total soil moisture content. The SM model parameters are fitted to the element-scale groundwater recharge rates, aggregated (upscaled) from the point-scale. These point-scale groundwater recharge rates are estimated using the TF approach, which is based on linear transfer functions. TF includes a new approach in which the parameters of the transfer function are obtained directly from widely available soil property data.

In GRASP the starting point is the point-scale. This is strongly motivated by the fact that the data available for soil and rock properties are generally point values. Therefore it seemed reasonable to start from there and then go up to larger scales (this was discussed in sections 2.3 and 2.10).

For the design of both SM and TF it was assumed that recharge to groundwater involves only the routing of infiltrating rainfall through the unsaturated zone to the phreatic surface. This was equivalent to considering the unsaturated zone to be like a black box with properties that delay and smooth the transport of water from the soil's surface to the groundwater. The SM approach is based on a study to establish a

relationship between groundwater recharge rates and total soil moisture content and the TF approach relies on an input-output (infiltration and recharge rates respectively) analysis using linear transfer functions.

5.2 - SM (Soil Moisture content) Approach

In this approach an attempt is made to represent groundwater recharge rates as a function of total soil moisture content. The time series of total soil moisture content and groundwater recharge from FULCRUM were used in this study. In addition an unsuccessful attempt is made to derive a relationship between the parameterisation in the SM approach and soil physical properties.

5.2.1 - Total Soil Moisture Content and Groundwater Recharge

Figure 5.1 shows the values of recharge rate plotted against total soil moisture content for three combinations of soil type and depth to phreatic surface (LL). A number of modelling approaches have been studied to represent recharge rates as a function of total soil moisture content and it was observed that when a displacement in time is applied to the values of total soil moisture content (i.e. values of groundwater recharge at a current time step are related to total soil moisture content at a previous time), the plots have much less scatter (Figure 5.2) than those in Figure 5.1. This suggests the following functional form for calculating recharge from total soil water content:

$$r_t = DD*(Wuz_{t-\delta} - Weq) \qquad \text{eqn. (5.1)}$$

where,

r_t - groundwater recharge rate at time t (mm/h);

DD and δ - constant parameters (DD in h^{-1} and δ in hours);

Wuz - unsaturated zone total soil moisture content simulated by FULCRUM (mm);

Weq - soil moisture content for equilibrium over the unsaturated soil column (mm)

Weq is the initial condition for total soil moisture content in all FULCRUM simulations. It is the total soil moisture content in the soil column for which both infiltration and groundwater recharge are equal zero.

(a) soil 1 - LL = -1.0 m

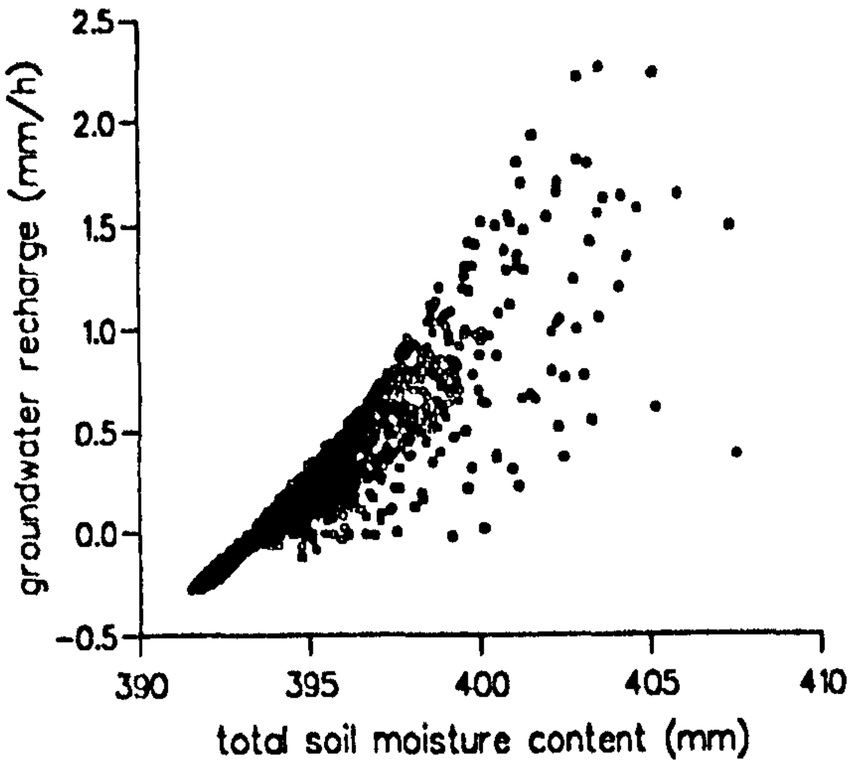

(b) soil 1 - LL = -3.0 m

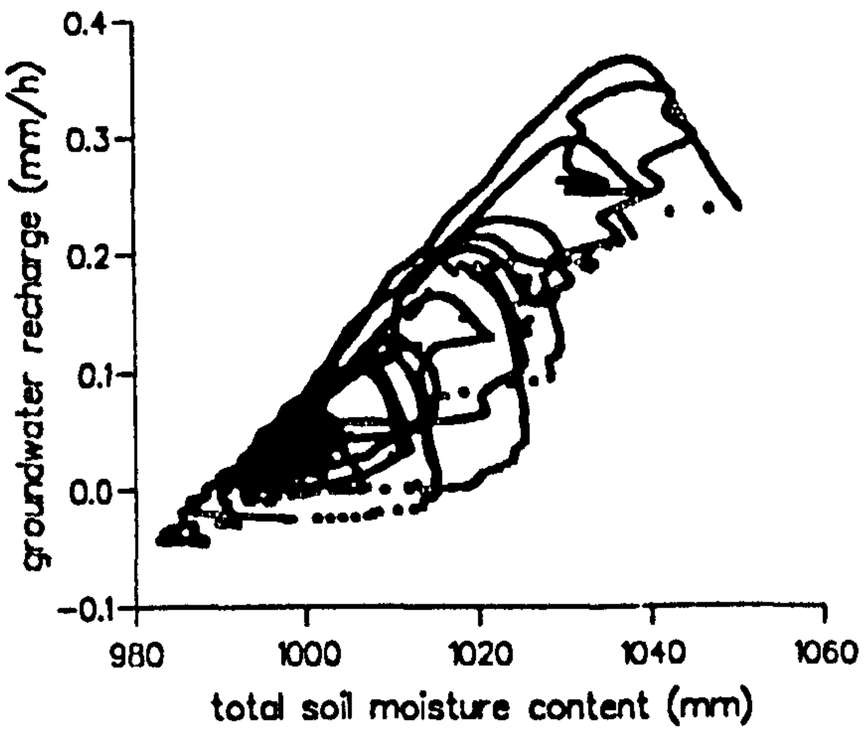

(c) soil 5 - LL = -1.5 m

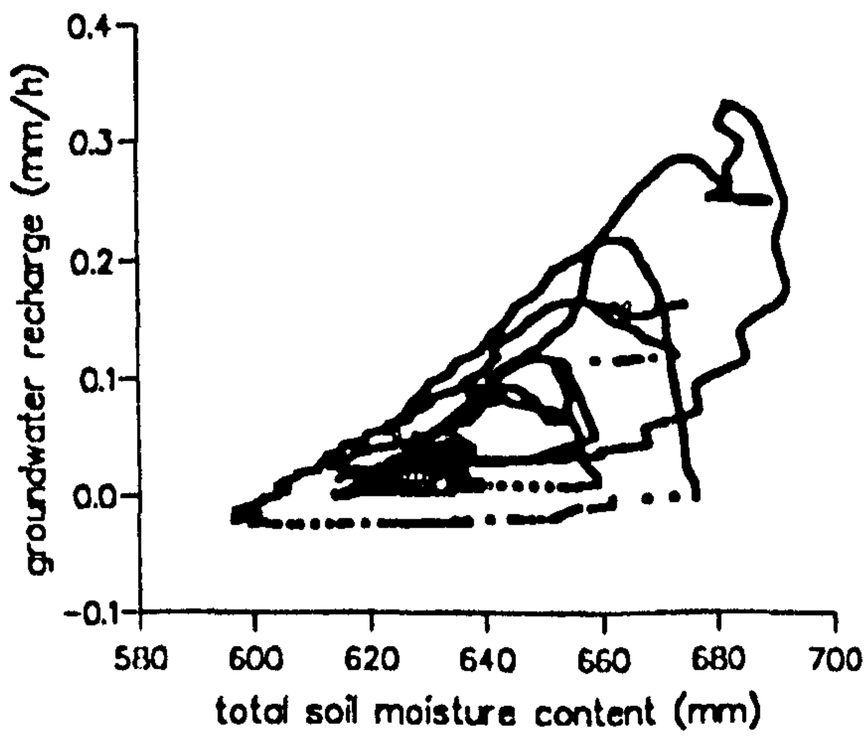

Figure 5.1 - Plots for total soil moisture content and groundwater recharge: no time lag considered

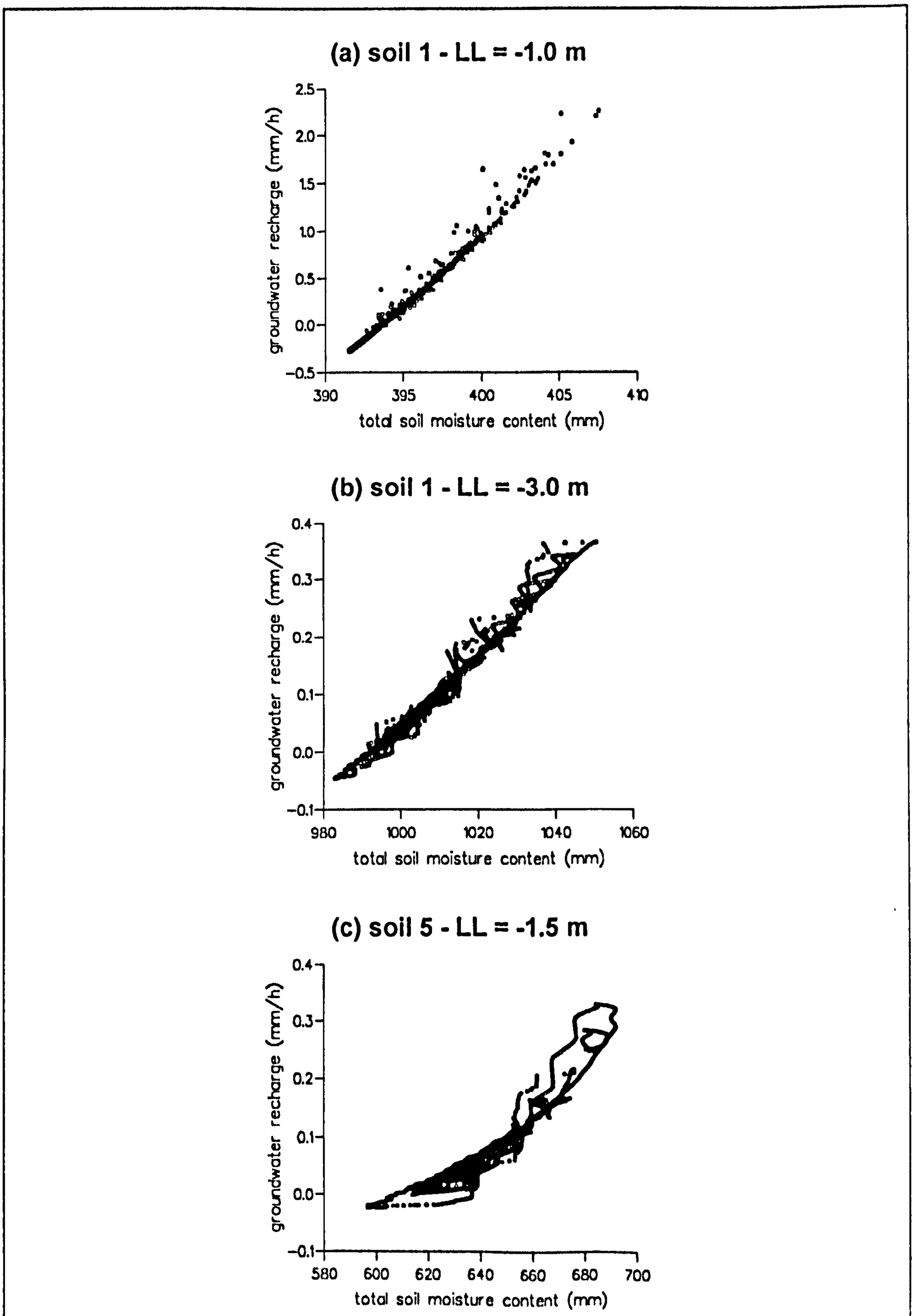

Figure 5.2 - Plots for total soil moisture content and groundwater recharge: time lag considered

The values of Weq can be eliminated from the eqn. (5.1) using the continuity equation, given by:

$$\frac{d}{dt}(WW_t) = input_t - r_t \qquad \text{eqn. (5.2)}$$

where,

WW_t - $(Wuz_{t-\delta} - Weq)$, in mm;

$input_t$ - (infiltration – transpiration) at time t, in mm/h.

The SM approach results from the application of both eqns. (5.1) and (5.2).

The values of the parameters DD and δ (eqn. 5.1) for each soil column and phreatic surface depths were adjusted by automatic calibration using the time series simulated by FULCRUM. The routine AMOEBA (which is based on the Nelder and Mead (1968) direct search method; Press et al., 1992) was applied using a minimum least squares function for the objective function. Table 5.1 shows the calibration results.

The regression results are generally quite good. The coefficient of determination is always around 0.9, except for the silt clay soil. For this soil, recharge rates for phreatic surface depths (LL) greater than 1.0m are extremely small and the hydrographs are very smooth. Therefore, simulations with LL greater than 1.0m were excluded from further analysis for the silt clay soil.

The best value for parameter δ varies throughout the year, so the values fitted by the optimisation represent average values over a year. In the case of soils 1, 3, 5 and 8 the variation through the year is relatively small. However, the poor result for soil 2 (silt clay soil) is due to the high variability of δ over the year. Figures 5.3 to 5.12 show some examples of groundwater recharge rates simulated using the SM approach (i.e. using eqns. 5.1 and 5.2) and rates calculated using FULCRUM. The differences between the two simulated recharge rates are also plotted, given by subtracting the recharge rates using the SM approach from the values using FULCRUM. These results show that eqns. 5.1 and 5.2 represent very well the recharge rates given using FULCRUM (note, the time period simulated is the time period used in the calibration of DD and δ, and the purpose is to show that the SM approach can produce good simulations of recharge rate, despite the simplicity of the SM equations).

Table 5.1 - Calibration results for DD and δ from the SM approach

soil no.	soil type	LL (m)	DD ($hours^{-1}$)	δ (hours)	R^{2} *
1	upper sand	1.0	1.54×10^{-01}	02	0.988
		1.5	4.93×10^{-02}	05	0.995
		2.0	2.07×10^{-02}	10	0.993
		3.0	6.33×10^{-03}	38	0.986
2	silt clay	1.0	6.25×10^{-04}	74	0.739
3	lower sand	1.0	7.510	00	0.992**
		1.5	1.550	00	0.970**
		2.0	6.63×10^{-01}	01	0.935
		3.0	2.81×10^{-01}	01	0.995
5	Anglezarke A	1.0	9.06×10^{-03}	25	0.932
		1.5	3.19×10^{-03}	77	0.889
		2.0	1.76×10^{-03}	157	0.856
8	Blackwood A	1.0	7.99×10^{-03}	28	0.923
		1.5	2.86×10^{-03}	89	0.874
		2.0	1.60×10^{-03}	175	0.842
soil 1 - 3	half soil type 1 and half soil type 3	1.0	2.53×10^{-01}	01	0.991
		2.0	3.26×10^{-02}	06	0.995
		3.0	9.92×10^{-03}	22	0.984

* $R^2 = 1 - \frac{\sum_{t=1}^{end} (r_t - r_t^{FULCRUM})^2}{\sum_{t=1}^{end} (r_t^{FULCRUM} - r_t^{FULCRUM})^2}$, where r_t and $r_t^{FULCRUM}$ are the recharge rates predicted using the SM approach and FULCRUM respectively.

** when delay is zero the model is reduced to a one-parameter model.

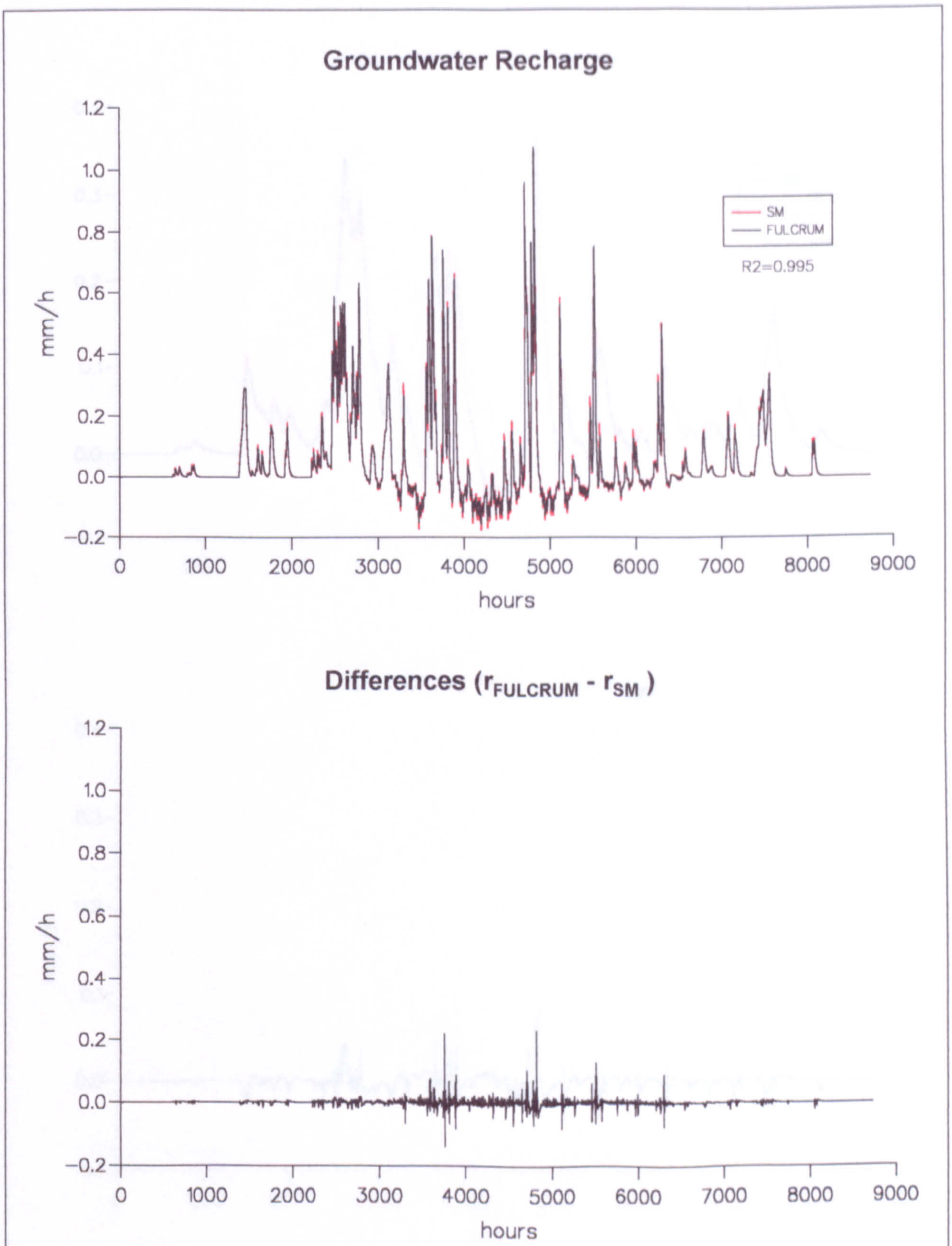

Figure 5.3 - SM approach: results for soil 1 (LL = -1.5 m)

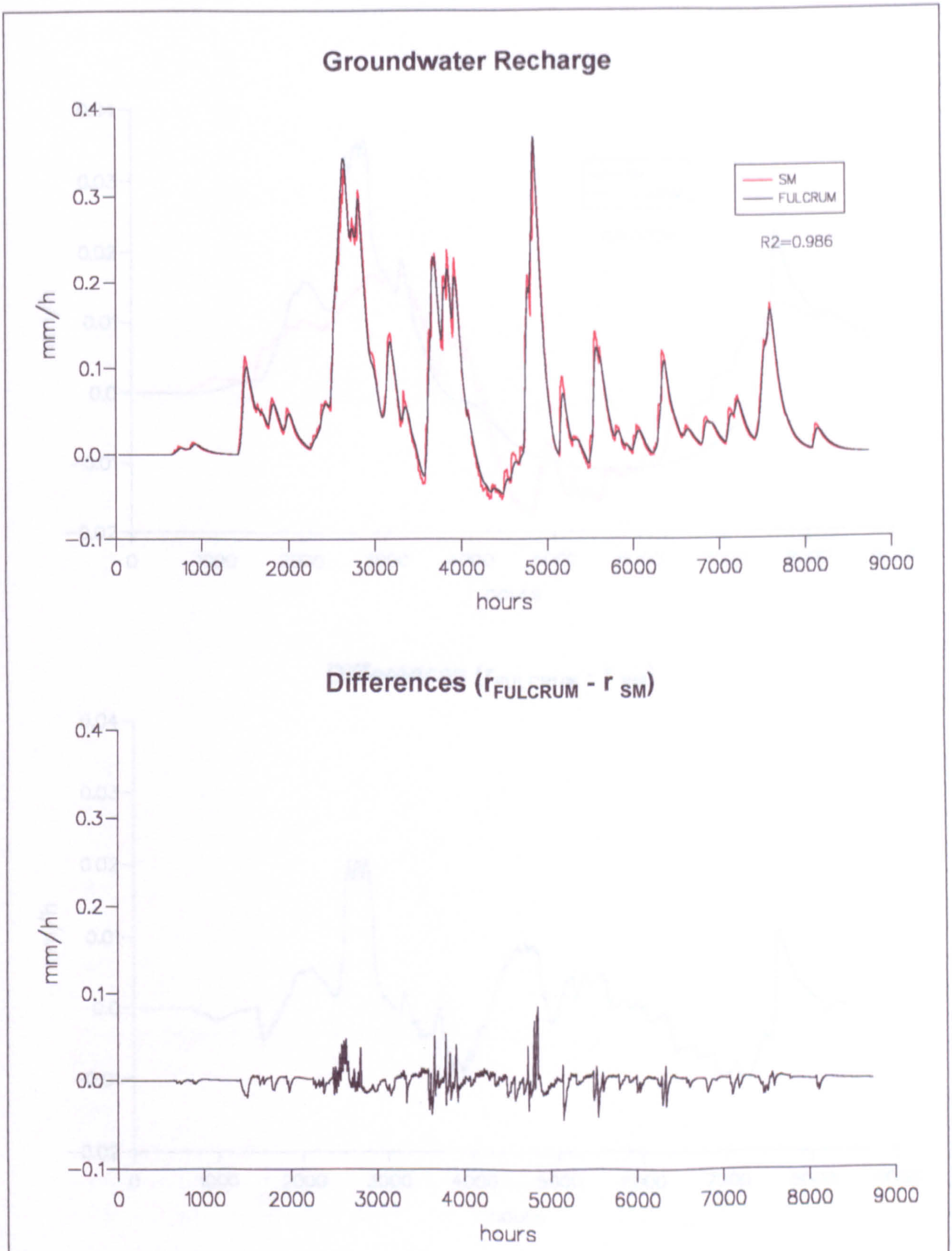

Figure 5.4 - SM approach: results for soil 1 (LL = -3.0 m)

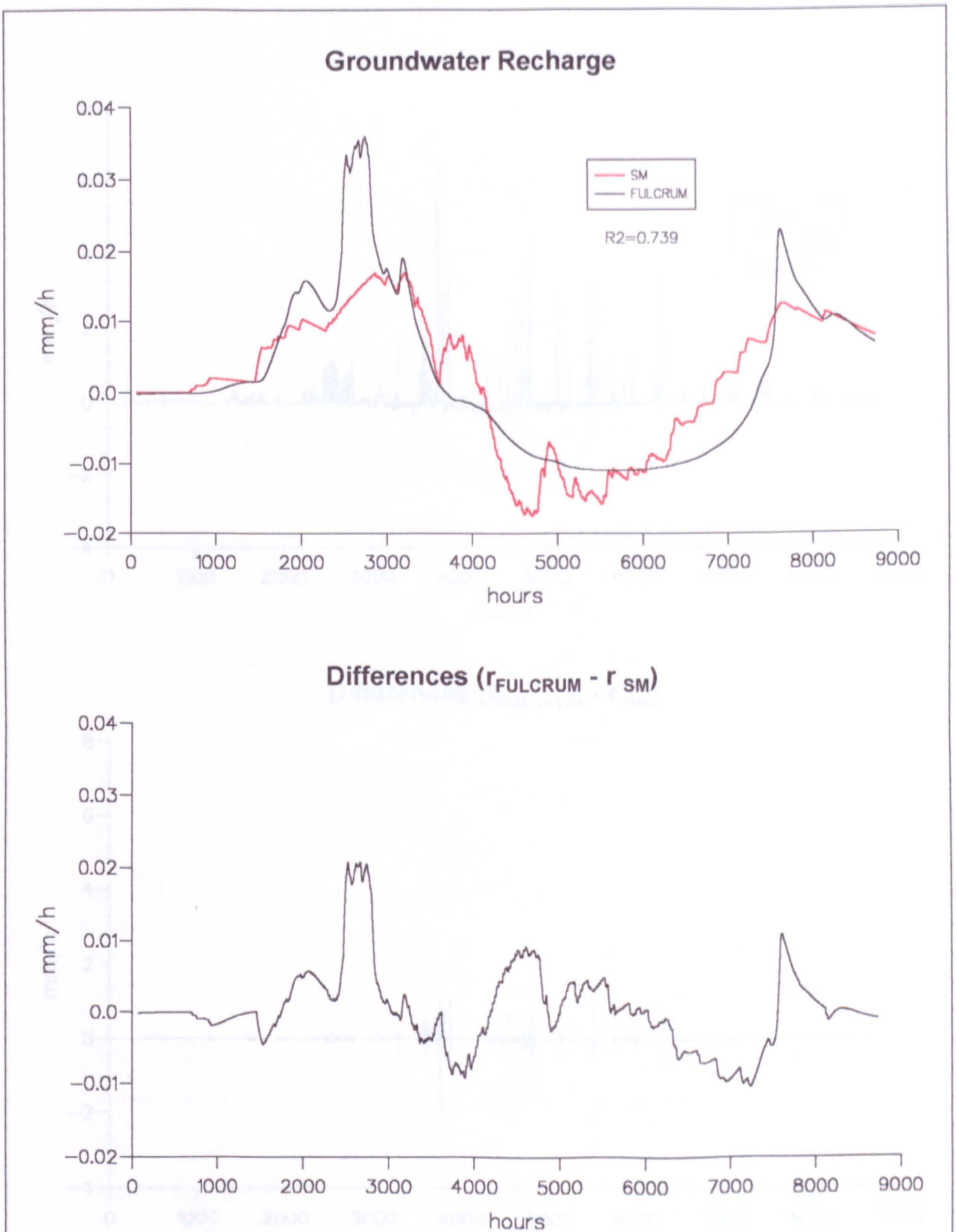

Figure 5.5 - SM approach: results for soil 2 (LL = -1.0 m)

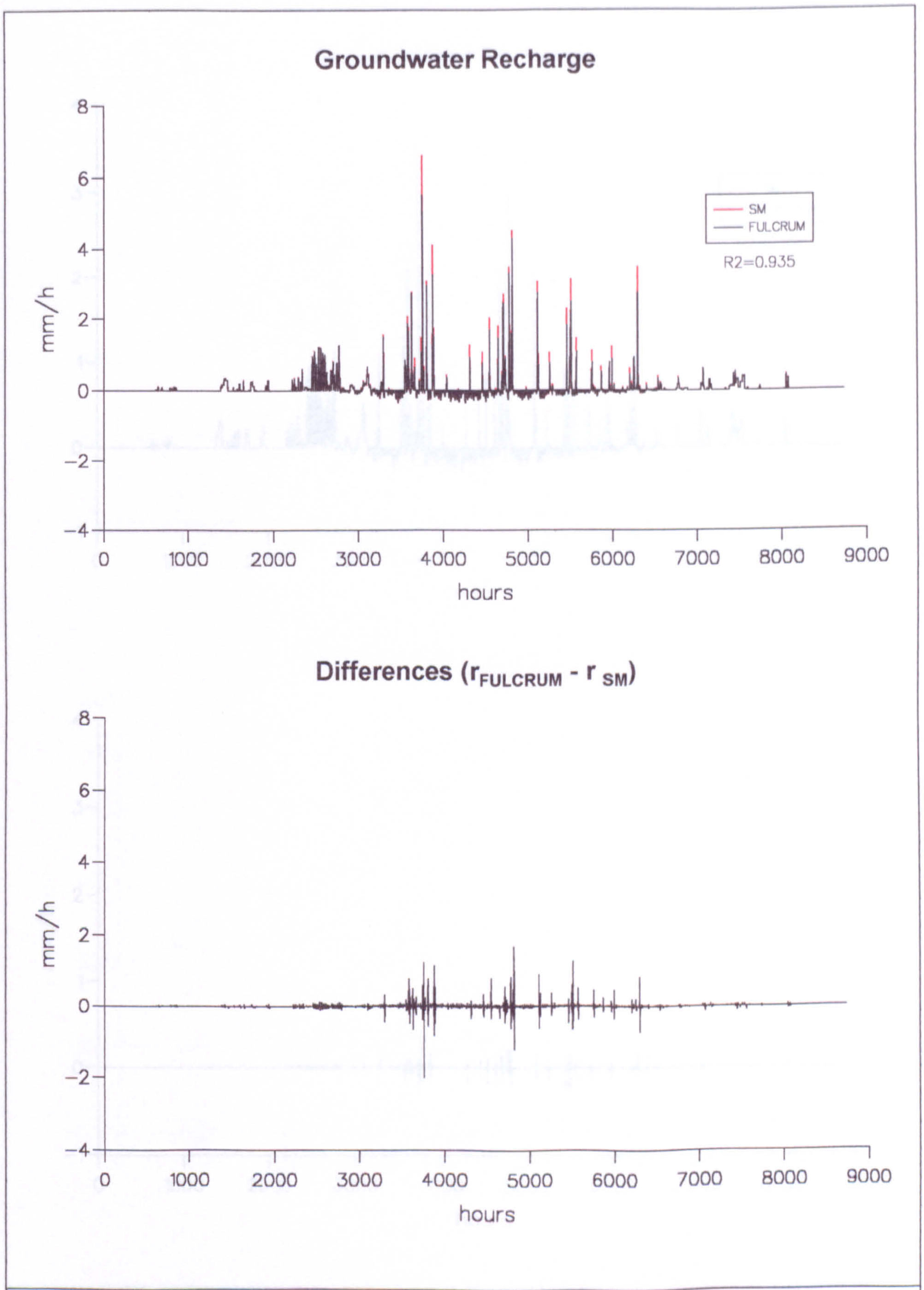

Figure 5.6 - SM approach: results for soil 3 (LL = -2.0 m)

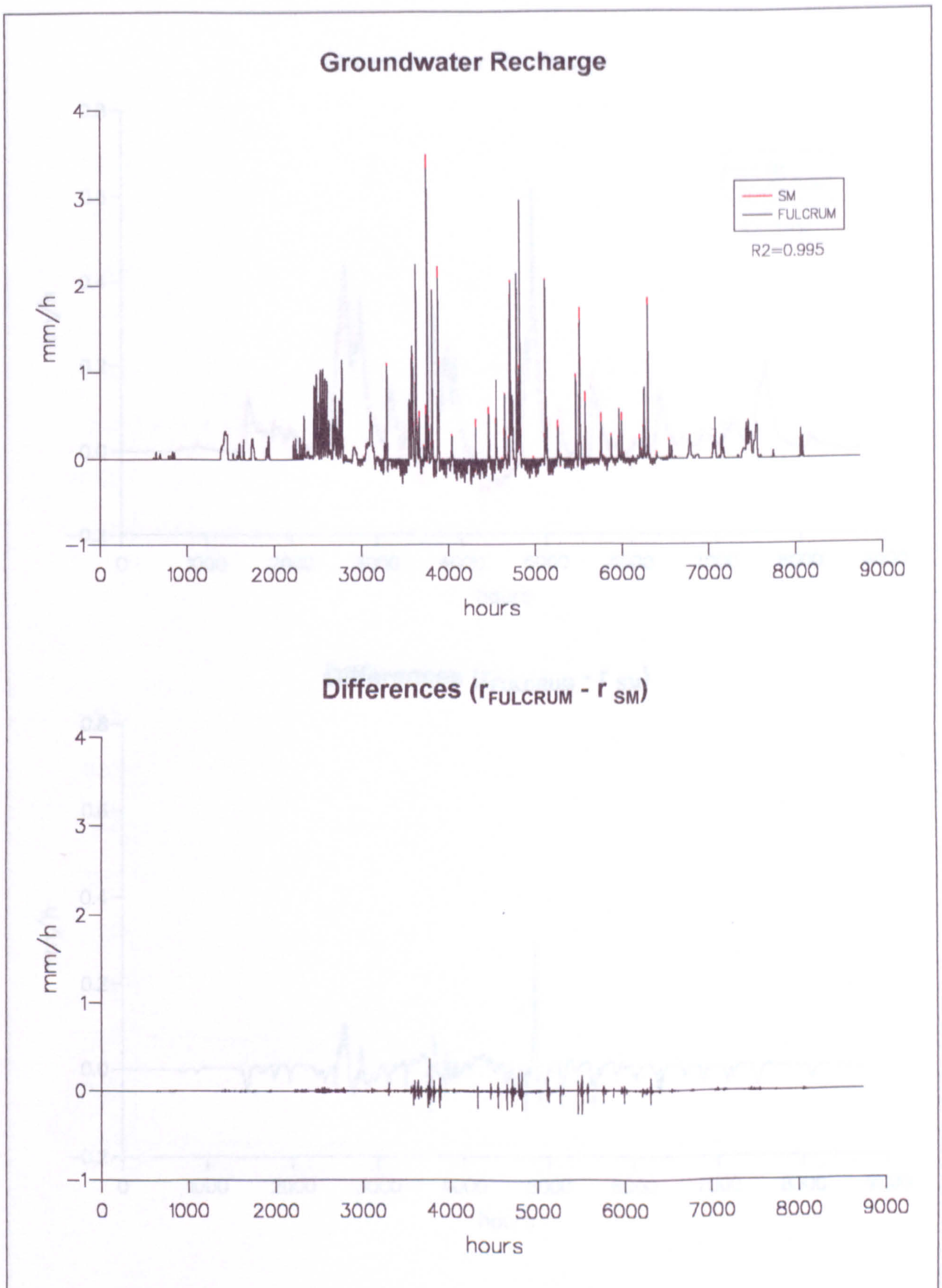

Figure 5.7 - SM approach: results for soil 3 (LL = -3.0 m)

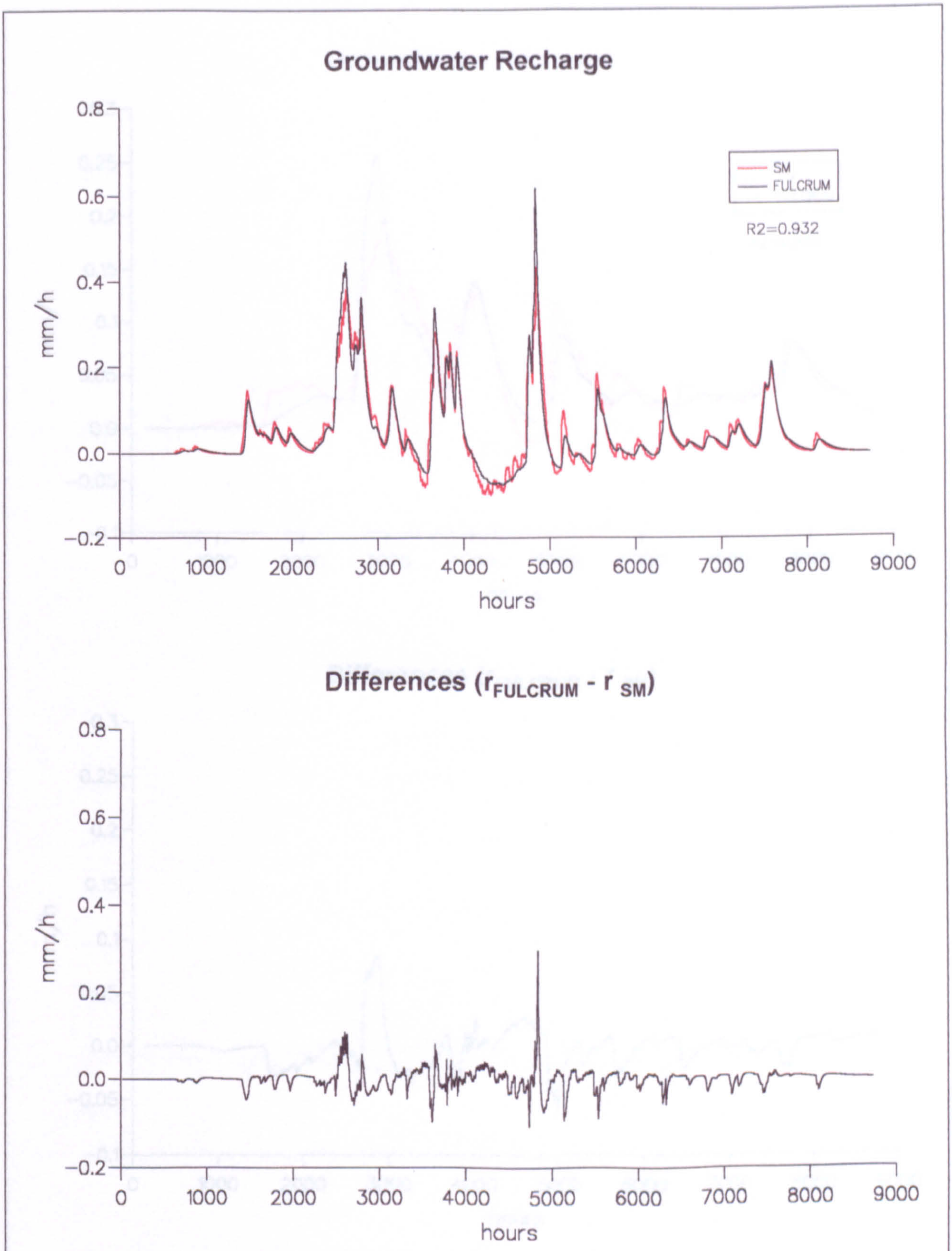

Figure 5.8 - SM approach: results for soil 5 (LL = -1.0 m)

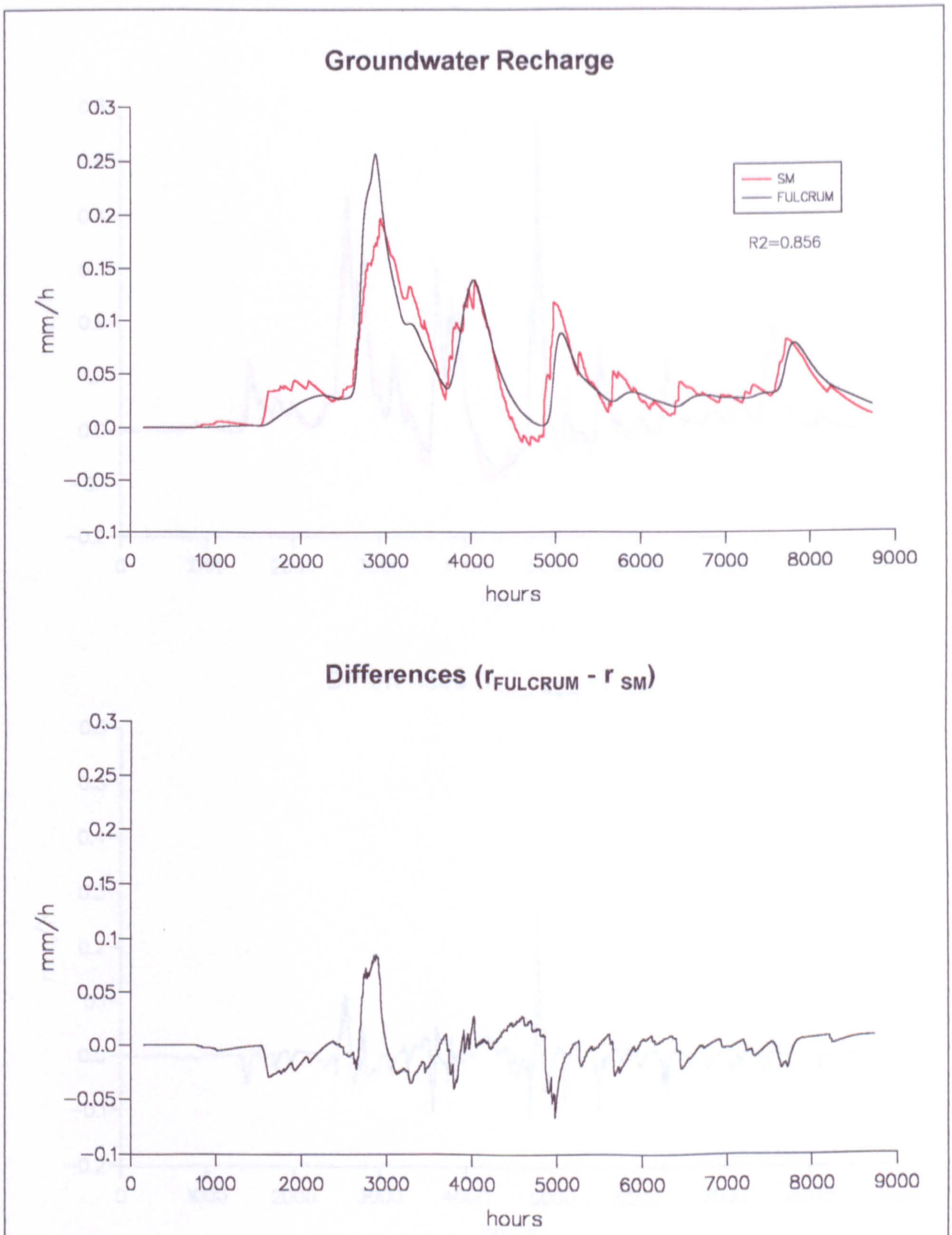

Figure 5.9 - SM approach: results for soil 5 (LL = -2.0 m)

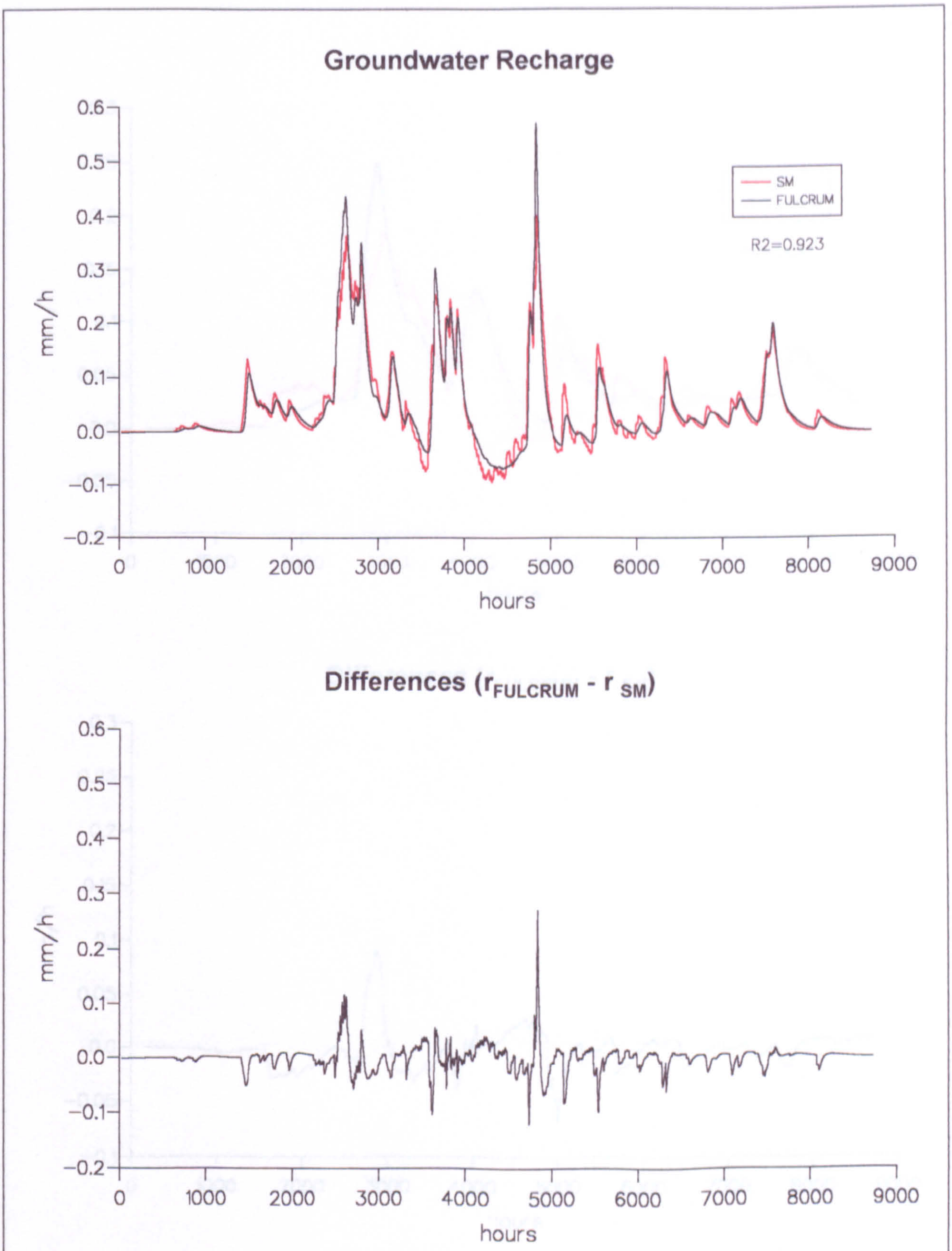

Figure 5.10 - SM approach: results for soil 8 (LL = -1.0 m)

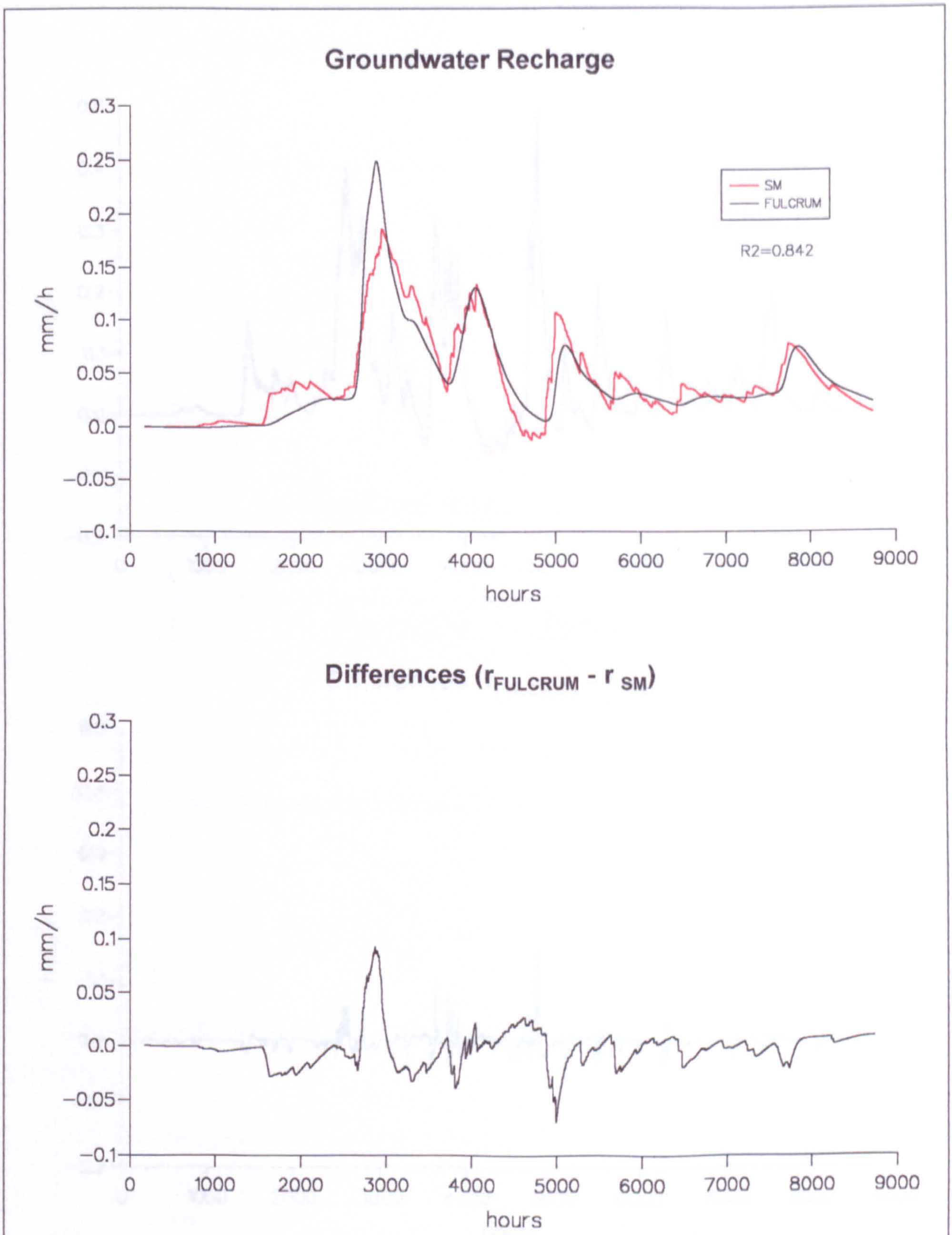

Figure 5.11 - SM approach: results for soil 8 (LL = -2.0 m)

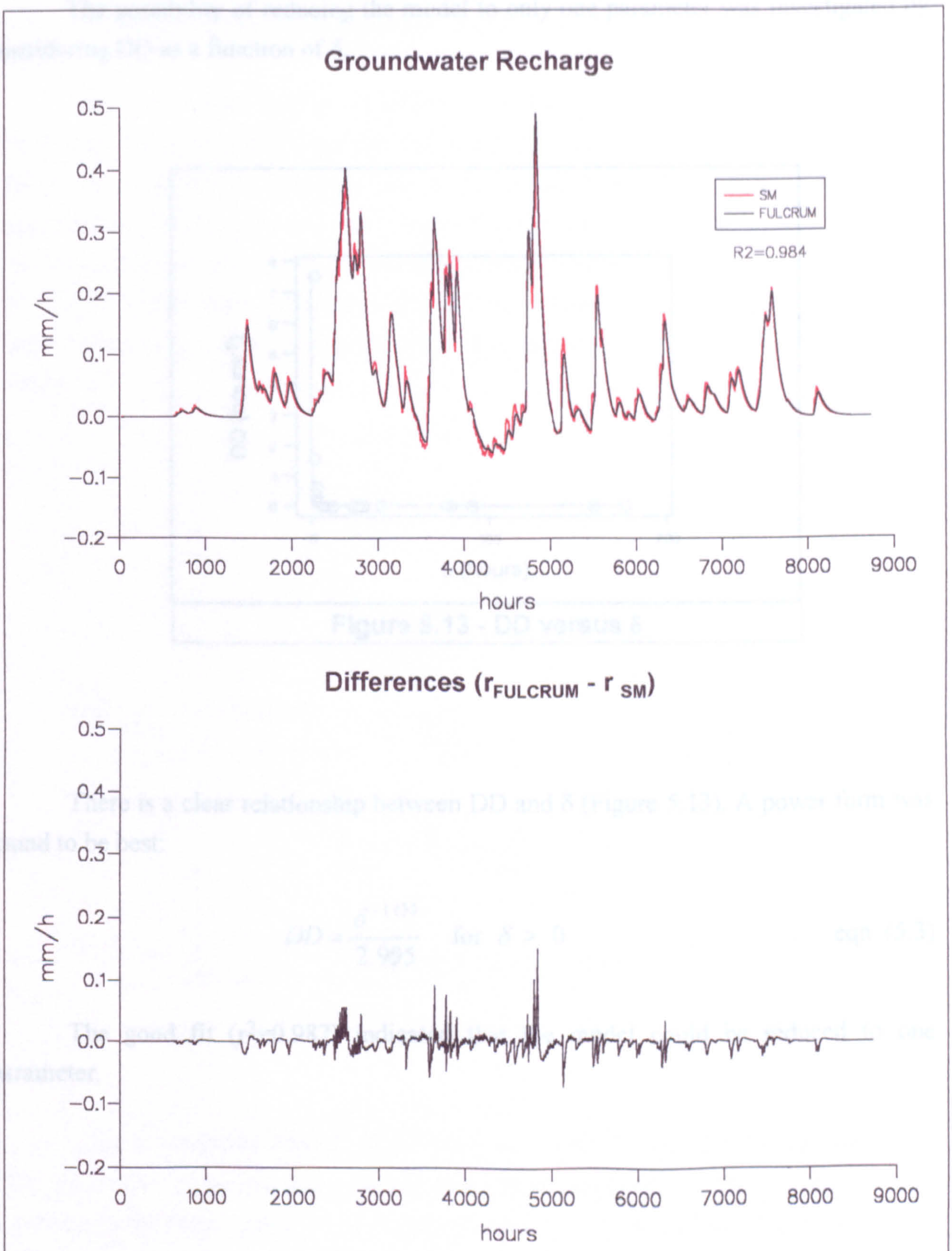

Figure 5.12 - SM approach: results for soil 1-3 (LL = -3.0 m)

The possibility of reducing the model to only one parameter was investigated by considering DD as a function of δ.

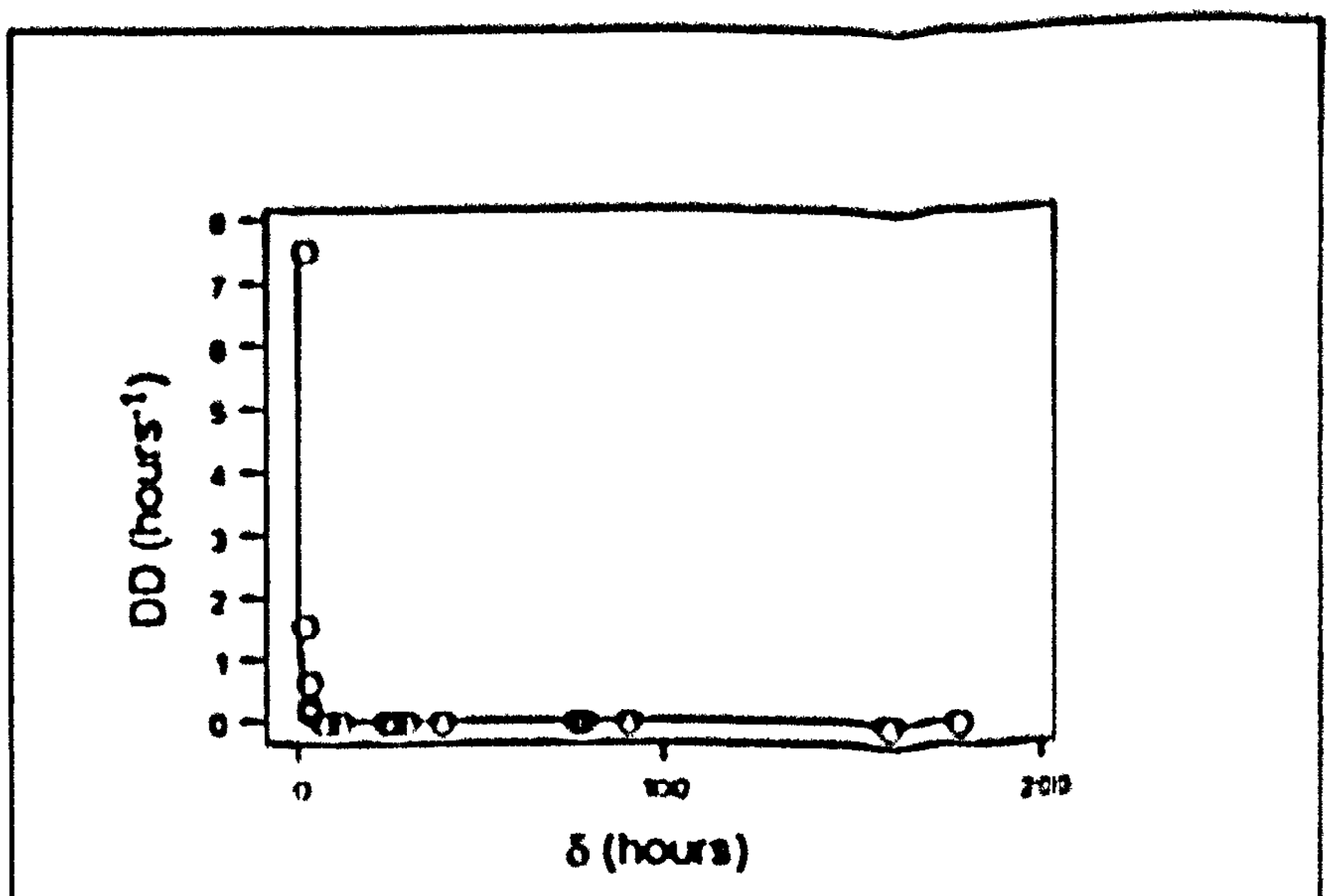

Figure 5.13 - DD versus δ

There is a clear relationship between DD and δ (Figure 5.13). A power form was found to be best:

$$DD = \frac{\delta^{-1.005}}{2.995} \quad \text{for } \delta > 0 \qquad \text{eqn (5.3)}$$

The good fit (r^2=0.987) indicated that the model could be reduced to one parameter.

5.2.2 - Parameter δ (SM approach) and Soil Properties

It is not an easy task to establish a mathematical relationship between δ and soil properties. Apart from the uncertainty of which soil characteristics should be considered, there are a number of pathways that could be taken for the analysis. The approach applied here is quite intuitive and simple. The soil hydraulic characteristics chosen for the analysis are widely known or considered easy to obtain. The δ parameter is thought to be related to the water travel time through the unsaturated zone towards the saturated zone. Figure 5.14 shows δ versus the phreatic surface depth (LL) for all the cases listed in Table 5.1.

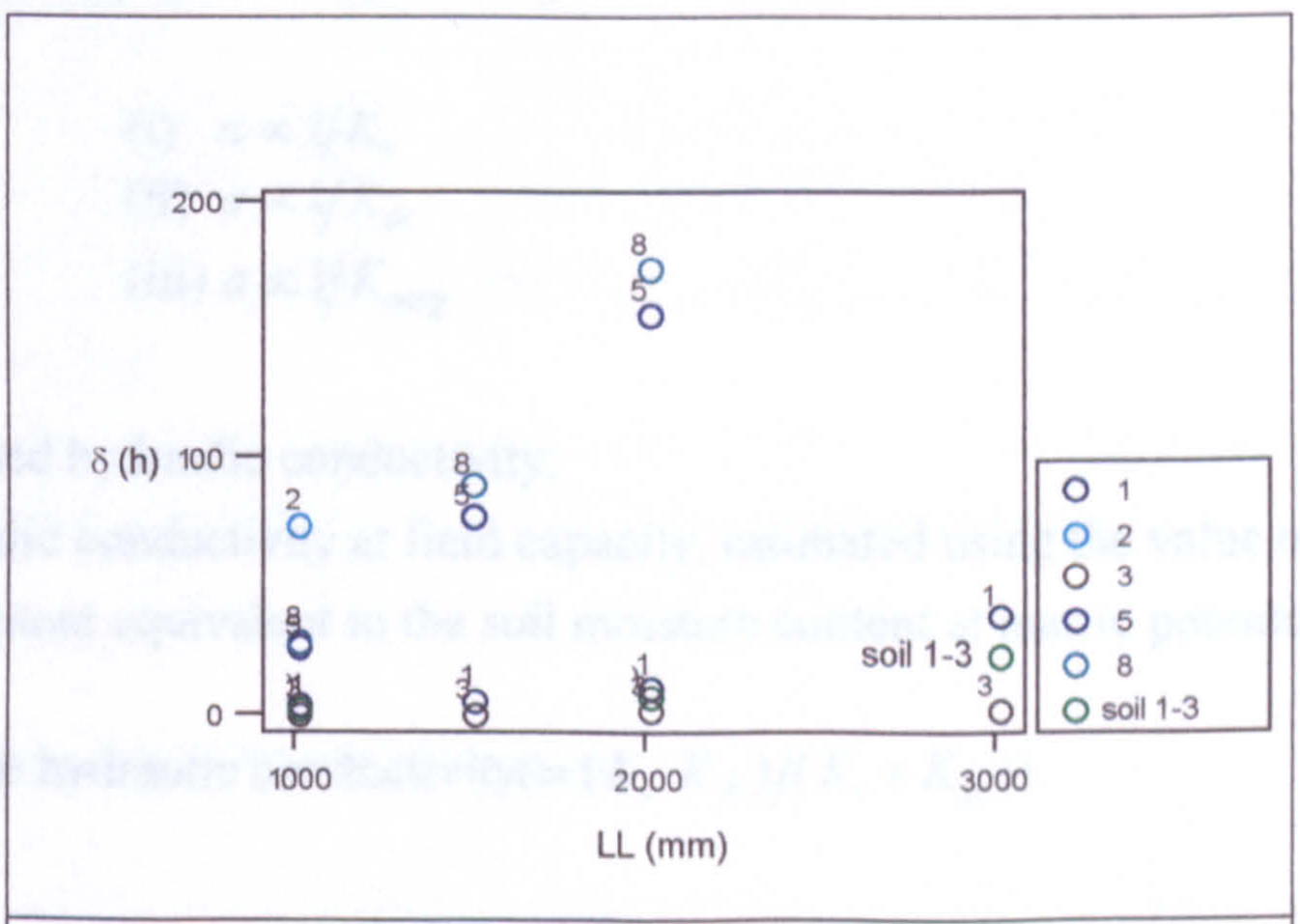

Figure 5.14 - δ versus LL

The δ parameter appears to generally increase with phreatic surface depth (LL). The dispersion of points shows clearly that the gradients of the fitted functions would increase in the order: soil 3, soil1-3 (composed soil column: half soil 1 and half soil 3), soil 1, soil 5, soil 8 and soil 2. So, it seems that soil 3 is the one which transfers water fastest and; soil 8 and, apparently (because only one simulation has been considered for soil 2), soil 2 the slowest.

δ and an Analogy to the Flux Average Velocity

This attempt is very intuitive and purely assumes that parameter δ is associated with the time taken for water to reach the saturated zone from surface:

$$\delta = \frac{LL}{v}, \text{ where } v \text{ is an average flux velocity.}$$

In order to relate parameter δ to soil properties, attempts have been made to find soil properties that could be associated with the values of the gradient (*a*, constant for each soil type) of the lines that could be fitted to the plots in Figure 5.14. Three different hypotheses that could explain the values of *a* were considered, using different characteristic values of hydraulic conductivity:

(i) $a \propto 1/K_s$
(ii) $a \propto 1/K_{fc}$
(iii) $a \propto 1/K_{avrg}$

where,

K_s - soil saturated hydraulic conductivity;

K_{fc} - soil hydraulic conductivity at field capacity, estimated using the value of moisture content equivalent to the soil moisture content at matric potential equal to -333 cm;

K_{avrg} - soil average hydraulic conductivity($= (K_s . K_{fc})/(K_s + K_{fc})$).

Table 5.2 shows these values for each soil type. By inspecting Figure 5.14, *a* follows the pattern:

$$a_{soil2} > a_{soil8} > a_{soil5} > a_{soil1} > a_{soil1-3} > a_{soil3}$$

Turning to Table 5.2 it can be observed that both of K_{fc} and K_{avrg} seem to follow a similar pattern (inverse order). However, if $a = 1/K_{fc}$ or $a = 1/K_{avrg}$, the estimated values for parameter δ are very poor compared to those obtained by optimisation. Therefore, some other variable is necessary to explain the values of the coefficient *a*. In one attempt to improve the definition of a, the depth to the phreatic surface (LL) was reduced by a factor proportional to soil porosity, in order to account for the presence of the matrix. These plots are shown in Appendix B. This, however, was not successful. Other attempts

involved using soil saturated hydraulic conductivity, porosity and depth to the phreatic surface in a multiple regression analysis. However, as for the above attempts, the results were not encouraging.

Table 5.2 - Soil hydraulic conductivity characteristics

soil no.	(1) θ_s	(2) θ_r	(3) θ_{fc}	(4) $(\theta_s-\theta_r)$	(5) $(\theta_s-\theta_{fc})$	(6) K_s (cm/h)	(7) K_{fc} (cm/h)	(8) K_{avrg} (cm/h)
1	0.430	0.090	0.247	0.340	0.183	2.75	0.426×10^{-02}	0.425×10^{-02}
2	0.530	0.220	0.397	0.310	0.133	0.0042	0.198×10^{-04}	0.197×10^{-04}
3	0.360	0.060	0.294	0.300	0.066	7.917	0.545	0.510
5	0.602	0.135	0.275	0.467	0.327	8.833	0.885×10^{-04}	0.885×10^{-04}
8	0.595	0.093	0.230	0.502	0.365	12.625	0.710×10^{-04}	0.710×10^{-04}
soil 1-3	0.395	0.075	0.271	0.320	0.124	4.082	0.845×10^{-02}	0.844×10^{-02}

(8) $K_{avrg} = (K_s * K_{fc})/(K_s + K_{fc})$

The values of saturated, residual, field capacity moisture content for soil 1-3 were obtained by averaging the values for soils 1 and 3. And $K_s = 2/(1/K_s^{soil1} + 1/K_s^{soil3})$ - K for composite columns.

δ and Soil Infiltration Modelling Parameters

In this case the study involved an analogy with infiltration modelling. It has been considered in a number of studies involving infiltration modelling that the wetting front moves with a velocity inversely proportional to the square root of the time. This is equivalent to:

$$x_f \propto \sqrt{t}$$

where x_f is the depth of the wetting front and t is the time for water to reach the wetting front from the surface. Villela and Mattos (1975) reported the following relationship:

$$x_f = \sqrt{\frac{K\Delta H}{\theta_s}}\sqrt{t} \qquad \text{eqn. (5.4)}$$

where,

K - hydraulic conductivity;

θ_s - soil saturated moisture content;

ΔH - variation of the matric potential between the wetting front and ground surface.

For this study it was supposed that the depth of the wetting front (x_f) would be equivalent to the depth of the phreatic surface (LL) and the time taken for water to reach the saturated zone (t) would be equivalent to parameter δ. Figure 5.15 shows the plots of LL versus $\sqrt{\delta}$. The plots obtained look reasonably linear. Furthermore eqn. (5.4) was applied in this study, with K assumed to be the soil saturated hydraulic conductivity (K_s) and ΔH to be associated to H_s and H_f of the Green and Ampt (Green and Ampt, 1911) infiltration model, equal to the pressure at the ground surface (the water depth in the case of ponding) and the pressure head at the wetting front, respectively.

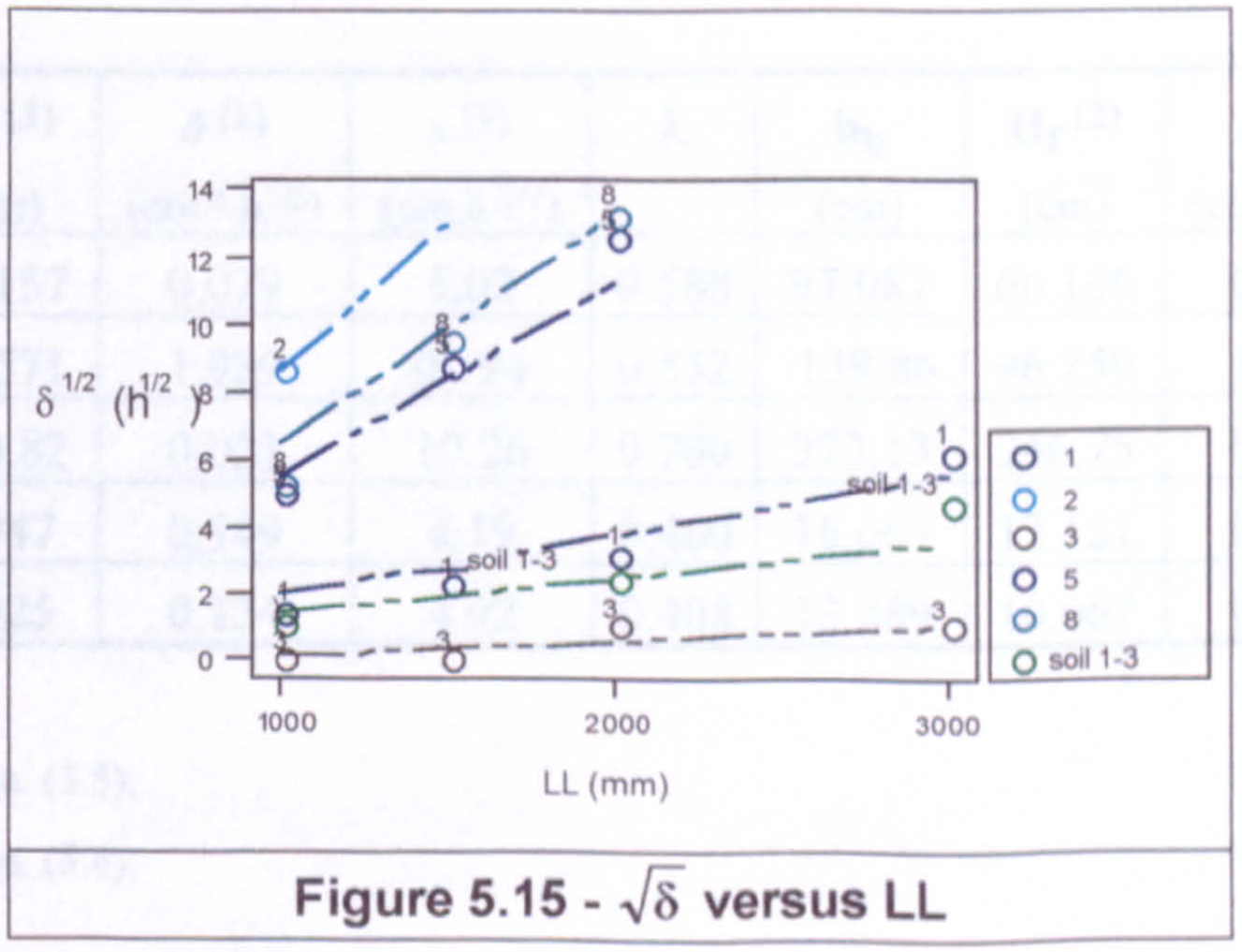

Figure 5.15 - $\sqrt{\delta}$ versus LL

H_s was taken to be zero (Rawls et al., 1992). H_f is difficult to determine and is quite variable in time. Many applications consider these variables (i.e. H_s and H_f) as fitting parameters. Mein and Larson (1973) used the expression:

$$H_f = \int_{\psi(\theta_i)}^{\psi(\theta_s)} \frac{K(\psi)}{K_s} d\psi \qquad \text{eqn. (5.5)}$$

$K(\psi)$ is the hydraulic conductivity function (in this case the van Genuchten-Mualem model was applied). The initial soil moisture content (θ_i) is assumed measured. Rawls et al. (1992) suggested values of soil moisture content corresponding to pressure of -100 cm, -333 cm (suction at field capacity) and -15000 cm (suction at wilting point) for wet, average and dry conditions respectively, when measured values are not available. The value at field capacity was adopted here, and $K(\psi)$ was integrated numerically by the Simpson's method, using steps for ψ of 1cm within the interval (0, -333cm). Table 5.3 shows the values of H_f given in this manner. For the moment, the layered soil is excluded from this analysis.

Table 5.3 - H_f and sorptivity

soil no.	$\int K$ (cm^2/h)	$H_f^{(1)}$ (cm)	$\hat{a}^{(1)}$ ($cm^{-1}.h^{1/2}$)	$s^{(1)}$ ($cm.h^{-1/2}$)	λ	h_b (cm)	$H_f^{(2)}$ (cm)	$\hat{a}^{(2)}$ ($cm^{-1}.h^{1/2}$)	$s^{(2)}$ ($cm.h^{-1/2}$)
1	69.183	25.157	0.079	5.03	0.588	97.087	66.106	0.049	8.16
2	0.141	33.571	1.939	0.194	0.552	139.86	96.259	1.145	0.328
3	798.23	100.82	0.021	10.26	0.700	373.13	246.75	0.014	16.06
5	26.911	3.047	0.149	4.19	0.400	16.667	12.121	0.075	8.37
8	33.136	2.625	0.134	4.92	0.408	13.889	10.067	0.068	9.63

Key for Table 5.3:

$H_f^{(1)}$ given using eqn. (5.5);

$H_f^{(2)}$ given using eqn. (5.6);

$\hat{a} = \left(\frac{K_s \Delta H}{\theta_s} \right)^{-1/2}$ (from eqn. 5.4), being $\hat{a}^{(1)}$ given using $H_f^{(1)}$ and $\hat{a}^{(2)}$ given using $H_f^{(1)}$;

$s^{(1)}$ soil sorpitivity given using eqn. (5.7) adopting $H_f^{(1)}$.

$s^{(2)}$ soil sorpitivity given using eqn. (5.7) adopting $H_f^{(2)}$.

The values of H_f (1) (Table 5.3) appear to be overestimated, especially for soil 3 (sand soil). Parlange and Haverkamp (1989) reported values of 26.551cm for a clayey soil and 13.993cm for a sandy soil. It should be noted that in general the sandy soils presented by Parlange and Haverkamp (1989) had saturated hydraulic conductivities greater than for the soils here. In addition, H_f was also determined as a function of the Brooks and Corey $K(\psi)$ model parameters (Rawls and Brasenkiek, 1983, 1989),

$$H_f = \frac{2+3\lambda}{1+3\lambda}\frac{h_b}{2} \qquad \text{eqn. (5.6)}$$

where,
λ is the pore-size distribution index;
h_b is the bubbling pressure head.

These parameters (λ and h_b) are related to the the van Genuchten-Mualem model parameters (Rawls and Brakensiek, 1989) by:

$$\alpha = h_b^{-1}$$
$$n = \lambda + 1$$

Table 5.3 presents the values of h_b, λ and H_f (referred as superscript 2) given by eqn. (5.7).

As for H_f given by eqn. (5.5), the values given by eqn. (5.6) also appear to be overestimated. It was found that in both cases (i.e. using H_f estimated by eqn. 5.6 and by eqn. 5.5) the values for a (linear coefficient, Table 5.3) pattern was not consistent with the pattern in Figure 5.15,

$$a_{soil2} > a_{soil8} > a_{soil5} > a_{soil1} > a_{soil1-3} > a_{soil3}$$

Apart from this, the values of parameter δ estimated in this manner resulted in very poor estimates for δ compared to the values obtained by calibration.

In another attempt to relate a to soil properties, the pattern of soil sorptivities from the Philip Infiltration Equation was compared with the pattern of *a*. Sorptivity (s) can be calculated from (reported by Rawls and Brakensiek, 1989):

$$s^2 = 2K_s(q_s - q_i)(H_s + H_f) \qquad \text{eqn. (5.7)}$$

Table 5.3 show the values of sorpitivity for all the soils using both eqns. (5.5) and (5.6) to estimate H_f. H_s was taken as zero. In both cases, sorpitivity did not follow the same pattern for *a* as in Figure 5.15.

δ and the Parameters of van-Genuchten-Mualem Hydraulic Properties Model

Although the van Genuchten-Mualem model is empirical, the model parameters α n and m are related to the pore size distribution. The possibility of one of these parameters being related to *a* was considered. Table 5.4 shows the values for the van Genuchten-Mualem model parameters for each soil type. The product m.n determines the extension of the pore size distribution towards finer soil pores sizes and m/n the extension towards larger pores sizes (Durner, 1994). None of them follow the pattern for *a*.

Table 5.4 - Parameters of van Genuchten-Mualem model

soil no.	α (cm^{-1})	n	m	m.n	m/n
1	1.03×10^{-02}	1.588	0.370	0.588	0.233
2	7.15×10^{-03}	1.552	0.356	0.553	0.229
3	2.68×10^{-03}	1.700	0.412	0.700	0.242
5	6.00×10^{-02}	1.400	0.286	0.400	0.204
8	7.20×10^{-02}	1.408	0.290	0.408	0.206

5.2.3 - Summary

A good simple equation (eqn. 5.1) has been found which relates the at-a-point recharge rate to the soil water content in the unsaturated zone. The equation has two parameters, which are strongly related allowing reduction to a single parameter. Several ways of relating the parameter directly to physical property data were considered, following methods successfully used by others for the description of moisture movement in porous media (including the use of simple scaling with $\sqrt{t}$). These proved unsuccessful. A method is developed later, however, which does allow the parameters to be estimated from soil property data without running FULCRUM or any other RE model. This method makes use of the results produced using the transfer function (TF) approach, discussed in the next section.

5.3 - TF (Transfer Function) Approach

In this approach an attempt is made to design a method for creating transfer functions relating recharge to infiltration for at-a-point modelling. The method consisted of an input-output analysis in which the unsaturated soil-column is considered as a linear black box, the infiltration rate being the input and groundwater recharge the output.

Other studies have attempted to relate rainfall infiltration to recharge rates. Besbes and de Marsily (1984) made an equivalent assumption and attempted to define and quantify the difference between soil water infiltration and recharge to an aquifer. They concluded that average infiltration and average recharge are identical over a long period of time and that the distinction accounts only for the time delay and smoothing imposed by soil's unsaturated zone. It is reported that measurements have shown that the water content below the root zone does not vary a great deal with time in temperate climates. For the analysis carried out in this study, the input was taken to be equal to infiltration minus transpiration, rather than the flux immediately below the root zone, as used by Besbes and de Marsily (1984). Wu et al. (1996) also proposed a linear model based on rainfall rates for representing recharge rates. Their approach was proposed for shallow groundwaters (up to 1.5 m deep) and was based on recharge rates derived from in-situ observations using lysimeters.

The study that resulted in the TF approach involved two different major steps:

(i) The derivation and parameterisation of the transfer functions;
(ii) A study to relate the transfer function parameterisation to soil physical property data.

The derivation of the transfer functions for the time series of soil water infiltration rates and groundwater recharge (obtained from FULCRUM) is described in section 5.3.1. The parameterisation of these transfer functions was derived by fitting them to the characteristic pulse response function of the Convection-Diffusion Equation (CDE). This is described in section 5.3.2. The association of the TFs and soil physical property data is discussed in sections 5.3.3 and 5.3.4.

5.3.1 - Transfer Functions

The transfer functions were determined by applying the theory of linear systems (e.g. Chow et al., 1988). Output (r_n, n=1,2,...,N - recharge rates) is given by the discrete convolution equation (eqn. 5.8) which is a function of input ($input_m$, m=1,2,...,M - soil water net infiltration) and the transfer function or pulse response (U_{n-m+1}):

$$r_n = \sum_{m=1}^{M} input_m U_{n-m+1} \qquad \text{eqn. (5.8)}$$

There are different ways of calculating the transfer function from eqn. (5.8); in this study the reverse process called deconvolution is used (i.e. given $input_m$ and r_n, U_{n-m+1} is determined). The time series of soil water net infiltration (discounting evapotranspiration) and groundwater recharge rates from FULCRUM were used to identify transfer functions for each pair of soil type and phreatic surface depth (LL). Some of these transfer functions are shown in Figure 5.16. For the deconvolution the Singular Value Decomposition Method (Press et al., 1992) was applied using the routine F04JAF (Singular Values Decomposition Method for solving linear problems) from the NAG package of subroutines.

5.3.2 - Transfer Functions and the Pulse Response for the Convection-Diffusion Equation

By inspection of Figure 5.16 it can be seen that the shape of the transfer functions are similar to the shape of the characteristic pulse response of the Convection-Diffusion Equation (CDE). Therefore these transfer functions were fitted to the pulse response of the CDE, optimising the CDE parameters C (convective velocity) and D (diffusion). Taking the CDE in the form:

$$\frac{\partial Q}{\partial t}+C\frac{\partial Q}{\partial z}-D\frac{\partial^2 Q}{\partial z^2}=0 \qquad \text{eqn. (5.9)}$$

where,

Q - flow (L^3 / T);
C - constant, convective velocity (L / T);
D - constant, diffusion coefficient(L^2 / T);
t - time (T);
z - length (L).

The solution for eqn. (5.9) can be found by using Laplace transform (Carslaw and Jaeger, 1959) and for an impulse input at z=0 is given by:

$$Q(z,t)=\frac{z}{\sqrt{4\pi Dt^3}}\exp\left(-\frac{(z-Ct)^2}{4Dt}\right) \qquad \text{eqn. (5.10)}$$

where the boundary and initial conditions are;

$$Q(z=0,t)=\delta(t)\ and\ Q(z>0,t=0)=0$$

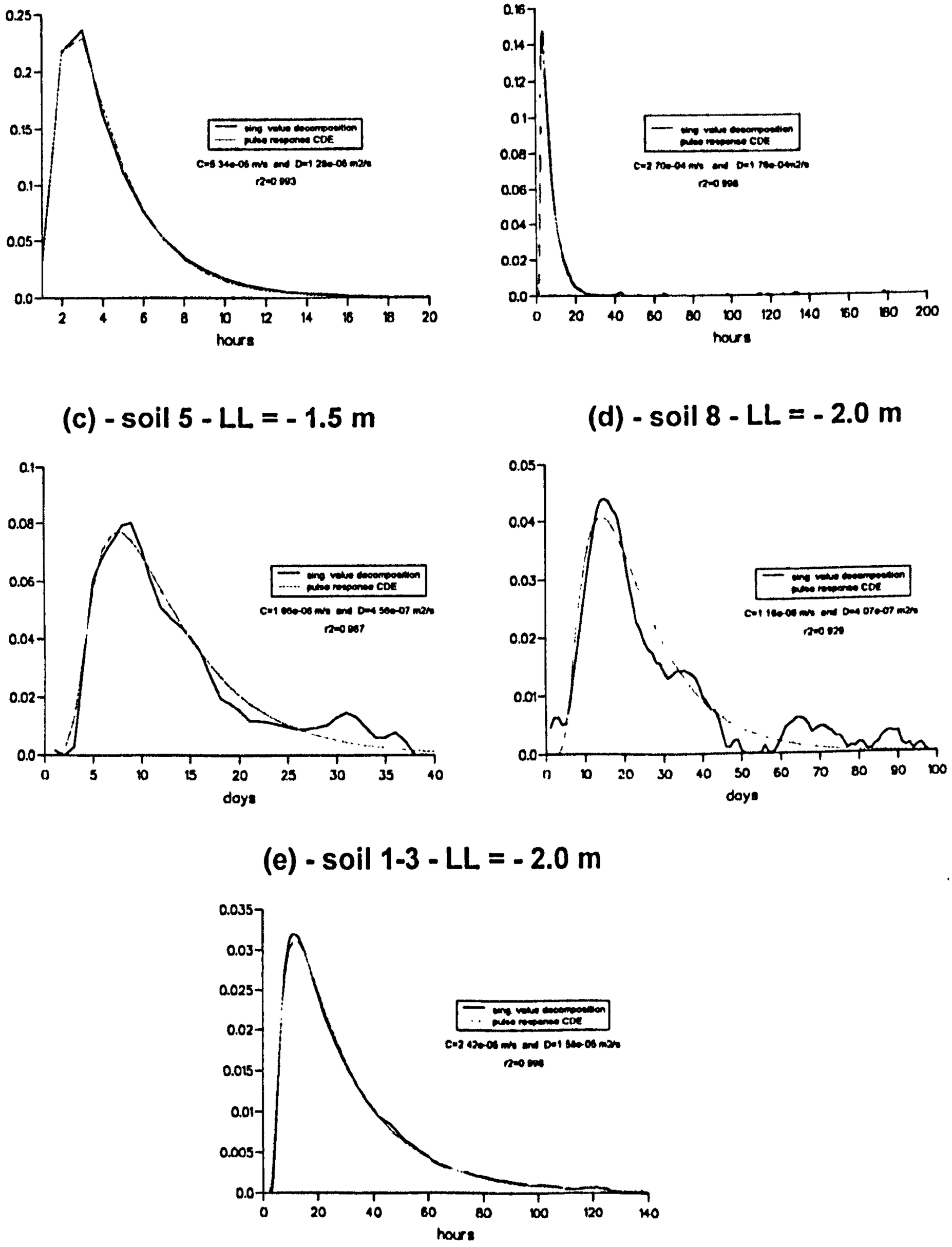

Figure 5.16 - Transfer functions: using the singular value decomposition method and fitting the characteristic pulse response of the convection-diffusion equation

By integrating eqn. (5.10) the step response function ($S_{x,t}$, equivalent to the S-curve in the Unit Hydrograph theory) can be determined:

$$S_{x,t} = \frac{1}{2}\left[erfc\frac{x - Ct}{2\sqrt{Dt}} + \exp\frac{Cx}{D} erfc\frac{x + Ct}{2\sqrt{Dt}} \right] \qquad \text{eqn. (5.11)}$$

where the complementary error function (erfc) can be evaluated from (Press et al., 1992):

$$\begin{aligned} erfc = {} & T \times \exp(-z \times z - 1.26551223 + T \times \\ & (1.00002368 + T \times (0.37409196 + T \times \\ & 0.09678418 + T \times (-0.18628806 + T \times \\ & (0.27886807 + T \times (-1.13520398 + T \times \\ & (1.48851587 + T \times (-0.82215223 + T \times \\ & 0.17087277))))))))) \end{aligned}$$

$$if \quad (x.lt.0) \quad \text{erfc} = 2 - \text{erfc}$$

and,

$$T = \frac{1}{(1. + 0.5 \times z)}$$

$$z = abs(Y_1)$$

$$Y_1 = \frac{(x - C \times T_a)}{(2. \times \sqrt{D \times T_a}}$$

$$T_a = I \times \Delta t, \quad I = 1, mem \text{ (memory of the transfer functions)}$$

The pulse response (or transfer function) H_t can be found from:

$$H_t = \frac{1}{\Delta t}\left[S_{x,t} * \Delta t - S_{x,t-1} * \Delta t \right] \qquad \text{eqn. (5.12)}$$

The values of C and D for each combination of soil type and LL were determined by automatic calibration in which the transfer functions determined using the Singular Value Decomposition Method (section 5.3.1) were fitted to the characteristic pulse response of the CDE (eqn. 5.12), optimising the parameters C and D. The AMOEBA routine (Press et al., 1992) which is based on Nelder and Mead's direct search method (Nelder and Mead, 1968) was applied. The objective function used in the calibration was

the minimum least squares. Table 5.5 shows the good calibration results achieved, and Figure 5.16 shows some of the transfer functions obtained by using optimised C and D.

Table 5.5 - Results for calibration of C and D of the CDE

soil no.	soil type	LL (m)	C (m/s)	D (m^2/s)	R^2 *
1	upper sand	1.0	5.34×10^{-05}	1.28×10^{-05}	0.993
		1.5	2.64×10^{-05}	9.45×10^{-06}	0.997
		2.0	1.51×10^{-05}	8.17×10^{-06}	0.997
		3.0	6.13×10^{-06}	5.26×10^{-06}	0.960
3	lower sand	1.0	3.88×10^{-04}	1.74×10^{-04}	1.000
		2.0	4.11×10^{-04}	1.23×10^{-04}	0.999
		3.0	2.70×10^{-04}	1.76×10^{-04}	0.998
5	Anglezarke A	1.0	2.93×10^{-06}	5.41×10^{-07}	0.980
		1.5	1.66×10^{-06}	4.56×10^{-07}	0.967
		2.0	1.23×10^{-06}	4.12×10^{-07}	0.929
8	Blackwood A	1.0	2.63×10^{-06}	4.85×10^{-07}	0.981
		1.5	1.49×10^{-06}	4.07×10^{-07}	0.960
		2.0	1.16×10^{-06}	4.07×10^{-07}	0.929
soil 1-3	half soil type 1 and half soil type 3	1.0	8.46×10^{-05}	1.90×10^{-05}	0.992
		2.0	2.42×10^{-05}	1.58×10^{-05}	0.998
		3.0	1.06×10^{-05}	8.84×10^{-06}	0.994

* - $R^2 = 1 - \frac{\sum_{t=1}^{end} (H_t - U_t)^2}{\sum_{t=1}^{end} (U_t - U_t)^2}$, where H_t is the pulse response and U_t is the transfer function derived as described in section 5.3.1.

To check the quality of the results achieved, the transfer functions associated with the calibrated values of C and D were used to simulate recharge for direct comparison with the FULCRUM results (Figures 5.17 to 5.25). The differences between the two results are plotted in each case. These results show that the use of transfer functions equivalent to the characteristic response of the convection-diffusion equation to simulate recharge rates agreed well with the recharge rates calculated using FULCRUM.

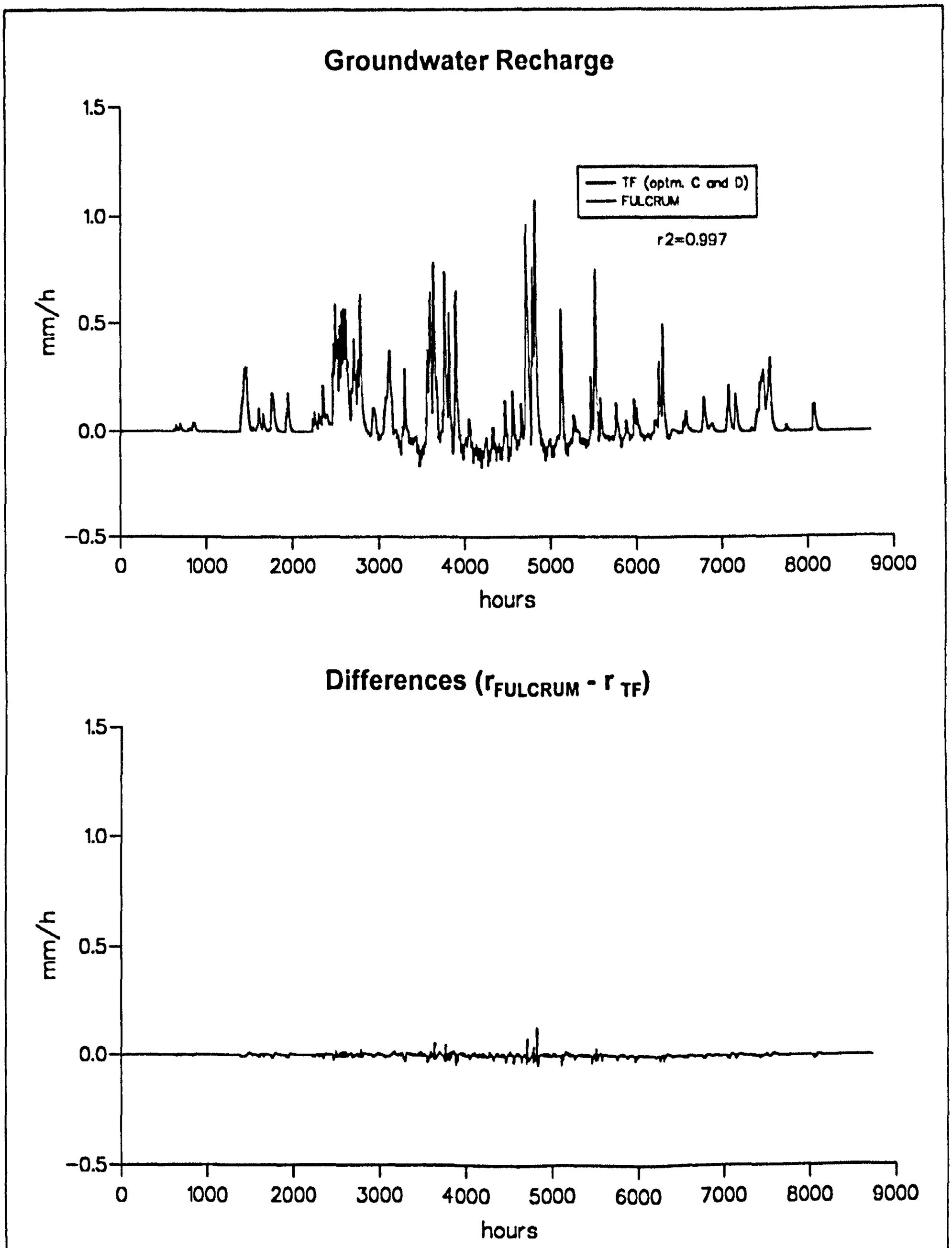

Figure 5.17-TF approach (optimising C and D):results for soil 1 (LL=-1.5m)

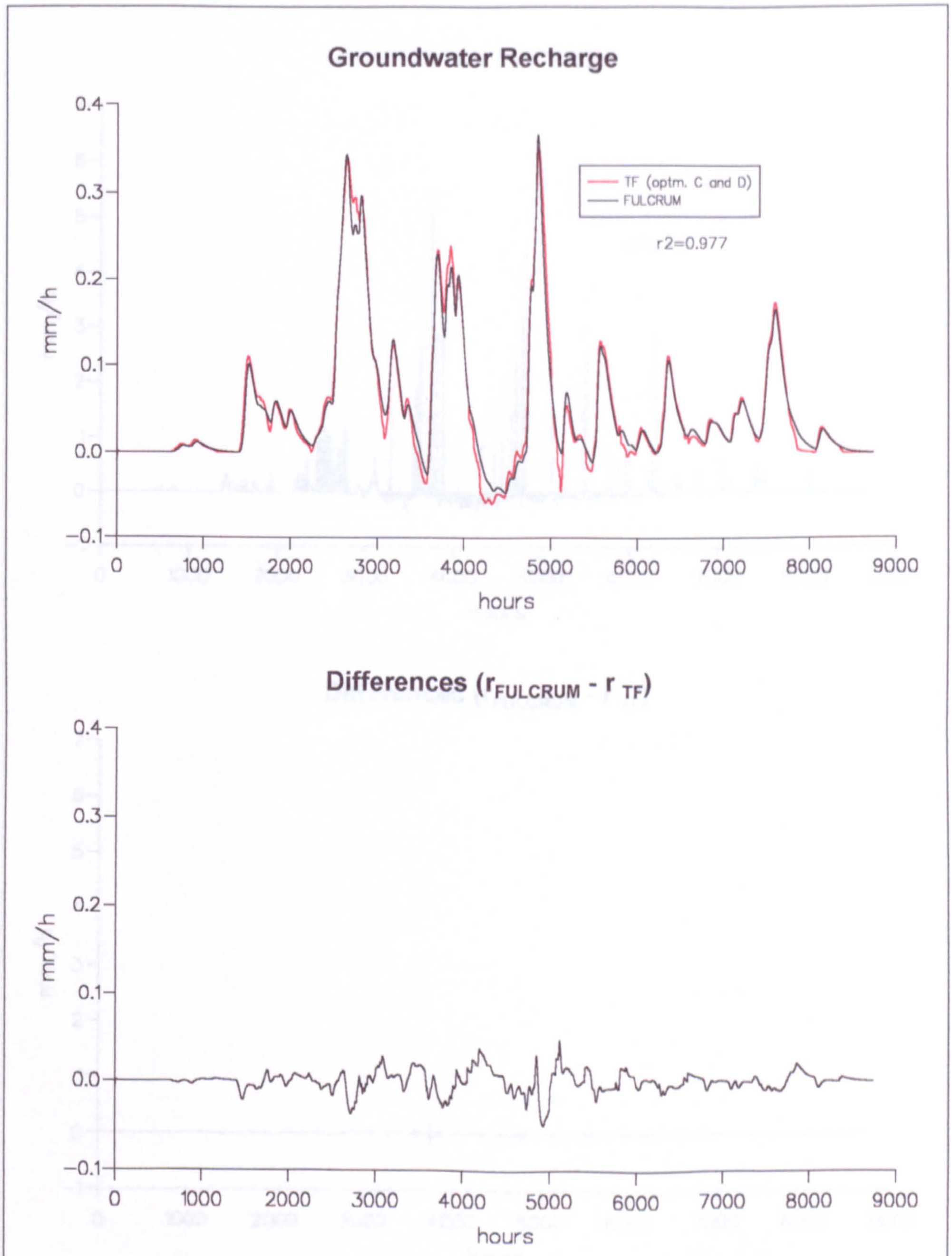

Figure 5.18-TF approach (optimising C and D):results for soil 1 (LL=-3.0m)

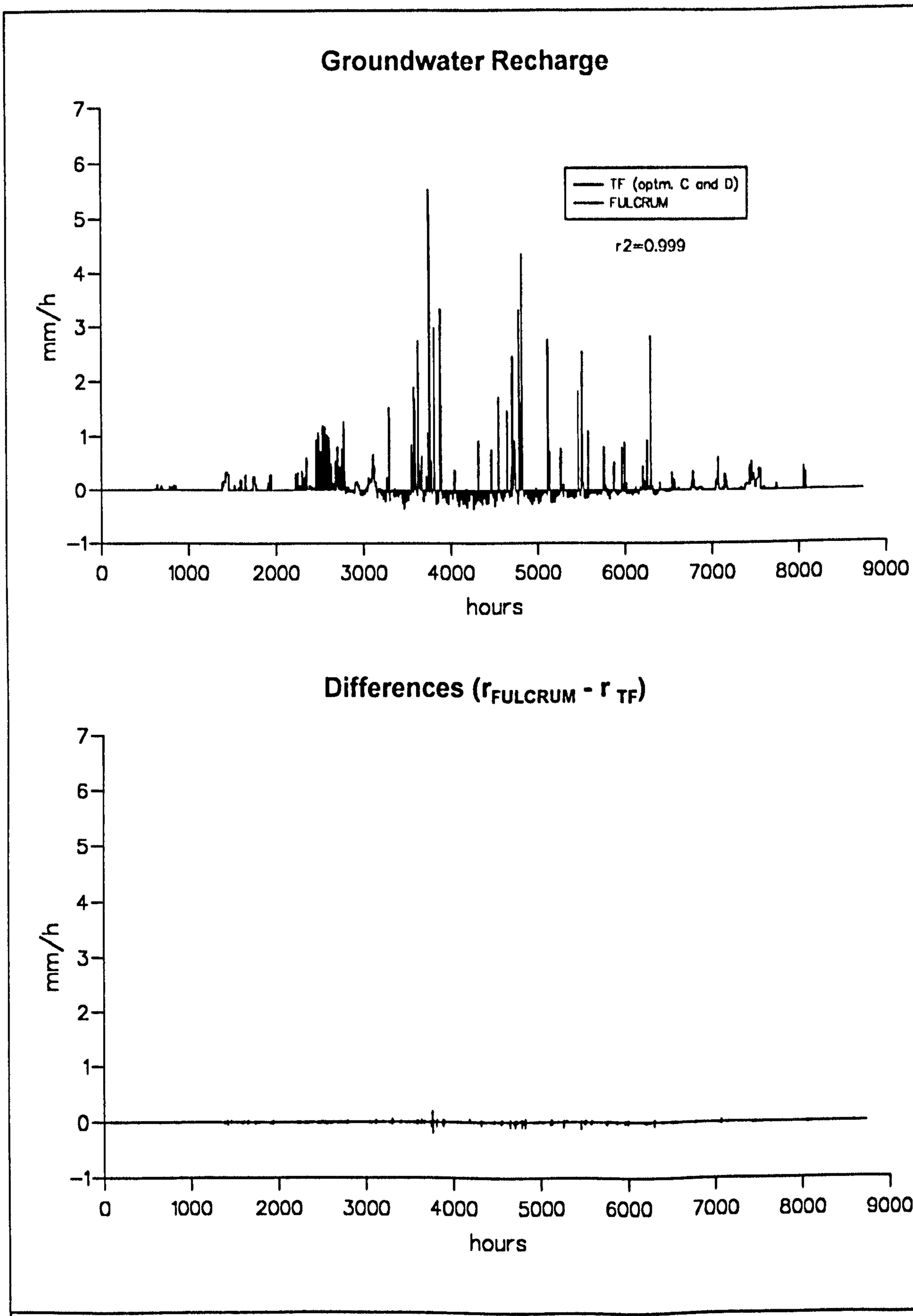

Figure 5.19-TF approach (optimising C and D):results for soil 3 (LL=-2.0m)

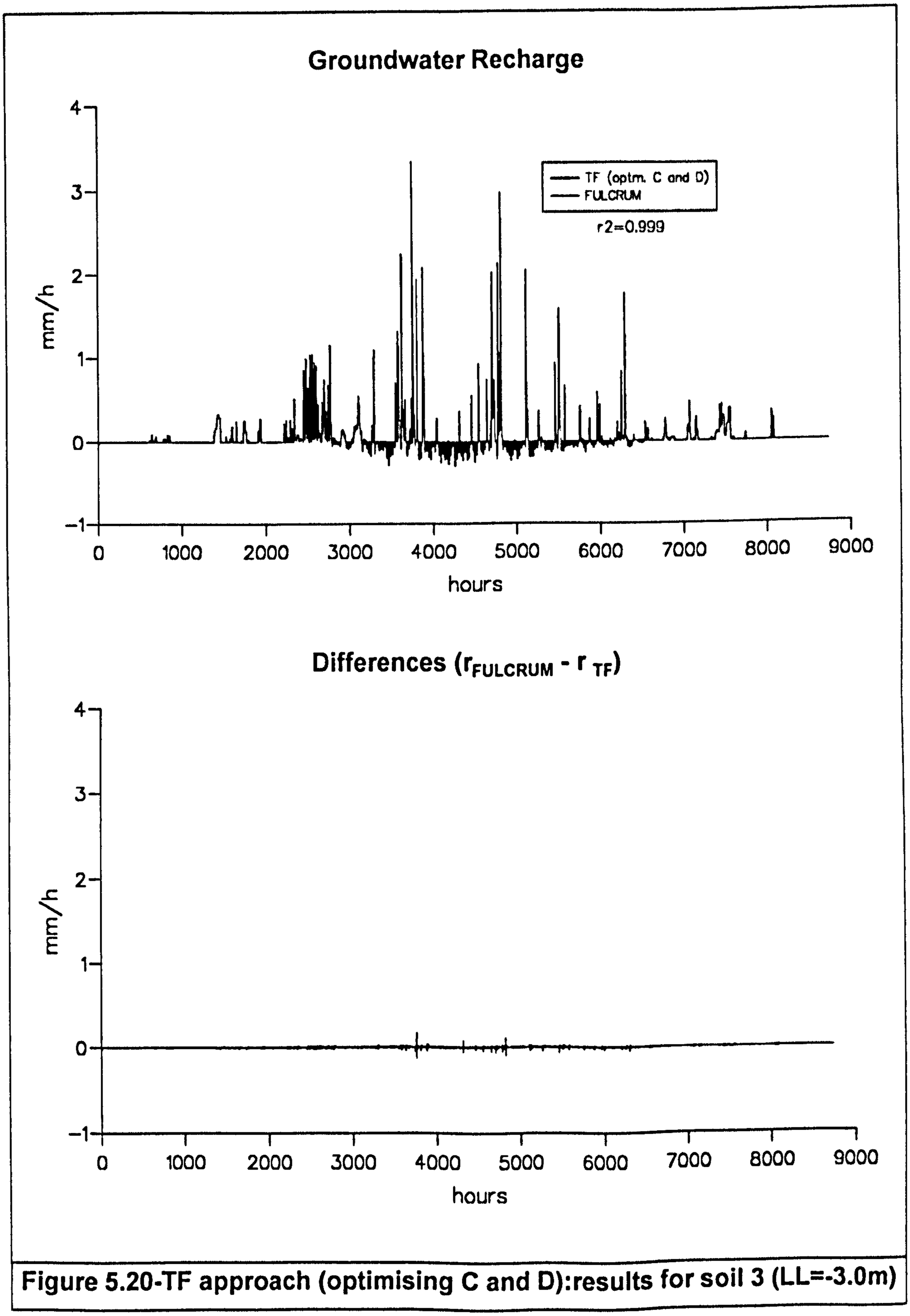

Figure 5.20-TF approach (optimising C and D):results for soil 3 (LL=-3.0m)

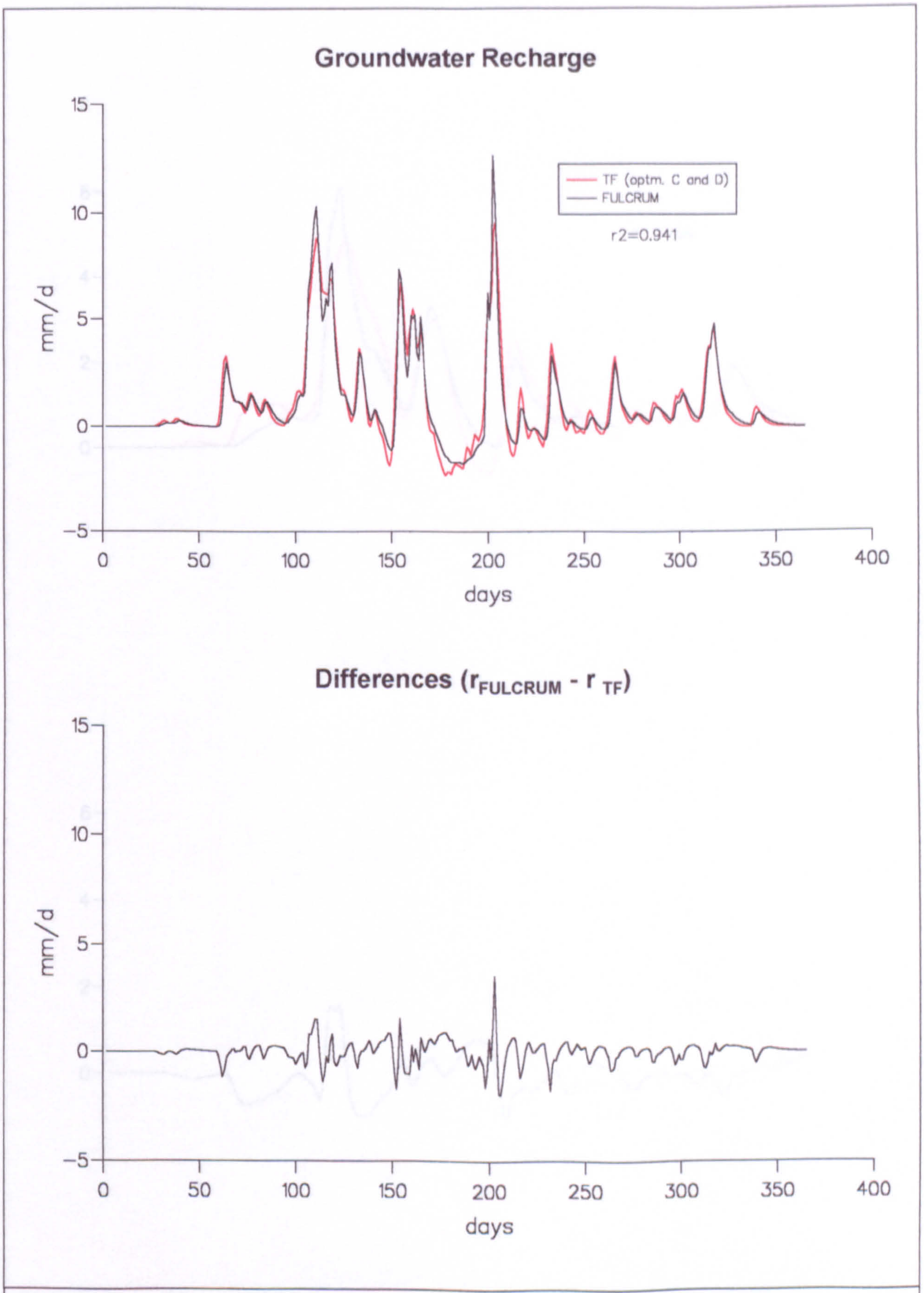

Figure 5.21-TF approach (optimising C and D):results for soil 5 (LL=-1.0m)

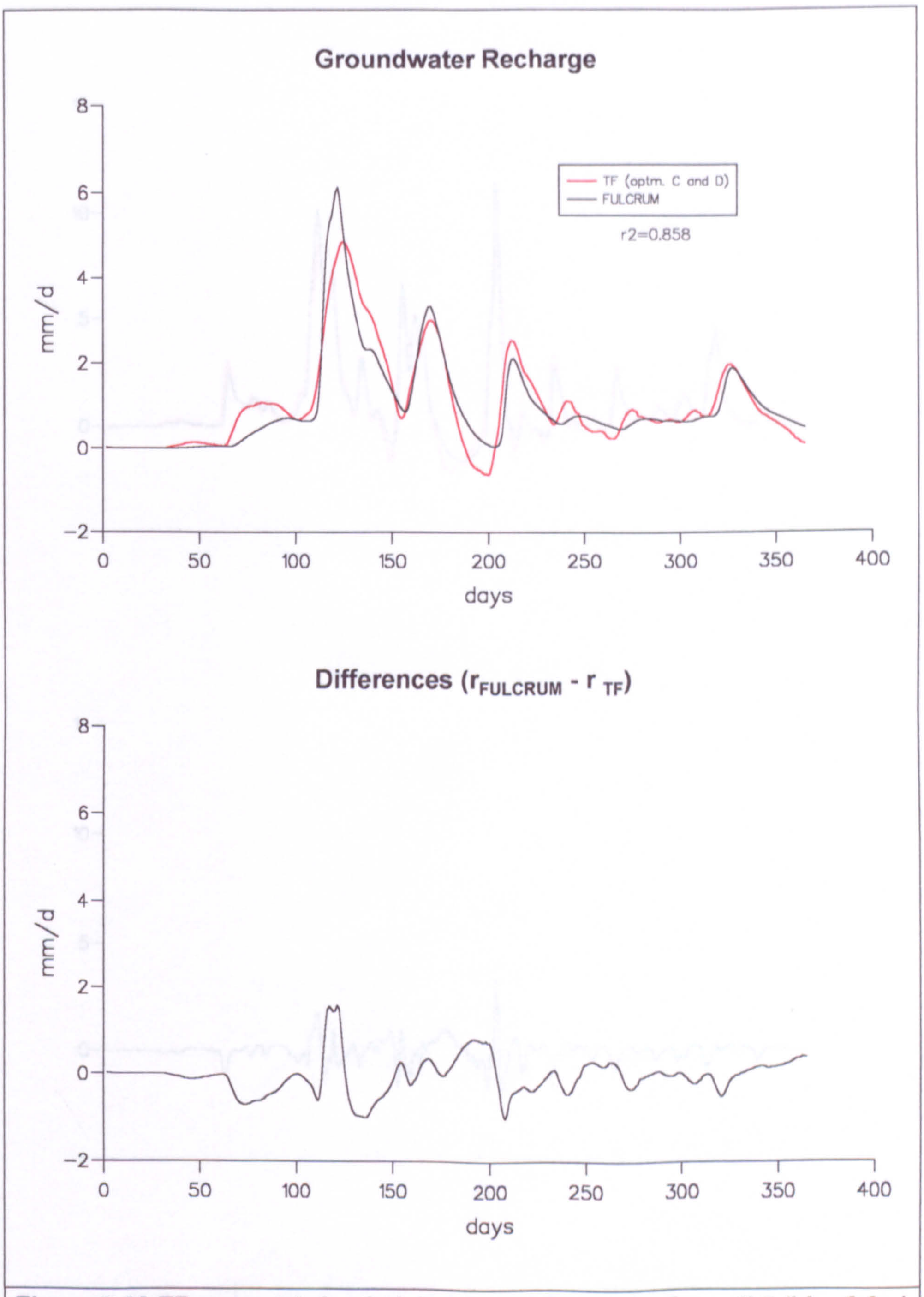

Figure 5.22-TF approach (optimising C and D):results for soil 5 (LL=-2.0m)

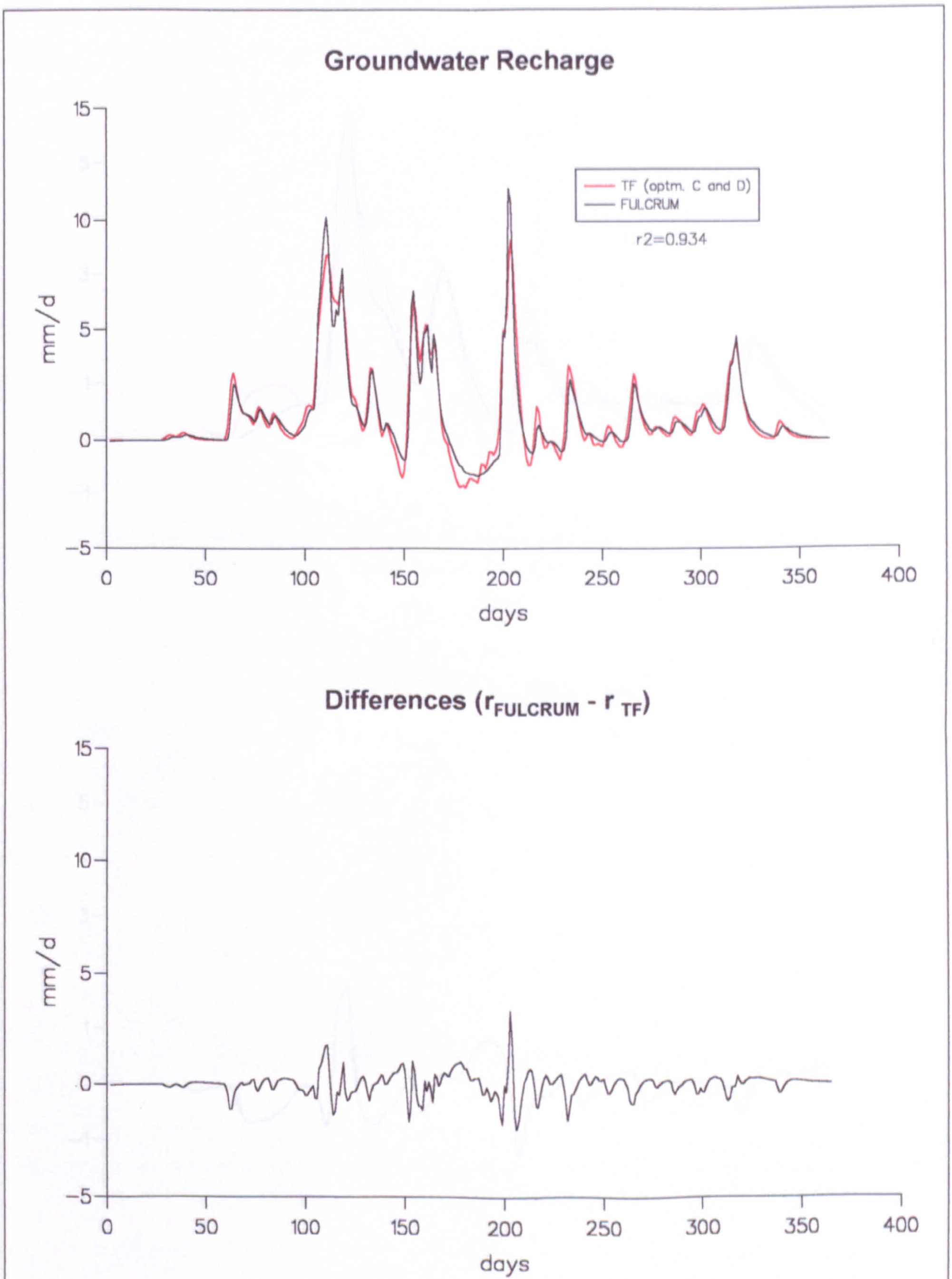

Figure 5.23-TF approach (optimising C and D):results for soil 8 (LL=-1.0m)

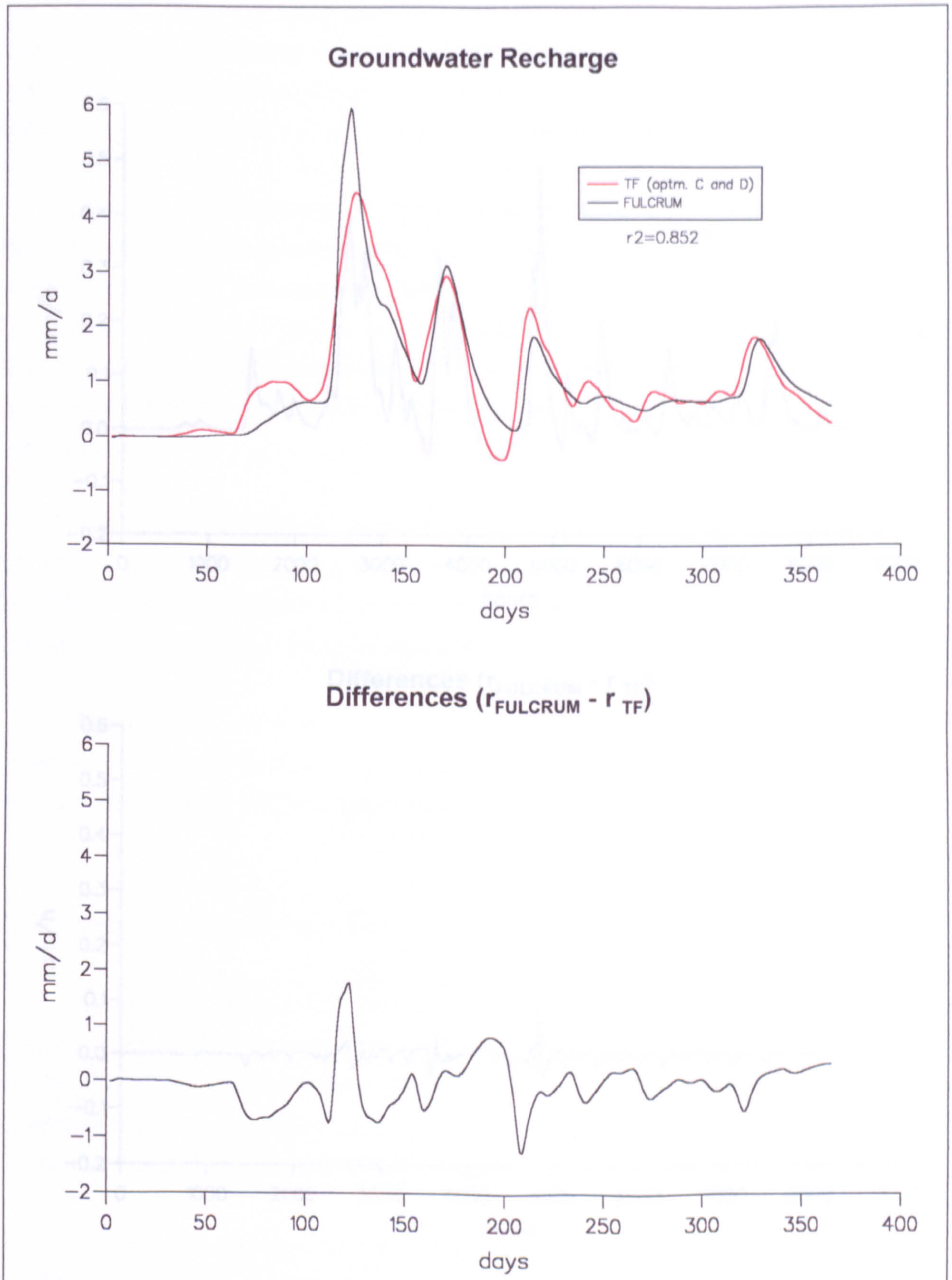

Figure 5.24-TF approach (optimising C and D):results for soil 8 (LL=-2.0m)

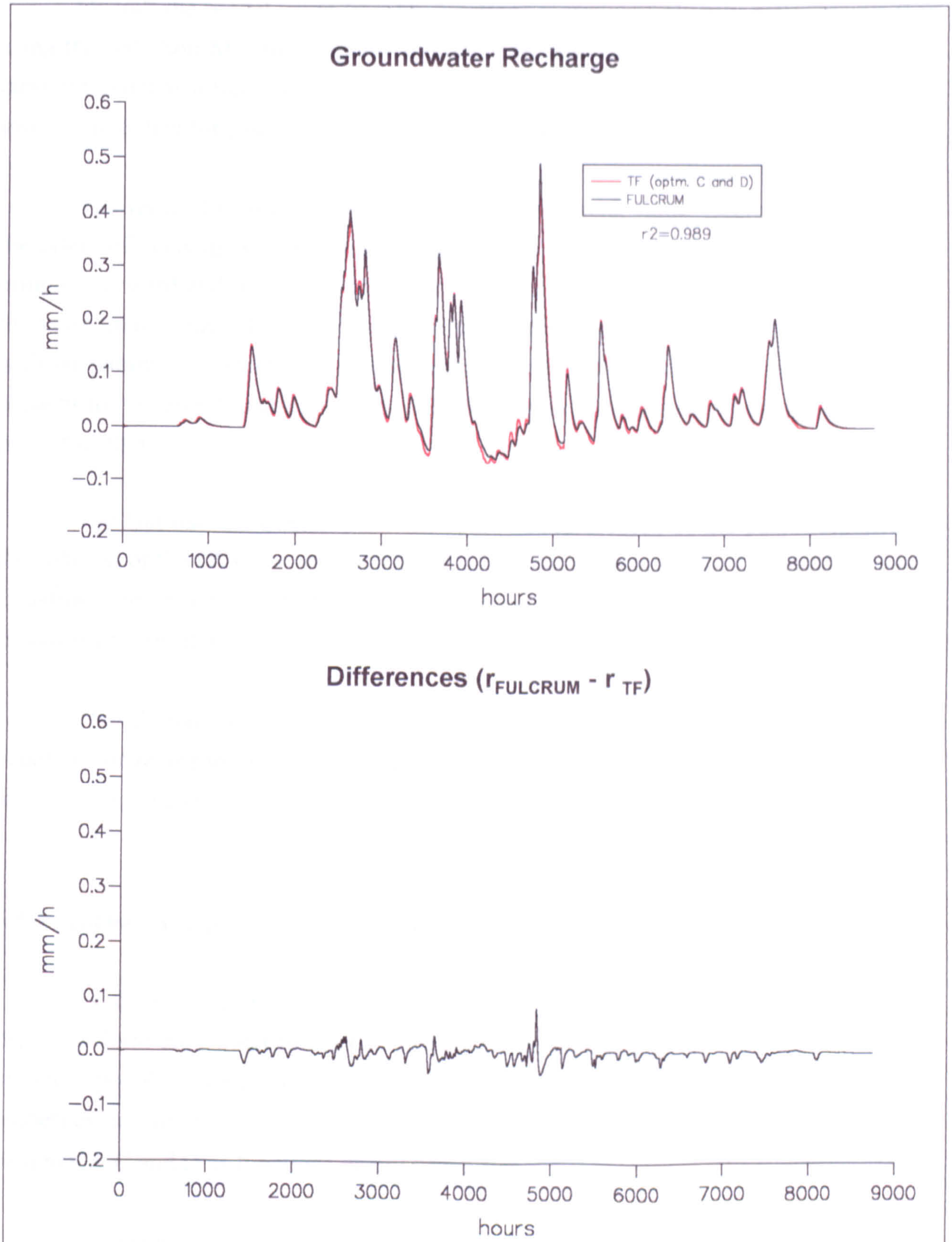

Figure 5.25 - TF approach (optimising C and D): results for soil 1-3 (LL = -3.0m)

Overall the model using transfer functions reproduced slightly better results than using the SM (Soil Moisture content approach, section 5.2) approach in which recharge rates are given as a function of total soil moisture content. Both models were poorer for soils 5 and 8 than for soils 1, 3 and soil 1-3. Soil 2 was excluded from this analysis.

The value of C influences the transfer function peak value. Decreasing C has both the effect of delaying and reducing the peak value, while increasing C has the effect of bringing forward and increasing the peak value. D has more influence on the recession limb and small values of D tend to produce a transfer function with a long tail. Compared with the parameters established in the previous section (DD and δ) C would more or less account for the effects caused by both DD (peak value) and δ (bring forward or postpone peak) together.

The fact that the transfer function could be represented by the pulse response for the solution of the CDE suggests some sort of similarity between the CDE and Richards' Equation. This is not unexpected, as some approximate analytical solutions for Richards' Equation are based on this similarity (see section 4.3).

The ultimate aim is to produce a method of determining the parameters of an equation for recharge directly from the physical properties of the porous media, so the similarity between the CDE and Richards equation is further explored below.

5.3.3 - Richards' Equation and the Convection-Diffusion Equation

As shown in section 4.3, there are different ways of writing Richards' Equation (RE) in a form equivalent to the Convection-Diffusion Equation (CDE). It is, therefore, in theory possible to estimate the recharge transfer function directly from soil hydraulic properties, by comparing both equations to find approximations for representing the CDE parameters C and D as functions of soil properties.

For example, after re-arranging RE written as in eqn. (4.15) and comparing it with the CDE (eqn. 5.9), $C=Ks/(\theta s-\theta r)$ and $D=C/\alpha$. Assuming an exponential form to represent soil hydraulic conductivity and soil retention functions (given by eqns. 4.13 and 4.14) as in Srivastava and Jim-Yeh (1991) these relationships are equivalent to $C=dK/d\theta$

and $D=Kd\psi/d\theta$. The same analysis can be carried out on relating RE to the Burgers' equation (eqn. 4.16). These approaches sometimes involve writing Richards' equation transforming the independent variable and the validation of their solutions are usually tied to some sort of simplification of the soil hydraulic conductivity and soil retention functions. In many cases these simplications do not give very realistic functions for field soils. Functions with the flexibility of the van Genuchten-Mualem are considered necessary to properly represent the general behaviour of field soils.

A new approach was sought for the transformation of RE to CDE, which would admit a more general representation of the soil hydraulic functions. A number of approaches using different dependent variables (e.g. 'K', 'θ', 'q' and 'q/K') were tried, and it was found that 'q/K' as the dependent variable was the most appropriate. This approach is described below.

The one-dimensional RE is derived from the combination of Darcy flow,

$$q = -K\left(\frac{\partial \psi}{\partial z} - 1\right)$$

and the continuity equation,

$$\frac{\partial \theta}{\partial t} = -\frac{\partial q}{\partial z}$$

where,

θ - local volumetric water content;

q - volumetric flux (Darcian flow) vertically downwards;

z - depth below soil surface;

t - is the time.

K - soil hydraulic conductivity function;

ψ - matric potential (negative in the unsaturated zone).

Rewriting the Darcy equation in terms of Q=q/K, and differentiating with respect to time, leads to,

$$\frac{\partial Q}{\partial t} = -\frac{\partial}{\partial t}\left(\frac{\partial \psi}{\partial z}\right) \qquad \text{eqn.(5.13)}$$

Expanding the continuity equation, and noting that q=QK, gives;

$$\frac{d\theta}{d\psi}\frac{\partial \psi}{\partial t} = -K\frac{\partial Q}{\partial z} - Q\frac{\partial K}{\partial z}$$

So, on multiplying throughout by $d\psi/d\theta$ (=ξ) and differentiating with respect to z:

$$\frac{\partial}{\partial z}\left(\frac{\partial \psi}{\partial t}\right) = -\xi K\frac{\partial^2 Q}{\partial z^2} - \frac{\partial \xi}{\partial z}K\frac{\partial Q}{\partial z} - \xi\frac{\partial K}{\partial z}\frac{\partial Q}{\partial z}$$

eqn. (5.14)

$$-\xi Q\frac{\partial^2 K}{\partial z^2} - \frac{\partial \xi}{\partial z}Q\frac{\partial K}{\partial z} - \xi\frac{\partial Q}{\partial z}\frac{\partial K}{\partial z}$$

Combining eqns.(5.13) and (5.14), and rearranging, then gives;

$$\frac{\partial Q}{\partial t} - \left(\frac{\partial}{\partial z}(\xi K) + \xi\frac{\partial K}{\partial z}\right)\frac{\partial Q}{\partial z} - \xi K\frac{\partial^2 Q}{\partial z} - \frac{\partial}{\partial z}\left(\xi\frac{\partial K}{\partial z}\right)Q = 0 \qquad \text{eqn.(5.15)}$$

Apart from the final term, the similarity of eqn. (5.15) to the CDE (eqn. 5.9) is clear. However, assuming conditions close to equilibrium, Q ≈ 0, eqn. (5.15) can be approximated by an equation which is a direct analogue of the CDE:

$$\frac{\partial Q}{\partial t} - \left(\frac{\partial}{\partial z}(\xi K) + \xi\frac{\partial K}{\partial z}\right)\frac{\partial Q}{\partial z} - \xi K\frac{\partial^2 Q}{\partial z} = 0 \qquad \text{eqn. (5.16)}$$

5.3.4 - The C and D parameters as Functions of Soil Hydraulic Properties

By comparing the convection-diffusion equation;

$$\frac{\partial Q}{\partial t} + C\frac{\partial Q}{\partial x} - D\frac{\partial^2 Q}{\partial x^2} = 0$$

with eqn. (5.16), C and D are given by:

$$C = -\frac{\partial}{\partial z}\left(K\frac{d\psi}{d\theta}\right) - \frac{d\psi}{d\theta}\frac{\partial K}{\partial z} \qquad \text{eqn. (5.17)}$$

$$D = K\frac{d\psi}{d\theta} \qquad \text{eqn. (5.18)}$$

The effective value for $\overline{C}$ for the soil column by analogy to the convective velocity in the CDE, can be written as:

$$\overline{C} = \frac{\text{distance}}{\text{travel time}}$$

In this case, then,

$$\overline{C} = \frac{LL}{\sum_{i=1}^{n}\frac{\Delta i}{C_i}} = \frac{n\,\Delta i}{\Delta i\sum_{i=1}^{n}C_i^{-1}}$$

where,

n - number of cells into which the soil unsaturated column is sub-divided;
Δi - thickness of each cell.

The same is valid for D.

The soil column effective values of C and D are then given by:

$$\bar{C} = \frac{n}{\sum_{i=1}^{i=n} C_i^{-1}} \qquad \text{eqn. (5.19)}$$

$$\bar{D} = \frac{n}{\sum_{i=1}^{i=n} D_i^{-1}} \qquad \text{eqn. (5.20)}$$

The derivatives needed to estimate parameters C and D for each depth were estimated from their analytical form using van Genuchten-Mualem soil hydraulic functions (van Genuchten, 1988). These are described in Appendix C.

Table 5.6 shows values of parameters C and D obtained from optimisation by fitting the transfer functions to the characteristic pulse response of the CDE (also given in Table 5.5, section 5.3.2) and the values obtained using direct calculation from the soil hydraulic functions (eqns. 5.19 and 5.20).

The agreement can be seen from Table 5.6 to be generally good. Some values, however, were underestimates, especially in the case of soils 5 and 8 (LL = -1.5 m and -2.0 m). For these cases, water is transferred more slowly throughout the unsaturated zone. Therefore, the soil moisture content varies more throughout the year. The parameters C and D for these transfer functions are estimated for soil moisture conditions close to equilibrium assuming zero infiltration and thus may be less representative, especially for high-flow periods. However, it should be considered that groundwater responses are generally slow, in which case the fast-response peaks that appear when looking at short time steps should be smoothed. In this case these transfer functions are likely to reproduce better agreements. Figures 5.26 to 5.39 show groundwater recharge simulated by FULCRUM and generated by the TF approach, which is being described here. The results tend to be better for shallower phreatic surface depths and for soils that transfer water faster (associated with smaller values for δ in the SM approach). Although overall the simulation results are good, the simulations for soils 5 and 8 (-2.0 m) did not reproduce good results and are not shown.

Table 5.6 - Effective values for Parameters C and D

soil no.	soil type	LL (m)	$C^{(1)}$ (m/s)	$C^{(2)}$ (m/s)	$D^{(1)}$ (m^2/s)	$D^{(2)}$ (m^2/s)
1	upper sand	1.0	5.34×10^{-05}	4.51×10^{-05}	1.28×10^{-05}	1.02×10^{-05}
		1.5	2.64×10^{-05}	1.80×10^{-05}	9.45×10^{-06}	5.36×10^{-06}
		2.0	1.51×10^{-05}	8.96×10^{-06}	8.17×10^{-06}	3.31×10^{-06}
		3.0	6.13×10^{-06}	3.16×10^{-06}	5.26×10^{-06}	1.63×10^{-06}
3	lower sand	1.0	3.88×10^{-04}	2.29×10^{-03}	1.74×10^{-04}	8.90×10^{-04}
		2.0	4.11×10^{-04}	6.57×10^{-04}	1.23×10^{-04}	3.75×10^{-04}
		3.0	2.70×10^{-04}	2.89×10^{-04}	1.76×10^{-04}	2.07×10^{-04}
5	Anglezarke A	1.0	2.93×10^{-06}	1.38×10^{-06}	5.41×10^{-07}	2.51×10^{-07}
		1.5	1.66×10^{-06}	5.02×10^{-07}	4.56×10^{-07}	1.34×10^{-07}
		2.0	1.23×10^{-06}	2.42×10^{-07}	4.12×10^{-07}	8.53×10^{-08}
8	Blackwood A	1.0	2.63×10^{-06}	1.15×10^{-06}	4.85×10^{-07}	2.07×10^{-07}
		1.5	1.49×10^{-06}	4.15×10^{-07}	4.07×10^{-07}	1.09×10^{-07}
		2.0	1.16×10^{-06}	1.99×10^{-07}	4.07×10^{-07}	6.94×10^{-08}
soil 1-3	half soil type 1 and half soil type 3	1.0	8.46×10^{-05}	5.14×10^{-05}	1.90×10^{-05}	1.25×10^{-05}
		2.0	2.42×10^{-05}	9.92×10^{-06}	1.58×10^{-05}	3.95×10^{-06}
		3.0	1.06×10^{-05}	3.45×10^{-06}	8.84×10^{-06}	1.92×10^{-06}

(1) - obtained by optimisation

(2) - estimated from soil hydraulic properties

Although in some cases the TF approach did not perform so well, it has the advantage of allowing overall good estimation of groundwater recharge rates which are completely independent of calibration and numerical simulations of RE. In addition, as the parameterisation is dependent on the soil's retention and hydraulic conductivity characteristics, it is likely to be quite sensitive to environmental changes.

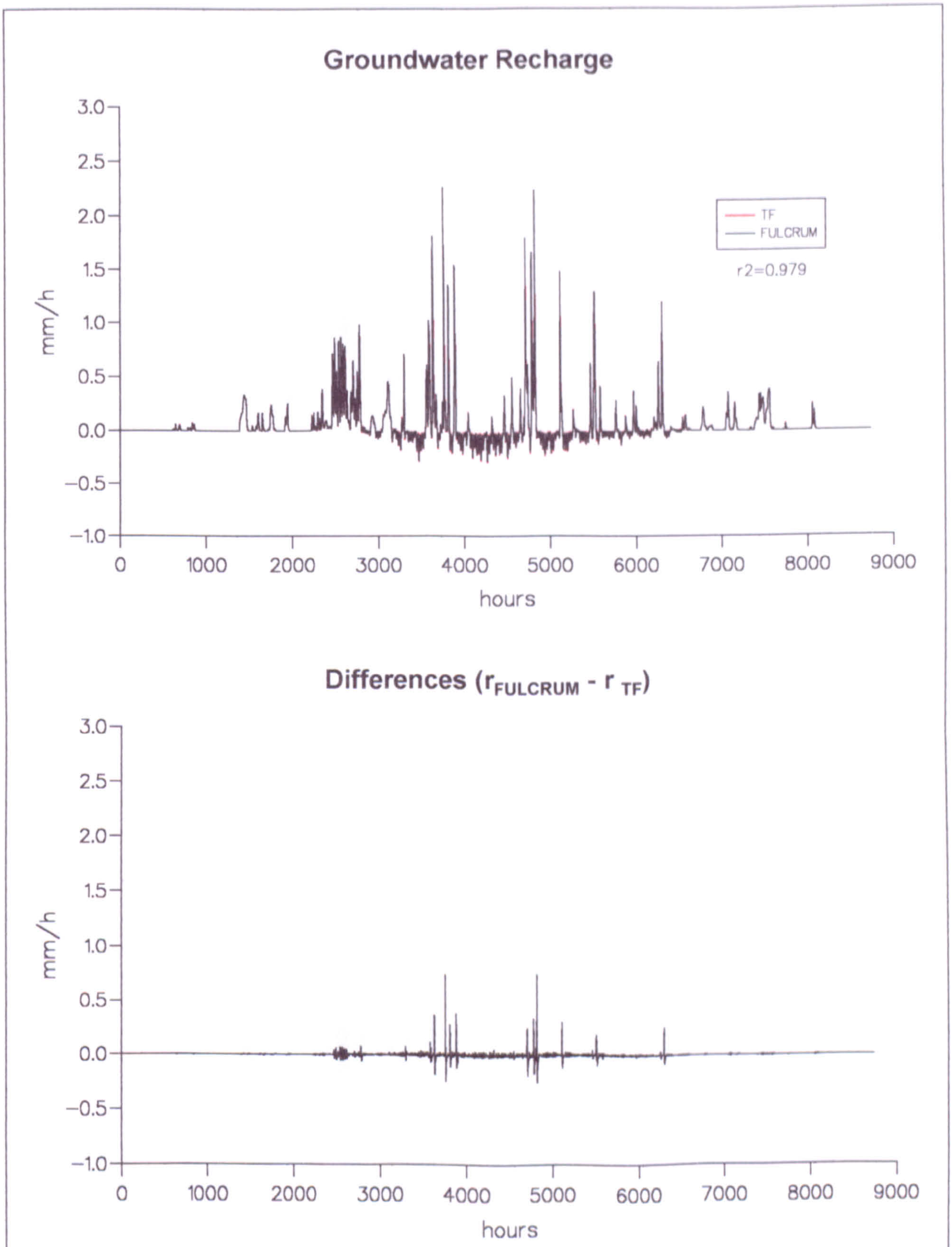

Figure 5.26 - TF approach: results for soil 1 (LL = -1.0 m)

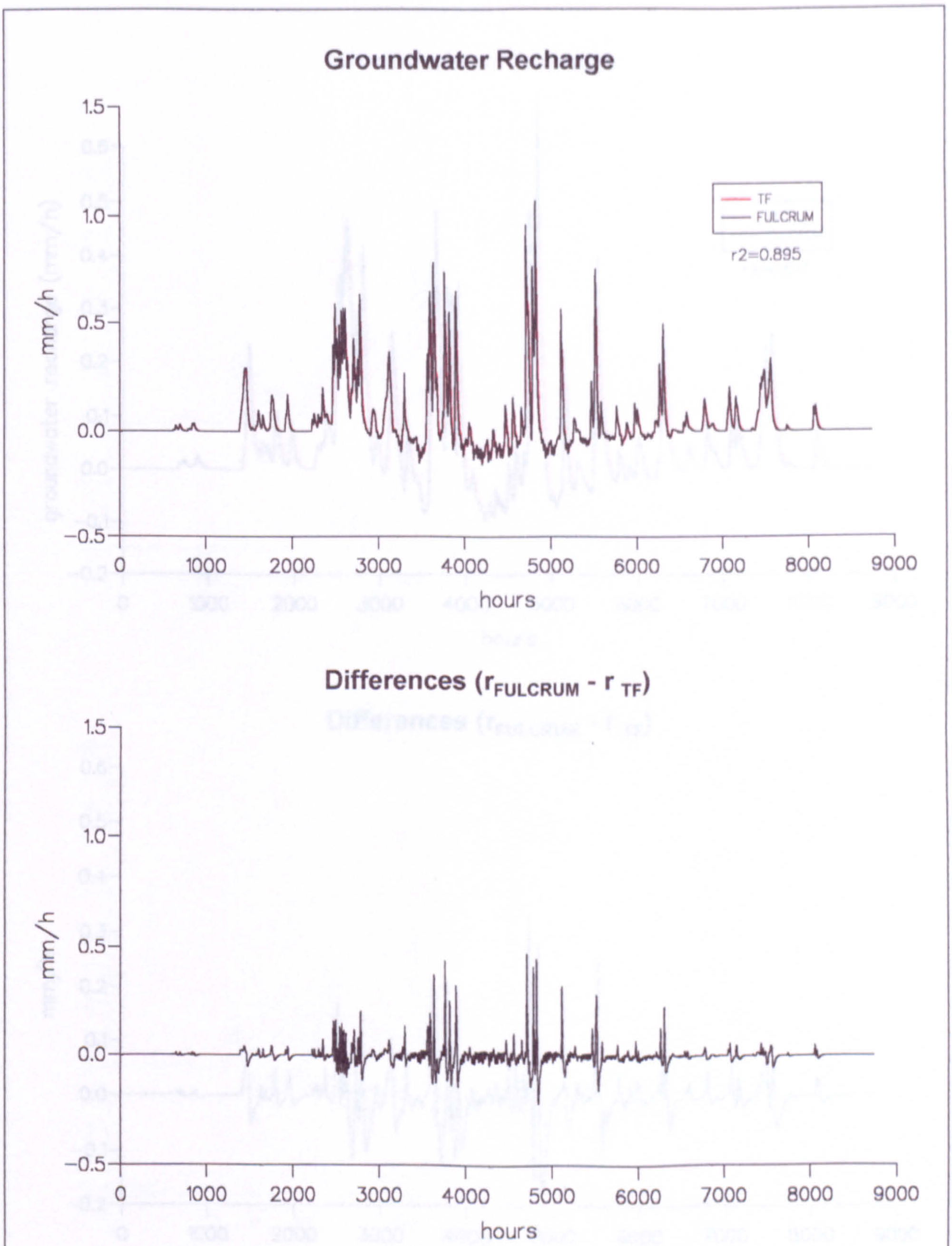

Figure 5.27 - TF approach: results for soil 1 (LL = -1.5 m)

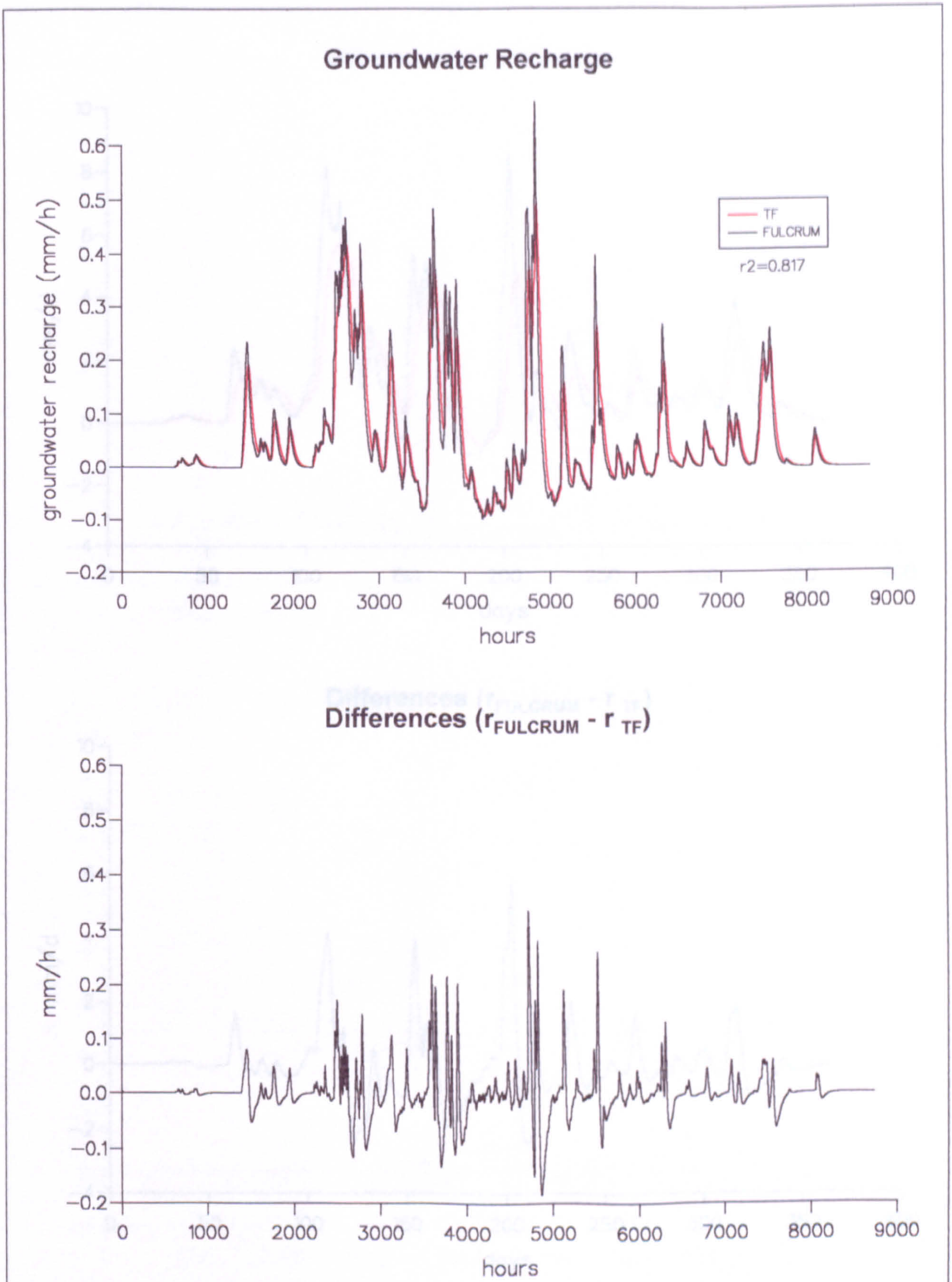

Figure 5.28 - TF approach: results for soil 1 (LL = -2.0 m)

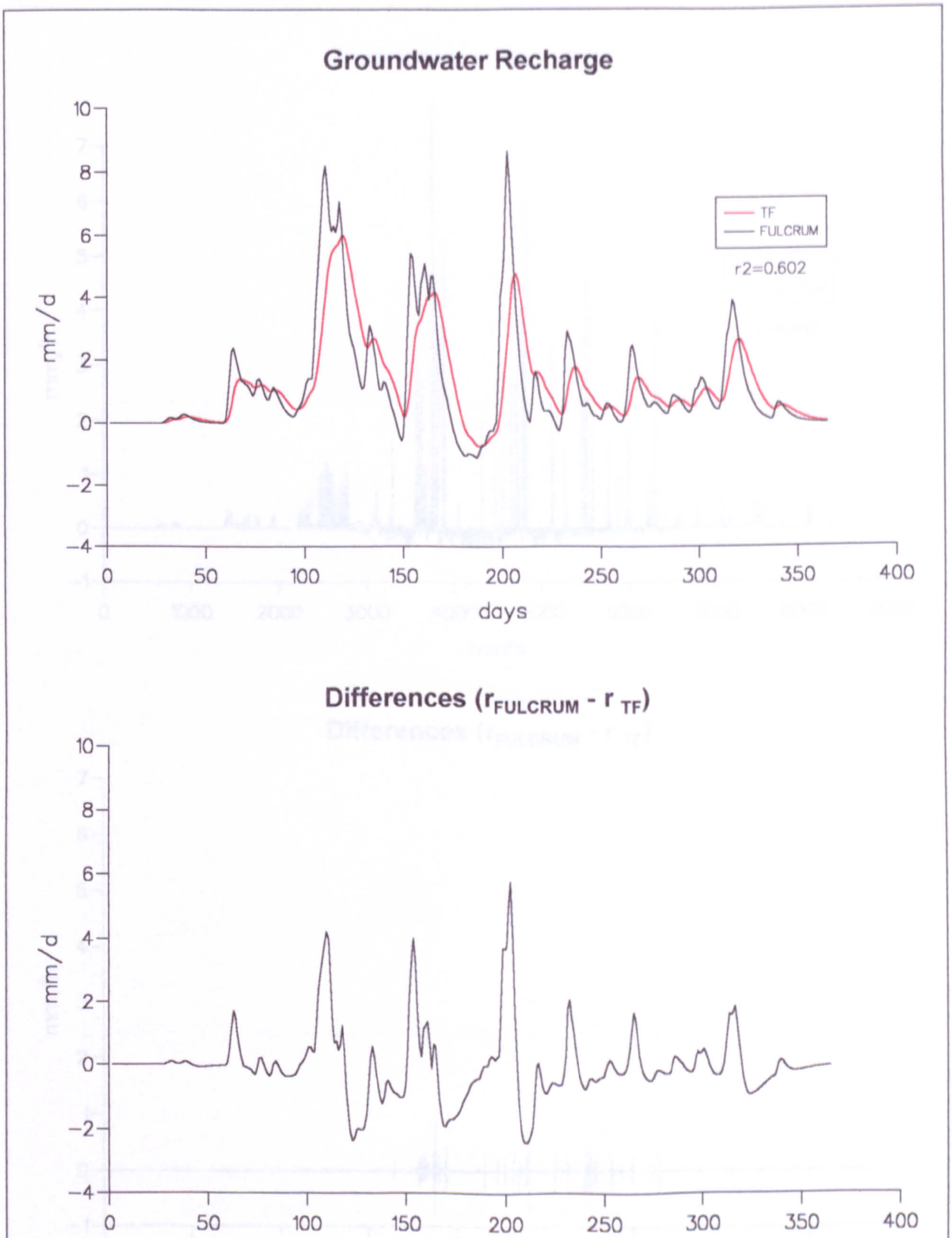

Figure 5.29 - TF approach: results for soil 1 (LL = -3.0 m)

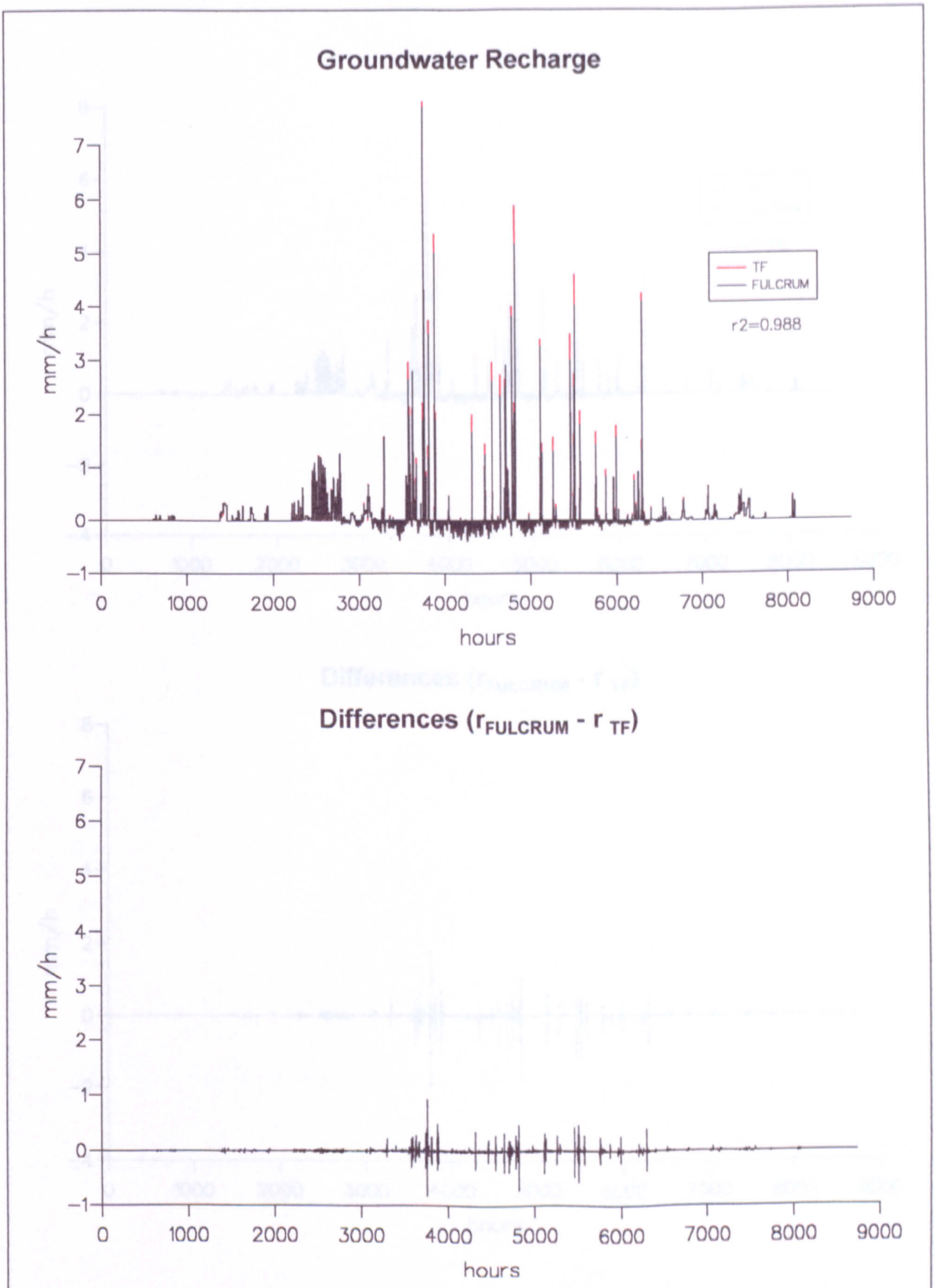

Figure 5.30 - TF approach: results for soil 3 (LL = -1.0 m)

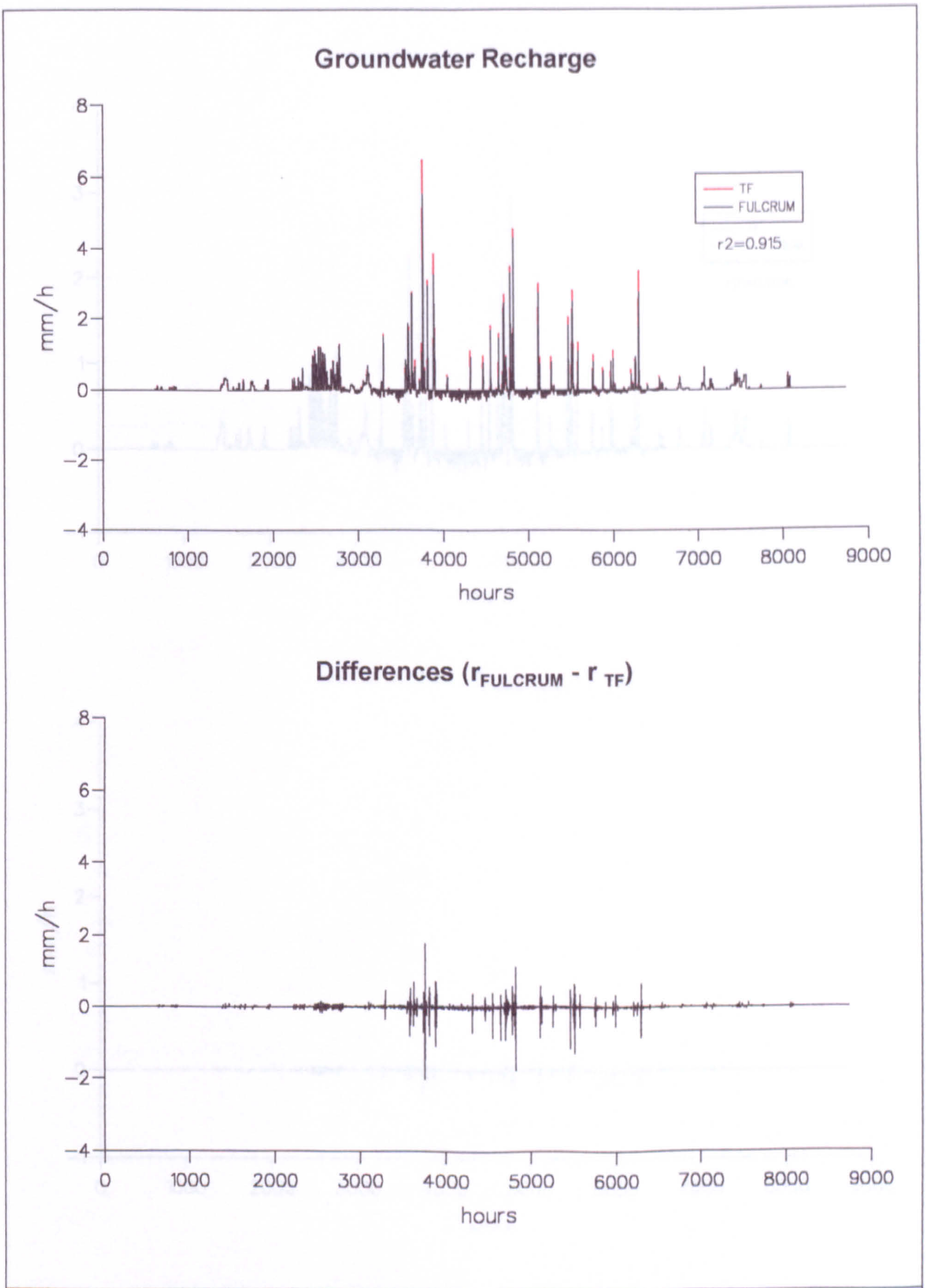

Figure 5.31 - TF approach: results for soil 3 (LL = -2.0 m)

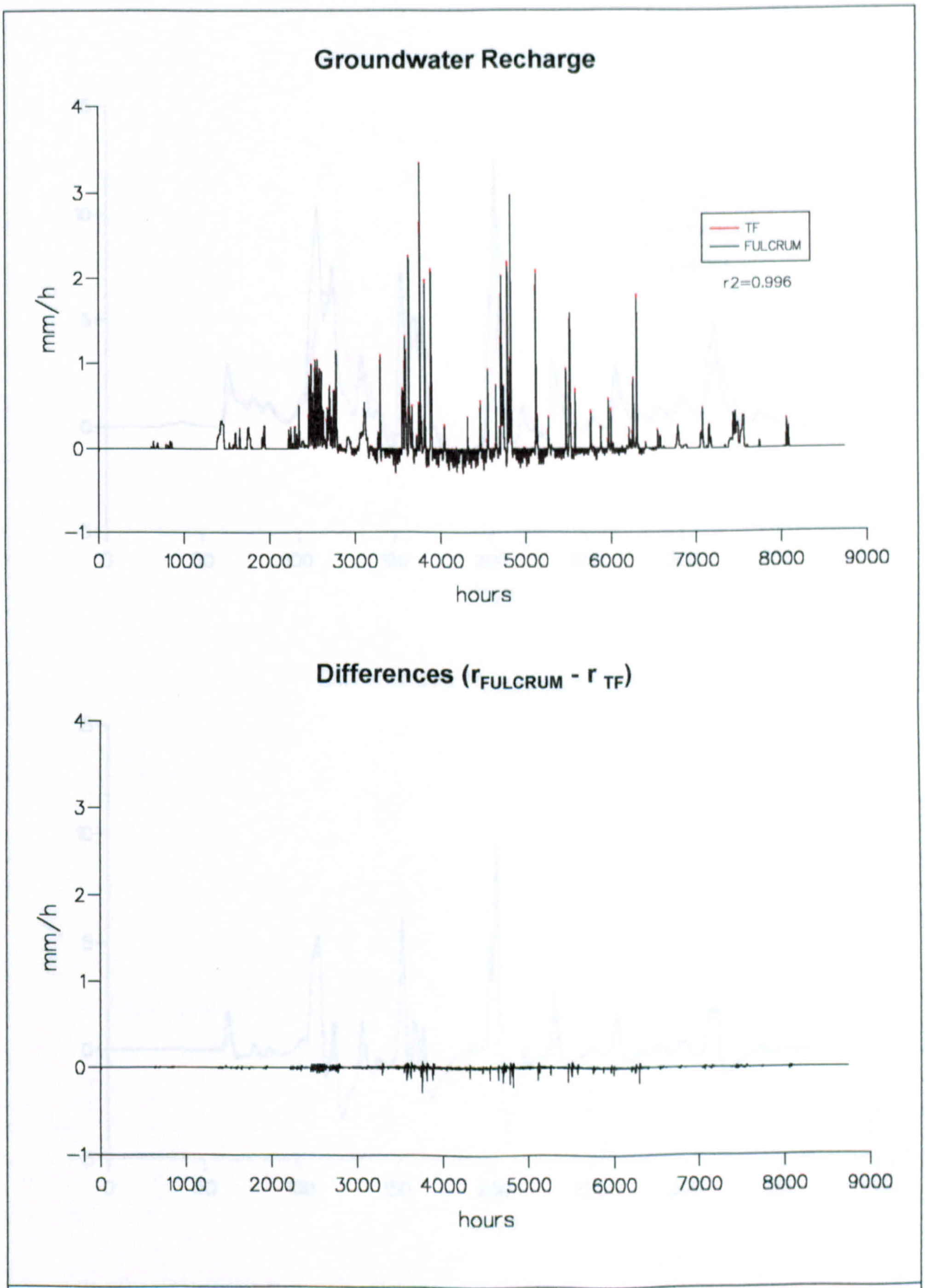

Figure 5.32 - TF approach: results for soil 3 (LL = -3.0 m)

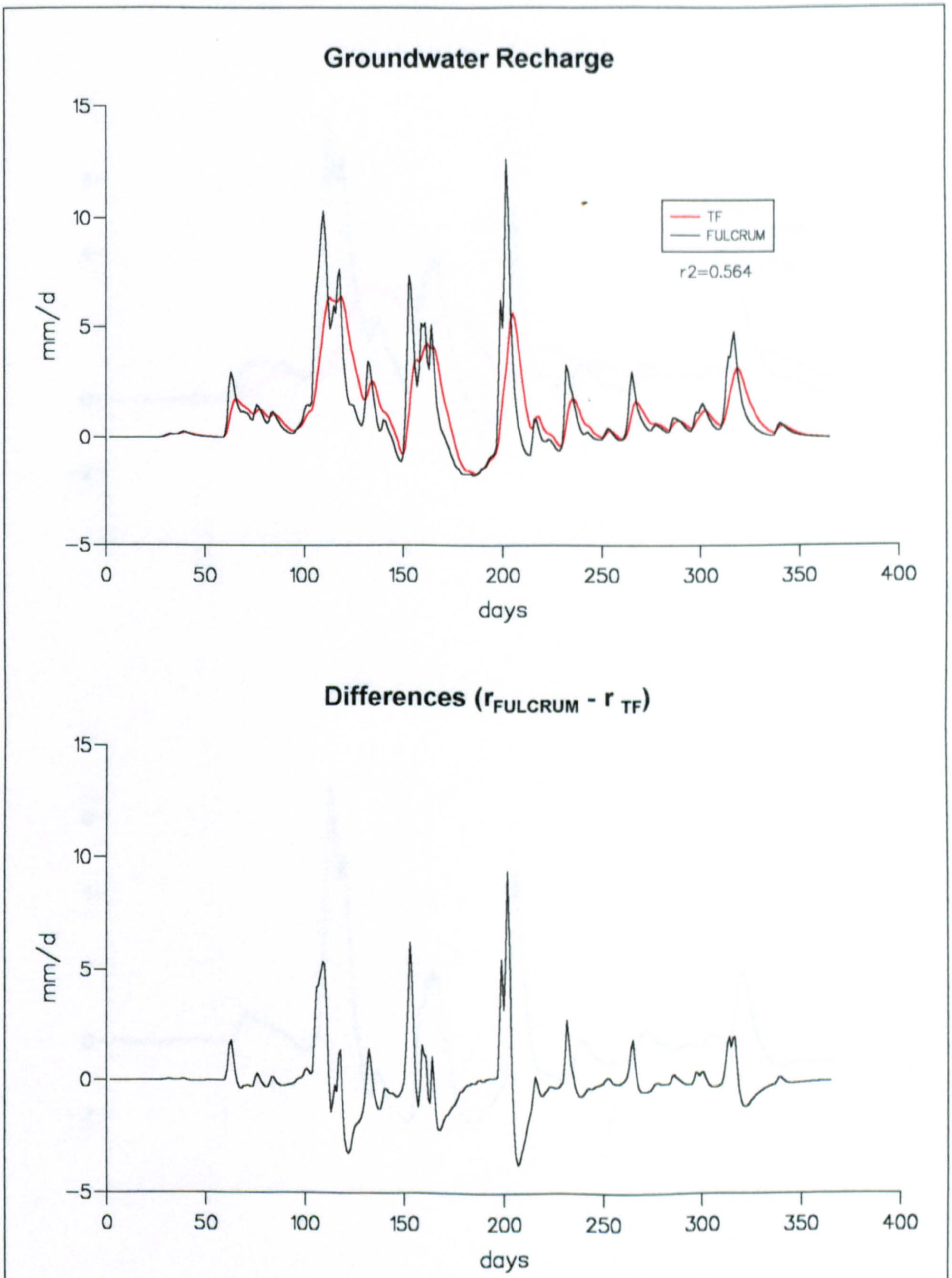

Figure 5.33 - TF approach: results for soil 5 (LL = -1.0 m)

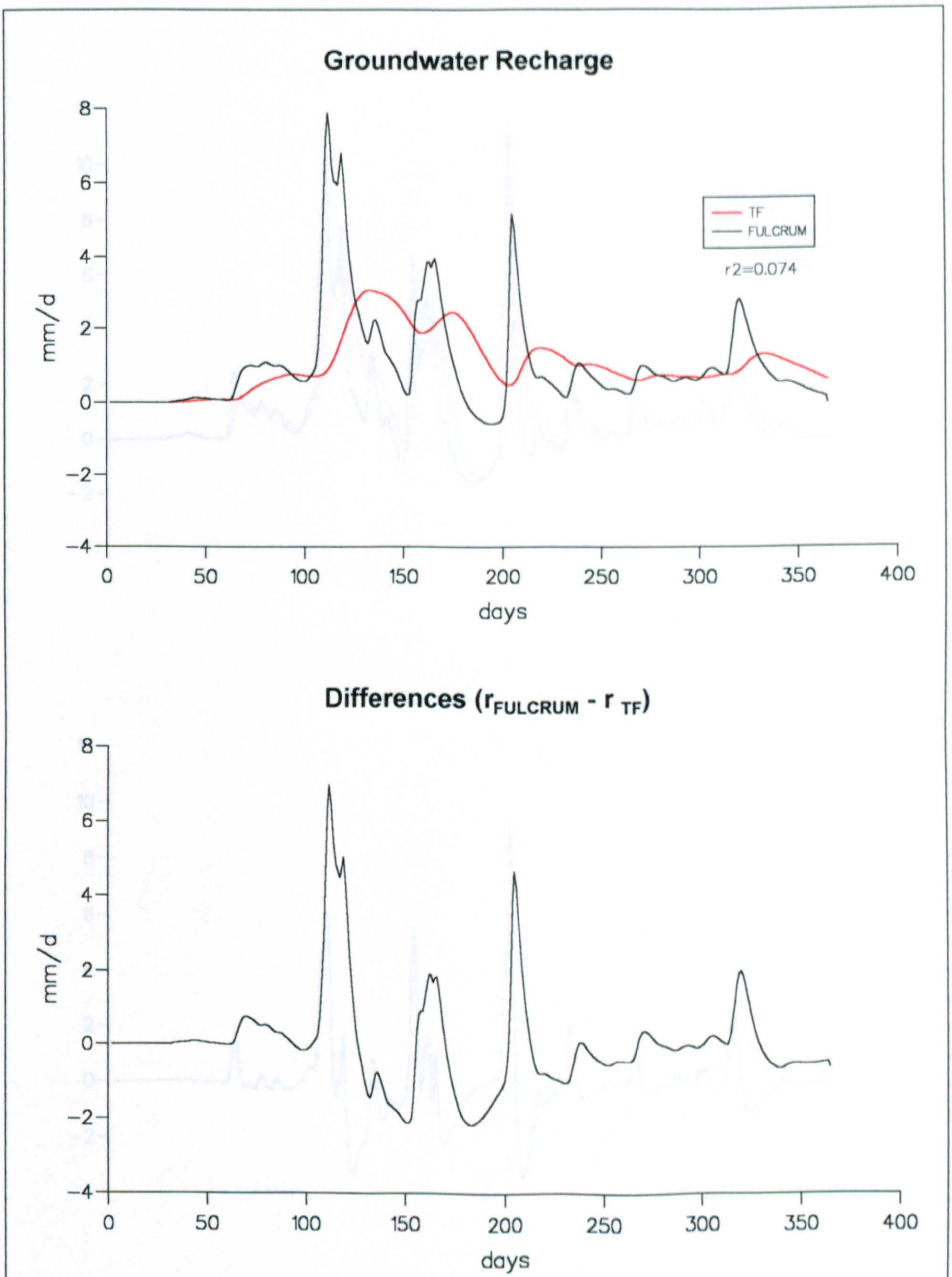

Figure 5.34 - TF approach: results for soil 5 (LL = -1.5 m)

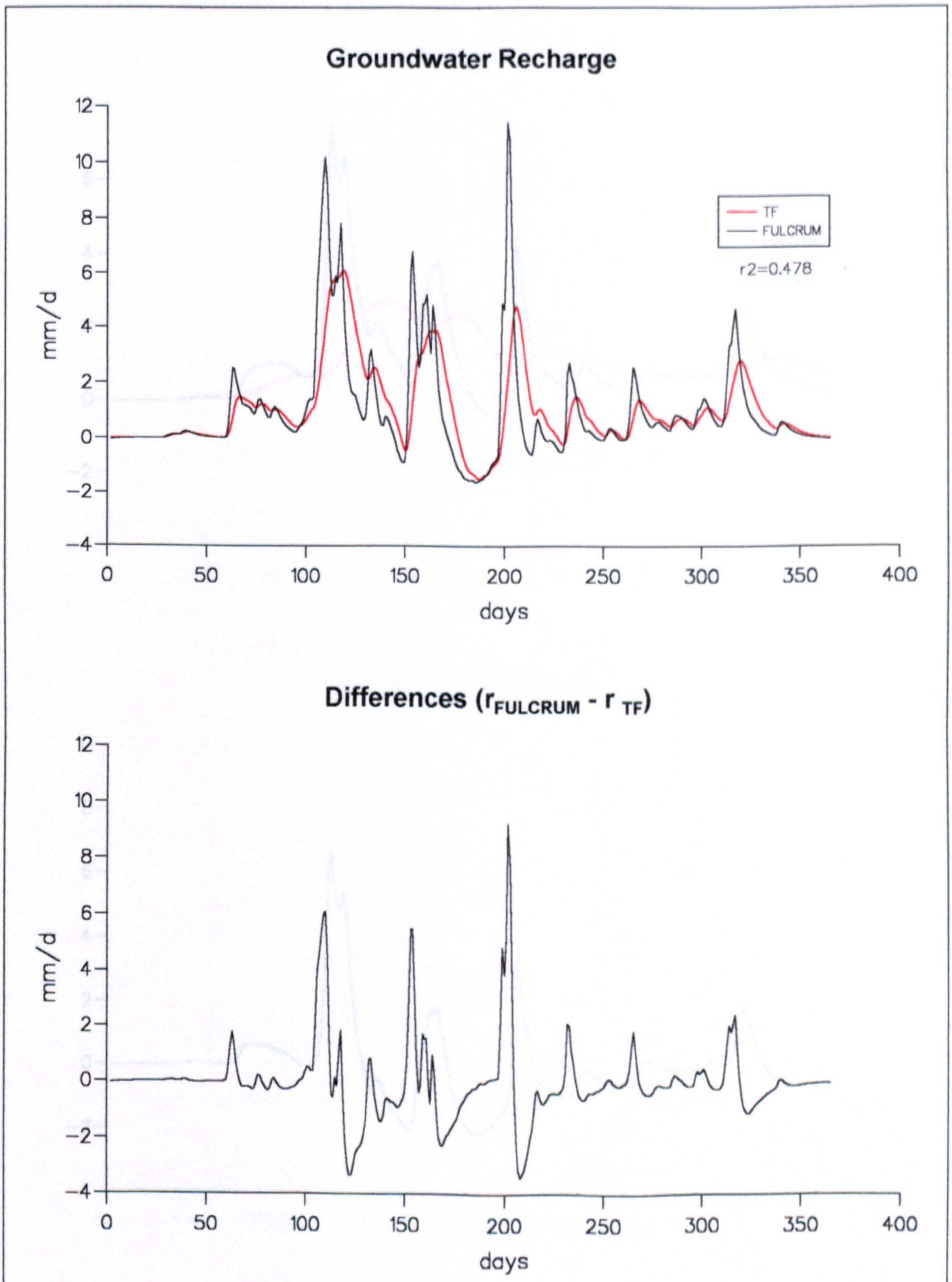

Figure 5.35 - TF approach: results for soil 8 (LL = -1.0 m)

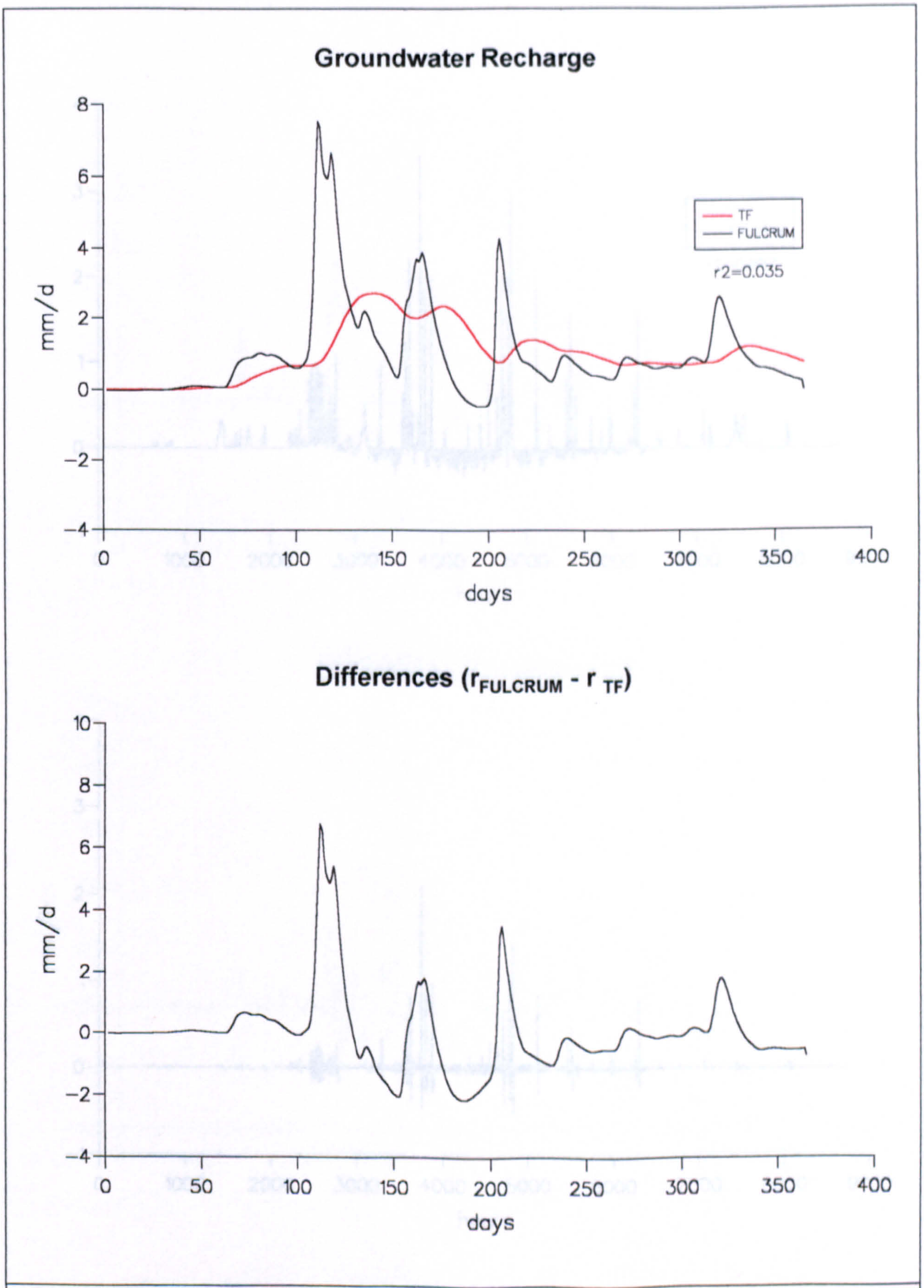

Figure 5.36 - TF approach: results for soil 8 (LL = -1.5 m)

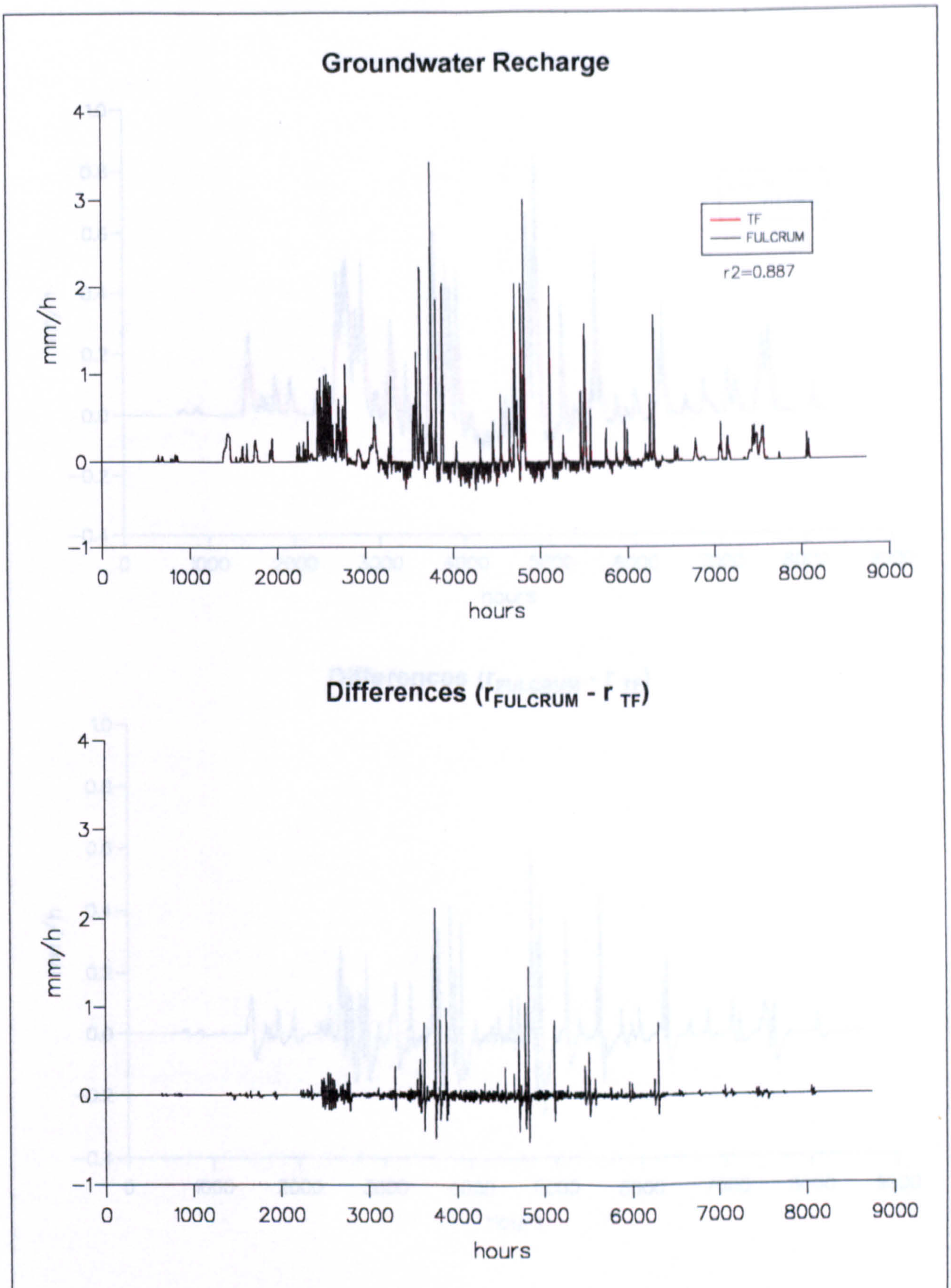

Figure 5.37 - TF approach: results for soil 1-3 (LL = -1.0 m)

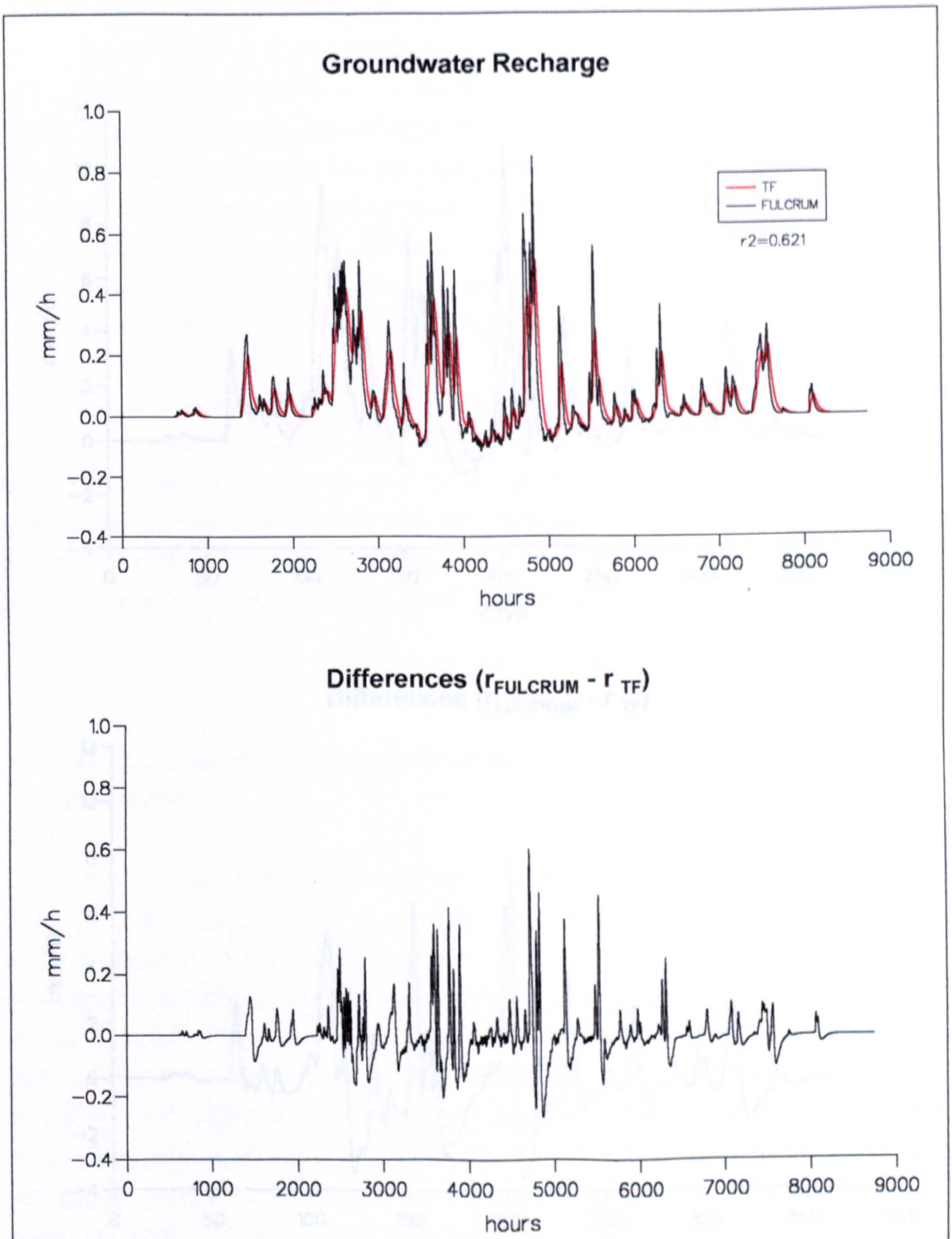

Figure 5.38 - TF approach: results for soil 1-3 (LL = -2.0 m)

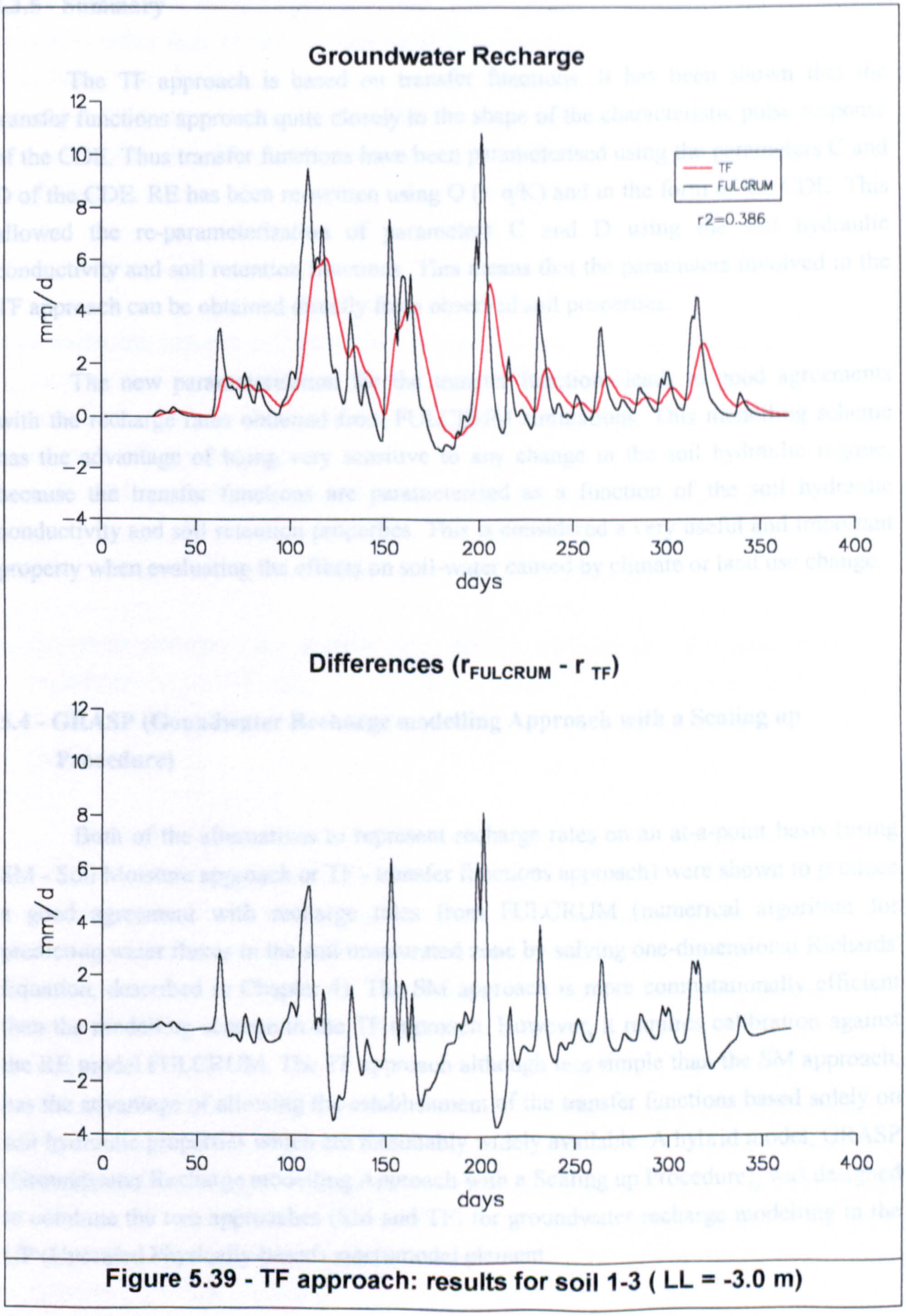

Figure 5.39 - TF approach: results for soil 1-3 (LL = -3.0 m)

5.3.5 - Summary

The TF approach is based on transfer functions. It has been shown that the transfer functions approach quite closely to the shape of the characteristic pulse response of the CDE. Thus transfer functions have been parameterised using the parameters C and D of the CDE. RE has been re-written using Q (= q/K) and in the form of the CDE. This allowed the re-parameterisation of parameters C and D using the soil hydraulic conductivity and soil retention functions. This means that the parameters involved in the TF approach can be obtained directly from observed soil properties.

The new parameterisation for the transfer functions leads to good agreements with the recharge rates obtained from FULCRUM simulations. This modelling scheme has the advantage of being very sensitive to any change in the soil hydraulic regime, because the transfer functions are parameterised as a function of the soil hydraulic conductivity and soil retention properties. This is considered a very useful and important property when evaluating the effects on soil-water caused by climate or land use change.

5.4 - GRASP (Goundwater Recharge modelling Approach with a Scaling up Procedure)

Both of the alternatives to represent recharge rates on an at-a-point basis (using SM - Soil Moisture approach or TF - transfer functions approach) were shown to produce a good agreement with recharge rates from FULCRUM (numerical algorithm for predicting water fluxes in the soil unsaturated zone by solving one-dimensional Richards' Equation, described in Chapter 4). The SM approach is more computationally efficient than the modelling scheme in the TF approach. However, it requires calibration against the RE model FULCRUM. The TF approach although less simple than the SM approach, has the advantage of allowing the establishment of the transfer functions based solely on soil hydraulic properties which are reasonably widely available. A hybrid model, GRASP (Groundwater Recharge modelling Approach with a Scaling up Procedure), was designed to combine the two approaches (SM and TF) for groundwater recharge modelling in the UP (Upscaled Physically-based) macromodel element.

In GRASP, the SM approach is the model applied at the scale of the UP element It is used rather than TF since it runs much more quickly than TF. To account for spatial variability, the SM model is parameterised by calibrating DD and δ against the aggregated responses derived using the TF at-a-point approach at a range of points within the catchment area. The process of applying GRASP within UP can be summarised by the following steps :

Pre-processing stage,

- estimate the parameters C and D for each point considered within the UP element;
- estimate the transfer functions;
- calculate recharge rates correspondent to each point and aggregate (by superposition) up to the UP element scale;
- fit the SM approach parameters δ and DD to the aggregated recharge response;

Second stage (part of the UP model main code),

- determine recharge rates at each time step by applying the SM model using the parameters δ and DD established in the pre-processing stage and total soil moisture content calculated from water mass balance for the soil water compartment of the UP model element.

Within the framework of the UP macromodel, GRASP will be fed by the UP model groundwater module with values for unsaturated zone depth (LL), with infiltration rates (this coupling is currently under development at the University of Newcastle) and evapotranspiration rates estimated in the canopy/snowmelt compartment. In addition, GRASP implies the need for a soil classification scheme. The modelling procedure for applying GRASP is demonstrated in detail in a case study in Chapter 6.

Overall, GRASP is a simple modelling scheme to simulate groundwater recharge for the UP model element. This new modelling scheme avoids the need for long and demanding RE simulations, giving results in good agreement with physically based simulations. Although GRASP was designed to work as a component of the UP model, it is believed that other modelling schemes can benefit from the approaches developed here to represent groundwater recharge.

5.5 - Summary and Conclusions

The modelling scheme GRASP was developed to represent the groundwater recharge component (percolation and capillary rise) in the UP model (Figure 3.1). GRASP comprises two modelling approaches (SM and TF) that have been formulated based on transient one-dimensional Richards' Equation (RE) simulations using FULCRUM (described in Chapter 4).

The two-parameter model in the SM approach has the advantage of being very simple to apply. It has also been shown that there is a potential to reduce the model to only one parameter. Several ways of relating the recharge parameters directly to physical property data were considered following methods successfully used by others for the description of moisture movement in porous media. A power relationship was verified between the parameter δ and LL (unsaturated zone depth) and the gradients of these curves were shown to be inversely proportional to the average hydraulic conductivity and to the hydraulic conductivity at field capacity. However, these parameters did not fully explain the values of the parameter δ found by optimisation. Overall, therefore, the analysis to relate parameters δ and DD to soil properties proved unsuccessful.

In the TF approach, it has been shown that the transfer functions calculated based on the time series from FULCRUM (numerical algorithm for predicting water fluxes in the soil unsaturated zone by solving one-dimensional RE, described in Chapter 4) approached quite closely to the shape of the characteristic pulse response of the Convection-Diffusion Equation (CDE). Based on this fact, a new form of writing RE was derived, which allowed the re-parameterisation of the parameters C and D of the CDE in terms of soil hydraulic and soil water retention properties. The new parameterisation for the transfer functions overall leads to good agreements with the recharge rates obtained by RE simulations. This modelling scheme has the advantage of being very sensitive to any change caused in the soil hydraulic regime, because the transfer function is parameterised as function of the soil's hydraulic conductivity and retention functions. This is a very useful and important property for evaluating the effects on soil-water caused by climate or land use change.

In GRASP, the SM approach is the model applied at the scale of the UP element It is used rather than TF since it runs much more quickly than TF. To account for spatial variability, the SM model is parameterised by calibrating DD and δ against the aggregated response derived using the TF at-a-point approach at a range of points within the catchment area.

In practice, good spatial resolution soil data is not always available. When this is the case, spatial variability and heterogeneity can be introduced to the model by creating an intermediate up-scaling procedure from the point scale to the patch (field site) scale. An example of this is shown by Desbarats (1995), in which probabilistic distribution functions are considered to scale up soil hydraulic functions.

The success of this hybrid approach indicates a possible relationship between the pairs of parameters C and D of the TF approach and δ and DD of the SM approach. Numerically, this linkage has proven successful. Future research could attempt to establish a direct analytical link. This could simplify the procedure involved in the model application.

At this stage no sensitivity study was attempted. This could be explored in the future, as the modelling approach is applied to a wider range of soil types. In addition, it is expected that a C, D and LL soil data base could be established, simplifying the pre-processing stage of modelling.

Chapter 6

Case Study

A small catchment with an area equivalent to that of a typical UP element was selected to demonstrate the use of GRASP. The catchment lies within the Red River Basin (Arkansas, USA) which is the basin chosen within the TIGER 3 programme for testing the UP model as a whole.

Summarising, GRASP involves the calculation of transfer functions at the point scale using the TF approach at several locations within the element area; each location having different pairs of characteristic soil retention and hydraulic functions. Aggregated (element average) recharges are then simulated using the transfer functions and parameters identified for the SM modelling approach. Once parameterised in this fashion, SM is used within the UP simulations to represent the upscaled recharge for the area of the element.

The groundwater recharge model developed in this thesis was completed before several of the other components of the UP modelling system and it was, therefore, not possible to fully test GRASP within the UP system. For example, the UP model infiltration module was not available for this application, so, infiltration and evaporation rates were simulated using FULCRUM. In addition, rainfall rates, unsaturated zone depth and land cover were considered to be uniformly distributed over the catchment area. These are not, however, limitations in GRASP and were considered here only to simplify the application, as the main objective was to demonstrate the groundwater recharge modelling procedure proposed.

6.1 - The Study Area

Little Washita catchment covers 610.20 km² and the Little Washita river is a tributary of the Washita River, southwest Oklahoma, USA. The catchment is in the southern part of the Great Plains (Figure 6.1).

The climate is classified as moist and sub-humid and average annual rainfall is around 747 mm. Summers are typically long, hot and relatively dry. Average daily high-temperature for July is around 34.4 °C and average cumulative rainfall is around 56 mm. Winters are typically short, temperate and dry. Most of the annual precipitation takes place over spring and autumn.

Surveys of the soils in the catchment were made by the US Soil Conservation Service. The soils are grouped into nine soil associations and on average are classified as loamy or sandy, fairly well drained and moderately deep. Permeabilities under saturated conditions for the central part of the catchment, where soils are sandier, are 50 mm/h or greater and where soils are finer permeability is generally less than 50 mm/h. Slopes in the catchment are generally gentle and the deepest soils in the catchment, located in the north-eastern section, are more than 1.5 m deep.

The soils are grouped into four hydrological groups according to the properties that are known to influence runoff: that is depth to the water table, infiltration rate and permeability of subsurface layers. Hydrological group A has the lowest runoff and group D the highest. Hydrologic group B is dominant, covering 72.3 percent of the catchment (US Department of Agriculture, 1991). A description of the soil hydrological groups is given in Table 6.1. The land is generally used for grassland and crops, with a small area of forest.

6.2 - Input Data used in the Simulations

The hydrometeorological data were obtained from the GEWEX initial data set (GIDS 1) CDROM. A period of about six months during spring and summer was selected for these simulations. Figure 6.2 shows the rainfall, temperature, net radiation and vapour pressure for Little Washita during the period used in the simulations.

Figure 6.1 - Location of Little Washita catchment

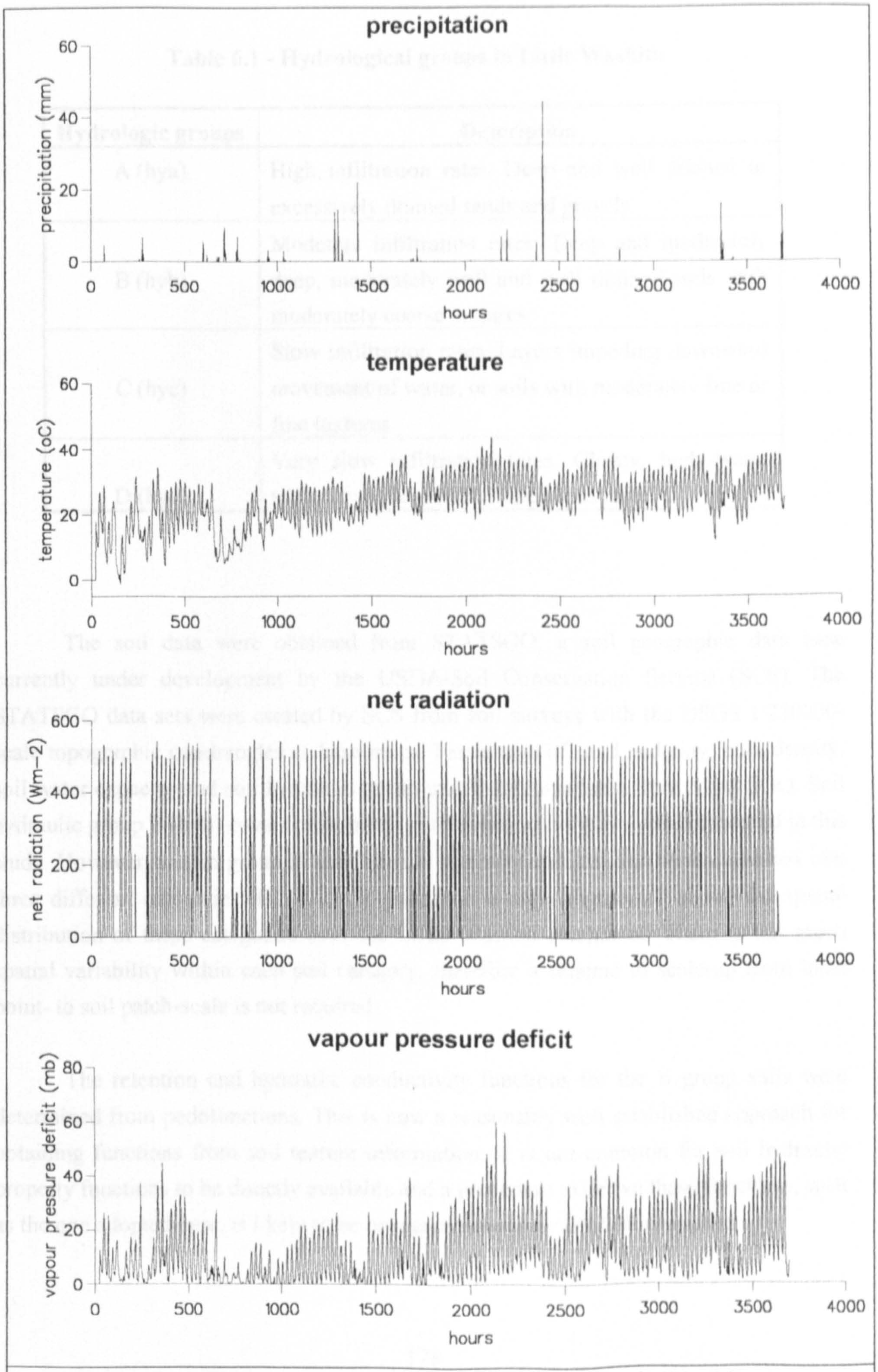

Figure 6.2 - Hydrometeorological data for Little Washita

Table 6.1 - Hydrological groups in Little Washita

Hydrologic groups	Description
A (hya)	High infiltration rates. Deep and well drained to excessively drained sands and gravels.
B (hyb)	Moderate infiltration rates. Deep and moderately deep, moderately well and well drained soils with moderately coarse textures.
C (hyc)	Slow infiltration rates. Layers impeding downward movement of water, or soils with moderately fine or fine textures.
D (hyd)	Very slow infiltration rates. Clayey, high water table, or shallow to an impervious layer.

The soil data were obtained from STATSGO, a soil geographic data base currently under development by the USDA-Soil Conservation Service (SCS). The STATSGO data sets were created by SCS from soil surveys with the USGS 1:250000-scale topographic quadrangles as base maps. Percentage of sand and clay, bulk density, soil water capacity and soil hydraulic group maps were available from STATSGO. Soil hydraulic group B (hyb) covers most of the catchment, so only hyb was considered in this study. However, within group B soils are not spatially uniform and were classified into three different categories (B1, B2, B3) based on texture. Figure 6.3 shows the spatial distribution of these categories over the Little Washita catchment. There is not much spatial variability within each soil category, therefore a scheme to scale-up from local point- to soil patch-scale is not required.

The retention and hydraulic conductivity functions for the B group soils were determined from pedofunctions. This is now a reasonably well established approach for obtaining functions from soil texture information. It is not common for soil hydraulic property functions to be directly available and a procedure to derive these functions, such as the one adopted here, is likely to be necessary whenever GRASP is applied.

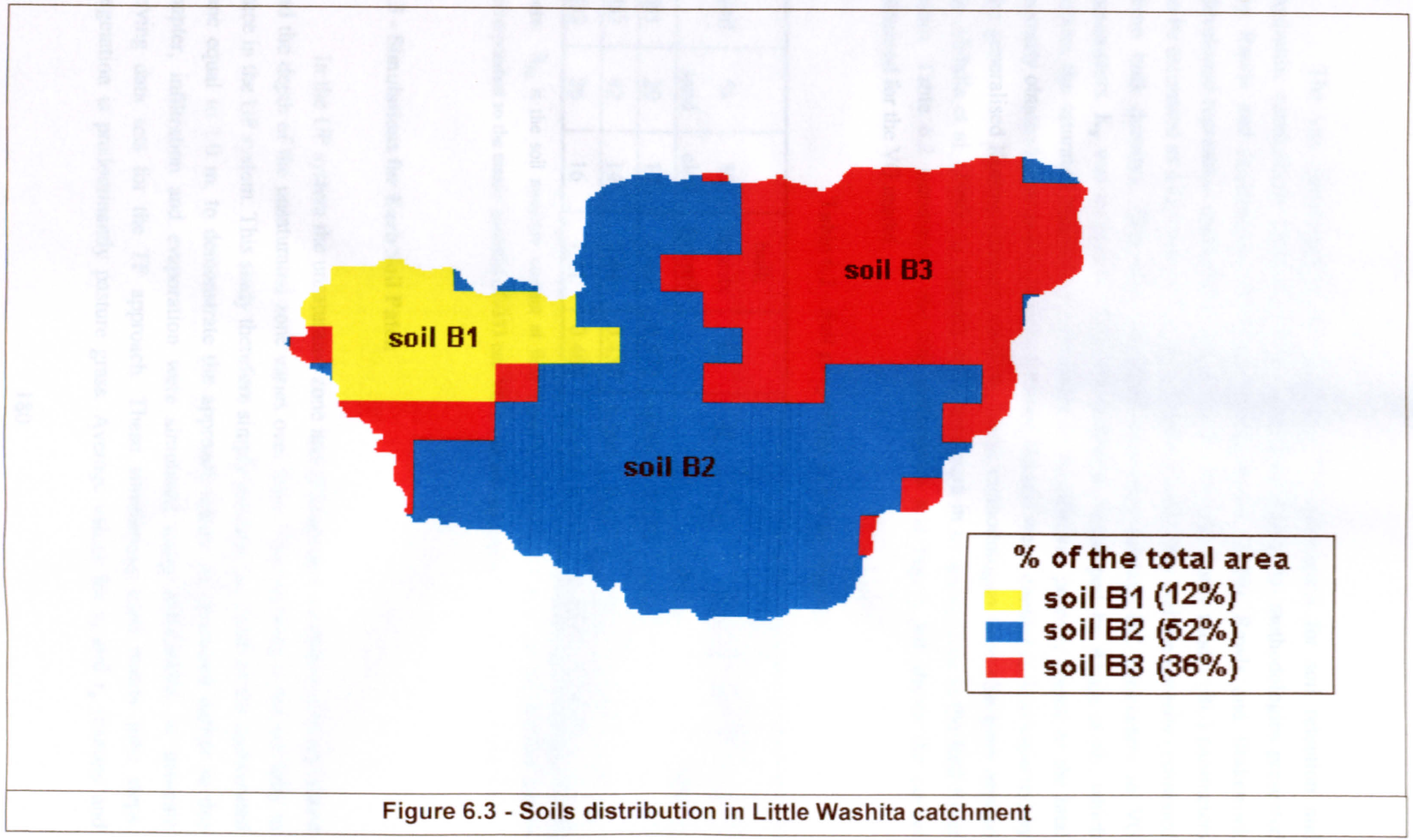

Figure 6.3 - Soils distribution in Little Washita catchment

The van Genuchten-Mualem model (VG) parameters for soil retention and hydraulic conductivity functions were obtained following the methodologies presented by Rawls and Brakensiek (1989) and Ahuja et al. (1989). Rawls and Brakensiek developed regression equations allowing the Brooks and Corey model (BC) parameters to be estimated as a function of the percentages of sand, clay and the porosity (estimated from bulk density). They also developed equations relating BC parameters to VG parameters. K_s was estimated using the technique developed by Ahuja et al., which relates the saturated hydraulic conductivity to an effective porosity (equal to the total porosity obtained from soil bulk density minus the soil water content at field capacity) by the generalised Kozeny-Carman equation. These methodologies have also been applied by Abdulla et al. (1996) to estimate soil parameters in an application to the Red River basin. Table 6.2 summarises the soil parameters and Figure 6.4 shows the curves obtained for the VG model.

Table 6.2 - Soil properties in Little Washita

soil	% sand	% clay	bulk density (g/cm^3)	θ_s	θ_r	θ_{fc}	K_s (m/day)	n	α (cm^{-1})
B1	20	17	1.40	0.472	0.067	0.273	0.393	1.330	2.19×10^{-2}
B2	42	14	1.44	0.457	0.066	0.217	0.836	1.358	4.20×10^{-2}
B3	26	16	1.41	0.468	0.066	0.257	0.499	1.338	2.58×10^{-2}

Note: θ_{fc} is the soil moisture content at field capacity, considered here to be the moisture content correspondent to the matric potential of -333 cm. VG model soil parameters were defined in section 4.2.

6.3 - Simulations for Each Soil Patch

In the UP system the unsaturated zone and groundwater compartments are linked and the depth of the unsaturated zone varies over time. This coupling is not yet fully in place in the UP system. This study therefore simply assumes the depth of the unsaturated zone equal to 1.0 m, to demonstrate the approach taken. As discussed earlier in this chapter, infiltration and evaporation were simulated using FULCRUM, to generate driving data sets for the TF approach. These simulations used hourly time steps. Vegetation is predominantly pasture grass. Average values for r_s and r_a (canopy and

aerodynamic resistance in the Penman-Monteith equation) equal to 40 and 80 sm^{-1} respectively were adopted. Soil types B1 and B3 have very similar physical properties, and for simplicity, it was assumed that infiltration and transpiration for both these soils were equal.

As described in Chapter 5, the transfer functions in TF have parameters C and D, as given in eqns. (5.17) to (5.20). Transfer functions were determined for each soil type. The values of the parameters C and D obtained for each soil type is shown on Table 6.3. Groundwater recharge for each simulated time step is given by the convolution of actual input rate (i.e. infiltration minus evaporation) and the current transfer function. Figure 6.5 shows the transfer functions for each soil patch considered in the simulations and figure 6.6 the recharge rates obtained. For soil B1, the recharge rates simulated by FULCRUM are also plotted showing the good agreement between the TF response and these obtained directly using Richards' equation. It can also be seen that the recharge rates are substantially different in the three soils, particularly for B2 compared to the other two. This shows that an aggregation approach (such as in the GRASP approach) is required if the effect of recharge spatial variability is to be properly simulated at the catchment scale.

Table 6.3 - Transfer function parameters C and D

Soil	C (m/s)	D (m^2/s)
B1	3.11×10^{-6}	6.59×10^{-7}
B2	1.57×10^{-6}	3.02×10^{-7}
B3	2.78×10^{-6}	5.72×10^{-7}

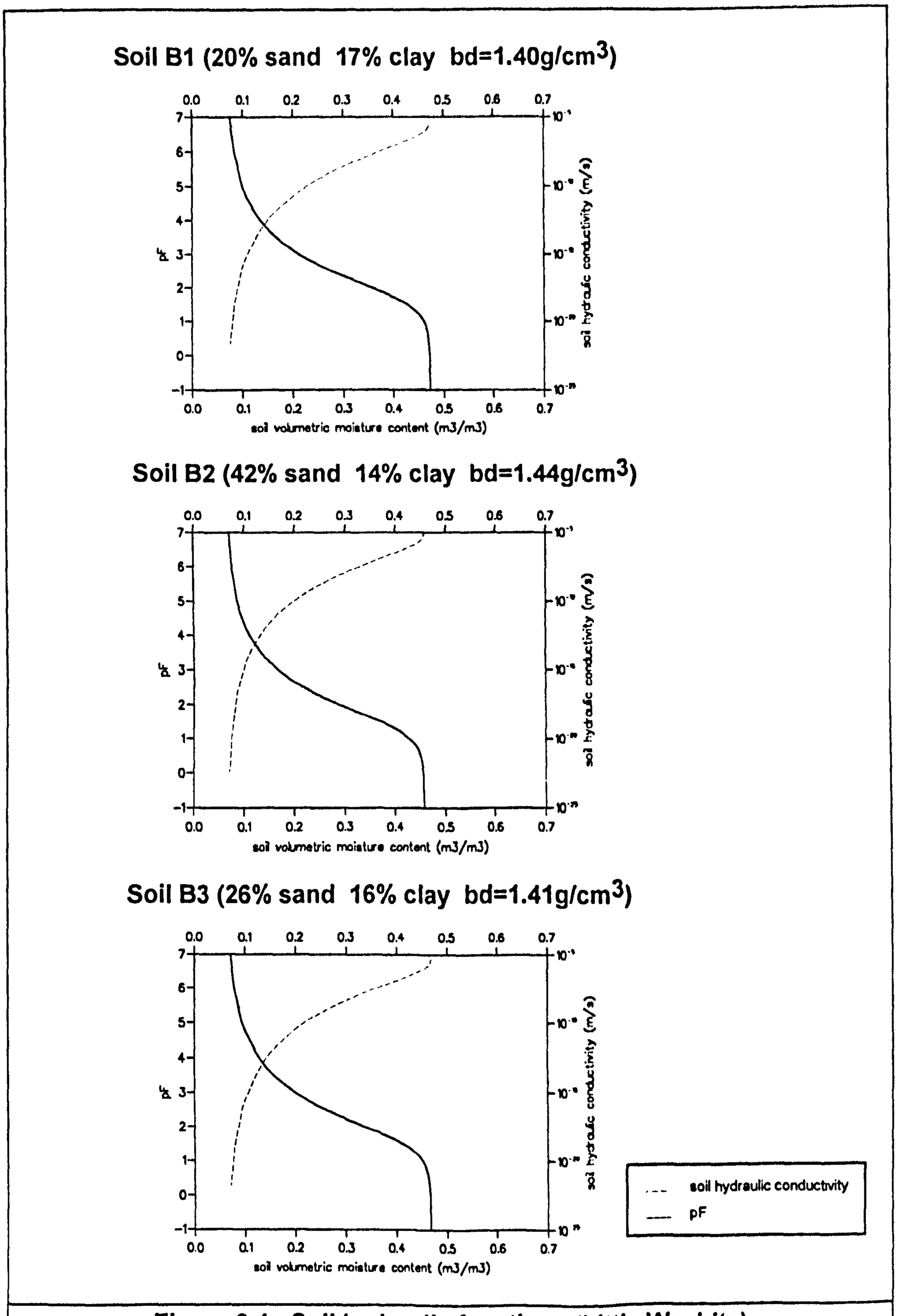

Figure 6.4 - Soil hydraulic functions (Little Washita)

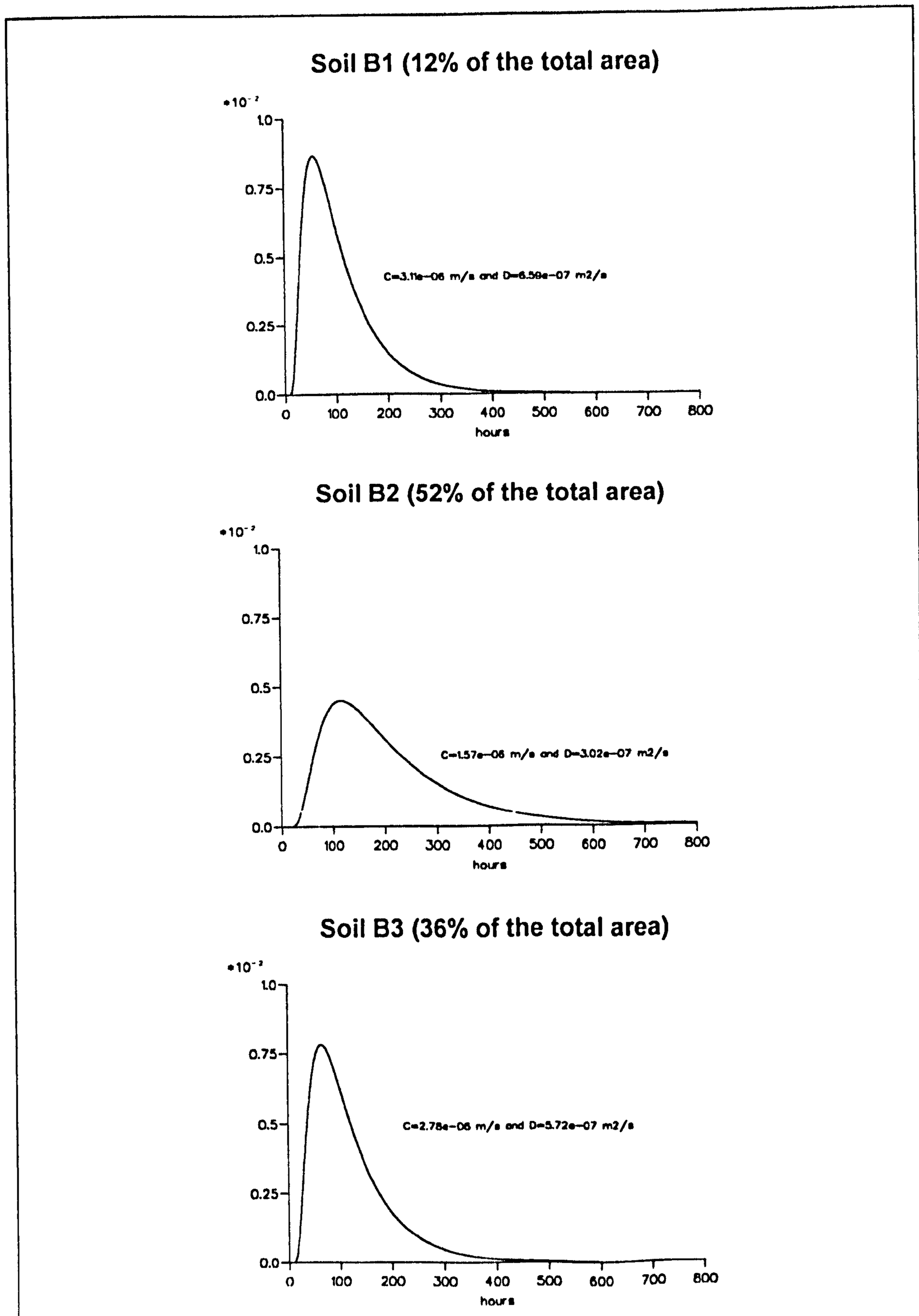

Figure 6.5 - Transfer functions for Little Washita

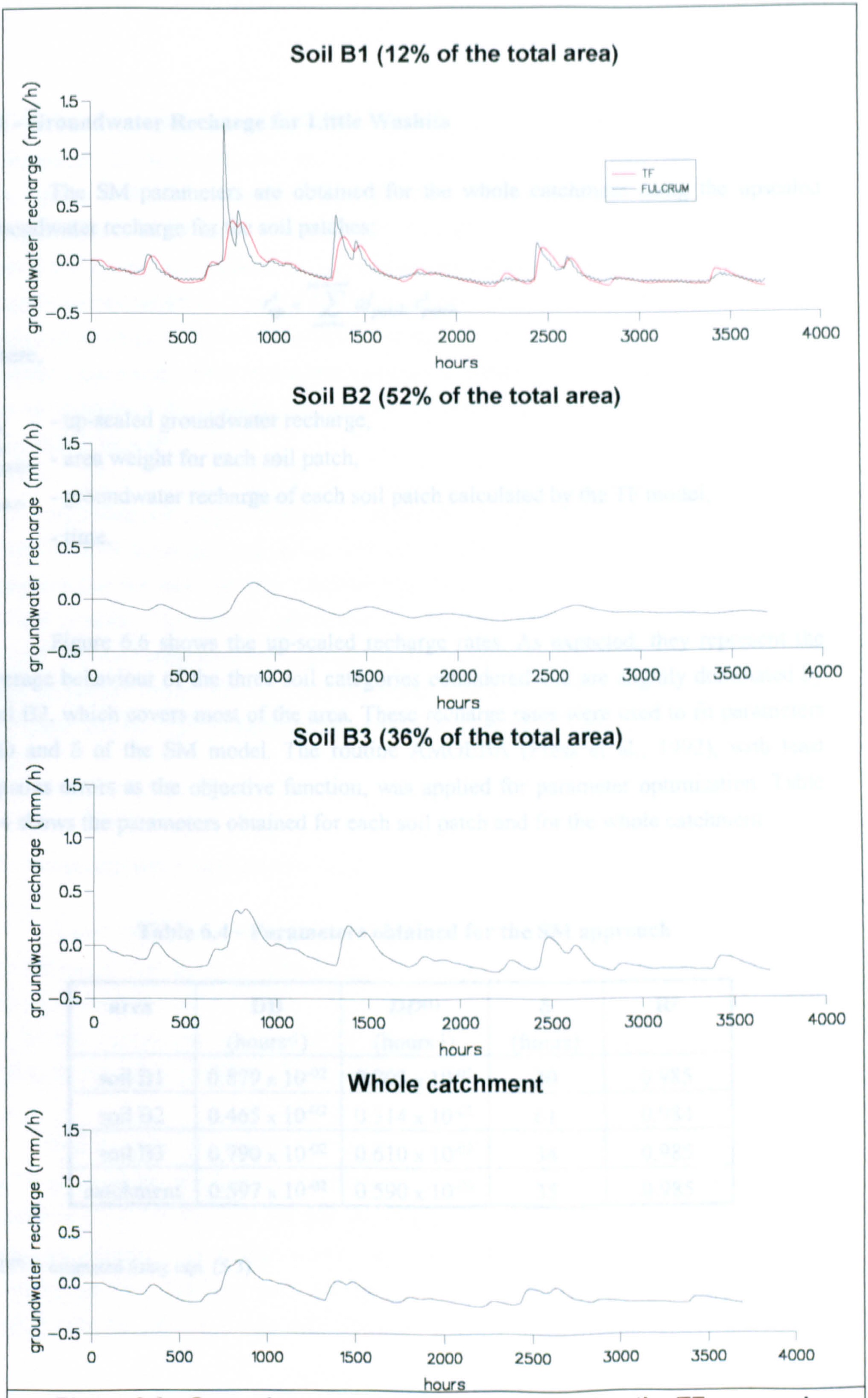

Figure 6.6 - Groundwater recharge simulated using the TF approach

6.4 - Groundwater Recharge for Little Washita

The SM parameters are obtained for the whole catchment using the upscaled groundwater recharge for the soil patches:

$$r_{up}^{t} = \sum_{patch=1}^{patch=end} \omega_{patch}^{t} \cdot r_{patch}^{t}$$

where,

r_{up}^{t} - up-scaled groundwater recharge,

ω_{patch}^{t} - area weight for each soil patch,

r_{patch}^{t} - groundwater recharge of each soil patch calculated by the TF model,

t - time.

Figure 6.6 shows the up-scaled recharge rates. As expected, they represent the average behaviour of the three soil categories considered and are slightly dominated by soil B2, which covers most of the area. These recharge rates were used to fit parameters DD and δ of the SM model. The routine AMOEBA (Press et al., 1992), with least squares errors as the objective function, was applied for parameter optimisation. Table 6.4 shows the parameters obtained for each soil patch and for the whole catchment.

Table 6.4 - Parameters obtained for the SM approach

area	DD (hours^{-1})	$DD^{(1)}$ (hours^{-1})	δ (hours)	R^2
soil B1	0.879×10^{-02}	0.703×10^{-02}	30	0.985
soil B2	0.465×10^{-02}	0.314×10^{-02}	61	0.984
soil B3	0.790×10^{-02}	0.610×10^{-02}	34	0.985
catchment	0.597×10^{-02}	0.590×10^{-02}	35	0.985

$DD^{(1)}$ - estimated using eqn. (5.3).

The fitting of the parameters DD and δ was very fast and no major problems were encountered. Several different start points were considered and the process of convergence to the solution was consistent. The results of the optimisation were good, with coefficients of determination around 0.980. Eqn. (5.3), which relates DD and δ, was applied and the values obtained for DD approached reasonably well to the values of DD obtained by optimisation (Table 6.4). As expected, the value of parameter DD for the catchment is close to the area-weighted average of the values of the soil patches. No apparent relationship across scales was verified for parameter δ. Further study is required in order to explore the possible relationships for scaling-up or -down parameters across scales using GRASP.

As a final comparison, Figure 6.7 shows the groundwater recharge rate calculated by the GRASP approach (i.e. using DD and δ, for catchment Table 6.4, in the SM approach) and the recharge rate obtained from aggregating the individual responses for the soil patches. The overall agreement is very good. Since it has been shown that GRASP properly represents the aggregated effects of soil patch responses, and the soil patch responses (using TF) properly represent Richards equation responses it can be concluded that GRASP properly upscales Richards' equation responses to the catchment scale.

6.5 - Summary and Conclusions

A case study was carried out to demonstrate the use of the GRASP approach. The area chosen for the study was the Little Washita, Red River basin, USA, which has an area equivalent to that of a typical UP element. Little Washita is the area chosen within the TIGER 3 programme for the testing of the UP model. The scope of this study was limited by the non-availability of some of the other components of the UP system.

Soil types B1, B2 and B3 (Tables 6.2 and 6.3) were considered. The sensitivity of the TF model to the soil hydraulic functions can be seen by comparing the recharge rates simulated using TF for soils B1 and B3 (Figure 6.6). The soil hydraulic functions for these two soils are very similar, which led to the application of the same infiltration and transpiration rates for both soils. However, recharge rates for soil B3 were generally smaller than for soil B1. Small differences in hydraulic functions do lead to differences

in recharge showing that, as it should be, the TF approach is sensitive to the soil hydraulic functions.

As expected, because of the linear upscaling approach taken, the recharge for the whole catchment represents the average recharge of the soil types considered, being slightly dominated by soil B2 which covers most of the catchment area.

When fitting parameters DD and δ, different starting points were used for the optimisation and the convergence was very fast and consistent. It was also noticed, as expected, that the value of DD for the catchment recharge rate is close to the area-weighted average of the values for the individual soils. No particular relationship across scales was identified for parameter δ. It would be interesting to continue this analysis and see if it is possible to identify a relationship to fully represent the way the upscaled model parameters vary across scales.

The estimations for parameter DD, using eqn. (5.3) that relates DD and δ, are in reasonable agreement with the values found by optimisation. This is encouraging and may, in the future, reduce the SM approach to one parameter.

The GRASP simulations seem to produce a very good general agreement.

To apply GRASP it is important to have a high resolution soil map: one was available in this case. In addition, this approach is likely to benefit from systems for classifying hydrologically similar units, which will save computing time. In this case, the catchment had previously been studied and the delineation of homogeneous patches was already available. Therefore, within each soil patch there was not much spatial variability, and average soil properties were assigned for each soil-patch. When this is not the case, spatial variability within the soil patches can be taken into account either by considering pdfs to scale up soil hydraulic functions from point- to the patch- scale or by sampling the occurrence of each soil type.

The pedofunctions (e.g. Rawls and Brakensiek, 1989) which estimate the parameters of the VG functions from soil particle analysis are very useful. Here, the functions adopted use only soil bulk density and the percentage of clay and sand. There are, however, other regression functions that take into account more soil characteristics,

such as soil moisture content at field capacity and wilting point. It is expected that as more information about the soil is introduced, more realistic functions are going to be produced. Texture analysis is not difficult to carry out, and texture is often one of the widely available soil properties. Nevertheless, it should be borne in mind that although the development of the regression curves of pedofunctions usually considers a large number of soils types in the regression analysis (in the case of Rawls and Brakensiek more than 1000 types have been considered), soils are quite variable, so pedofunctions should be applied cautiously to regions for which these functions have previously not been tested or applied.

It was assumed that the rainfall was uniformly distributed. This approximation was used to simplify the application as the main objective was to demonstrate the use of GRASP. Further studies should evaluate the effect of considering non-uniform distributed rainfall. The next major step, however, should be the analysis of the GRASP approach when used within the UP model.

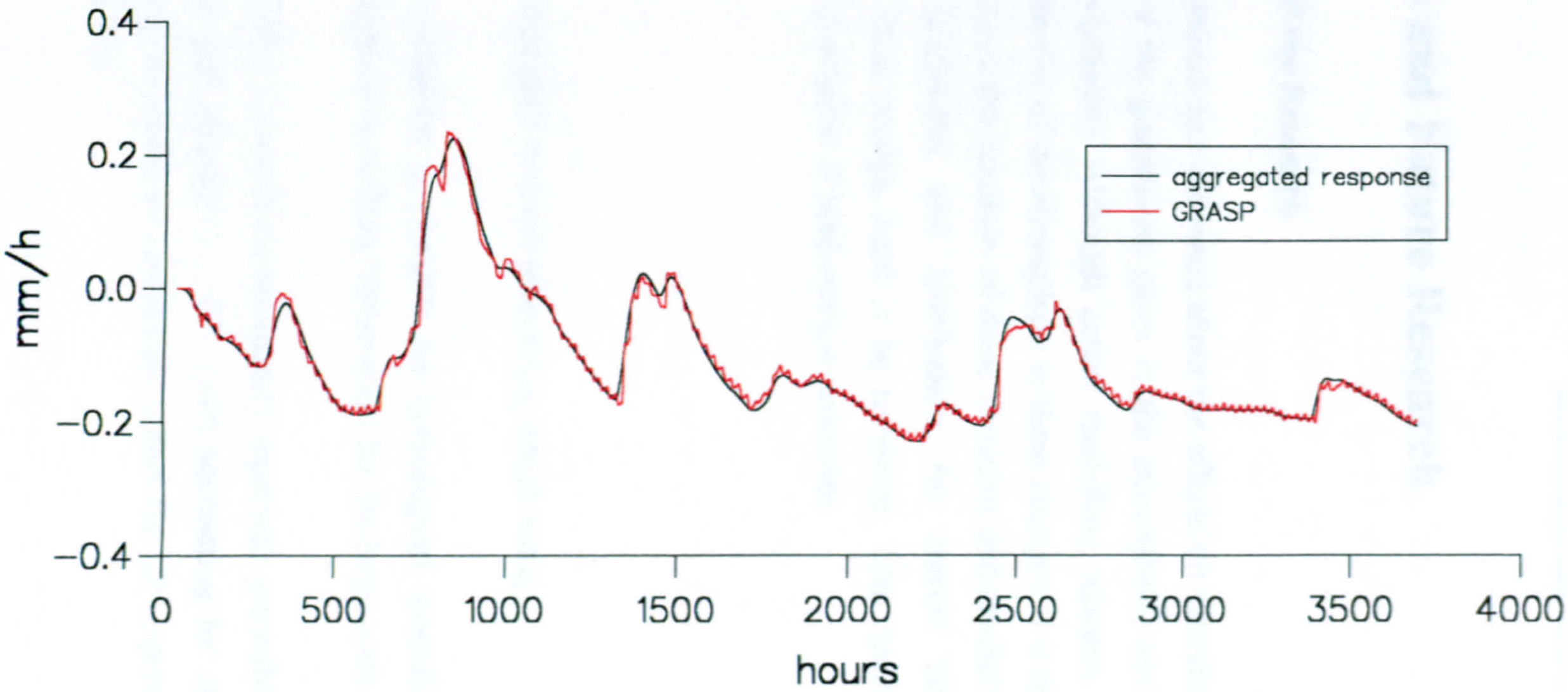

Figure 6.7 - Groundwater recharge for Little Washita

Chapter 7

Conclusions and Future Research

7.1 - Importance of the Research

Recently, concern has increased about the effects on climate of both a build up in the concentration of the greenhouse gases in the atmosphere, and large scale land use changes (e.g. deforestation). Although actual modelling schemes have been useful in identifying the sensitivity of the atmosphere to these changes, it is now widely recognised that in order to enhance the accuracy of these forecasts and predict the consequences for water resources availability and distribution, the current land-surface processes representations in these models need to be reviewed. This research is a contribution towards a new representation of land-surface processes.

7.2 - Conclusions

This research accomplished its main objectives, which were,

- Review current modelling procedures for hydrological modelling in support of the development of improved modelling frameworks for the large scale.

- Develop a modelling approach to adequately represent groundwater recharge for the small catchment or grid element (~ 100 km^2) accounting for spatial variability, and appropriate for use as the recharge component within the UP (Upscaled Physically-based) macromodel framework.

From the review it was concluded that a new approach is necessary in order to enhance land-surface (global hydrologic cycle) representation in GCMs, and a number of recommendations were drawn up for developing new hydrological approaches for the large scale. These can be summarised as:

- the model should represent explicitly named physical processes (e.g. exfiltration, groundwater recharge) as in the descriptive structure typical in ESMA (Explicit Soil Moisture Accounting) models;
- all aspects of the model should have a physical interpretation;
- the parameters in the model should be measurable or easily acquired from physical features (e.g. topography, mapped river networks, land cover, soil type, etc.), minimising the need for calibration;
- the parameters should be sensitive to environmental change;
- the required data should be, as far as possible, globally available;
- the model should be computationally efficient, fast and simple to run.

The model GRASP (Groundwater Recharge modelling Approach with a Scaling up Procedure) was proposed as a component of the UP macromodel (large scale hydrological model currently under development at the University of Newcastle as their contribution to the TIGER programme). GRASP works based on two modelling approaches, both based on the one-dimensional Richards equation. SM (Soil Moisture content approach) is applied at the small-catchment or grid-element scale (about 100 km^2). In SM, groundwater recharge is given as a linear function of soil moisture content. It has the advantage of being very simple to apply. In addition, it was suggested that there is potential for reducing the model to one parameter. Several ways of relating the recharge parameters directly to physical property data were considered, but none proved fully successful. The two parameters of SM are fitted to recharge rates upscaled (aggregated) from the point-scale, which are calculated using the TF (Transfer Function approach).

TF, the other modelling approach involved in GRASP, is applied at the point scale in the pre-processing stage of GRASP and involves the use of transfer functions. The two parameters of the transfer function are derived based on the soil retention and hydraulic conductivity functions. The expressions for estimating these parameters were

derived from the Richards equation re-written in terms of Q=q/K and in the form of the convection-diffusion equation. A case study, using data from Little Washita (which is located in the Red river basin-USA) was carried out to demonstrate the use of GRASP.

Both modelling approaches involved in GRASP (SM and TF) were able to simulate recharge rates that were in agreement with the recharge rates simulated by the one-dimensional Richards equation. This is evidence that simplified models based on partial analysis may successfully be used to represent complex systems, while allowing physical interpretation.

One of major advantages of this approach is that it allows for a connection between model parameters and physical characteristics that can be derived from field observations. This makes it possible to incorporate physical reality into modelling. Apart from this, the parameterisation of C and D of the transfer functions are based on the soil hydraulic functions which are expected to be sensitive to environmental changes.

Soil hydraulic functions may not be readily available for some regions of the globe. However, the possibilities introduced by the use of pedofunctions should be considered. These functions are mainly parameterised based on texture analysis elements, which are relatively easier to obtain and more widely available. The use of pedofunctions to derive the soil retention and hydraulic conductivity functions has been demonstrated in the case study. Nevertheless, these functions should be applied cautiously to regions for which they have not previously been applied or tested, even though the pedofunctions are derived based on regression analysis in which a large number of soil types are considered.

The use of GRASP was successfully demonstrated in the case study. The study was limited, however, by non-availability of some of the other components of the UP macromodel. Moreover, rainfall was considered to be uniformly distributed over the element. This approximation was used to simplify the application, as the main objective was to demonstrate the use of GRASP.

The general framework of the UP macromodel allows for a pre-processing stage for some of the components, and this is the case in GRASP. It is expected that with increasing model applications the pre-processing stage would be simplified by creating a soil database for C,D and LL.

Finally, although GRASP was designed mainly to be a component of the UP model, it is believed that the modelling approach adopted in GRASP can be used in other applications in hydrology.

7.3 - Recommendations for Future Research

Based on the previous discussion, recommendations for future research can be summarised as:

- GRASP was developed based on fully physically based one-dimensional simulations using Richards' equation. The data used in the simulations were real data, and soil types considered in the simulations covered a range of soil groups. In addition, the use of GRASP was demonstrated successfully for the completely independent soils data of Little Washita. However, soils are very variable, and future work should attempt to extend the validation of GRASP for other soils, as well as other climatological conditions. Thus, with these extended validation practices, the sensitivity of the parameters in GRASP could be better analysed. Moreover, from these studies a database of physically sound values for the parameters could be collected.

- The use of GRASP was demonstrated successfully in a case study using data from Little Washita. However, this study was limited, because the UP model is not fully developed. Future work should attempt to extend the validation of GRASP within the model as whole and its interaction with the other components, in particular the other components in the soil compartment as well as the groundwater compartment.

- Although it is expected that following future modelling applications the pre-processing stage would be simplified by creating a C, D, LL soil database, the approach in GRASP may be reduced to only one stage by relating the parameters in SM directly to soil physical properties. Several ways of relating the recharge parameters directly to physical property data were considered but, overall, none proved to be fully successful. SM and TF are in some way correlated. This relationship has been demonstrated numerically as it was possible to fit SM to responses from TF. Thus, in theory, it should be possible to relate the parameters in SM to the parameters in TF, creating a link between the parameters in SM and the soil retention and soil hydraulic conductivity functions. Future work could attempt to derive the pulse response for SM's storage function, and by comparison with the pulse response in TF, the link could be established.

REFERENCES

Abbott, M. B., Bathurst, J. C., Cunge, J. A., O'Connell, P. E. and Rasmussen, J., 1986a, An introduction to the European hydrological system - Système Hydrologique Européen, 'SHE', 1: history and philosophy of a physically-based distributed modelling system, J. Hydrol., 87, 45-59.

Abbott, M. B., Bathurst, J. C., Cunge, J. A., O'Connell, P. E. and Rasmussen, J., 1986b, An introduction to the European hydrological system - Système Hydrologique Européen, 'SHE', 2: structure of a physically-based distributed modelling System, J. Hydrol., 87, 67-77.

Abdulla, F. A., Lettenmaier, D. P., Wood, E. F. and Smith, J. A., 1996, Application of a macroscale hydrologic model to estimate the water balance of the Arkansas-Red River Basin, J. Geophys. Res., 101(D3) 7449-7459.

Ahuja, L. R., Cassel, D. K., Bruce, R. R. and Barnes, B. B., 1989, Evaluation of spatial distribution of hydraulic conductivity using effective porosity data, Soil Sci., 148, 404-411.

Anderton, S. P., Parkin, G. and Ewen, J., 1994, Simulations of the migration of ^{36}Cl and ^{129}I in a hypothetical catchment under a boreal climate (DSATE series), Department of Civil Engineering, University of Newcastle upon Tyne, UK.

André, J. C., Bougeault, P. and Goutorbe, J. P., 1990, Regional estimates of heat and evaporation fluxes over non-homogeneous terrain: examples from HAPEX-MOBILHY program, Boundary Layer Meteorol., 50, 77-108.

Arain, A. M., Michaud, J., Shuttleworth, W. J. and Dolman, A. J., 1996, Testing of vegetation parameter aggregation rules applicable to the Biosphere-Atmosphere Tranfer Schemes (BATS) and FIFE site, J. Hydrol., 177, 1-22.

Arnell, N. W., 1993, Data requirements for macroscale modelling of the hydrosphere, in Macroscale Modelling of the Hydrosphere, IAHS publ. no. 214, 139-150.

Avissar, R., 1992, Conceptual aspects of a statistical-dynamical approach to represent landscape sub-grid-scale heterogeneities in atmospheric models, J. Geophys. Res., 97(D3), 2729-2742.

Barry, D. A., Parlange, J. -Y., Sander, G. C. and Sivapalan, M., 1993, A class of exact solutions for Richards's equation, J. Hydrol., 142, 29-46.

Bathurst, J. C., 1986, Physically-based distributed modelling of an upland catchment using the Système Hydrologique Européen, J. Hydrol., 87, 79-102.

Bathurst, J. C., 1986, Sensitive analysis of the Système Hydrologique Européen for an upland catchment, J. Hydrol., 87, 103-123.

Bathurst, J. C. and O'Connell, P. E., 1992, Future of distributed modelling: the Système Hydrologique Européen, Hydrol. Process., 6, 265-277.

Bathurst, J. C. and Cooley, K. R., 1996, Use of SHE hydrological modelling system to investigate basin response to snowmelt at Reynolds Creek, Idaho, J. Hydrol., 175, 181-211.

Bear, J., 1972, Dynamics of fluids in porous media, Dover Publications Inc., New York.

Becker, A. and Nemec, J., 1987, Macroscale hydrologic models in support to climate research, IAHS Publ., no.168, 431-445.

Becker, A., 1992, Criteria for a hydrologically sound structuring of large scale land surface process models, in Advances in Theoretical Hydrology: a tribute to James Dooge, J. Philip O' Kane (ed.), Elsevier, New York, 97-111.

Besbes, M. and De Marsily, G., 1984, From infiltration to recharge: use of a parametric transfer function, J. Hydrol., 74, 271-293.

Betson, R. P., 1964, What is watershed runoff?, J. Geophys. Res., 69(8), 1541-1552.

Beven, K. and Kirkby, M. J., 1979, A physically-based, variable contributing area model of basin hydrology, Hydrol. Sci. Bull., 24(1), 43-69.

Beven, K. and O'Connell, P.E., 1982, On the role of physically-based distributed modelling in hydrology, Report no. 81, Institute of Hydrology, Wallingford, UK.

Beven, K. J. and Germann, P. F., 1982, Macropores and water flow in soils, Water Resour. Res., 18, 1311-1325.

Beven, K., Kirkby, M. J., Schoffield, N. and Tagg, A., 1984, Testing a physically-based, flood forecasting model TOPMODEL for three U.K. catchments, J. Hydrol., 69, 119-143.

Beven, K., Calver, A. and Morris, E. M., 1987, The Institute of Hydrology distributed model, Report No. 98, Institute of Hydrology, Wallingford, UK.

Beven, K., 1989, Changing ideas in hydrology - The case of physically-based models, J. Hydrol., 105, 157-172.

Beven, K., 1995, Linking parameters across scales: subgrid parameterizations and scale dependent hydrological models, Hydrol. Process., 9, 507-525.

Binley, A. and Beven, K., 1992, The future of distributed models: model calibration and uncertainty prediction, Hydrol. Process., 6, 279-298.

Birkinshaw, S., 1993, Testing and modifying FULCRUM, M.Sc. dissertation, Department of Civil Engineering, University of Newcastle upon Tyne, UK.

Blöschl, G. and Sivapalan, M., 1995, Scale issues in hydrological modelling: a review, Hydrol. Process., 9, 251-290.

Bouchet, R. J., 1963, Evapotranspiration réelle et potentielle, signification climatique, in Int. Assoc. Sci. Hydrol., Proceedings, Berkeley, Calif. Symp. Publ. 62, 134-142.

Broadbridge, P. and White, I., 1988, Constant rate rainfall infiltration: a versatile nonlinear model, 1. Analytical solution, Water Resour. Res., 24(1), 145-154.

Brooks, R. H. and Corey, A.T., 1966, Properties of porous media affecting fluid flow, J. Irrig. Drain. Amer. Soc. Civil Eng., IR2, 61-88.

Brun, C., Bernard, R., Vidal-Madjar, D., Gascuel-Odoux, C., Merot, P., Duchesne, J. and Nicolas, H., 1990, Mapping saturated areas with a helicopter-borne C-band scatterrometer, Water Resour. Res., 26(5), 945-955.

Brutsaert, W. and Stricker, H., 1979, An advection-aridity approach to estimating actual regional evaporation, Water Resour. Res., 15, 443-450.

Brutsaert, W., 1986, Catchment-scale evaporation and the atmospheric boundary layer, Water Resour. Res., 2(9), 39s - 45s.

Brutsaert, W., 1991, The formulation of evaporation from land surfaces, in Advances in the Modelling of Hydrologic Systems, D. S. Bowles and P. E. O'Connell (eds.), Kluwer Academic Publishers, 67 - 84.

Burgers, J. M., 1948, A mathematical model illustrating the theory of turbulence, Adv. Appl. Mech., 1, 171-179.

Calver, A., 1988, Calibration, sensitivity and validation of a physically based rainfall-runoff model, J. Hydrol., 103, 103-115.

Carsel, R. F. and Parrish, 1988, Developing joint probability distributions of soil water retention characteristics, Water Resour. Res., 24, 755-769.

Carslaw, H. S. and Jaeger, J. C., 1959, Conduction of heat in solids, Oxford University Press, Oxford.

Celia, M. A., Bouloutas, E. T. and Zarba, R. L., 1990, A general mass-conservative numerical solution for the unsaturated flow equation, Water Resour. Res., 26(7), 1483-1496.

Chen, F., Mitchell, K., Schaake, J., Xue, Y., Pan, H-L, Koren, V., Duan, Q. Y., Ek, M. and Betts, A., 1996, Modelling of land surface evaporation by four schemes and comparison with FIFE observations, J. Geophys. Res., 101(D3), 7251-7268.

Chen, Z., Govindaraju, R. S. and Kavvas, M. L., 1994a, Spatial averaging of unsaturated flow equations under infiltration conditions over areally heteregeneous fields, 1. Development of models, Water Resour. Res., 30(2), 523-533.

Chen, Z., Govindaraju, R. S. and Kavvas, M. L., 1994b, Spatial averaging of unsaturated flow equations under infiltration conditions over areally heteregeneous fields, 2. Numerical simulations, Water Resour. Res., 30(2), 535-548.

Chow, V. T., Maidment, D. R. and Mays, L. W., 1988, Applied Hydrology, McGrawHill, New York.

Cowpertwait, P. S. P., O'Connell, P. E., Metcalfe, A. V. and Mawdsley, J. A., 1996, Stochastic point process modelling of rainfall. II. Regionalisation and disaggregation, J. Hydrol., 175, 17-46.

Crawford, N. H. and Linsley, R. K., 1966, Digital simulation in hydrology: Stanford watershed model IV, Technical report No. 39, Dep. of Civil Eng., Stanford University.

Dawdy, D. R. and O'Donnell, T., 1965, Mathematical models of catchment behaviour, J. Hyd. Div. ASCE, 91(HYA), 123-137.

Desbarats, A. J., 1995, Upscaling capillary pressure-saturation curves in heterogeneous porous media, Water Resour. Res., 31(2), 281-288.

Dickinson, R. E., Henderson-Sellers, A., Rosenzweig, C. and Sellers, P. J., 1991, Evapotranspiration models with canopy resistance for use in climate models, a review, Agricultural and Forestry Meteorology, 54, 373 - 388.

Dooge, J. C. I., 1986, Looking for hydrologic laws, Water Resour. Res., 22(9), 46s-58s.

Dümenil, L. and Todini, E., 1992, A rainfall-runoff scheme for use in the Hamburg climate model, in Advances in Theoretical Hydrology: a tribute to James Dooge, J. Philip O' Kane (ed.), Elsevier, New York, 129-173.

Dunne, T., 1978, Field studies of hillslope flow processes, in Hillslope hydrology, M. J. Kirkby (ed.), John Wiley and Sons, 227-294.

Durner, W., 1994, Hydraulic conductivity estimation for soils with heterogeneous pore structure, Water Resour. Res., 30(2), 211-223.

Eltahir, E. A. B. and Bras, R. L., 1993, A description of interception over large areas, J. Climate, 6, 1002-1008.

Engman, E. T., Jackson, T. J. and Schmugge, T. J., 1983, Implications of complete watershed soil moisture measurements to hydrologic modelling, IEEE Int. Geoscience and Remote Sensing Symposium, San Francisco, Calif., 1(TA-1), 2.2-2.5.

Engman, E. T. and Gurney, R. J., 1991, Remote sensing in hydrology, Chapman & Hall, London.

Entekhabi, D. and Eagleson, P. S., 1989, Land surface hydrology parameterization for atmospheric general circulation models including sub-grid scale spatial variability, J. Climate, 2(8), 816-831.

Famiglietti, J. S. and Wood, E., 1994a, Multiscale modeling of spatially variable water and energy balance processes, Water Resour. Res., 30(11), 3061-3078.

Famiglietti, J. S. and Wood, E., 1994b, Application of multiscale water and energy balance models on a tallgrass prairie, Water Resour. Res., 30(11), 3079-3093.

FAO/UNESCO, 1974, Soil Map of the World, 1:5,000,000, FAO, Paris.

Fett, W., Neumann, P. and Schultz, G. A., 1990, Hydrological model based on satellite imagery and GIS, Int. Symosium on Remote Sensing and Water Resources, Enschede, The Netherlands.

Fleming, G., 1975, Computer simulation techniques in hydrology, Elsevier, New York.

Franchini, M. and Pacciani, M., 1991, Comparative analysis of rainfall-runoff models, J. Hydrol., 122, 161-219.

Franchini, M., Wendling, J., Obled, C. and Todini, E., 1996, Physical interpretation and sensitivity analysis of the TOPMODEL, J. Hydrol., 175, 293-338.

Fujita, H., 1952, The exact pattern of a concentration-dependent diffusion in a semi-infinite medium, 2, Textile Res. J., 22, 823-827.

Geyer, B. and Jarvis, P., 1991, A review of models of Soil - Vegetation - Atmosphere - Transfer - Schemes (SVATS): a report to the TIGER III Committee.

Goutorbe, J. P., Lebel, T., Tinga, A., Bessemoulin, P., Brouwer, J., Dolman, A. J., Engman, E. T., Gash, J. H. C., Hoepfiner, M., Kabat, P., Kerr, Y., Monteney, B., Prince, S., Said, F., Sellers, P. and Wallace, J. S., 1994, HAPEX-Sahel: a large scale study of land-atmosphere interactions in the semi-arid tropics, Annales Geophysicae, 12, 53-64.

Grayson, R. B., Moore, I. D. and McMahon, T. A., 1992, Physically based hydrologic modeling: 1. A terrain-based model for investigative purposes, Water Resour. Res., 26(10), 2639-2658.

Gregory, D. and Smith, R. N. B., 1993, Canopy, surface and soil hydrology, Unified Model Documation paper 25.

Gottardi, G. and Venutelli, M., 1993, Richards: Computer Program for the Numerical Simulation of One-Dimensional Infiltration Into Unsaturated Soil, Computers and Geoscience, 19(2), 1239-1266.

Green, W. H. and Ampt, G. A., 1911, Studies on soil physics, part I, the flow of air and water through soils, J. Agric. Sci., 4(1), 1-24.

Haverkamp, R., Vauclin, M., Touma, J., Wierenga, P. J. and Vachaud, G., 1977, Soil Sci. Soc. Am. J., 41, 285-294.

Hendrickson, J. D., Sorooshian, S. and Brazil, L. E., 1988, Comparison of Newton-type and direct search algorithms for calibration of conceptual rainfall-runoff models, Water Resour. Res., 24(5), 691-700.

Hewlett, J. D. and Hibbert, A. R., 1967, Factors affecting the response of small watersheds to precipitation in humids areas, in Forest Hydrology, W. E. Sopper and H. W. Lull (eds.), Pergamon, 275-290.

Hills, R. G. and Warrick, A. W., 1993, Burgers' equation: a solution for soil water flow in a finite length, Water Resour. Res., 29(4), 1179-1184.

Holwill, C. J. and Stewart, J. B., 1992, Spatial variability of evaporation derived from aircraft and ground-based data, J. Geophys. Res., 97(D17), 18,673 - 18,680.

Ibbit, R. P. and O'Donnell, T., 1971, Fitting methods for conceptual catchment models, J. Hydraul. Eng., 97(HY9), 1331-1342.

Intergovernmental Panel on Climate Change (IPCC), 1990, Climate Change, The IPCC Scientific Assessment, J.T. Houghton, G.J. Jenkins and J.J. Ephraums (eds.), Cambridge University, Cambridge.

International GEWEX Project Office, 1991, Continental-scale International Project (GCIP), Rep. 1, Washington, D.C..

International Geosphere-Biosphere Programme, 1990, The International Geosphere-Biosphere Programme: a study of global change, the initial core projects, Rep. 12, Stockholm.

Jackson, T. J. and Schmugge, T. J., 1981, Aircraft active microwave measuments for estimating soil moisture, Photogr. Eng. Remote Sensing, 47(6), 801-805.

Jensen, K. H. and Mantoglou, A., 1992, Future of Distributed Modelling, Hydrol. Process., 6, 225-264.

Johansson, P.-O., 1988, Methods for estimation of natural groundwater recharge directly from precipitation - comparative studies in sandy till, in Estimation of natural groundwater recharge, ed. by I. Simmers, D. Reidel Publishing Company, Netherlands, 239-270.

Johnson, K.D., Entekhabi, D. and Eagleson, P., 1993, The implementation and validation of improved land-surface hydrology in an atmospheric general circulation model, J. Climate, 6, 1009-1026.

Johnston, P. R. and Pilgrim, D., 1976, Parameter optimisation for watershed models, Water Resour. Res., 12(3), 477-486.

Khaleel, R., Relyea, J. F. and Conca, J. L., 1995, Evaluation of van Genuchten-Mualem relationships to estimate unsaturated hydraulic conductivity at low water contents, Water Resour. Res., 31, 11, 2659-2668.

King, A.W., 1991, Translating models across scales in the landscape, Ecological Studies, 82, 479-517.

Kirchhoff, G., 1894, Vorlesungen über die Theorie der Wärme, Barth, Leipzig.

Kite, G. W., Dalton, A. and Dion, K., 1994, Simulation of streamflow in a macroscale watershed using general circulation model data, Water Resour. Res., 30(5), 1547-1559.

Kouwen, N., Soulis, E. D., Pietromiro, A., Donald, J., and Harrington, R. A., 1993, Grouped Response Units for Distributed Hydrologic Modelling, Journal of Water Resources Planning and Management, 199(3), 1-17.

Kuchment, L. S., 1992, The construction of continental scale models of terrestrial hydrological cycle: an analysis of the state of the art and future prospects, in Advances in Theoretical Hydrology: a tribute to James Dooge, J. Philip O' Kane (ed.), Elsevier, New York, 113-127.

Kuhnel, V., Dooge, J. C. I., O'Kane, J. P. J. and Romanowicz, R. J., 1991, Partial analysis applied to scale problems in surface moisture fluxes, Surv. Geophys., 12, 221-247.

Levin, S.A., 1992, The problem of pattern and scale in ecology, Ecology, 73, 6, 1943-1967.

Liesbscher, H. J., 1993, Hydrology for the Water Management of Large River Basins, Hydrol. Sci. Bull., 38(1), 1-13.

Loaiciga, H. A., Valdes, J. B., Vogel, R., Garvey, J. and Schwarz, H., 1996, Global warming and the hydrological cycle, J. Hydrol., 174, 83-127.

Lopes, J. E. G., Braga, B. P. F. and Conejo, J. G. L., 1981, SMAP, a simplified hydrologic model, International Symposium on Rainfall-Runoff Modeling, Mississipi State University, Mississipi.

Manabe, S., 1969, Climate and ocean circulation: 1.The atmospheric circulation and the hydrology of the earth's surface, Mon. Wea. Rev., 97, 739-774.

McFarlane, N. A., Boer, G. J., Blanchet, J. P. and Lazare, M., 1992, The Canadian Climate Centre Second-Generation General Circulation Model and Its Equilibrium Climate, J. Climate, 5, 1013-1044.

Mein, R. G. and Larson, C. L., 1973, Modeling infiltration during a steady rain, Water Resour. Res., 9(2), 384-394.

Milly, P. C. D., 1991, Some current themes in physical hydrology of the land-atmosphere interface, IAHS publ. no. 204, 3-9.

Mishra, S. and Parker, J. C., 1989, Effects of parameter uncertainty on predictions of unsaturated flow, J. Hydrol., 108, 19-33.

Mitchell, J. B. F., 1989, The 'greenhouse effect' and climate, Rev. Geophys., 27, 115-139.

Monteith, J. L., 1973 , Principles of Environmental Physics, Edward Arnold, London.

Moore, I. D. and Grayson, R. B., 1991, Terrain-based catchment partitioning and runoff prediction using vector elevation data, Water Resour. Res., 27(6), 1177-1191.

Moore, R. D. and Thompson, J. C., 1996, Are water table variations in a shallow forest soil consistent with the TOPMODEL concept?, Water Resour. Res., 32(3), 663-669.

Moore, R. J. and Clarke, R. T., 1981, A Distribution Function Approach to Rainfall - Runoff Modelling, Water Resour. Res., 17(5), 1367-1382.

Moore, R. J., 1983, The probability-distributed approach to spatial conceptual rainfall-runoff modelling, Report to Floods Protection Comission, Institute of Hydrology, Wallingford, UK.

Moore, R. J., 1985, The Probability-Distributed Principle and Runoff Production at a Point and Basin Scales, Hydrol. Sci. Bull., 30(2), 273-297.

Moore, R. J., Cooper, D. M., Harding, R. J., Roberts, G. and Calver, A., 1991, Large Scale Hydrological Modelling: A Systems Analysis, Institute of Hydrology, Wallingford.

Morel-Seytoux, H. J. and Miracapillo, C., 1989, Prediction of Water Table Mound development and Aquifer Recharge from an Infiltrating Area, in Unsaturated flow in hydrologic modeling: theory and practice, H.J. Morel-Seytoux (ed.), Kluwer Academic Publishers, 241-272.

Morton, F. I., 1965, Potential evaporation and river basin evaporation, J. Hydraul. Eng., 91(HY6), 67-97.

Morton, F. I., 1983, Operational estimates of areal evaporation and their significance to the science and practice of hydrology, J. Hydrol., 66, 1-76.

Mualem, Y., 1976, A new model for predicting the hydraulic conductivity of unsaturated porous media, Water Resour. Res., 12, 513-522.

Naden, P. S., 1993, A routing model for continental-scale hydrology, in Macroscale Modelling of the Hydrosphere, IAHS publ. no. 214, 67-79.

Nelder, J. A. and Mead, R., 1965, A simple method for function minimization, Comp. Journal, 7(4), 309-313.

Shukla, J., Nobre, C. A. and Sellers, P. J., 1990, Amazonia deforestation and climate change, Science, 247, 1322-1325.

O'Connell, P. E., Introduction: a historical perspective, in Advances in the modelling of hydrologic systems, D. S. Bowles and P. E. O'Connell (eds.), Kluwer Academic Publishers, 3-30.

O'Loughlin, E. M., 1981, Saturation Regions in Catchments and their Relations to Soil and Topographic Properties, J. Hydrol., 53, 229-246.

O'Loughlin, E. M., 1986, Prediction of Surface Saturation Zones in Natural Catchments by Topographic Analysis, Water Resou. Res., 22(5), 794-804.

Ott, M., Su, Z., Schumann, A. H. and Schultz, G. A., 1991, Development of a distributed hydrological model for flood forecasting and impact assessment of land-use change in the international mosel river basin, IAHS Publ. no. 201, 183-194.

Parlange, J. -Y. and Haverkamp, R., 1989, Infiltration and ponding time, in Unsaturated flow in hydrologic modeling: theory and practice, H.J. Morel-Seytoux (ed.), Kluwer Academic Publishers, 95-126.

Philip, J. R., 1957, The theory of infiltration: 1. The infiltration equation and its solution, Soil Sci., 83(5), 345-357.

Philip, J. R., 1974, Recent progess in the solution of nonlinear diffusion equations, Soil Sci., 117, 257-264.

Pimentel da Silva, L., 1990, Automatic calibration of rainfall-runoff models using smoothing techniques: an application to the SMAP-II model, M.Sc. thesis, COPPE, Universidade Federal do Rio de Janeiro, Rio de Janeiro, Brazil (in Portuguese).

Press, W. H., Teukolsky, S. A., Vetterling, W. T. and Flannery, B. P., 1992, Numerical recipes in fortran: The art of scientific computing, Cambridge University Press, Cambridge.

Price, J. C., 1982, Estimation of regional scale evapotranspiration through analysis of satellite thermal-infrared data, IEEE Trans. Geosci. Remote Sensisng, GE-20, 286-292.

Pullan, A. J., The quasilinear approximation for unsaturated porous media flow, Water Resour. Res., 26, 6, 1219-1234.

Quinn, P., Beven, K., Chevallier, P. and Planchon, O., 1991, The prediction of hillslope flow paths for distributed hydrological modelling using digital terrain models, Hydrol. Process., 5, 59-79.

Ragab, R. and Cooper, J. D., 1990, Obtaining soil hydraulic properties from field, laboratory and predictive methods, UK Nirex Ltd., UX/96/242.

Ragab, R., 1995, Towards a continuous operational system to estimate the root-zone soil moisture from intermittent remotely sensed surface moisture, J. Hydrol., 173, 1-25.

Rassmusson, E. M., Dickinson, R. E., Kutzbach, J. E. and Cleaveland, M. K., 1992, Climatology, in Handbook of hydology, D. R. Maidment (ed.), McGraw-Hill.

Rathfelder, K. and Abriola, L. M., 1994, Mass conservative numerical solutions of the head-based Richards' equation, Water Resour. Res., 30, 9, 2579-2586.

Rawls, W. J., Brakensiek, D. L. and Miller, N., 1983, Green-Ampt infiltration parameters from soils data, J. Hydraul. Div., Am. Soc. Civ. Eng., 109(1), 62-70.

Rawls, W. J. and Brakensiek, D. L., 1989, Estimation of soil water retention and hydraulic properties, in Unsaturated flow in hydrologic modeling: theory and practice, H.J. Morel-Seytoux (ed.), Kluwer Academic Publishers, 275-300.

Rawls, W. J., Ahuja, L. R., Brakensiek, D. L. and Shirmohammadi, A., 1992, in Handbook of hydology, D. R. Maidment (ed.), McGraw-Hill.

Richards, L. A., 1931, Capillary conduction of liquids through porous mediums, Physics, 1, 318-333.

Rogers, C., Stallybrass, M. P. and Clements, D. L., 1983, On two-phase infiltration under gravity and with boundary infiltration: An application of a Bäcklund transformation. Nonlinear Anal., Theory Math. Appl., 7, 785-799.

Ross, P. J., 1990, Efficient numerical methods for infiltration using Richards' equation, Water Resour. Res., 26(2), 279-290.

Rossi, C. and Nimmo, J. R., 1994, Modelling of soil water retention from saturation to oven dryness, Water Resour. Res., 30(3), 701-708.

Russo, D., 1988, Determining soil hydraulic properties by parameter estimation: on the selection of a model for the hydraulic properties, Water Resour. Res., 24(3), 453-459.

Sander, G. C., Parlange, J. -Y., Kuhnel, V., Hogarth, W. L., Lockington, D. and O'Kane, J. P. J., 1988, Exact nonlinear solution for constant flux infiltration, J. Hydrol., 97, 341-346.

Saxton, K. E., Rawls, W. J., Romberger, J. S. and Papendick, R. I., 1986, Estimating Generalized Soil-Water Characteristics from Texture, Soil Sci. Soc. Am. J., 50, 1031-1036.

Sellers, P. J., Mintz, I., Sud, Y. C. and Dalcher, A., 1986, A Simple Biosphere (SiB) Model for use within General Circulation Models, J. Atmos. Sci., 43, 505-531.

Sellers, P. J., Hall, F. G., Asrar, G., Strebel, D. E. and Murphy, R. E., 1992, An overview of the First International Satellite Land Surface Climatology Project (ISLSCP) Field Experiment (FIFE), J. Geophys. Res., 97, D17, 18345-18371.

Sharma, M. L., 1986, Measurement and prediction of natural groundwater recharge - An overview, J. Hydrol. (N.Z.), 25, 1, 49-56.

Shouse, P. J., van Genuchten, M. Th. and Sisson, J. B., 1991, A gravity-drainage/scaling method for estimating the hydraulic properties of heterogeneous soils, IAHS publ. no. 204, 281-291.

Shuttleworth, W. J., 1988a, Evaporation from Amazonian rainforest, Pro. R. Soc. London Ser. B, 233, 321 - 346.

Shuttleworth, W. J., 1988b, Macrohydrology - The new challenge for process hydrology, J. Hydrol., 100, 31-56.

Shuttleworth, W. J., 1991, The Modellion Concept, Rev. Geophys., 29(4), 585-606.

Shuttleworth, W. J., Gash, J. H. C., Roberts, J. M., Nobre, C. A., Molion, L. C. B. and Ribeiro, M. N. G., 1991, Post-deforestation Amazonian climate: Anglo-Brazilian research to improve prediction, J. Hydrol., 129, 71-86.

Shuttleworth, W. J., 1992, Evaporation, in Handbook of hydology, D. R. Maidment (ed.), McGraw-Hill.

Sivapalan, M., Beven, K. and Wood, E.F., 1987, On Hydrological Similarity, 2. A Scaled Model of Storm Runoff Production, Water Resour. Res., 23(12), 2266-2278.

Sklash, M. G. and Farvolden, R. N., 1979, The role of groundwater in storm runoff, J. Hydrol., 43, 45-65.

Solomon, S. I., Denouvillieez, J. P., Chart, E. J., Woolley, J. A. and Cadou, C., 1968, The use of a square grid system for computer estimation of precipitation, temperature and runoff, Water Resour. Res., 4(5), 919-929.

Sorooshian, S. and Gupta, V. K., 1985, The analysis of structural identifiability: theory and application to conceptual rainfall-runoff models, Water Resour. Res., 21(4), 487-495.

Sorooshian, S., Duan, Q. and Gupta, V. K., 1993, Calibration of rainfall-runoff models: application of global optimization to the sacramento soil moisture accounting model, Water Resour. Res., 29(4), 1185-1194.

Srivastava, R. and Jim Yeh, T. C., 1991, Analytical Solutions for One-Dimensional, Transient Infiltration Toward the Water Table in Homogeneous and Layered Soils, Wat. Resour. Res., 27(5), 753-762.

Su, N., 1994, A formula for computation of time-varying recharge of groundwater, J. Hydrol, 160, 123-135.

Tallaksen, L. M., 1995, A review of baseflow recession analysis, J. Hydrol., 165, 349-370.

Theis, S. W., Blanchard, B. J. and Newton, R. W., 1984, Utilization of vegetation indices to improve microwave soil moisture estimates over agricultural lands, IEEE Trans. Geosci. Remote Sensing GE-22, 490-496

Thomas, G., 1990, The regional hydrologic impacts of global climate change: the role of climate models, Palaeogeogr., Palaeoclimatol., Palaeoecol., 82, 343-368.

Thomas, H. R. and Rees, S. W., 1991, A comparison of field-monitored and numerically predicted moisture movement in unsaturated soil, Int. J. Numer. Anal. Methods Geomech., 157, 417-431.

Thompson, N., Barrie, I. A. and Ayles, M., 1981, The Meteorological Office rainfal and evaporation calculation system: MORECS, Met. Office, UK.

Todini, E., 1996, The ARNO rainfall-runoff model, J. Hydrol., 175, 339-382.

UNEP/WMO, 1983, A Square Grid Hydrological Study of the Amazon River Basin, Progress Report No. 8 (1022-02-1-83), on Project BRA/72/010, Shawinigan Eng. Comp. Ltd..

US Department of Agriculture, 1991, Hydrology of the Little Washita river watershed, Oklahoma: data and analysis, ARS-90, Agricultural Research Service.

van de Griend, A. A. and Engman E. T., 1985, Partial-Area Hydrology and Remote Sensing, J. Hydrol., 81, 211-251.

van Genuchten, M. Th., 1980, A closed-form equation for predicting the hydraulic conductivity of unsaturated soils, Soil Sci. Soc. Am. J., 44, 872-898.

van Genuchten, M. Th. and Nielsen, D. R., 1985, On describing and predicting the hydraulic properties of unsaturated soils, Ann. Geophys., 3(5), 615-628.

Villela, S. W. and Mattos, A., 1975, Applied hydrology, McGraw-Hill, São Paulo (in Portuguese).

Vorösmarty, C. J., Moore III, B., Grace, A. L., Gildea, M. P., Melillo, J. M., Peterson, B. J., Rastetter, E. B. and Steudler, P. A., 1989, Continental scale models of water balance and fluvial transport: an application to South America, Global Biogeochem. Cycles, 3, 241-265.

Vorösmarty, C. J., Gutowski, W. J., Person, M., Chen, T. -C. and Case, D., 1993, Linked atmosphere-hydrology models at the macroscale, in Macroscale Modelling of the Hydrosphere, IAHS publ. no. 214, 3-27.

Wang, Q. J., 1991, The genetic algorithm and its application to calibrating conceptual rainfall-runoff models, Water Resour. Res., 27(9), 2467-2471.

Wang, Q. J. and Dooge, J. C. I., 1994, Limiting cases of water fluxes at the land surface, J. Hydrol., 155, 429-440.

Warrick, A. W., Islas, A. and Lomen, D. O., 1991, An analytical solution to Richards' equation for time-varying infiltration, Water Resour. Res., 27(5), 763-766.

Warrick, A. W. and Parkin, G. W., 1995, Analytical solution for one-dimensional drainage: Burgers' and simplified forms, Water Resour. Res., 31(11), 2891-2894.

Wessman, C. A., 1992, Spatial Scales and Global Change: Bridging the Gap from Plots to GCM Grid Cells, Annu. Rev. Ecol. Syst., 23, 175-200.

Whittaker, S. K., 1992, Contaminant transport in the unsaturated zone, MSc dissertation, Civil Engineering Department, University of Newcastle upon Tyne, UK.

Wood, E. F., Sivapalan, M., Beven, K. and Band, L., 1988, Effects of spatial variability and scale with implications to hydrologic modelling, J. Hydrol., 102, 29-47.

Wood, E. F., 1991a, Global scale hydrology: advances in land surface modelling, Rev. Geophys., supplement, 193-201.

Wood, E. F., Lettenmaier, D. P. and Wallis, J. R., 1991b, Comparison of an alternative land surface parameterization with GFDL high resolution climate model, IAHS publ. no. 204, 53-64.

World Climate Research Programme, WCRP, 1991, Draft science plan for the GEWEX continental-scale international project, WMO Bull., Geneva.

WRSRU/NERC - University of Newcastle upon Tyne, 1992, Continental Scale Modelling, TIGER III.3 Proposal.

Wu, J., Zhang, R. and Yang, J., 1996, Analysis of rainfall-recharge relationships, J. Hydrol., 177, 143-160.

Xavier, A. E., 1982, Hyperbolic penalization: a new method for resolution of optimisation problems, M.Sc. thesis, COPPE, Universidade Federal do Rio de Janeiro, Rio de Janeiro, Brazil (in Portuguese).

Zhao, R. J., Zuang, Y. L., Fang, L. R., Liu, X. R. and Zhang, Q., 1980, The Xinanjiang Model, Hydrological Forecasting, Proceedings of Oxford Symposium, IAHS Publ., no. 129, 351-356.

Yeh, W. W. -G., 1986, Review of parameter identification procedures in groundwater hydrology: the inverse problem, Water Resour. Res., 22(2), 95-108.

APPENDIX A

A New Drainage Component for ARNO Model

A.1 - Introduction

During early stages of this work the possibility of using the ARNO modelling scheme (Todini, 1996) for large scale land-surface parameterisation was studied. The ARNO model, described in section 2.6.2, is a conceptual ESMA type model (Explicit Soil Moisture Accounting Models, O'Connell (1991), described in section 2.4.3). In the runoff parameterisation spatial variability is represented by incorporating the contributing area concept and applying the power probability distribution function given in Zhao et al., 1980 (see eqn. 2.4). The model includes evapotranspiration and deep percolation losses, outflow as subsurface flow (drainage) and a detailed routing component that considers transfers both within sub-catchments and from sub-catchments to the outlet of the catchment. As a part of this initial study the drainage component of the ARNO model was reviewed.

A.2 - ARNO Model Drainage Component

The drainage component is given by eqn. (2.6):

$$D(t) = D_{\min} \frac{w}{w_{\max}}, \; w < w_{\lim}$$

$$D(t) = D_{\min} + D_{\max} \left(\frac{w - w_{\lim}}{w_{\max} - w_{\lim}} \right)^{d\exp}, \; w \geq w_{\lim}$$

where, D_{max} (maximum allowed drainage), D_{min} (minimum allowed drainage) and dexp are parameters. This function is empirical, is linear for $w < w_{lim}$ and can be linear or nonlinear (depending on the value of dexp) for $w \geq w_{lim}$. Along with the deep percolation function (also empirical), the drainage function controls the hydrograph recession limb behaviour. In ARNO all the parameters in these functions are obtained by calibration.

A.3 - Recession Analysis

This analysis was carried out in an attempt to improve the hydrograph recession representation in the ARNO model. A number of single-peak discharge events were selected for a catchment comprising the Featherstone and Alston sub-catchments of the Tyne basin, Northeast England (Figure A.1). The analysis carried out involved searching for a parameterisation giving discharge as a function of catchment storage, obtained by integrating the recession curves, assuming the storage is zero at the end of the time interval. The SHE model has been extensively applied to the Tyne basin and in this study evaporation rates from SHE simulations were used. All these recession segments have been shifted together to form a characteristic recession (Figure A.2).

A.4 - New Drainage Component

First, based on the shapes seen in Figure A.2, fitting was attempted using two line segments, one parallel to the 'x' axis and the other with a positive gradient. This was relatively successful. However, this function type would introduce a threshold structure in the model. To overcome this, a hyperbolic-form function was fitted to the data.

$$D_t = \mathbf{DR1} + \frac{\tan\left(\frac{\pi-\alpha}{2}\right)}{\tan^2\left(\frac{\pi-\alpha}{2}\right)-1}\left(-G+\sqrt{G^2+\mathrm{d}^2\frac{\left(\tan^2\left(\frac{\pi-\alpha}{2}\right)-1\right)^2}{\tan^2\left(\frac{\pi-\alpha}{2}\right)}}\right),$$

$$\alpha = \arctan(\mathbf{DR3})$$

$$G = \mathbf{DR3}*(\mathbf{DR2}-W_t)$$

This function is analogous to equation 2.3 (Xavier, 1982), which was previously applied by Pimentel da Silva (1990) to smooth threshold structures in a typical ESMA model (see section 2.4.3). Figure A.2 shows the best fit of the hyperbolic-function to the discharge x storage points for the group of discharge events used in this study.

The use of this modelling scheme would simplify the original ARNO approach, and the new function has the advantage of being continuous, overcoming the problems caused by threshold structures in conceptual models (discussed in section 2.4).

The new drainage approach was integrated with the Xinanjiang runoff function (Zhao et al., 1980) and some simulations carried out (Figure A.1). This approach, however, was not tested extensively.

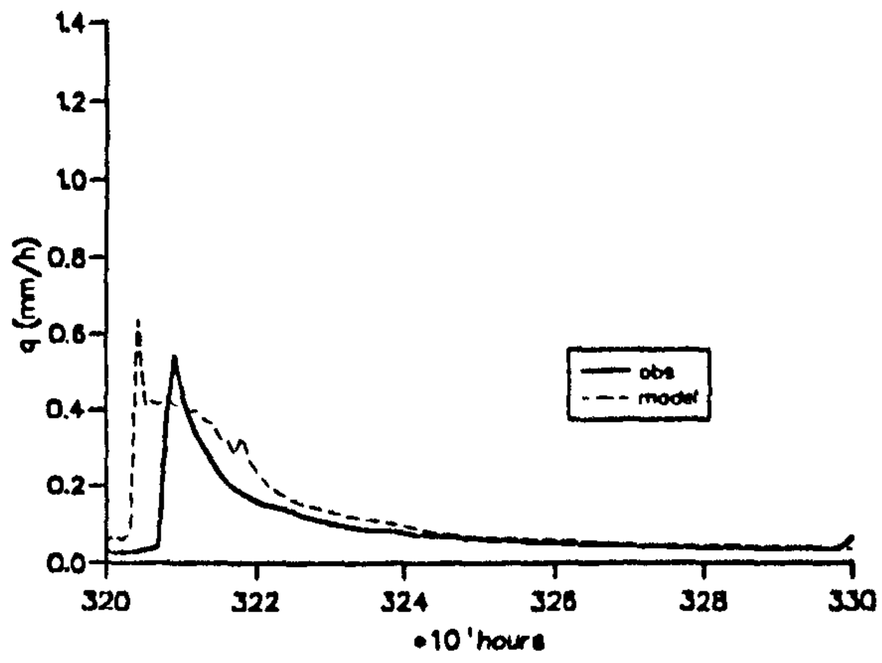

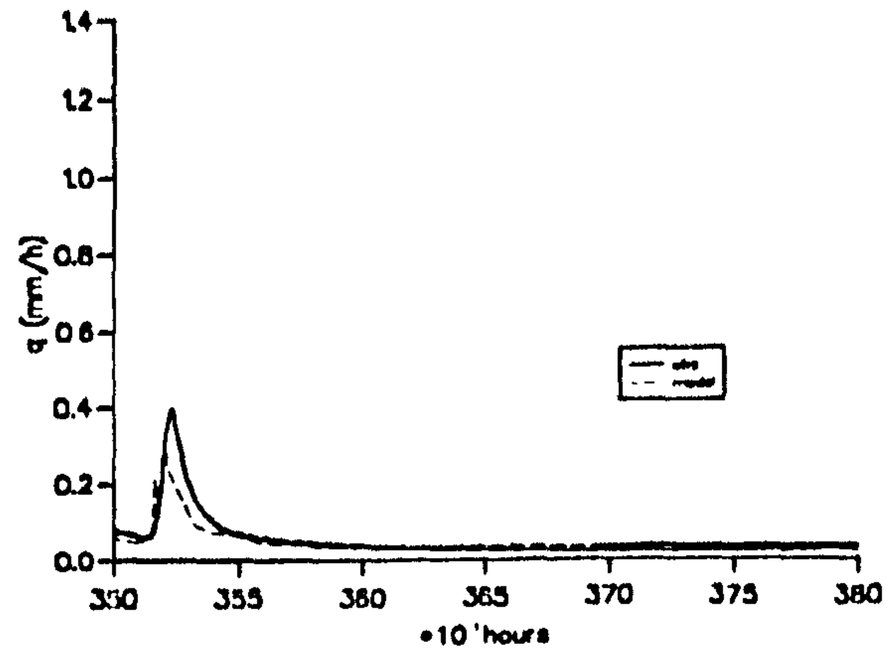

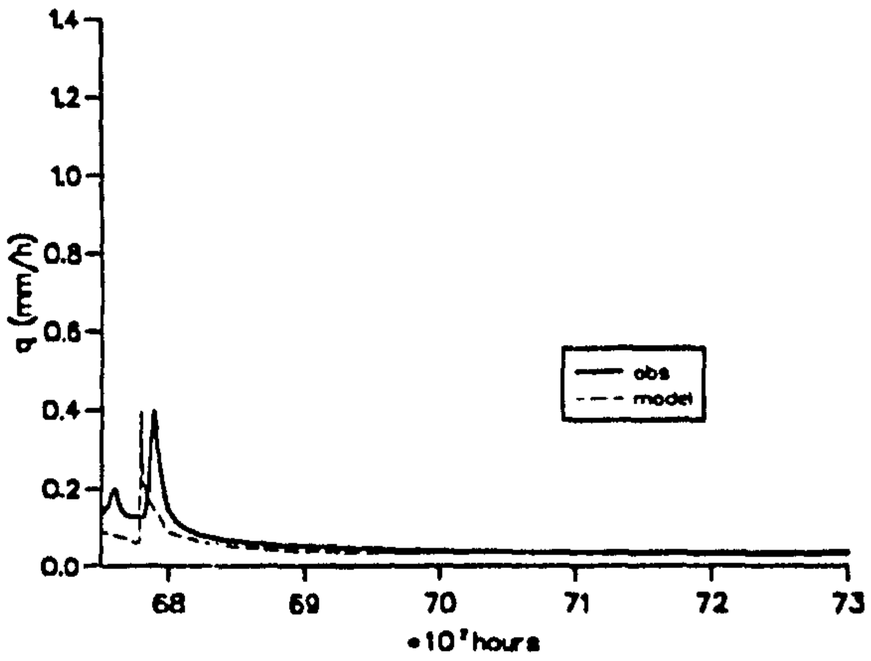

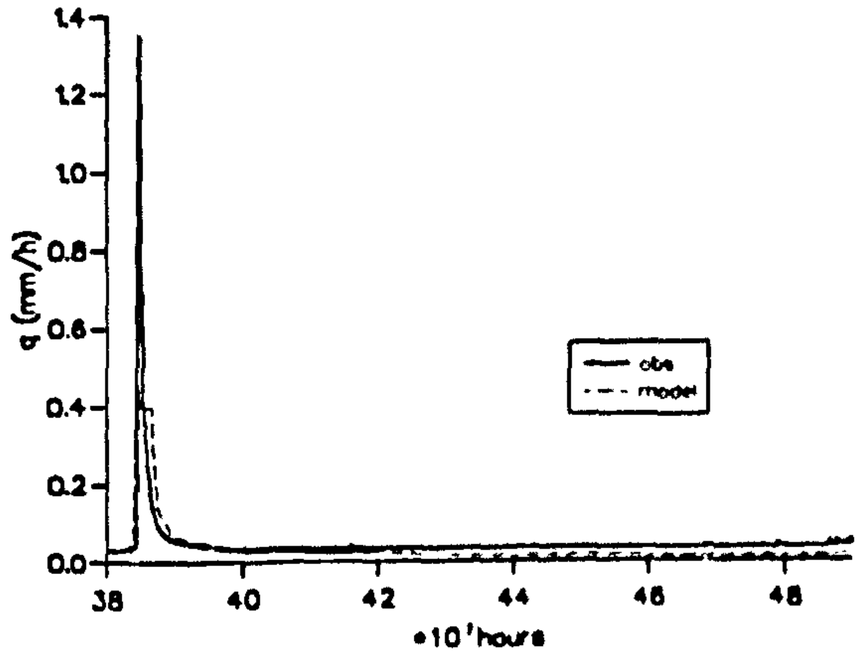

Figure A.1 - Discharge events (Alston and Featherstone)

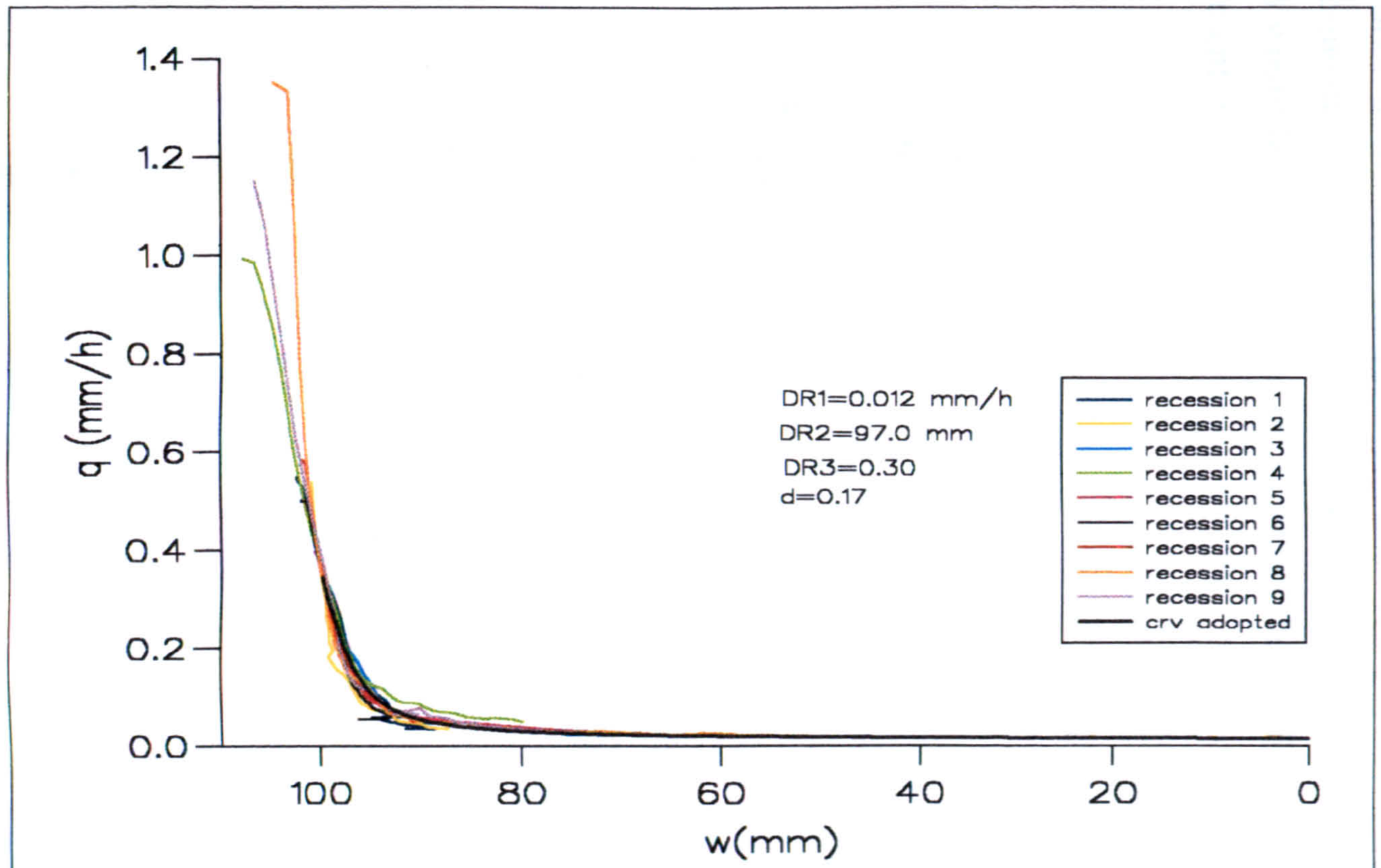

Figure A.2 - Recessions shifted together and new function

APPENDIX B

Parameter δ of the SM Approach and Soil Physical Properties

In the formulation of the SM approach of the GRASP model an unsuccessful study was made to associate the parameter δ to soil physical properties. Some plots produced during these attempts are shown here. If a good association is found the points on the plots would fall on a straight line or simple curve. This Appendix complements the study presented in section 5.2.2.

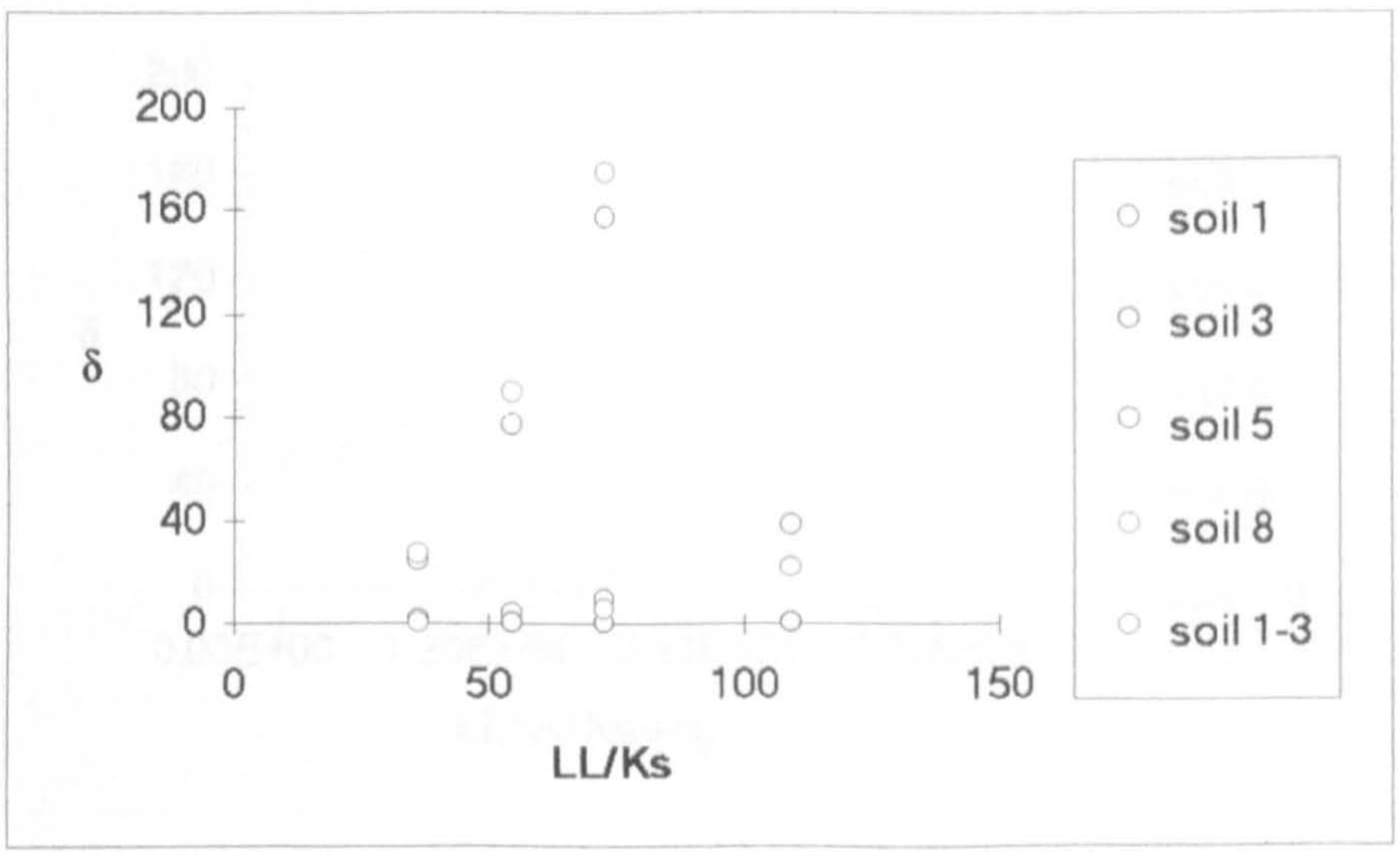

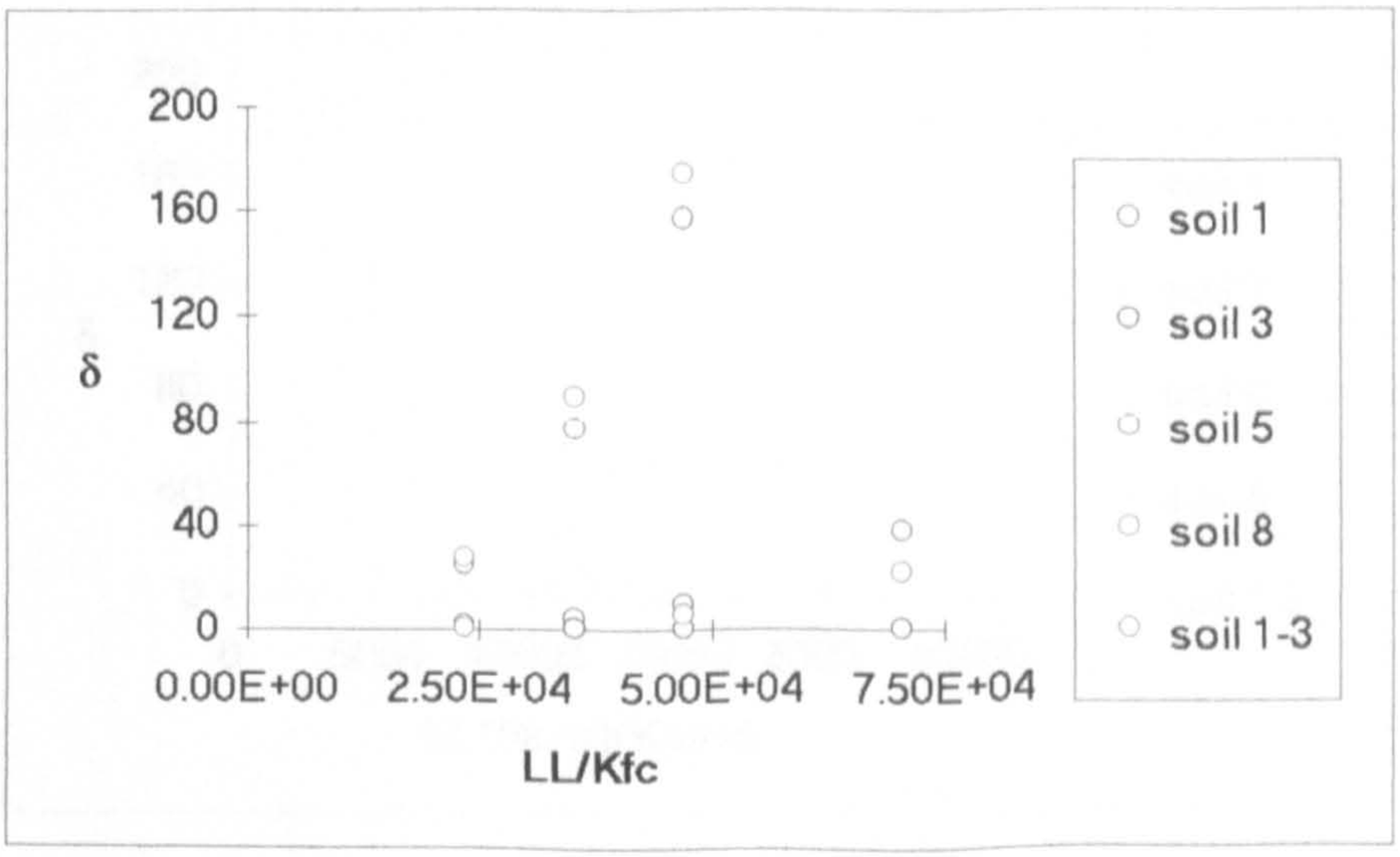

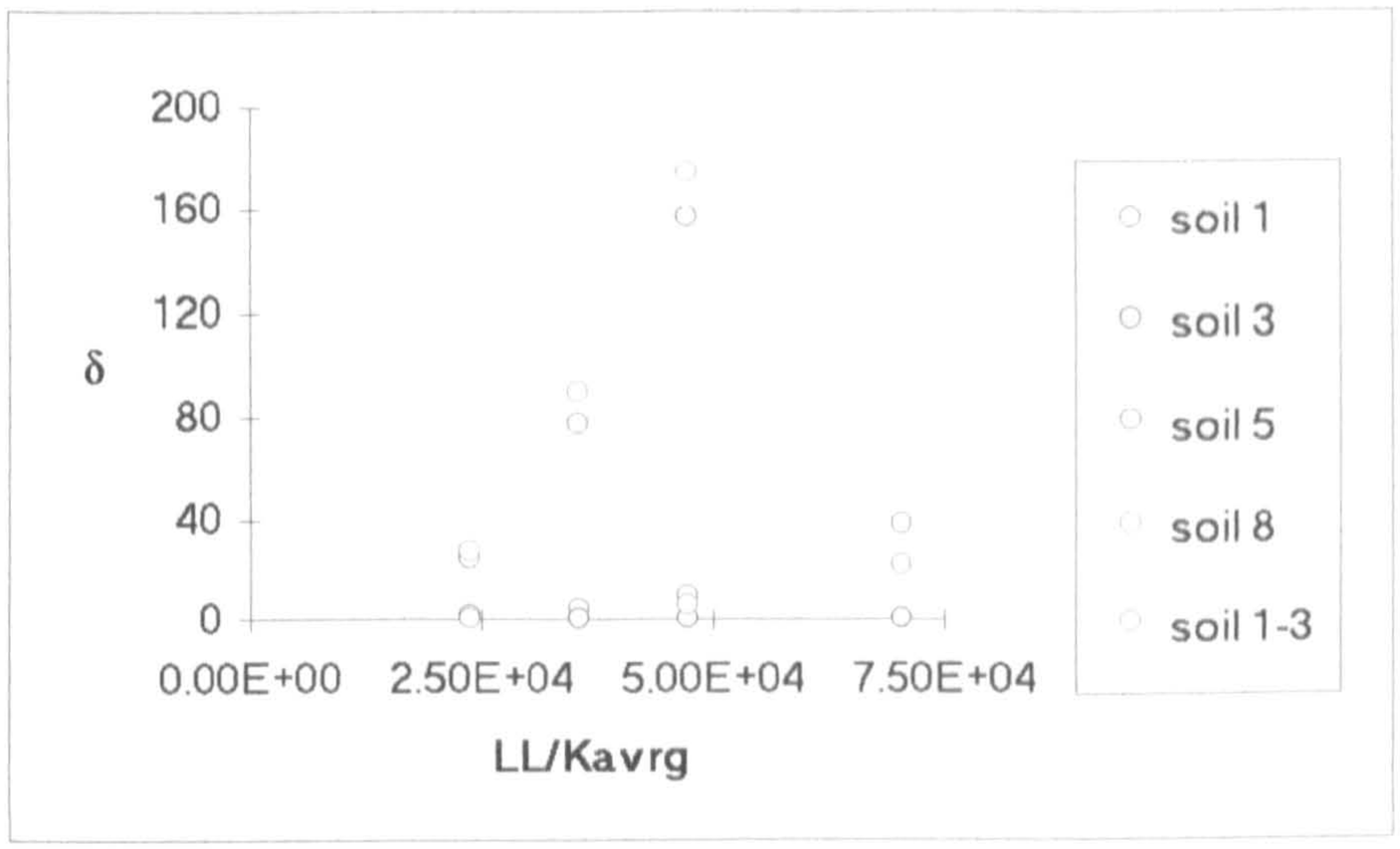
200
160
120
δ
80
40
0
0.00E+00
2.50E+04
5.00E+04
7.50E+04
LL/Kavrg
soil 1
soil 3
soil 5
soil 8
soil 1-3

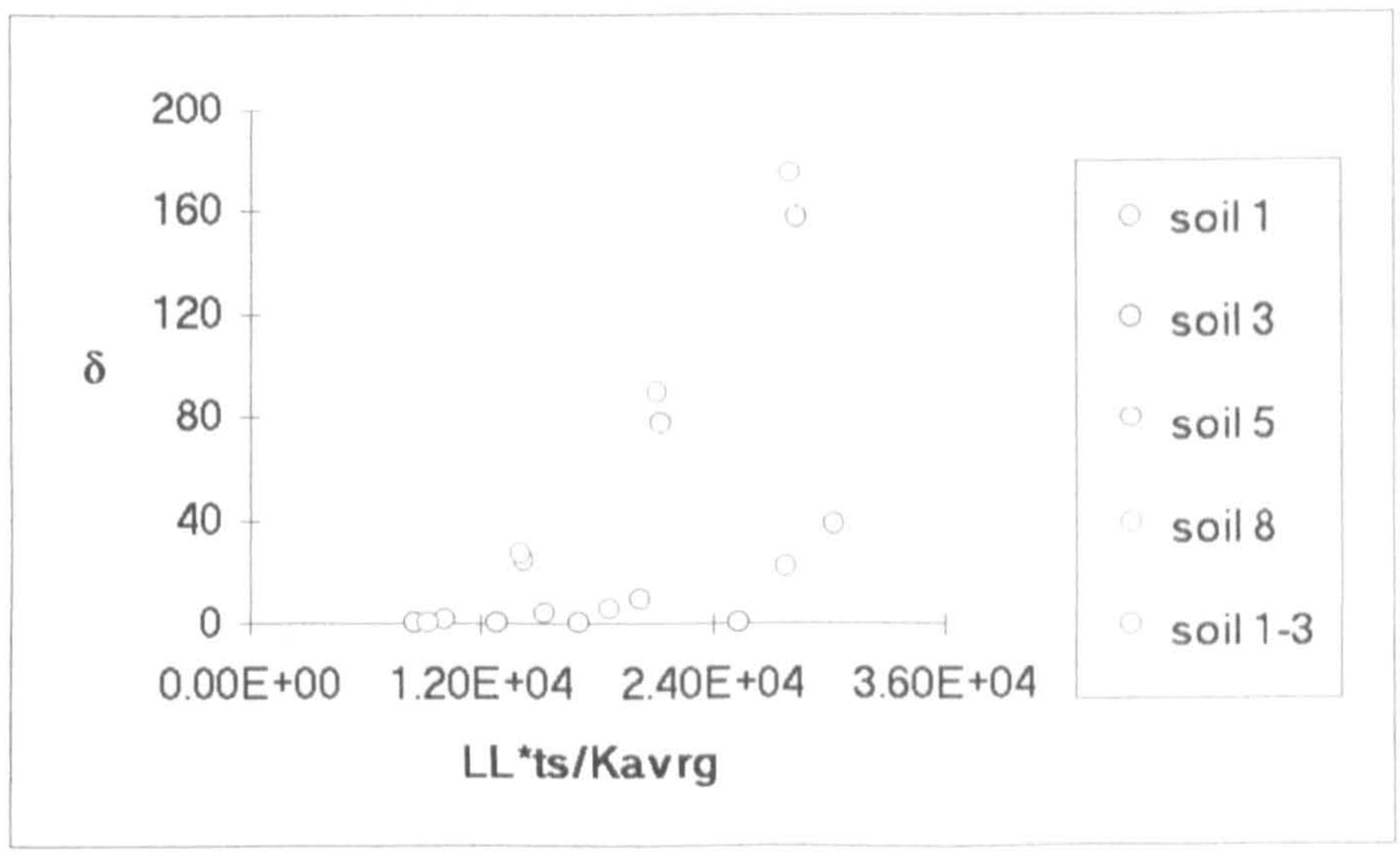
200
160
120
δ
80
40
0
0.00E+00
1.20E+04
2.40E+04
3.60E+04
LL*ts/Kavrg
soil 1
soil 3
soil 5
soil 8
soil 1-3

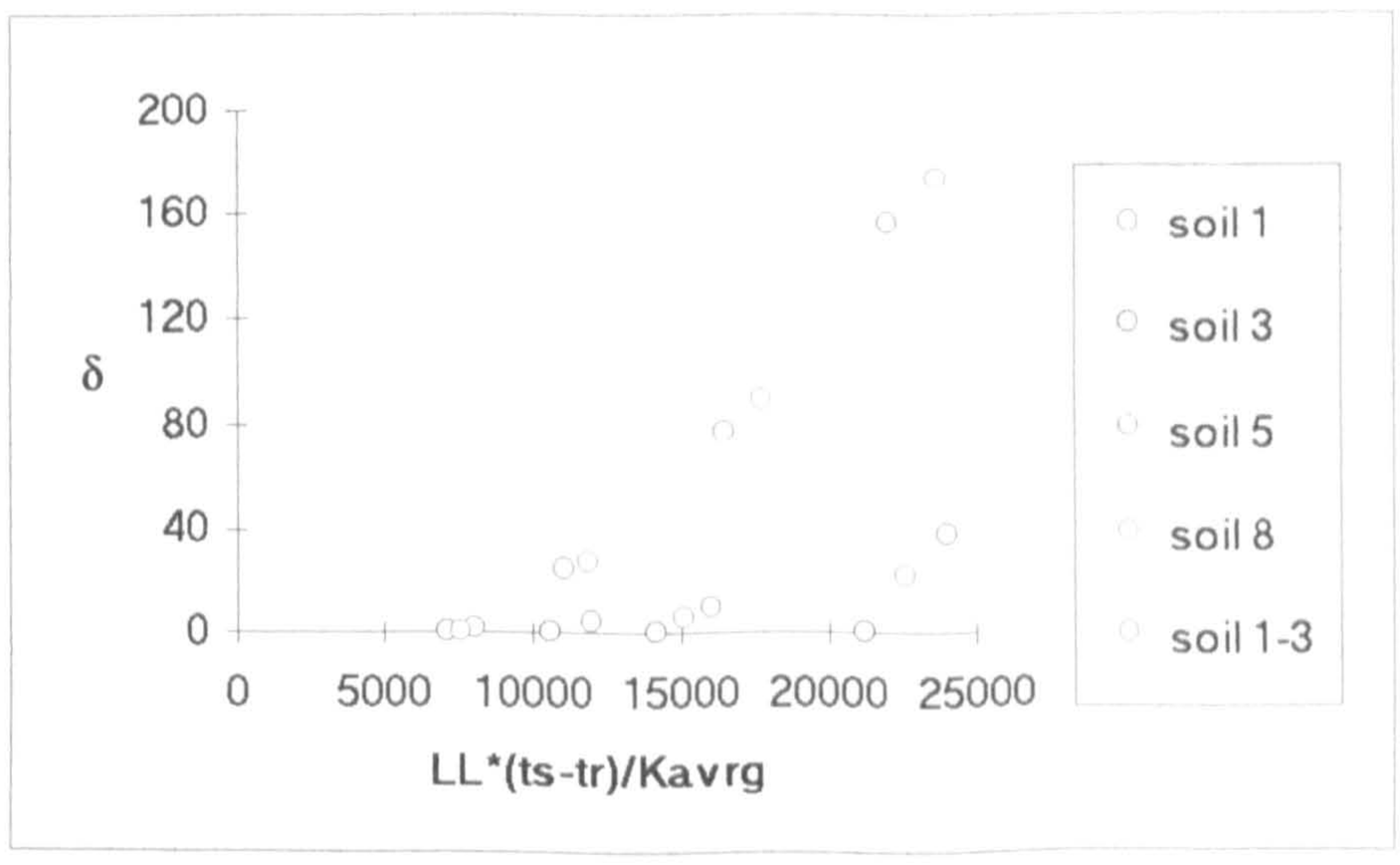
200
160
120
δ
80
40
0
0
5000
10000
15000
20000
25000
LL*(ts-tr)/Kavrg
soil 1
soil 3
soil 5
soil 8
soil 1-3

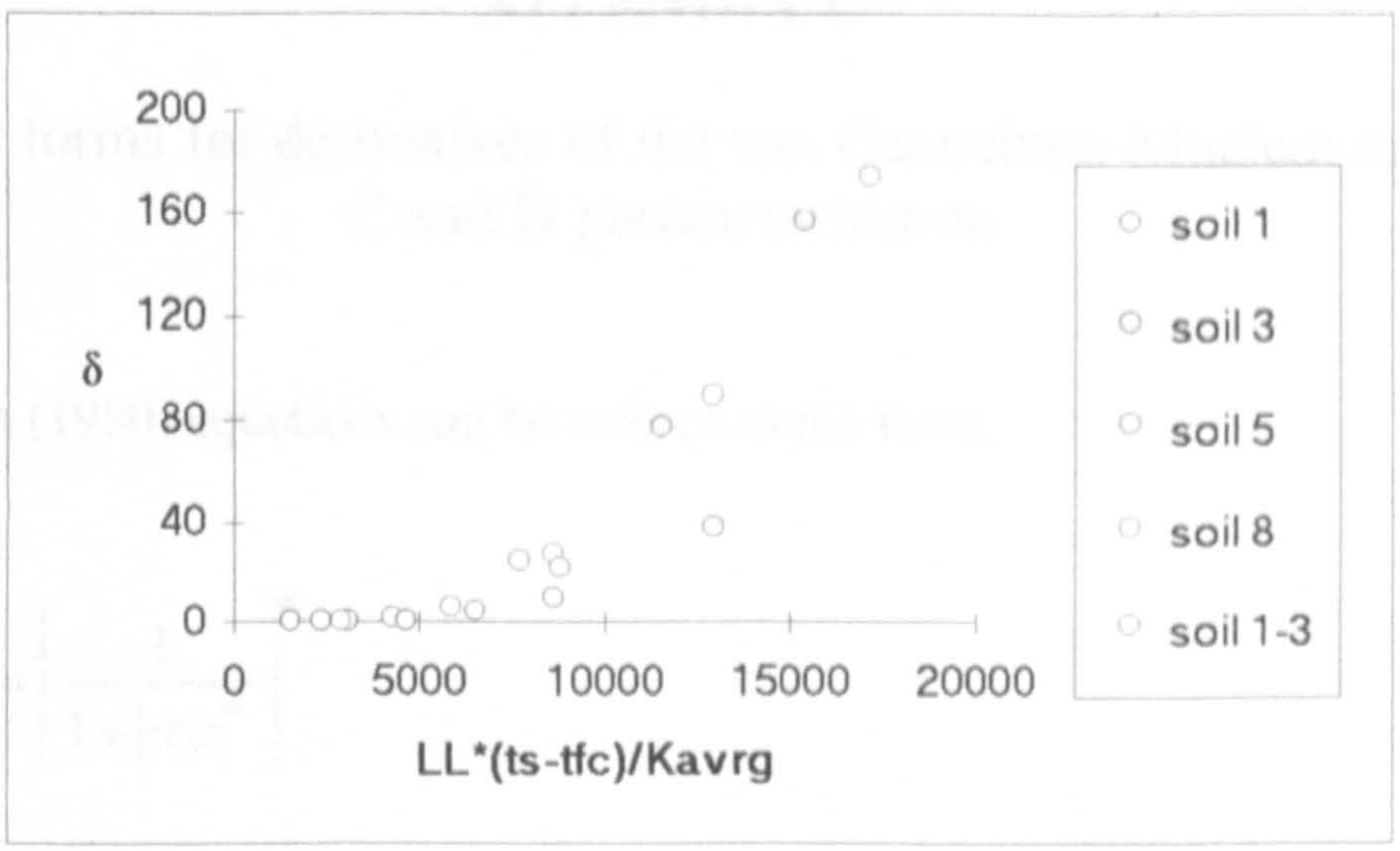

Notes:

- The scale for both axes in these plots is hours; LL is the depth to the phreatic surface; K_s the soil saturated hydraulic conductivity; K_{fc} the soil hydraulic conductivity at field capacity, the volumetric moisture content at a matric potential of -333 cm; and K_{avrg} the soil harmonic average hydraulic conductivity($= (K_s . K_{fc}) / (K_s + K_{fc})$).

- ts is the saturated moisture content (porosity); tr the residual moisture content (from van-Genuchten model); and tfc the moisture content at field capacity, correspondent to a matric potential of -333cm.

As can be seen the points on the plots are very scattered and it is not practical to determine a simple functional relationship between δ and the six groups of physical properties.

APPENDIX C

Analytical forms for derivatives of the van Genuchten-Mualem model for C and D parameterisation

van Genuchten (1980) equations can be written in the form,

$$\frac{(\theta-\theta_r)}{(\theta_s-\theta_r)}=\left[\frac{1}{1+|\alpha\psi|^n}\right]^m \qquad \text{eqn. (C.1)}$$

and K(ψ), as in Ragab and Cooper (1990),

$$K(\psi)=K_s\frac{\left\{\left[1+|\alpha\psi|^n\right]^m-|\alpha\psi|^{n-1}\right\}^2}{\left[1+|\alpha\psi|^n\right]^{m(x+2)}}, \text{ (x=0.5; Mualem, 1976))} \qquad \text{eqn. (C.2)}$$

and K(θ), as in Shouse et al. (1991),

$$K(\theta)=K_{sat}S^{1/2}\left\{1-\left[1-S^{1/m}\right]^m\right\}^2 \qquad \text{eqn. (C.3)}$$

where,

$$S=\frac{(\theta-\theta_r)}{(\theta_s-\theta_r)}$$

and,

θ - soil moisture content;
θ_s - saturated moisture content (porosity);
θ_r - residual moisture content;
K_{sat} - saturated hydraulic conductivity;
ψ - matric potential;
α - soil parameter;
n - soil parameter;
m - soil parameter (=1-(1/n)).

Parameter C (eqn. 5.17) is given by;

$$C_i = -\frac{\partial}{\partial z}\left(K\frac{d\psi}{d\theta}\right) - \frac{d\psi}{d\theta}\frac{\partial K}{\partial z}$$

which is equivalent to;

$$C_i = -\frac{\partial \psi}{\partial z}\left(K\frac{\partial}{\partial \psi}\left(\frac{d\psi}{d\theta}\right) + 2\frac{\partial K}{\partial \psi}\frac{d\psi}{d\theta}\right)$$

However, as $\psi = -z$ for equilibrium, then;

$\frac{\partial \psi}{\partial z} = -1$, and C becomes;

$$C_i = K\frac{\partial}{\partial \psi}\left(\frac{d\psi}{d\theta}\right) + 2\frac{\partial K}{\partial \psi}\frac{d\psi}{d\theta}$$

Expanding $\partial K/\partial \psi$,

$$C_i = K\frac{\partial}{\partial \psi}\left(\frac{d\psi}{d\theta}\right) + 2\frac{\partial K}{\partial \theta}\frac{d\theta}{d\psi}\frac{d\psi}{d\theta}$$

which results on,

$$C_i = K\frac{\partial}{\partial \psi}\left(\frac{d\psi}{d\theta}\right) + 2\frac{\partial K}{\partial \theta}$$

D (eqn. 5.18) is given by;

$$D_i = K.\frac{d\psi}{d\theta}$$

C.1 - $\frac{d\psi}{d\theta}$

$$-\psi(\theta) = \frac{1}{\alpha} \cdot \left[\frac{A}{1-A}\right]^{(1-m)} \qquad \text{eqn. (C.4)}$$

Where,

$$A = 1 - S^{1/m}$$

In which S, is given by,

$$S = \frac{\theta - \theta_r}{\theta_s - \theta_r}$$

Deriving eqn. (C.4),

$$\frac{d\psi}{d\theta} = -\frac{1}{\alpha}(1-m)\left[\frac{A}{1-A}\right]^{-m} \frac{\partial Y}{\partial \theta}\,, \qquad \text{eqn. (C.5)}$$

In which Y is given by,

$$Y = A.(1-A)^{-1}$$

So,

$$\frac{\partial Y}{\partial \theta} = \frac{\partial A}{\partial \theta}.(1-A)^{-1} + A.(-1).(1-A)^{-2}.(-\frac{\partial A}{\partial \theta}) \qquad \text{eqn. (C.6)}$$

Where,

$$\frac{\partial A}{\partial \theta} = -\frac{1}{m} S^{(\frac{1}{m}-1)} \frac{\partial S}{\partial \theta} \qquad \text{eqn. (C.7)}$$

and,

$$\frac{\partial S}{\partial \theta} = \frac{1}{(\theta_s - \theta_r)} \qquad \text{eqn. (C.8)}$$

Substituting eqn. (C.8) in eqn. (C.7),

$$\frac{\partial A}{\partial \theta} = -\frac{1}{m.(\theta_s - \theta_r)} S^{(\frac{1}{m}-1)} \qquad \text{eqn. (C.9)}$$

Substituting eqn. (C.9) in eqn. (C.6),

$$\frac{\partial Y}{\partial \theta} = -\frac{1}{S.m.(\theta_s - \theta_r)}\left(1+\frac{A}{1-A}\right) \qquad \text{eqn. (C.10)}$$

Finally, substituting eqn. (C.10) in eqn. (C.5),

$$\frac{\partial \psi}{\partial \theta} = -\frac{(m-1)}{\alpha.m.(\theta_s - \theta_r).A^m.(1-A)} \qquad \text{eqn. (C.11)}$$

C.2 - $\frac{\partial}{\partial \psi}\left(\frac{d\psi}{d\theta}\right)$

Deriving eqn. (C.11),

$$\frac{\partial}{\partial \psi}\left(\frac{d\psi}{d\theta}\right) = \frac{m-1}{\alpha.m.(\theta_s - \theta_r)}.[A^m.(1-A)]^{-2}.[m.A^{m-1}.\frac{\partial A}{\partial \psi}.(1-A) \qquad \text{eqn. (C.12)}$$

$$+A^m(-\frac{\partial A}{\partial \psi})]$$

S is given by,

$$S = \frac{(\theta - \theta_r)}{(\theta_s - \theta_r)} = \left[\frac{1}{1+|\alpha\psi|^n}\right]^m$$

and,

$$A = 1 - S^{1/m}$$

Then, A can be given as a function of matric potential by,

$$A = 1 - [1 + |\alpha\psi|^{\frac{1}{1-m}}]^{-1}$$

and,

$$\frac{\partial A}{\partial \psi} = -\frac{\alpha}{1-m}.[1 + |\alpha\psi|)^{\frac{1}{1-m}}]^{-2}.|\alpha\psi|^{\frac{m}{1-m}} \qquad \text{eqn. (C.13)}$$

$\frac{\partial}{\partial \psi}\left(\frac{d\psi}{d\theta}\right)$ is given by substituting eqn. (C.13) into eqn. (C.12).

C.3 - $\frac{\partial K}{\partial \theta}$

In which "$\partial K/\partial 6$" is given by,

$$\frac{\partial K}{\partial \theta} = \frac{K_{sat}.S^{-1/2}}{(\theta_s - \theta_r)}.(1 - A^m).\left[\frac{1}{2} + 2.(1 - A).\frac{A^m}{A} - \frac{1}{2}.A^m\right] \qquad \text{eqn. (C.14)}$$

given by Shouse et al. (1991). Substituting "S" in eqn. (C.14) by,

$S = (1 - A)^m$, eqn. (C.14) becomes,

$$\frac{\partial K}{\partial \theta} = \frac{K_{sat}.(1 - A)^{-m/2}}{(\theta_s - \theta_r)}.(1 - A^m).\left[\frac{1}{2} + 2.(1 - A).\frac{A^m}{A} - \frac{1}{2}.A^m\right] \qquad \text{eqn. (C.15)}$$